BIOCHEMICAL AND MOLECULAR GENETIC ASSESSMENT OF BACTERIAL BIOPOLYMER

A thesis submitted

in partial fulfillment of the requirements for the degree of

Doctor of Philosophy

By

Pinkee Phukon

Registration No. 014 of 2009

School of Science

Department of Molecular Biology & Biotechnology

Tezpur University

Napaam, Tezpur - 784028

Assam, India

June, 2013

Dedicated to Deuta and Maa.....

ABSTRACT

The ever increasing population has led to accumulation of non degradable waste materials in the environment affecting the very survival of the living world. Petro-derived plastics are widely used to make a variety of industrial and consumer products. But their intrinsic durability and resistivity towards degradation renders them pollutants in the environment. There is no effective method for the degradation of these recalcitrant materials. Considering the huge economic and ecological costs involved in the ever depleting environment from such petro-derived plastics, the idea of substituting non-degradable synthetic plastics with ecofriendly biodegradable plastics has drawn considerable attention world over. Among the various biodegradable plastics available, polyhydroxyalkanoate (PHA) is a promising natural polyester produced by bacteria as their intracellular storage energy material while suffering from a particular stress[1]. PHA is not only biodegradable and biocompatible, but also known to possess same physical properties as that of conventional plastics thereby making it suitable for the various applications.

It is known that the petroleum hydrocarbon contaminated soils harbor a large number of microbes constituting an environment of excess carbon with limited nitrogen, and as such these sites could be the potential source for PHA producing bacteria. Assam is rich in petroleum and the first oil well was discovered in Digboi more than a hundred years ago. The state has over 1.3 billion tones of proven crude oil and 156 billion cu mt of natural gas reserves. The premier Indian Oil companies like ONGC, OIL and IOCL are involved in exploration, development and production of crude oil and natural gas, transportation of crude oil and production of LPG. In view of the above background information, the present investigation was taken up with the following objectives:

1. Screening of biopolymer producing bacteria
2. Isolation and purification of PHA
3. Physical and chemical characterization of PHA
4. Molecular genetic assessment of PHA producing bacterial isolates

Bacterial strains were isolated from the soil samples collected from crude oil contaminated sites of Assam and Assam Arakan Basin, ONGC; waste disposal site of Numaligarh Refinery Limited, Assam and non-petroleum industrial site of Jagiroad Paper Mill, Nagaon, Assam for the isolation of PHA producing bacteria. A

total of 13 pure bacterial strains were isolated and screened for PHA production. The standard staining procedures enabled selection of 3 isolates such as BPC1, BPC2 and BP2 for assessing their potential PHA production.

Morphological characterization (colony size, pigmentation, forms, margin and elevation) displayed wide variations. All biochemical tests were carried out to characterize the bacterial strains. The optimum growth conditions of the bacterial isolates were assessed by subjecting them to different growth phase, pH and temperature regimes. The optimal conditions for PHA production were- pH 7.0, 37 °C temperature and 72 h culture period.

For molecular characterization of the biopolymer producing bacterial isolates BPC1 and BPC2, 16s rDNA analysis was performed. Genomic DNA isolated from the bacterial isolates was used for the amplification of 16S rDNA by PCR and then sequenced. Subsequently, data generated were deposited in the GenBank of NCBI, compared with published sequences and phylogenetic tree was constructed using ClustalW by the distance matrix analysis and the neighbour-joining method. Phylogenetic analysis indicated a comparative search for the sequence of BPC1 and BPC2 revealed 99% homology to other known *Pseudomonas aeruginosa* 16S rDNA gene sequences and accordingly they were named as *P. aeruginosa* BPC1 (JQ796859) and *P. aeruginosa* BPC2 (JQ866912), respectively. The bacterial strain BP2 was previously identified by our laboratory and named as *Bacillus circulans* MTCC8167.

The bacterial strains were subjected to growth kinetic study in the different culture media supplemented with the carbon substrates like glucose, glycerol, *colocassia* starch, propionic acid, soy oil, waste mobile, sugarcane molasses and glycerol byproduct of kitchen chimney dump lard (KCDL). The bacterial strain *P. aeruginosa* JQ866912 possessed the higher accumulation of PHA as compared to *B. circulans* MTCC8167 followed by *P. aeruginosa* JQ796859. Comparatively, when the glycerol byproduct (waste of KCDL) was used as the carbon source, *P. aeruginosa* JQ866912 showed the highest PHA accumulation in comparison to the other carbon sources, followed by *P. aeruginosa* JQ796859 and *B. circulans* MTCC8167. Similar results were obtained in the case of biomass yield by the bacterial strains with the use of the above stated carbon sources.

The biopolymer was isolated following the soxhlet extraction method with chloroform as the solvent, and purified by washing repetitively with ice cold methanol[2]. Subsequently, the chemical and structural characterization was done using UV-Vis spectroscopy, FTIR, GCMS and ^{1}H and ^{13}C NMR methods. The results confirmed the isolated PHAs from *P. aeruginosa* JQ796859, *B. circulans* MTCC8167 and *P. aeruginosa* JQ866912 to be poly (3-hydroxyvalerate) co- (5-hydroxydecenoate) (P-3HV-5-HDE), poly-3-hydroxybutyrate-co-3-hydroxyvalerate (P-3HB-3HV) and poly-3-hydroxyvalerate-co-5-hydroxydecenoate-co-3-hydroxyoctadecenoate (P-3HV-5HDE-3HODE) respectively. The molecular weight of the biopolymers was assessed by GPC and the value was found to be in the order *B. circulans* MTCC8167> *P. aeruginosa* JQ866912 > *P. aeruginosa* JQ796859. XRD analysis was carried out to study the crystalline behavior of the polymers. The degradation profile and melting point of the extracted biopolymers were tested by using TGA and DSC analysis, respectively. All three biopolymers possessed thermal as well as melting stability. The photoluminescence property of the biopolymers was studied by photoluminescence spectrophotometer (PL) and all of them showed luminescence property. SEM analysis was done to examine the surface morphology of the extracted biopolymers.

In vitro degradation of the biopolymers from *P. aeruginosa* JQ796859 and *P. aeruginosa* JQ866912 was done by treating with different soil bacteria like *Alacaligens faecalis* (MTCC8164), *B. circulans* (MTCC8167), *P. aeruginosa* (MTCC7815) and *Mycobacterium* spp (G-35I); and the biopolymer from *B. circulans* MTCC8167, by *B. subtilis* strains BP4, BP5, BP7 and fungal strains *Candida albicans* (MTCC 3017) and *Fusarium oxysporum* (NCIM 1281). FTIR and SEM analysis was done to assess the pattern of degradation of the biopolymers. All these analyses supported biodegradability of the biopolymers when exposed to microbial action.

Silver nanoparticle (SNP) has been extensively used in biomedical studies, cosmetics, antibacterial-water filter and also as drug carrier. The natural hydrophobic biopolymers such as PHA could be an effective alternative and renewable source for the aforementioned applications. SNP synthesized from $AgNO_3$ was impregnated by dispersing in PHA colloid (0.085%) using $NaBH_4$. *In situ* formation of the SNP-PHA colloid was confirmed by FTIR analysis. The

stability was tested by wave length scanning using a UV-Vis spectrophotometer and finally with a transmission electron microscope (TEM). The composite of SNP-PHA was found to be stable for 30 days as compared to the lower stability of SNP solution alone. In the present investigation, the PHA polymer of *B. circulans* MTCC8167 was used for stabilizing the size of SNP particles which in turn would provide advantage for their application in synthesis, transportation of SNP colloids and their use in different biomedical formulations.

The change in photoluminescence properties in doping of the copper, zinc and nickel oxide nanoparticles with PHA polymer of *P. aeruginosa* JQ866912 was studied using XRD, UV-Vis spectroscopy and PL. XRD analysis and the same showed the successful incorporation of nanoparticles in the polymer matrix. The PL spectra of the materials showed a dramatic change in the emission nature to that of the virgin polymer.

Malaria is a vector-borne infectious disease and continues to be a major health problem in the tropics and subtropics. The antimalarial drug artemisinin has successfully been used in the treatment of growing resistance of *Plasmodium falciparum* for more than two decades. But there was a case of significant liver inflammation due to prolonged use of relatively high-dose of artemisinin. In view of the importance of artemisinin in treatment of malaria, several methods have been developed for quantitative analysis of its metabolites. But, none of the existing methods could determine the trace amount of artimisinin in the biological fluids like urine as well as in pharmaceutical formulations. As such there is a need for development of an efficient technique to detect the lowest possible traceable amount of artimisinin in biological fluids and pharmaceutical formulations. Accordingly, a highly sensitive method was developed using a selective biosensor comprised of PHA-gold nanoparticles (AuNPs) composite synthesized on indium–tin oxide (ITO) glass plate for direct determination of artimisinin in pharmaceutical formulations and biological fluids. The sensor was fabricated by adsorbing horseradish peroxidase (HRP) enzyme on the electrode surface for which cyclic voltametry (CV) was used to monitor the electro-catalytic reduction of artemisinin under diffusion controlled conditions. Electrochemical interfacial properties and immobilization of enzyme onto PHA-AuNPs film were evaluated and confirmed by CV, Electrochemical impedance spectroscopy (EIS) and SEM techniques. The tested biosensor exhibited

low LOD values, high levels of repeatability and reproducibility in pharmaceutical formulations and also in the spiked human serum. The PHA/AuNPs/HRP/ITO biosensor based nanocomposite probe has potential as a good analytical alternative in comparison to other existing methods presently available for such tests.

To determine the presence of PHA biosynthesis genes in *P. aeruginosa* strains JQ796859 and JQ866912, PCR based molecular technique was used for their elucidation. The amplification was carried out using two primer-pairs, I-179L and I-179R. The PCR product of 540 bp representing the partial coding sequences of the genes phaC1 and C2 was obtained. The same has evidenced for the presence of PHA biosynthesis genes in the concerned two bacterial strains.

References

1. Berlanga, M., et al. Rapid spectrofluorometric screening of poly-hydroxyalkanoate-producing bacteria from microbial mats, *Int Microbiol.* **9**, 95--102, 2006.
2. Ashby, R.D., et al. Poly (ethylene glycol)-mediated molar mass control of short-chain- and medium-chain-length poly (hydroxyalkanoates) from *Pseudomonas oleovorans, Appl. Microbiol. Biotechnol.***60**, 154--159, 2002.

DECLARATION BY THE CANDIDATE

The thesis entitled "**BIOCHEMICAL AND MOLECULAR GENETIC ASSESSMENT OF BACTERIAL BIOPOLYMER**" is being submitted to the Tezpur University in partial fulfillment for the award of the degree of Doctor of Philosophy in Molecular biology & Biotechnology is a record of bonafide research work accomplished by me under the supervision of Prof. B. K. Konwar.

All helps received from various sources have been duly acknowledged.

No part of this thesis has been submitted elsewhere for award of any other degree.

Pinkee Phukon.

Date: 28.06.2013

Place: Tezpur

Pinkee Phukon
Dept. of Mol Biol & Biotechnology
Tezpur University

TEZPUR UNIVERSITY
SCHOOL OF SCIENCE
DEPARTMENT OF MOLECULAR BIOLOGY & BIOTECHNOLOGY
NAPAAM, TEZPUR-784028, ASSAM, INDIA

B. K. Konwar, Ph. D (London), DIC (Imperial)
Professor
Presently Vice Chancellor
Nagaland University (Central)

Ph (O): 03712-275402
Fax: 03712-267005/6
Email: bkkon@tezu.ernet.in
vicechancellornu@yahoo.co.in

CERTIFICATE OF THE PRINCIPAL SUPERVISOR

This is to certify that the thesis entitled **"BIOCHEMICAL AND MOLECULAR GENETIC ASSESSMENT OF BACTERIAL BIOPOLYMER"** submitted to the School of Science, Tezpur University in partial fulfillment for the award of the degree of Doctor of Philosophy in Molecular biology & Biotechnology is a record of research work carried out by Ms. Pinkee Phukon under my supervision and guidance.

All help received by her from various sources have been duly acknowledged.

No part of this thesis has been submitted elsewhere for award of any other degree.

Date: 28.06.2013
Place: Tezpur

B. K. Konwar
Signature of the Principal Supervisor

TEZPUR UNIVERSITY
SCHOOL OF SCIENCE
DEPARTMENT OF MOLECULAR BIOLOGY & BIOTECHNOLOGY
NAPAAM, TEZPUR-784028, ASSAM, INDIA

CERTIFICATE BY THE EXTERNAL EXAMINER AND ODEC

This is to certify that the thesis entitled **"BIOCHEMICAL AND MOLECULAR GENETIC ASSESSMENT OF BACTERIAL BIOPOLYMER"** submitted by Ms. Pinkee Phukon to Tezpur University in the Department of Molecular biology & Biotechnology under the school of Science in partial fulfillment of the requirement for the award of the degree of Doctor of Philosophy in Molecular biology & Biotechnology has been examined by us on 25/11/13 and found to be satisfactory.

The committee recommends for the award of the degree of Doctor of Philosophy.

Signature of:

Principal Supervisor
Date: 25/11/13

External Examiner
Date: 25/11/13

Acknowledgement

First of all, I express my utmost gratefulness and allegiance to the Almighty for bestowing upon me his generous blessings and benediction and for giving me the strength, perseverance and endurance to complete my work successfully.

I convey my heartfelt gratitude to my supervisor Prof. B. K. Konwar, (presently, Vice Chancellor, Nagaland University) for his valuable suggestion, corrections, constructive criticism and extensive discussions on the subject right from the beginning of research work to the completion of the thesis, which has enabled me to complete this thesis.

I convey my sincere thanks to Prof. S. K. Dolui and Prof. A. K. Mukherjee; members of my doctoral committee for their useful suggestions and informative discussions.

My sincere gratitude goes to Prof. A. K. Buragohain, Prof. S. Baruah (HOD), Dr. S.K. Rai, Dr. M. Mandal, Dr. A. Ramteke, Dr T. Medhi, Dr. R. Dole, Dr. E. Kalita, Dr. S. P. G. Ponnam, Dr. R. Mukhopahyay, Dr. S. Saha, Dr. A. N. Jha, Dr. N. D. Namsa and Dr. L. Bora of our department for their help and support.

I am thankful to Dr Kalyan Hazarika, Dr Naba Bordoloi, Pronobda, Dipakda and Samar da of the department for their help and encouragements.

I would like to acknowledge the sophisticated instrument facilities and infrastructure received from the Dept. of Chemical Sciences and other Departments of Tezpur University.

My sincere thanks go to Dr. Raju Khan and Dr. Keisham Radhapyari, CSIR-NEIST, Jorhat for giving me the opportunity to carry out the biosensor application work in their laboratory.

I am truly thankful to my lab mates Dr. J. P. Saikia, Pranjal, Mayur, Anggana, Krishna, Kalpana, Yasir and Salam Pradeep for their assistance and

encouragement to carry out the research work and making the stay in the lab very enjoyable and comfortable.

I would also like to thank my seniors and friends during my stay at Tezpur University, Muhsina ba, Nabanita ba, Barnali, Nimisha, Shreemaye, Furzee, Trisha, Monalisha, Chandramika, Rekha, Sweety, Binod da, Bikash, Dhruba, and all the Ph. D colleagues of Mol Biol &Biotech department for their support and cooperation.

Words are insufficient to thank Rajib and Dhaneswar for their help, support, co operation and encouragement that have helped me in carrying out the work.

I would like to express my respect and gratitude to all my family members for their love, support, inspiration and constant encouragement throughout the Ph. D work.

I owe my special thanks to my husband Utpol for his generous help during the work and for bearing all the pains I put him throughout.

I take this opportunity to sincerely acknowledge INBIGS, ONGC, Jorhat, for providing me Senior Research Fellowship, which helped me to perform the ph. D work comfortably.

Finally, I would like to thank the authorities of Tezpur University for granting me the permission to do this research work.

In addition to this, I owe my sincere gratitude to each and every one who has knowingly and unknowingly helped me in the successful completion of the Ph. D work.

Pinkee phukon

Contents

List of Tables

Search Tool (BLAST) from National Centre for Biotechnology Information (NCBI). The 16S-rDNA sequences from microbes showing upto 99% identity are shown.

List of Figures

Abbreviations used in the thesis

PHA	Polyhydroxyalkanoate
PHB	Polyhydroxybutyrate
Scl-PHA	Short chain length Polyhydroxyalkanoate
mcl-PHA	Medium chain length Polyhydroxyalkanoate
UV	Ultra violet
FTIR	Fourier transform infrared
GCMS	Gas chromatography and Mass spectrometry
NMR	Nuclear magnetic resonance
DSC	Differential scanning calorimetry
TGA	Thermo gravimetric analyser
XRD	X ray diffraction spectrophotometer
PL	Photoluminescence spectrophotometer
GPC	Gel permeation chromatography
SEM	Scanning electron microscopy
TEM	Transmission electron microscopy
CV	Cyclic voltammetry
EIS	Electrochemical impedance spectroscopy
PCR	Polymerase chain reaction
gL^{-1}	Gram per liter
$^{\circ}C$	Degree celcius
mL	Mili liter
w/v	Weight by volume
w/w	Weight by weight
v/v	Volume by volume
$mL.min^{-1}$	Mili liter per minute
θ	Theta
λ	Wave lenght
Tg	glass transition temperature
Tm	Melting temperature
Da	Dalton
EDTA	Ethidium bromide tetra acetate

CHAPTER 1

INTRODUCTION

1.1 General

The introduction of synthetic polymer materials has turned out to be a vital part of our contemporary life due to their various attractive properties which has molded society in many ways that make life both easier and safer. In the present world, the most hunted synthetic polymers are petroleum derived synthetic plastics. The plastic materials are composed of different synthetic or semi synthetic products and can be manipulated chemically to have better strength and shapes as per our interest. The vast majority of these polymers are based on chains of carbon atoms alone or with oxygen, sulfur, or nitrogen as well. The backbone of plastic polymers is the part of the chain on the main "path" linking a large number of repeating units together. They have high molecular weight ranging from 501,000 kDa. The fine tuning of the repeating unit's molecular structure of plastics has allowed them to become an indispensable part of the twenty-first century. They have many desirable properties such as high chemical resistance, variable elasticity, malleability and non-toxicity, and hence find applications in many durables, disposable goods and packaging materials in our day to day life. But the synthetic materials also leave harmful imprints on the environment. The main cause of inconvenience of plastics towards the environment is their disposal as they are recalcitrant to microbial degradation. Evidence is mounting that the chemical building blocks that make plastics so versatile are the same components that might harm people and the environment. As a consequence of durability of plastics and their disposable usage, plastic wastes contribute to an array of environmental problems like:

- Chemicals added to plastics are absorbed by human bodies and some of these compounds affect normal hormonal behavior or effect potential human health.
- Chemicals used in plastic production are shown to leach from landfill and contaminate aquatic habitats and are often ingested by marine animals, injuring and poisoning the aquatic life.
- Plastic buried deep in landfills can leach harmful chemicals that spread into groundwater, and those floating on the field or water impart unaesthetic look to cities, beaches and land fields.

In recent years, there has been increasing public concern over the harmful effects of petrochemical-derived plastic materials to the environment. This has prompted many countries to start developing biodegradable plastic retaining the same physical and chemical properties of conventional synthetic plastics. According to an estimate, around 8 per cent of world's oil production is used to make plastics and the production of plastic has crossed 300 million tonnes per annum by 2010. This problem is compounded with the fact that the resources for crude oil is also decreasing.

Existing methods to degrade plastics are inefficient. Incineration is an alternate option in dealing with non-degradable plastics, but in addition to its high cost, harmful chemicals like hydrogen chloride and hydrogen cyanide are emitted during incineration[1]. Therefore, in response to these problems, the idea of substituting non-degradable synthetic plastics with greener ecofriendly biodegradable plastics has drawn interest from both academic and commercial world. This alternative has come in the form of biodegradable plastic materials. While it retains the desired physical and chemical properties of the conventional synthetic plastics, it is recyclable and can be produced from renewable resources.

1.2 Biopolymer

Biopolymers are diverse and versatile class of materials that have potential applications in virtually all sectors of the economy. Biopolymers are natural biodegradable polymers that are synthesized and catabolized by various live agents like microorganisms, plants and animals[2, 3, 4, 5, 6] and they do not cause toxic effect in the host and have certain advantages over petroleum-derived plastics[7, 8, 9, 10, 11, 12, 13, 14]. Various types of naturally occurring biopolymers defined on the basis of the chemical structure of their monomeric units tend to indicate the function of these polymers in living organisms. Some such biopolymers are nucleic acids, proteins, polysaccharides, polyphosphates, polyphenols, polysulfates and polyesters. Biopolymers are prone to enzymatic degradation as they are the products of enzymatic polymerization in their synthesis.

1.3 Classification of biopolymers

Depending on the evolution of the synthesis process, various classifications of the different biodegradable polymers have been proposed. Based on their origin and production, biopolymers can basically be divided as follows:

Category 1: Polymers from biomass such as agro-polymers from agro-resources (starch, cellulose) are biodegradable.

Category 2: Polymers obtained by microbial production or genetically modified bacteria, the polyhydroxyalkanoates.

Category 3: Polymers conventionally and chemically synthesized using renewable biobased monomers obtained from agro-resources, the poly (lactic acid), a biopolyester polymerized from lactic acid monomers, and are biodegradable.

Category 4: Polymers whose monomers are obtained conventionally by chemical synthesis that are specifically petroleum based. They can also be used for making biodegradable polymers such as aliphatic aromatic copolyesters. Though these polymers are manufactured from synthetic components, they are completely compostable and bio-degradable.

1.3.1 Category1: Polymers from biomass such as agro-polymers from agro resources

The biopolymers of category 1 are the most common in the environment and are extracted from marine and agricultural animals and plants. Some examples of these polymers are as follows:

Starch

Starch is the storage polysaccharide of cereals, tubers and legume plants and widely available agro-resources suitable for a variety of industrial uses. It is composed of large number of glucose molecules joined by glycosidic bonds. It is

economically competitive with petroleum and has been used in several methods for preparing compostable plastics.

Cellulose

Cellulose is one of the most abundant constituents of biological matter and principal component of plant cell walls. It is a linear polymer of anhydroglucose. Its regular structure and tendency to form hydrogen bonded crystalline microfibrils and fibers make it the main context of packaging material.

Chitosan

Chitosan is a natural biodegradable polysaccharide found as an exoskeleton of crustaceans and cell walls of certain fungi. Chemically it is a linear polysaccharide of randomly distributed β-(1-4)-linked D-glucosamine (deacetylated unit) and N-acetyl-D-glucosamine (acetylated unit). Chitosan has a number of uses in commercial and biomedical field. Its antimicrobial property makes it a good packaging material; it is further used as a natural seed treatment and plant growth enhancer and also as an eco-friendly biopesticide substance.

Proteins: casein, keratin, collagen, gluten, soy

Casein, keratin and collagen are natural animal derived proteins. Gluten and soy proteins are found in plants like wheat, corn and leguminous plants. They are insoluble in water and difficult to process due to their complex structure.

Lignin

Lignin is a complex hydrophobic aromatic compound most commonly derived from wood and an integral part of the secondary cell walls of plants[15]. It is one of the most abundant organic polymers on earth after cellulose. Lignin is unusual because of its heterogeneity and lack of a defined primary structure. It is covalently linked to hemicellulose and, therefore, crosslinks different plant polysaccharides conferring mechanical strength to the cell wall and by extension the plant as a whole. Lignin plays a crucial part in conducting water in plant stem. It is

one of the most slowly decomposing components of dead vegetation, contributing a major fraction of the material that becomes humus as it decomposes.

Hyaluronic acid

Hyaluronic acid is a type of carbohydrate; more specifically a mucopolysaccharide naturally found in all vertebrate tissues and also occurs as an extracellular polysaccharide in a variety of bacteria. It plays an important physiological role in organisms at it provides a protective matrix for reproductive cells, serves as a regulator in the lymphatic system, and acts as a lubricating fluid in joints. This characteristic makes it most beneficial substance in the fields of orthopedics and eye surgery.

1.3.2 Category 2: Polymers obtained by microbial production or genetically modified bacteria

Polyhydroxyalkanoates

In recent years, considerable attention has been paid to microbial biopolymers. Polyhydroxyalkanoates (PHAs) belong to the family of microbial polyesters that accumulate as storage material in microbial cells under the stress conditions[16, 17, 18, 19, 20]. They are aliphatic polyesters of various hydroxyalkanoates synthesized by microorganisms as storage carbon and energy compounds and reported to be stored in inclusion bodies within the cytoplasm of the microbial cells[21, 22], usually when an essential nutrient such as nitrogen or phosphorus is limited in the presence of excess carbon source[23, 24, 25]. PHAs extracted from the bacterial cells are considered to be strong biodegradable materials having properties similar to various synthetic thermoplastics and elastomers, from polypropylene to synthetic rubber[26].

Beijerinck first observed lucent granules of PHA in bacterial cells in 1888[27]. The composition of PHAs was first described by Lemoigne as constituent of the bacterium *Bacillus megaterium* as an unknown material in the form of a homopolyester of 3-hydroxybutyric acid, called polyhydroxybutyrate (PHB)[28] which is a prototype of PHA family. More than 100 PHA monomers with different

attributes and structures have been reported[29]. Polymers of the PHA family are constantly increasing in number due to the continuous discovery of new homopolymers and copolymers which ultimately results in the availability of PHAs with a wide range of chemical structures and an assortment of properties[21, 30, 29, 31]. Many microorganisms have the ability to degrade these biopolymers by intracellular depolymerases[32] and upon disposal, are converted to water and carbon dioxide under aerobic conditions and to methane under anaerobic conditions.

Xanthan

Xanthan gum is a complex microbial polysaccharide derived from the bacterial coat of *Xanthomonas campestris* and is produced by the fermentation of glucose, sucrose or lactose. The remarkable properties of xanthan gum make it an attractive polymer for different industrial and biological purposes.

Pullulan

Pullulan is a linear polysaccharide extracellularly produced by several species of yeast specifically by *Aureobasidium pullulans*. Its long chain consists of maltotriose units connected with each other by glycosidic bond. It has many uses as an industrial plastic, in food industry.

Bacterial cellulose

Bacterial cellulose is a straight chain polymers consisting of glucose units held together by beta-linkages. Many microorganisms like fungi, bacteria (mainly of the genera *Acetobacter, Sarcina ventriculi and Agrobacterium*) and algae contain cellulose. Its chemical and physical nature also correlates with the cellulose found in plants[33]. In natural habitats, the majority of bacteria synthesize cellulose outside their cell to form protective envelopes around the cells. Nowadays bacterial cellulose is widely used for a variety of commercial applications with modifications in their synthesis.

1.3.3 Category 3: Polymers conventionally and chemically synthesized using renewable biobased monomers obtained from agro-resources

Polylactic acid (PLA)

Polylactic acid (PLA) is a biodegradable thermoplastic aliphatic polyester derived from the fermentation of carbohydrate feedstock such as maize, wheat and agricultural waste products like whey, molasses, green juice etc. Bacterial fermentation of sugars is used for the production of lactic acid monomer which is ultimately oligomerized and catalytically dimerized to form lactic acid polymer[34]. PLA is currently used in a number of biomedical applications, and has agricultural and manufacturing uses as well.

1.3.4 Category 4: Polymers whose monomers are obtained conventionally by chemical synthesis process that are specifically petroleum based

Polyglycolic acid (PGA)

Polyglycolic acid (PGA) is a simplest linear, aliphatic, thermoplastic, biodegradable polymer. It can be prepared by polycondensation or ring opening polymerization of glycolic acid monomer molecule. Though PGA is considered as a tough fiber-forming polymer, but due to its hydrolytic instability owing to the presence of the ester linkage in its backbone, it has very limited use. Now a days polyglycolide and its copolymers [poly(lactic-co-glycolic acid) with lactic acid, poly(glycolide-co-caprolactone) with ε-caprolactone, and poly (glycolide-co-trimethylene carbonate) with trimethylene carbonate] are extensively used as a material for the synthesis of absorbable sutures and are being evaluated in the biomedical field. Their degradation processes are erosive and easily hydrolyzed in aqueous environment. After hydrolysis PGA is converted into some nontoxic product which is again metabolized into water and carbon dioxide and excreted through urine.

Polycaprolactone

Polycaprolactone (PCL) is a biodegradable thermoplastic polyester obtained by chemical synthesis from crude oil with a low melting point of around 60 °C. PCL is prepared by ring opening polymerization of ε-caprolactone using a catalyst such as stannous octoate[35]. Since this polymer is compatible in nature, therefore it can be mixed with other materials to improve its processing characteristic, quality and biodegradability. In suitable physiological conditions, PCL is easily degraded by hydrolysis of its ester linkages. Due to its lower melting temperature, high biodegradability and good biocompatibility, PCL has been widely used in different biomedical fields eg. tissue engineering, drug delivery systems etc. In particular, it is especially interesting for the preparation of long term implantable devices owing to its degradation which is even slower than that of polylactide.

Polyvinyl alcohol (PVA)

Polyvinyl alcohol (PVA) is a water-soluble synthetic polymer prepared by hydrolyzing polyvinyl acetate in ethanol with potassium hydroxide in a continuous process. It is an odorless, tasteless, translucent, white or cream colored granular powder. Depending on the degree of polymerization and the degree of hydrolysis, PVA can be used for different functional purposes. It is emulsifying, adhesive and has high tensile strength, flexibility, high oxygen and aroma barrier properties. It is fully degradable and dissolves quickly. Since PVA can undergo pyrolysis at high temperatures therefore, it decomposes rapidly above 200 °C.

1.4 Polyhydroxyalkanoates

Polyhydroxyalkanoates (PHAs) are the most versatile group of naturally occurring biodegradable and biocompatible polymers that belong to the aliphatic polyester family as shown in Fig. 1.1[36]. In the cytoplasm of bacteria, PHAs accumulate as water insoluble inclusions for storage compounds of carbon and energy during imbalanced growth[37] (by various microorganisms, i.e., in the presence of an excess of a carbon source and nutrient limiting conditions e.g., nitrogen, phosphorus). Certain bacteria, however, produce them without being subjected to any kind of nutritional constraints, e.g. *Alcaligenes latus*[23]. PHAs can contribute up

to 90% (w/w) of the cell dry weight matter of cells or even more. The number per cell and size of inclusion bodies of PHA varies among different species[23, 36].

The resulting granules are coated with a layer of phospholipids and proteins. The granule-associated proteins play a major role in the synthesis and degradation of PHAs and in the formation of PHA granules.

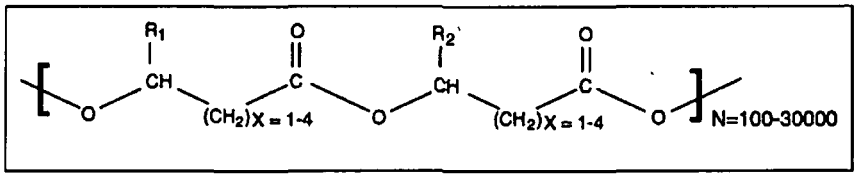

Fig. 1.1 General structure of polyhydroxyalkanoate. R_1 and R_2 are alkyl groups (C_1–C_{13})[36]

More than 100 different types of monomer units with different structures have been identified as constituents of the PHA (Fig.1.1). By changing the growth conditions and carbon source used, the monomer composition of PHA can be manipulated and thereby varying their structures[38, 39, 40]. This creates a possibility for producing different types of biodegradable polymers with an extensive range of properties. Members of the PHA family can exist as homopolymers of hydroxyalkanoic acids, as well as copolymers of two or more hydroxyalkanoic acids. These polymers are formed by bonding of the carboxyl group of one monomer with the hydroxyl group of the neighbouring monomer through an ester linkage[37]. PHAs are synthesized by numerous gram positive bacteria; aerobic (cyanobacteria) and anaerobic (non-sulfur and sulfur purple bacteria) photosynthetic bacteria, gram negative bacteria as well as some archaebacteria through the fermentation of carbon compounds[23, 17]. The molecular mass of PHA is in the range of 50–1,000 kDa and varies with the PHA producer. Owing to the stereo specificity of biosynthetic enzymes present inside the bacterial cell the monomer units of the PHA polymers are all in D-configuration type[41, 42]. Low solubility, high molecular weight and specifically water insoluble property of PHAs make them an ideal

carbon-energy storage material which exerts negligible osmotic pressure on the bacterial cell[17, 43].

The members of the PHA family have polymer characteristics that are similar to conventional plastics such as polypropylene[37]. Other biodegradable polymers such as chemically synthesized plastics (e.g. Polyglycolic acid and polylactic acid) and starch-based plastics (e.g. starch-polyethylene) have also prospects but they lack variability in structure and extensive material properties. As PHAs are biodegradable and immunologically inert, they have promising future applications particularly in medical related fields.

The use of PHA in wide range of applications has been hampered mainly due to their high cost of production as compared to petrochemical-based polymers[44, 45]. Exploring its production from locally available and renewable carbon sources such as agro-horticultural wastes like corn, cassava etc. would be of economic interest. With the aim of commercializing PHA, a great deal of effort has been devoted to reduce the production cost by the development of superior bacterial strains most likely recombinant microbial strains and more efficient fermentation and recovery processes[46, 47, 48]. Analysis of the entire process for the production and recovery of PHA will allow to design the most efficient method of PHA production and to evaluate the approximate price of PHA produced on a commercial scale. Additionally, further research is required to enhance the physical properties of PHAs[49].

Industrial producers are currently working towards decreasing the cost price of these biopolymers by increasing the volumetric production capacity of fermentor systems and improving process technology, especially the downstream processing. The utilization of open mixed microbial cultures facilitates the use of mixed substrates since the microbial population can adapt continuously to changes in substrate. Also the need for sterilization and sterile fermentation systems is prevented.

1.5 Occurrence of PHA

The first discovery of PHA was monitored by a French scientist Maurice Lemoigne[28] in *Bacillus megaterium* in 1926 and the PHA discovered was the short

chain length PHA, poly (3-hydroxybutyrate), P (3HB), which is one of the most well studied PHAs. Several bacteria synthesize and accumulate PHA as a sink for carbon and energy storage materials for redundant reducing power under the condition of limiting nutrients in the presence of excess carbon source[24, 50, 51, 52]. Prokaryotic organisms are known to produce Polyhydroxybutyrate amounting to as much as 80% of their cellular dry weight. In 1983, medium chain length mcl-PHA was discovered when *Pseudomonas oleovorans* was grown in octane[53]. So far, more than 90 different genera of archae and eubacteria have been reported to accumulate PHAs[9]. A wide variety of PHA copolymers have been isolated from bacteria and many cyanobacteria found in different environmental samples including marine sediments[54].

Bacteria were mainly divided into two major groups for the production of PHAs based on the culture conditions required for PHA synthesis[55]. First group of bacteria can synthesize PHA with the limitation of an essential nutrient such as nitrogen, phosphorus, magnesium, or sulphur and with an excess source of carbon after the growth phase. The bacteria included in this group are *Ralstonia eutropha*, *Protomonas extorquens*, and *Pseudomonas oleovorans*. The second group of bacteria can synthesize PHA during growth phase and does not require nutrient limitation. Some of the bacteria belonging to this group include *Alcaligenes latus*, a mutant strain of *Azotobacter vinelandii* and recombinant *Escherichia coli*. These characteristics are regarded as important while production of PHA. The molecular structure of the PHA depends directly on the used organism, culture conditions and carbon substrate used for the organism's growth[23].

Many workers have reported new PHA synthesizing bacteria like *Axobacter, Azospirillum, Beggiatoa, Beijerinckia, Caulobacter, Clostridium, Halobacterium, Leptothrix, Methylocystis, Rhizobium, Rhodospirillum, Thiocaspa, Cyanobacteria, Paracoccus denitrificans, Pseudomonas stutzeri, P. aeruginosa*, recombinant *Bacillus subtilis, Delftia acidovorans, Azotobacter chroococcum, Azobacter vinelandii, Comamonas sp, Streptomyces aureofaciens* and *Aeromonas hydrophila.*

However, for the industrial production of PHA, recombinant *E. coli* with all functional genes have been introduced. These bacteria can use a wider range of cheap carbon sources, and also it is relatively easier to extract and purify the

polymer from these bacteria. Many new recombinant organisms like different microbes, yeasts and plants have been introduced for PHA synthesis from cheap carbon sources like molasses, sucrose, lactose, glycerol, oils and methane.

Now-a-days mixed culture can also be used to synthesize PHA. The mixed cultures are usually used in waste water treatment. Activated sludge, a well-known mixed culture, is able to store PHA as carbon and energy storage material under unsteady conditions.

1.6 Substrates used for PHA production

Since PHAs are considered as an environmentally benign substitute for the petroleum-derived polymer material, several factors need to be critically investigated for the production of PHAs at the industrial scale. However, the major problem behind its commercial production and application is the high cost of bacterial fermentation which makes bacterial PHA production 5-10 times more expensive than the petroleum-derived polymers such as polyethylene and polypropylene. The ability of the bacteria to utilize cheap carbon sources is very important because the significant factor for the production cost of PHA is the cost of carbon substrates[56]. Therefore, PHA production is mainly focused on the renewable resources where bacteria can utilize waste generated from food, agricultural and industrial procedures and fatty acids as carbon sources.

Research works have been carried out to develop recombinant bacterial strains having the ability to use cheap carbon sources, while corresponding fermentation strategies have been developed and optimized to improve productivity. Some workers have tried alternative carbon sources to make PHAs production more economical. Crude carbon substrates such as corn oil[57], palm oil[58,59], plant oil[60, 61, 62, 63], molasses[64, 65, 66], starch[67, 68], whey[69], and industrial wastes[70, 71, 72, 73] are excellent substrates for the growth and polymer production and are used by different bacteria. Utilization of these plant derivatives are actually an indirect way of using atmospheric carbon dioxide as the carbon source for PHAs production[74]. However, the polymer concentration and content obtained were considerably lower than those obtained using purified carbon substrates. Therefore, there is a need for development

of more efficient fermentation strategies for production of these polymers from a cheap carbon source.

Compared to other processes, the use of mixed cultures has gained much attention as the most effective, cheaper and potential means of producing PHAs[75]. In most cases of mixed cultures, the organic acids contained in wastewater or transformed from other industrial wastes were used as carbon source for production of PHAs. Consequently, mixed culture procedures do not only help to solve the environmental pollution problem caused by organic wastes but also help them to convert into useful materials which are important for sustainable development and environmental protection.

1.7 Structure and classification of PHA

1.7.1 Structure of PHA Granules

The structure of PHA granules has not been fully determined but the major constituents with small amounts of proteins and lipids are known. PHA synthesis occurs intracellularly in multiple cytoplasmic inclusion bodies that are generally 200-500 nm in size and surrounded by a membrane to which proteins are bound[23]. The hydrophobic polyester core is largely amorphous. The initial investigations on PHA granules from bacteria were performed by Williamson and Wilkinson[21] and also by Griebel *et al.*[76] PHA granules may be surrounded by a phospholipid monolayer that contains specific granule associated proteins (Fig. 1.2) such as (i) PHA synthase (PhaC) (ii) PHA depolymerases and 3HB-oligomer hydroxylase (PhaZi) (iii) phasins (PhaPs), which are thought to be the major structural proteins of the membrane surrounding the PHA-containing inclusion bodies and (iv) the regulator of phasin expresssion (PhaR) and also cytosolic proteins that may be non-specifically attached to the granules via hydrophobic interactions.

The polyester core is known to be surrounded by a 4 nm boundary layer, which most likely comprises of a phospholipid monolayer[77] with embedded and attached proteins. Recently atomic force microscopy (AFM) studies on PHB granules in *Comamonas acidovoran*[78] and *R. eutropha*[79] provided further evidence for the existence of an envelope surrounding the PHB granules. PHB inclusions from sonicated cells of *R. eutropha* revealed on one hand, a rough and ovoid, and on

the other hand, a smooth and spherical surface structure and shape. Furthermore, splits and fissures are identified at the surface of rough PHB granules. Measurements of the splits indicated a thickness of the boundary layer of 4 nm. With electron microscopy, Lundgren *et al.*[80] showed that the surface of PHA granules from *B. megaterium* and *B. cereus* is covered by a membrane with about 15–20 nm thickness. AFM analysis has shown that PHA granules have an additional network layer with globular areas with 35 nm in diameter most likely also incorporating structural phasin proteins. This was also used to show porin-like structures in the surrounding membrane which have been suggested to provide a portal to the amorphous polymer core and be the site of PHA metabolism and depolymerisation. When the layer is damaged during the isolation of the granules the crystallinity increases by 50–60%. Two physical states of the polyester occur in PHB granules: intracellular native amorphous granules and partially crystalline granules[81].

(i) PHA Synthase (PhaC)

In *Ralstonia eutropha,* PhaC is a soluble protein in the cytoplasm, which becomes insoluble with granule binding following the onset of PHA accumulation under the cultivation conditions permissive for PHA accumulation. This is due to the PHA chain which remains covalently linked to the enzyme until synthesis of the polymer has finished[82, 83]. However, PHA synthase becomes PHB-granule-bound during PHB biosynthesis only when the growing hydrophobic polyester molecules are covalently linked to the enzymes during polymerization; conferring amphiphilicity to the enzyme-polyester complex. According to the substrate specificities and sequence homologies, four different classes of PHA synthases were distinguished:

(a) Class I PHA synthases synthesize PHAs of hydroxyalkanoates of short-chain-length (PHA-scl).

(b) Class II PHA synthases prefer coenzyme A thioesters of hydroxyalkanoates of medium-chain-length (PHA-mcl) comprising 6-14 carbon atoms as substrates and occur in strains belonging to the genus *Pseudomonas* of the rRNA homology

group- I. However, in contrast to class I and class II PHA synthases, these enzymes are composed of two different subunits designated as PhaE and PhaC.

(c) The class III synthase investigated in detail is the enzyme of *A. vinosum*. Class III PHA synthases exhibit also substrate specificities with PHA-scl.

(d) Class IV PHA synthases are also composed of two different types of subunits and occur in species belonging to the genus *Bacillus*[84]. Although the PhaC protein of class IV PHA synthases revealed high homologies to PhaC of class III PHA synthases, an activator, PhaR, is required for PHA synthase activity.

The class I and class III PHA synthases of α-proteobacterium *R. eutropha* and ç-proteobacterium *A. vinosum*, respectively, are regarded as model enzymes for studying PHA-scl biosynthesis in bacteria, whereas the PHA-mcl synthases of *P. oleovorans* and *P. putida* represent the most detailed studied class II PHA synthases. PHA synthases are also responsible for the molecular weight of PHA synthesized. Metabolic factors for PHA synthesis are the intracellular concentration of the PHA synthases, the enzyme-to-substrate ratio, and probably also enzymes' capability to hydrolyze PHAs, such as intracellular PHA depolymerases or esterases and lipases[85, 86]. The absence of PHA depolymerases results in the formation of PHAs exhibiting a higher molecular mass as shown for recombinant strains of *E. coli* expressing the PHA operon from *R. eutropha*[87]. Also the level of PhaC expression has a significant influence on the molecular mass of the synthesized polyester. A higher concentration of active PHA synthase protein resulted in a lower molecular mass of the resulting PHA molecules[88, 89].

(ii) PHA depolymerase (PhaZi)

Several bacteria express extracellular depolymerases which are secreted into the environment to degrade PHA released from dead bacteria. The immature extracellular depolymerases (PhaZe) contain in general N-terminal signal peptides of 25-58 amino acids, a large catalytic domain at the N-terminal region, a substrate binding domain localized at the C-terminal region, and a linking domain connecting

the catalytic domain with the substrate-binding domain[90]. In contrast to the well-studied extracellular PHA depolymerases, intracellular PHA depolymerases (PhaZi) have been far less investigated although they play an important role for the overall PHA metabolism. In *B. megaterium, Zooglea ramigera, Sinorhizobium melioti*, and *R. eutropha,* PHA hydrolyzing activity has been demonstrated. Very recently four additional intracellular PHA depolymerases were identified in *R. eutropha* by York and co-workers (PhaZ2 and PhaZ3)[91], Schwartz *et al.* (PhaZ4)[92], and Potter *et al.* (PhaZ5)[93].

(iii) Phasins (PhaP1)

The structural protein phasins (PhaP1) represent a class of probable non-catalytic proteins consisting of a hydrophobic domain which associates with the surface of the PHB granules, and of a predominantly hydrophilic/amphiphilic domain exposed to the cytoplasm of the cell. PhaP1 adheres very tightly *in vivo* to native as well as *in vitro* to artificial PHB granules. PhaP1 is synthesized in large quantities under storage conditions and represents as much as 5% of the total protein[94]. By this, PhaP1 provides protection to the host cell by contributing to coverage of the hydrophobic surface of the polymer, preventing other proteins falsely binding to the hydrophobic granules[95]. In the PHA-Scl accumulating bacteria *Rhodococcus ruber*, the anchoring region was located at the carboxy terminus, and it was demonstrated that phasin molecules truncated at the carboxy-terminal region lost their capability to bind to PHA granules[96]. The addition of phasins accelerates the PHA synthesis rate and regulates the size of PHA inclusions. Over expression of PhaP, on the other hand, results in the formation of many small granules in the cell. The addition of PhaP isolated from *R. eutropha* increased the activity of class II PHA synthase from *P. aeruginosa* by approximately 50%. Reverse transcription and polymerase chain reaction (RT-PCR) analysis clearly demonstrated that PhaP2, PhaP3, and PhaP4 were also transcribed under conditions permissive for PHB biosynthesis and accumulation[93].

(iv) Transcriptional Repressor (PhaR)

Transcriptional repressor PhaR, the regulator of phasin expression was first detected in *R. eutropha.* PhaR is proposed to be a repressor protein of transcription that binds to the PhaP1 upstream region in *R. eutropha*, thereby repressing expression of PhaP1. Derepression of PhaR requires biosynthesis and accumulation of PHB. PhaR has the capability to bind to at least three different targets in cells of *R. eutropha*: (i) the promoter region of PhaP1, (ii) the promoter region of PhaR, and (iii) the surface of PHB granules. PhaR can work on 5 different situations to regulate PhaP: A: if cells are cultivated under conditions not permissive to PHB biosynthesis, PhaR cannot bind to PHB granules because they do not exist in the cells. The cytoplasmic concentration of PhaR is sufficiently high to repress transcription of PhaP1and no PhaP1 protein is formed and detectable in the cytoplasm, B: If conditions permissive for PHB biosynthesis start with the constitutively expressed PHA synthase (PhaC) which starts to synthesize PHB molecules that remain covalently linked to the enzyme. At the beginning, small micelles are formed which gradually become larger and constitute the nascent PHB granules. PhaC no longer covers the PHB granule surface entirely, and proteins with a binding to the hydrophobic surface like PhaR to the granules. This lowers the cytoplasmic concentration of PhaR, C: From a certain point the cytoplasmic concentration of PhaR becomes so low that it can no longer repress transcription of PhaP1. Following synthesis it binds to the PHB granules. The concentration of soluble PhaP1 in the cytoplasm remains beyond a detectable level, D: The PHB granules grow and reach their maximum size; PhaP protein is being continuously synthesized in sufficient amounts, E: When the PHB granules have reached the maximum possible size according to the physiological conditions, almost the entire surface will be covered by PhaP1 protein, and the latter is displacing PhaR protein from the PHB granules. Consequently, the cytoplasmic concentration of PhaR increases and it will exceed the threshold concentration required to repress again transcription of PhaP1. As a consequence, PhaP1 protein is no longer synthesized. This mode of regulation ensures that PhaP1 is not produced in higher amounts than required to cover the surface of PHB granules. In addition, the binding capacity of PhaR to the promoter

region of its own gene prevents over expression of this repressor protein that is, therefore, under auto-control.

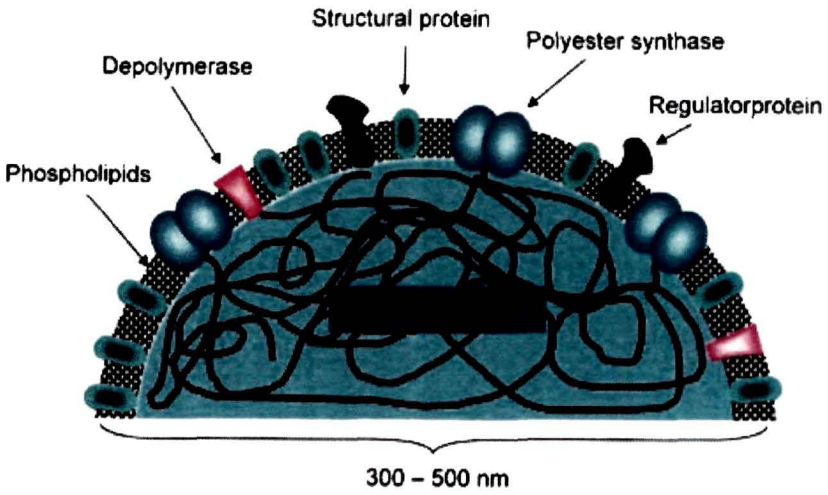

Fig. 1.2 Schematic presentation of a PHA granule with granule associated proteins according to Rehm[97] such as: Polyester synthase: PHA synthase (PhaC), Depolymerase: PHA depolymerase (PhaZi), Structural protein: Phasins (PhaP), Regulator protein: Transcriptional Repressor (PhaR) and Phospholipids: Embedded and attached with proteins

1.7.2 Classification of PHA

Depending on the substrate provided, many microorganisms can include a wide variety of 3-hydroxy fatty acids in the PHA. More than 100 different monomer units have been identified as constituents of PHA in >300 different microorganisms[98].

Depending on the number of carbon atoms in the monomeric unit, PHAs are classified into two different types.

i) Short chain length PHAs (scl-PHAs, 3-5 C-atoms)

ii) Medium chain length PHAs (mcl-PHA, 6 or more C-atoms)

Also, depending on the kind of monomer present, PHAs can be homopolymers containing only one type of hydroxyalkanoate as the monomer unit, e.g., P(3HB), P(3HHx) or heteropolymers containing more than one kind of hydroxyalkanoate as monomer units, e.g., poly(3-hydroxybutyrate-co-3-hydroxyvalerate), P(3HB-co-3HV), poly(3-hydroxyhexanoate-co-3-hydroxyoctanoate), P(3HHx-co-3HO) and poly-(3-hydroxybutyrate-co-3-hydroxyhexanoate), P(3HB-co-3HHx)[44, 99]. Due to the continuous discovery of new homopolymers and copolymers, the polymers of the PHA family are constantly increasing in number. Moreover saturated, unsaturated, halogenated, branched and aromatic side chains in (R)–3HA monomeric units have also been found in the sequence of microbial PHA[100, 101]. This is in turn resulting in the availability of PHAs with a wide range of chemical structures and an assortment of properties. The properties of PHAs vary significantly depending on their monomer content and consequently can be customized by controlling their compositions. The differences in their properties have also been shown to greatly affect the mode/rate of degradation in aqueous or biological media.

1.7.3 Metabolic pathway of PHA biosynthesis

Microorganisms are capable of producing intracellular PHA inclusions in their stationary growth phase under nutritional unbalanced growth conditions but with an excess of carbon source. Different types of enzymes are involved to run the metabolic process of the bacteria for the formation of inclusion bodies. Based on the types of monomers incorporated into PHA, various metabolic pathways have been shown to be involved in the PHA biosynthesis. The schematic illustration of the metabolic pathway of PHA biosynthesis is shown in Fig. 1.3 in broad-spectrum.

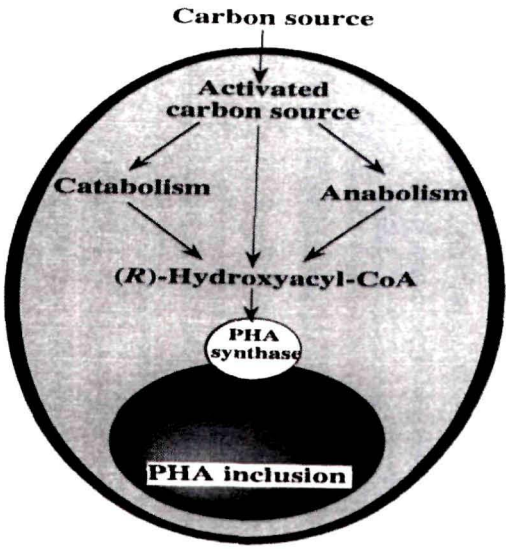

Fig. 1.3 General scheme for the metabolic pathways of PHA synthesis from different carbon sources within a bacterial cell according to Sudesh *et al.*[17]

1.7.4 Enzymes involved in the PHA biosynthesis

Depending on functions, there are three main enzymes involved in the PHA biosynthesis. The key enzyme in PHA biosynthesis is PHA synthase (PhaC) which mainly polymerize the monomeric groups of carbon source intake by the microorganisms. The second type of enzyme is β-ketothiolase (PhaA) which is involved in the intermediate metabolic pathway programme. The third type of enzyme is acetoacetyl CoA reductase (PhaB) which basically reflects the main role in oxidation-reduction reaction in PHA metabolism process. Moreover, the genes and enzymes involved in PHAs synthesis have evolved features according to different microbial groups.

1.7.4.1 PHA synthase (PhaC)

This enzyme is mainly associated with the polymerization reaction of hydroxyalkanoic acids as substrates. The substrate specificity of PHA synthases may determine the ability of microorganisms to synthesize a particular form of PHA.

PHA synthases may be divided into four classes based on their primary structure, the sub unit composition and the substrate specificity[97, 102] (Fig. 1.4).

(i) Class I PHA synthases consists of only one type of subunit (PhaC). Its molecular weight ranges between 61 and 73 kDa and catalyzes polymerization of 3-5 carbon atoms and mainly utilizes CoA thioesters of 3-HAs, 4-HAs, and 5-HAs[103].

(ii) Class II type of PHA synthases is encoded by two different genes, phaC1 and phaC2, 61 to 73 kDa in size. Each catalyses the polymerisation of CoA thioesters of various $3HA_{Mcl}$ comprising 6-14 carbon atoms[102]. The two phaC genes are separated by the phaZ gene encoding the PHA depolymerase.

(iii) Class III synthases are composed of two subunits (PhaC and PhaE) with molecular weights 40 kDa each and possess substrate specificities similar to class I type. These PHA synthases prefer coenzyme A thioester of $3HA_{Scl}$ with 6-8 carbon atoms[104].

(iv) Class IV synthases are composed of two subunits (PhaC and PhaR) that can utilize coenzyme A thioester of R-3-hydroxyfatty acids with 3-5 carbon atoms[105]. The molecular weights of the two subunits are 40 kDa and 22 kDa respectively.

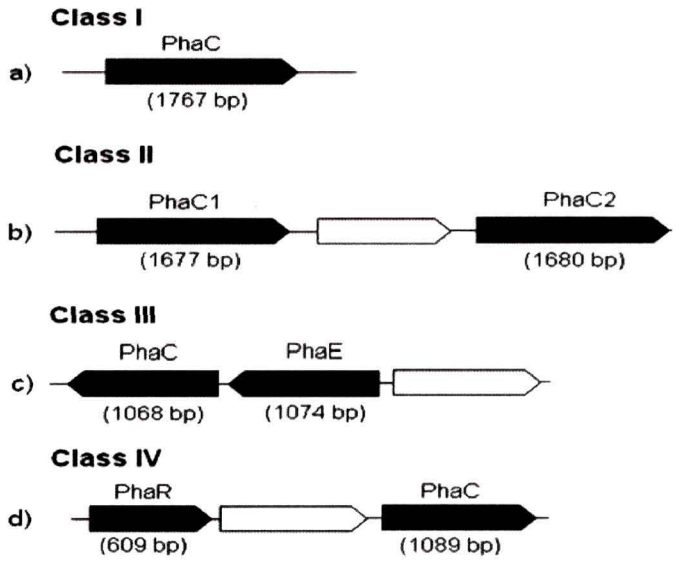

Fig. 1.4 Schematic representation of different classes of the PHA synthases according to Rehm[97]

1.7.4.2 β-ketothiolase (PhaA)

This enzyme is mainly responsible for the degradation of fatty acids by thiolytic cleavage in PHA biosynthetic process. Based on the substrate specificity, this enzyme is divided into two groups[37]. The first group of β-ketothiolase has broad substrate specificity with C_4-C_{16} and mainly involved in the degradation of fatty acids. The second group of β-ketothiolase has a narrow range of substrate specificity with C_3-C_5 and mainly responsible for the biosynthesis. Both the types of β-ketothiolase exist as homotetramer with molecular mass of 160-190 kDa.

1.7.4.3 Acetoacetyl CoA reductase (PhaB)

The acetoacetyl CoA reductase (PhaB) is NADH/NADPH dependent enzyme and catalyzes the second step in PHB biosynthetic pathway by converting the acetoacetyl CoA into 3-hydroxybutyryl CoA through oxidation-reduction process. These are basically of two types depending on their origin from different genera: (i) NADH dependent and (ii) NADPH dependent. PhaB is a homotetramer with molecular masses ranging from 85-140 kDa.

1.7.5 PHA biosynthesis pathway

Bacteria can undergo PHA biosynthesis through three different biosynthetic pathways. Depending on the precursor carbon source provided, three types of pathways are suggested which are summarized in a single schematic diagram (Fig. 1.5).

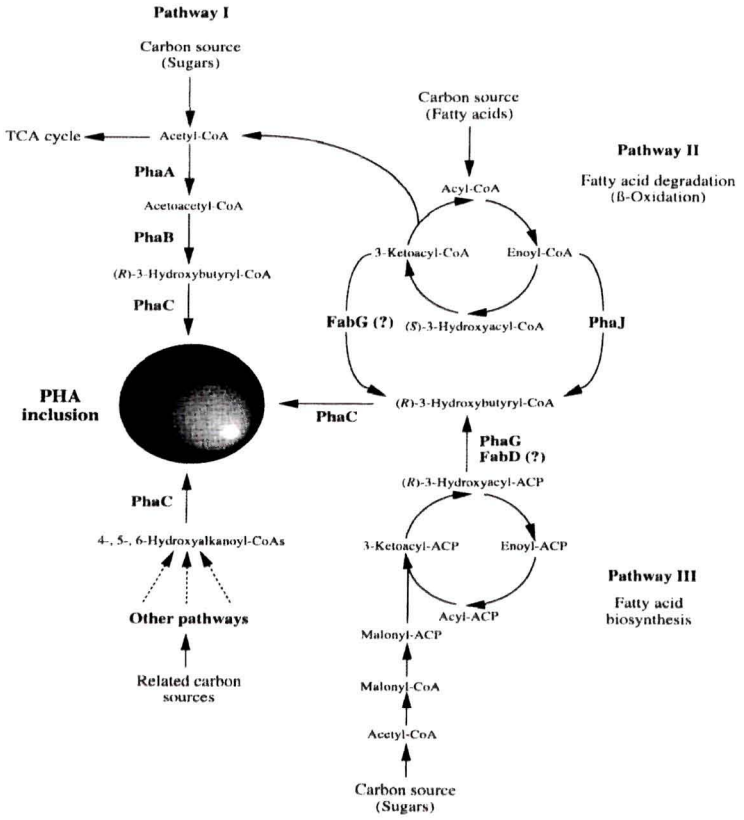

Fig. 1.5 Cyclic metabolic nature of P (3HB) biosynthesis and degradation in bacteria according to Sudesh *et al.*[17] PhaA, β-ketothiolase; PhaB, NADPH-dependent acetoacetyl-CoA reductase; PhaC, PHA synthase; PhaZ, PHA depolymerase;1, dimer hydrolase;2, (R)-3-hydroxybutyrate dehydrogenase;3, acetoacetyl-CoA synthetase;4, NADH-dependent acetoacetyl-CoA reductase

Pathway I

Pathway I is mainly related to the formation of scl-PHA molecules and the precursor molecule is acetyl CoA provided by glycolysis process within the bacterial cell. In the case of *R. eutropha* pathway I is generally observed. This pathway consists of 3 enzymatic reactions catalyzed by three different enzymes (Fig. 1.5, Pathway I). Two acetyl-CoA moieties are condensed to acetoacetyl-CoA by a β-ketothiolase (PhaA). The product then undergoes reduction by an NADPH-dependent reductase (PhaB) which produces (R)-isomer of 3-hydroxybutyryl-CoA[106]. On the other hand, in *Rhodospirillum rubrum* which shares almost similar PHA biosynthesis pathway as *R. eutropha*, the reductase which is an NADH-dependent isoenzyme gives rise to (S)-isomer of 3-hydroxybutyryl-CoA. Lastly, (R)-3-hydroxybutyryl-CoA monomers are polymerized by PHA synthase (PhaC) to P (3HB).

Pathway II

Another type of PHA biosynthesis pathway is mainly involved in the mcl-PHA synthesis through fatty acid β-oxidation pathway (Fig. 1.5). This pathway is exhibited by the *Pseudomonads* belonging to rRNA-homology-group I which derives the 3-hydroxyacyl-CoA substrates of C_6-C_{14} for mcl-PHA synthase to synthesize mcl-PHA from various alkanes, alkanols or alkanoates[39, 17]. Here, the fatty acids are first converted to the corresponding acyl-CoA thioesters which are then oxidized by fatty acid ß-oxidation via trans-2-enoyl-CoA and (S)-3-hydroxyacyl-CoA to form 3-ketoacyl-CoA. 3-ketoacyl-CoA is then cleaved by a ß-ketothiolase to form acetyl-CoA and an acyl-CoA comprising of two less carbon atoms as compared to the acyl-CoA that entered the first cycle. Specific enzymes such as the enoyl-CoA hydratase (PhaJ) and 3-ketoacyl-CoA reductase (FabG) are apparently involved in the conversion of fatty acid β-oxidation which intermediates into suitable monomers that can be polymerized by the PHA synthase to synthesis mcl-PHA. This pathway is mainly referred to as the *P. oleovorans* PHA biosynthetic pathway.

Pathway III

The third type of PHA biosynthesis pathway occurs in most *Pseudomonads* belonging to rRNA homology group I except *P. oleovorans* which can also synthesize mcl-PHA from structurally unrelated, simple and inexpensive carbon sources such as glucose, sucrose and fructose[106]. Therefore this pathway is also referred to as *P. aeruginosa* PHA biosynthetic pathway. In this case, 3-hydroxyacyl monomers are derived from the *de novo* fatty acid biosynthesis pathway. Since the fatty acid biosynthesis intermediate is in the form of (R)-3-hydroxyacyl-ACP, an additional biosynthetic step is needed to convert it into (R)-3-hydroxyacyl-CoA form. Therefore, an enzyme 3-hydroxyacyl-CoA-ACP transferase (PhaG) is involved in channeling the intermediates of the *de novo* fatty acid biosynthesis pathway to PHA biosynthesis[107].

1.8 Detection, extraction and characterization of PHAs

1.8.1 Detection method

Since PHAs are hydrophobic in nature, lipophilic dyes such as Sudan black B[108], Nile blue A[109] and Nile red[110] have been used to stain these granules for detection. Such staining methods provide for easier identification between PHA accumulating and non accumulating strains. The lipophilic dye Sudan black B is more soluble in lipid material and imparts a black blue colour to the PHA granule. Nile blue A, a water soluble basic oxazine dye has an advantage over that of Sudan black in that it does not stain other inclusion bodies such as glycogen and polyphosphate. Hence it has more specific affinity to stain only PHAs[109] and gives bright orange fluorescence at a wavelength of 460 nm. Nile red has been observed to produce a strong orange fluorescence (emission maximum, 598 nm) with an excitation wavelength of 543 nm (maximum) upon binding to P (3HB) granules in cells of *Cupriavidus necator*[111].

1.8.2 Extraction of PHAs

The recovery of PHA contributes significantly to the cost of production of the polymer. A variety of methods have been adopted for PHAs extraction from bacterial cells. For the extraction of PHA, the bacterial cell biomass is harvested

from their broth using conventional procedures such as centrifugation, filtration, or flocculation-centrifugation. The harvested cells are then lyophilized and then subjected to various extraction methods that employ solvent extraction or non PHA biomass digestion[112].

1.8.2.1 Solvent extraction

Solvent extraction methods proposed for PHAs recovery involve their extraction using chlorinated solvents such as methylene chloride, propylene carbonate, dichloroethane or chloroform. After extraction of the polymer, the dissolved polymer is filtered to remove cellular debris, concentrated and then precipitated by using chilled non solvents such as methanol or ethanol by vigorous shaking. However, this method has some drawbacks for the commercial purposes. Some of them require large volumes of solvents and are therefore commercially unattractive[113, 36], it creates hazards for the operators and for the environment and while extraction, destroys the natural morphology of PHA granules that is useful in certain applications such as the production of strong fibers[114]. On the contrary, solvent extraction has some advantages over some other recovery methods. They do not degrade the polymer and can be useful for some medical application by the elimination of endotoxin found in gram negative bacteria[115].

1.8.2.2 Digestion methods

1.8.2.2.1 Digestion by surfactants

Surfactants, such as anionic sodium dodecyl sulfate (SDS) disrupt cells by incorporating itself into the lipid bilayer membrane of the bacteria. Higher concentration of the surfactant breaks the cellular membrane to produce surfactant micelles and membrane phospholipids, which leads to the release of P (3HB). Surfactant solubilizes not only proteins but also other non-PHA cellular materials and thus surfactant alone cannot give a high purity PHA (>97%). Furthermore, higher dose of surfactant is not cost effective.

1.8.2.2.2 Digestion by sodium hypochlorite

Sodium hypochlorite digestion method is another recovery method for PHA extraction. Sodium hypochlorite breaks open the bacterial cells which solubilizes non PHA material and thus liberates the intracellular granules. However, sodium hypochlorite digestion causes severe degradation of the polymer, with up to 50% reduction in its molecular weight[116]. The combination of chloroform and sodium hypochlorite can significantly reduce the molecular weight of PHA. Here, the hypochlorite digests the cells releasing the PHA, which immediately dissolves in chloroform and thus gets protected from degradation[117]. But this also imparts environmental hazards and leads to a higher cost.

1.8.2.2.3 Enzymatic digestion

Different enzymes such as alcalase, neutrase, lecitase, and lysozyme are in use for the enzymatic digestion method which has to be followed by washing with an anionic surfactant like SDS to solubilize non P (3HB) cellular material. Solubilized and non-solubilized cell compounds are separated by centrifugation following which washing with anionic surfactant and flocculation is carried out. Enzymatic digestion is a good recovery process for PHA extraction but leads to high cost.

1.8.3 Quantification and compositional analysis of PHA

1.8.3.1 Quantification of PHA

Quantification of PHA is done by gravimetric measurement from lyophilized cell biomass. The freeze dried biomass is digested using sodium hypochlorite and the sediment material extracted by chloroform, followed by precipitation with diethyl ether, methanol or acetone. Law and slepecky[118] has developed another method for PHA quantification. In this method PHA is converted to crotonic acid by treating with concentrated sulphuric acid and the product is measured by taking optical density at 235 nm. However, this method of estimation is less accurate because chloroform solubilizes impurities of crude polymer which absorb the UV and retain the same even after the acetone and alcohol washing, which would interfere with the assay giving incorrect values of PHA concentration.

1.8.3.2 FTIR spectroscopy

FTIR spectroscopy has been in use to characterize the intracellular PHA molecules which gives insight into the chemical structure without prior hydrolysis of the polymer molecule. This method facilitates rapid identification of the polymer and requires very less amount (0.5-1.0 mg) of sample[119]. Rapid screening of scl and mcl-PHAs in lyophilized bacterial cells can be done by using FTIR. For scl-PHAs, the band at 1,185 cm^{-1} occurs due to C-O stretching and the band at 1,282 cm^{-1} corresponds to –CH group[119]. Similarly for mcl-PHAs, the characteristic peak of ester carbonyl band occurs at 1,742 cm^{-1} and the band at 1,165 cm^{-1} occurs due to C-O stretching[120].

1.8.3.3 Gas chromatography and mass spectroscopy (GCMS)

GCMS analysis has enabled quantitative information of PHA including the total amount, mass and concentration of monomers present in the polymer at very low concentrations of sample[121]. In this method, the lyophilized cells are subjected to direct acid or alkaline methanolysis, followed by gas chromatography (GC) of the methyl esters. This method is fast, susceptible and reproducible.

1.8.3.4 NMR spectroscopy

NMR spectroscopy such as ^{13}C, ^{1}H and 2D INADEQUATE (Incredible Natural Abundance Double Quantum Transfer Experiments) are in use for characterizing and quantifying the pure PHAs. By this method the exact location of the double bonds in the monomer and also the exact configuration of the polymer can be determined.

1.9 Physical properties

The physical properties of the polymer are mainly dependent on the chemical formulation and structure of the polymer itself. PHB is an optically active, compact helical structure, which is most similar to that of polypropylene which also has a compact configuration[122]. Characteristics of biopolymers are similar to those of conventional plastics like polypropylene[123, 124].

The molecular weight of the bacterial polymers is in the range of $2x10^5$ to $3x10^6$ Da with polydispersity (M_w/M_n) of around 2.0[125]. The crystallinity value of poly (3HB) is in the range of 55-80%[126, 127]. Poly (3HB) crystals usually show a lamellar morphology and form spherulites when crystallized from the melt to the bulk material. Poly (3HB) is a relatively stiff, rigid material and has a tensile strength comparable to that of polypropylene. Some of the scl-PHAs may be too brittle and rigid which may lack the superior mechanical properties required for biomedical and packaging film applications. Mcl-PHAs may be elastomeric and have very low mechanical strength. Copolymers like PHBV or mcl-PHAs are less stiff and brittle than PHB whereas most of the other mechanical properties are the same.

1.10 Biodegradation of PHA

Biodegradation is a process of degradation where break down of complex compound into simple compounds takes place as a result of microbial action without the release of any hazardous substances to the environment. Different types of biodegradation occur in environment such as Hydro-biodegradation, Photo-biodegradation and Oxo-biodegradation.

Biodegradation of PHA can be distinguished into two parts: intracellular and extracellular PHA degradation. Intracellular degradation occurs in the endogenous storage reservoir by the accumulating bacterium itself and intracellular PHA depolymerases catalyze the degradation process. On the contrary, extracellular degradation is the utilization of an exogenous polymer released by accumulating cells after death. Here, different microbes present in the environment secrete extracellular PHA depolymerases and PHA hydrolases[128, 129] to hydrolyze solid PHA into water soluble oligomers and monomers, and subsequently utilize the resultant products as nutrients within the cells. After degradation of PHA, the polymer is converted into carbon dioxide and water under aerobic conditions and into methane under anaerobic conditions. In biological systems PHAs can be degraded using microbial depolymerases as well as by non-enzymatic and enzymatic hydrolysis in animal tissue[130]. Biodegradation of PHAs is influenced by numerous factors such as molecular mass, monomeric composition, chemical structure, crystallinity[4] etc. The

rate of polymer biodegradation depends on a variety of factors including surface area, microbial activity of the environment, pH, temperature, moisture and pressure of other nutrient materials. Ultra violet rays can also accelerate degradation of PHAs[131].

1.11 Applications of PHA

PHAs have been drawing considerable attention as biocompatible plastics for a wide range of applications[126] due to its biocompatibility, biodegradability and uniform chirality. A number of different companies are developing PHAs for use in the plastic industry. Currently, some US and Japanese companies are actively trying for commercialization of PHA biopolymers. They can also be used to manufacture medical-surgical garments, carpet, packaging, compostable bags, lids or tubs and flushables. The extensive range of physical properties of PHA provides them a broad range of potential applications to mankind[132, 133].

In the recent years, nanoparticles have been gaining importance for diverse biomedical applications like antioxidant, cytotoxic, antibacterial properties etc. in the daily human life. Silver is used in many different biomedical fields for therapeutic uses. The novelty of the material helps a lot in its use in different composites in both liquid and solid forms. The antibacterial property of the silver nanoparticles (SNP) was well reported by different researchers. Many workers reported on the stability problem of the colloidal silver nanoparticles. Owing to the bactericidal properties of silver ions, its nano dispersions can form a basis for the development of new classes of bactericides and different medicinal substances. The preparation of a dispersed system with the required stability in time and resistance to the action of external factors remains to be the major problem. Different surfactants like PVP (Polyvinylpyrrolidone), Tween, CTAB (Cetyl trimethylammonium bromide) etc were used to stabilize the SNP. The natural hydrophobic polymers such as PHA from bacteria are expected to be the effective alternative renewable source for such uses. PHAs can be applied for:

- Blow molded bottles, containers, creating agent on paper and electronic products especially from the composites of PHA.
- Biodegradable carrier for long term dosage of drugs, medicines, insecticides, herbicides. PHAs have been studied as drug carrier scaffolds for controlled drug delivery because the physical properties like strength, modulus and elongation of the scaffolds are comparable to that of other drug delivery systems.
- Due to the slow hydrolytic degradation inside the human body, PHAs can be more advantageous for their use in reconstructive surgery.
- PHAs can also be used as starting material for other chemicals taking advantage of their uniform chirality.
- PHAs have a potential role as a pollution bioindicator in preliminary assessments of environmental health[134].
- In bone and blood vessel replacements and
- In biosensor applications

1.12 Molecular identification of bacterial isolates

The identification of bacteria on the basis of phenotypic characteristics is generally not as accurate as identification based on genotypic methods. To accurately identify the bacteria, ribotyping is used as the most common molecular biological approach. It is also commonly used as a rapid tool for the identification of poorly described, rarely isolated, or phenotypically aberrant and non-cultured unknown bacteria up to the species level.

Ribotyping involves the fingerprinting of genomic DNA restriction fragments containing all or part of the genes coding for the 16S and 23S rRNA. 16S rRNA genes are mainly used for classification and identification of bacteria. These genes are universally present in all bacteria and have highly conserved and variable regions that will discriminate the genus or species level. Moreover, 16S rRNA genes are located on the mitochondrion and as a result numerous copies are available. This is adequately distinctive from its eukaryotic, archaeal, and chloroplastic homologs, so that each can be amplified separately. Since it is enough conserved, its amplification can be performed using specific primers. The 16S rRNA gene

sequence is about 1,550 bp long and is composed of both variable and conserved regions. The gene is large enough, with sufficient interspecific polymorphisms of 16S rRNA gene to provide distinguishing and statistically valid measurements. The DNA is used as the template for PCR to amplify a segment of about 500 or 1,500 bp of the 16S rRNA gene sequence. Broad-based or universal primers complementary to conserved regions are usually chosen so that the region can be amplified from any bacteria. The primers are used at the beginning of the gene and at either the 540-bp region or at the end of the whole sequence (about the 1,550-bp region), and the sequence of the variable region in between is used for the comparative taxonomy. The other advantage of this gene is that for describing a new species, it is mandatory to sequence and deposit in an available site (e.g. NCBI), so that everyone can have access to the sequences of all described species and use them to identify any bacteria of interest.

By digesting the 16S rRNA genes with a specific restriction enzyme, fragments of different lengths are generated. By performing a gel electrophoresis of the digested samples, the fragments can be visualized as a smear on the gel, where larger fragments are at the top of the gel, and smaller fragments further down. These smears form a unique pattern for each species and can be used to identify the origin of the DNA.

The 16S rRNA gene sequence identification of organisms is dependent on accurate sequences in databases, appropriate names associated with those sequences, and an accurate sequence of the isolate to be identified. The conservation in the 16S rRNA gene sequence relationships in *Bacillus* spp was first stated by Dubnau *et al.*[135]. Although the absolute rate of change in the 16S rRNA gene sequence is not known, it does mark evolutionary distance and relatedness of organisms. In general, the comparison of the 16S rRNA gene sequences allows differentiation between organisms at the genus level across all major phyla of bacteria, in addition to classifying strains at multiple levels, including at their species and subspecies level. The occasional exceptions to the usefulness of 16S rRNA gene sequencing usually relate to more than one well-known species having the same or very similar sequences.

Aims and objectives of the present study

Since North-eastern part of India is considered as the one of the mega biodiversity hot spots of the world, therefore, screening of microbial diversity from the environment is prospective to develop different biotechnological products and processes for the different application purposes. The present investigation was commenced for the production of PHA from microorganisms starting with selection of potent strains, optimization of production processes, extraction and purification of polymers and also the economic production of PHAs from the bacteria. Researchers have developed various extractions as well as purification processes for PHA recovery. Moreover, the applicability of PHA in different areas has been highlighted.

In view of the above mentioned background information, the present research project was undertaken with the following objectives:

1. Screening of biopolymer producing bacteria,
2. Isolation and purification of PHA,
3. Physical and chemical characterization of PHA, and
4. Molecular genetic assessment of PHA producing bacterial isolates

CHAPTER 2

REVIEW OF LITERATURE

Research was carried out to inform the scientific society with new knowledge or discovery. However, it is not to be expected that everybody would willingly believe what we tackle in our whole research work. Thus, to make our research more convincing we support it with other works which have spoken about the same topic that we have for our research. This is where literature review comes in. Literature review establishes a clear tie between the works that we have cited and the topic that we have written about. Literature review justifies the reason for research and allows establishing our theoretical framework and methodological focus. It acts as a springboard for the whole thesis and shows the originality and relevance of our research problem. It is a critical discussion and summary of literature that is of 'general' and 'specialized' relevance to our particular area and topic of the research problem.

This chapter will present an overview of the previous work carried out by different researchers and knowledge about the PHA producing bacteria, their diversity, inexpensive carbon sources for the culture of biopolymer producing bacteria, PHAs biodegradability and their application in different areas. The chapter is divided in following sections to cover all the aspects.

PHAs are polyesters of various hydroxyalkanoates accumulated in the form of intracellular granules by a large variety of bacteria when, bacterial growth is limited by depletion of nitrogen, phosphorus[136] or oxygen and an excess amount of carbon source. If the general physiological fitness of bacteria is not affected they can store excess nutrients inside their cells and by polymerizing soluble intermediates into insoluble molecules and the cells do not undergo alterations in its osmotic state. Peters and Rehm[43] have reported the prevention of leakage of these PHA compounds from bacterial cells thereby allowing the availability of the nutrient stores at a low maintenance.

2.1 Screening of PHA production in bacteria

According to Byrom[51] about 8-13 granules per cell having diameter of 0.2-0.5 μm were observed in *A. eutrophus*. These granules appear as highly refractive inclusion bodies under electron microscope. Simbert[137] has reported the presence of PHB granules in bacterial cells which can be detected by staining with Sudan Black B. However, Ostle and Holt[109] advocated the use of Nile Blue A, a water soluble

basic oxazine dye that has a greater affinity and higher specificity than Sudan Black B for PHB, and that gives a bright orange fluorescence at a wavelength of 460 nm, as other inclusion bodies do not stain with Nile Blue A, thereby emphasizing its usefulness. The oxazine dye Nile blue A and its fluorescent oxazone form, Nile red, were used to develop a simple and highly sensitive staining method to detect PHB and other PHAs directly in growing bacterial colonies[138]. PHB granules of Nile red-stained living cells of *Caryophanon latum* at the early stage of PHB accumulation were frequently found at or close to the cytoplasmic membrane which were determined by confocal laser scanning fluorescence microscopy[139]. The identity of polyhydroxyalkanoates (PHA) storing bacteria selected under aerobic dynamic feeding conditions, using propionate as carbon source, was determined by applying reverse transcriptase–polymerase chain reaction (RT-PCR) on micromanipulated cells and confirmed by fluorescence *in situ* hybridization (FISH)[140].

2.2 PHA production in specific bacteria

Production of PHA has been reported by numerous bacteria. *R. eutropha* is by far the most extensively studied bacteria used for PHB and PHBV production. Vaneechoutte[141] reported that *R. eutropha* has the ability to produce PHB with the use of simple carbon source. *R. eutropha* NCIMB 11599 can produce 121 gL^{-1} PHB under controlled glucose and nitrogen limitation conditions in fed-batch culture[142]. Mixtures of glucose, propionic acid and either 4-hydroxybutyric acid or β-butyrolactone as carbon sources in fed-batch cultures of *R. eutropha* led to production of a P (3HB-4HB-3HV) terpolymer[143].Volova[144] reported *R. eutropha* B8562 produced PHAs upto 90% of the cell dry weight by using different carbon sources (CO_2, fructose and glucose).

By the virtue of their ability to use methanol as a carbon substrate, *Methylobacterium* species are of interest for the production of PHB. *M. rhodesianum, M. extorquens, M. organophilum, M. rhodenium, M. zatmanii, M. radiotolerans, Mycoplana rubra, Paracoccus denitrificans*[145, 146] and *Proteomonas extorquens*[147, 148] are some of the bacterial species which uses methanol as a carbon source for PHB accumulation. Bourque[149] reported *M. extorquens* accumulated 30% (CDW) of P (3HB) with a molecular mass of 250 kDa with methanol concentration of 1.7 gL^{-1}, and addition of complex nitrogen source.

P. putida can efficiently incorporate monomers in the range of C_8–C_{10} during PHA synthesis. De Smet[54] observed the presence of intracellular granules consisting of poly (3-hydroxyoctanoate) in *P. oleovorans* strain ATCC29347 grown in two-phase medium containing 50% v/v octane. Haywood[150] examined various *Pseudomonas* spp. for growth and polyester accumulation with C_6-C_{10} straight-chain alkanes, alcohols and alkanoic acid as the sole carbon source. The accumulation of PHAs containing mcl-3HB (C_6-C_{12}), but not 3-HB, appears to be a characteristic of the fluorescent *Pseudomonas* spp. to accumulate these PHAs[151]. Several studies have shown that *P. putida* and *P. aeruginosa* strains are able to convert acetyl-CoA to medium-chain-length monomers for PHA synthesis[152]. Ayub[153] reported that *Pseudomonas* spp. 14-3 strain accumulated large quantities of PHB when grown on octanoate isolated from Antarctic environment. This isolate was characterized on the basis of phenotypic features and partial sequencing of its 16s ribosomal RNA gene. *Pseudomonas* spp. 14-3 showed increased tolerance to both thermal and oxidative stress.

Other important strains recently studied include- *Bacillus* spp., *Alcaligenes* spp., *Rhodopseudomonas palustris, E. coli, Burkholderia* spp. and *Halomonas boliviensis.*

A number of *Bacillus* spp. has been reported to accumulate 9-44% dry cell weight of PHB. By comparison, *B. mycoides* RLJ B-017 contained 69.4±0.4% dry cell weight PHB. Therefore, this strain has been considered as a potent organism for industrial interest[154]. The tropical marine and mangrove microflora from the mid-west coast of India possessed a high potential to accumulate important polymers such as PHA. Among these isolates, seven cultures accumulated more than 1 gm of PHA per litre of culture broth[155]. Tajima[156] reported the isolation of a PHA accumulating gram-positive bacterium *Bacillus* sp. INT005 from gas field soil. The species was identified by comparing its morphological and physiological properties and partial nucleotide sequence (500 bp) of its 16s rRNA. Construction of recombinant *B. subtilis* was also done for the production of PHA co polymer[157].

Lakhman[158] reported that strains of *Rhizobium* spp. isolated from leguminous plants and standard strains accumulated 27% to 57% PHA of their cell biomass while using sucrose as a sole carbon source. Van-Thuoc[159] produced PHB by

utilizing *H. boliviensis* culturing in cheap and readily available agro-residue as cheap carbon source in order to reduce the cost of production.

The use of recombinant *E. coli* as PHA producer has drawn tremendous scientific attention as it is genetically well characterized. *E. coli* is not being a natural PHA accumulator; its production has to be metabolically engineered. Moreover it does not have any depolymerase activity to degrade the accumulated PHA. Although *R. eutropha* produces high levels of P (3HB), but they have certain limitations which impedes genetic manipulations. Therefore, the expression of PHA biosynthetic genes of *R. eutropha* in *E. coli* for P (3HB) synthesis opened up the possibility for PHA production by recombinant organisms[160,161,162]. Genetically and metabolically engineered *E. coli* can synthesize a variety of polymers, such as P (3HB-3HV), P (3HB-4HB), P (4HB) and P (3HO-3HH). Expression of *P. aeruginosa* PHA synthases, phaC1 and phaC2 in *E.coli* fadB mutant resulted in msc-PHA accumulation when grown in presence of C_8-C_{14} fatty acids[163, 164]. Recombinant *E. coli* DH5α (pQKZ103*)* has been shown to accumulate PHB up to 85% of the cell dry weight when cultured in minimal glucose medium[165]. PHA synthase gene (pha C1) from indigenous *Pseudomonas* spp. LDC-5 was amplified by PCR and cloned in *E. coli* which is a potential candidate for the large-scale production of polymer[166].

2.3 Production of PHA in higher organisms

2.3.1 Yeasts

PHA production from yeast is still in its infantile stage. Only a few reports of PHA production by different metabolically engineered yeasts are available[167, 168]. Poirier[169] reported transformation of PHA synthase from *P. aeruginosa* modified at the carboxy-end for peroxisomal targeting in methylotrophic yeast *Pichia pastoris*. The PHA synthase was expressed under the control of the promoter of *P. pastoris* acyl-CoA oxidase gene and accumulated up to 1% medium-chain-length PHA per g dry weight as inclusions within the peroxisomes. Buelhamd[170] reported production of PHAs in a transgenic yeast *Saccharomyces pombe* harboring the PHB synthesis genes encoding β-ketothiolase (phbARe), acetoacetyl-CoA reductase (phbBRe) and PHB synthase (phbCRe) of *R. eutropha*. The transgenic yeast accumulated about 9%

(w/w) of PHB under optimized conditions. Abu-Elreesh[167] reported PHA accumulation of about 7% (w/w) by metabolically engineered *Kloeckera* yeast cells.

2.3.2 Insects

Williams *et al.*[171] reported a novel pathway for the synthesis of P-3HB which was engineered by simultaneous delivery of two genes into insect cells *Spodoptera frugiperda* by use of individual baculovirus vectors. This system includes expression of a dehydrase-domain mutant rat fatty acid synthase cDNA and the phbC gene encoding polyhydroxyalkanoate synthase from *A. eutrophus*. Approximately 1 mg of PHB was isolated from a one-litre culture of these cells corresponding to 0.16% of cell dry weight.

2.3.3 Plants

Plants are capable of producing significant amounts of numerous useful chemicals at a low cost, when compared to bacteria or yeast[172]. Commercialization of plant derived PHA will require the creation of transgenic crop plants with the addition of high product yields[173]. Transgenic plants can produce PHAs from photosynthetically fixed CO_2 and water which after disposal degrade back to CO_2 and water. Therefore, it might be possible to produce PHA at a similar low costs which are comparable to those of other biopolymers already obtained from plants. *Arabidopsis thaliana* was the first targeted model for transgenic studies in plants[37]. Poirier[174] reported synthesis of PHA in plants which was initially explored by the expression of PHA biosynthetic genes of the bacterium *R. eutropha* in the well-studied plant *A. thaliana*. But scanty (0.1%) accumulation of PHB was achieved from the plant. Recently all three genes necessary for PHB biosynthesis were transformed to *A. thaliana* in a single transformation event[175]. These plants accumulated more than 4% of their fresh weight (approximately 40% of their dry weight) of PHB in leaf chloroplasts. John and Keller[176] reported the novel perspective on the use of PHA synthesis in cotton fiber cells by the expression of the *R. eutropha* PHB biosynthetic pathway. Analysis of the transgenic fibers showed PHB accumulation up to 0.3% of dry weight exhibiting better insulating properties. Moreover PHA biosynthetic genes also have been expressed in some agricultural crops such as *Brassica napus,Gossypium hirsutum, Nicotiana tabacum, Solanum tuberosum and Zea mays*[176, 177, 178, 179, 29]. By transforming threonine deaminase gene

from *E. coli* and PHB biosynthetic genes from *R. eutropha*, PHBV were produced by engineered Arabidopsis and Brassica plants in their leaves and seeds respectively[180]. An optimized genetic construct for plastid transformation of tobacco plant *Nicotiana tabacum* for the production of polyhydroxybutyrate (PHB) was reported by Bohmert-Tatarev *et al.*[181]. This plant has been designed using an operon extension strategy and bacterial genes encoding the PHB pathway enzymes were selected for use in this construct based on their similarity to the codon usage and GC content of the tobacco plastome.

2.4 Fermentation process

Fermentation strategies for the production of high concentration of P (3-HB-co-3-HV) with different 3-HV fractions by recombinant *E. coli* harboring *A. latus* PHA biosynthesis genes were developed[46]. *A. latus* when transformed with its own cloned phaC gene, exhibited increase in PHB synthesis as well as increase in PHB content[182]. The recombinant *A. latus* synthesized maximum concentration from 3.1-3.7 gL^{-1} and content of PHB from 50.2-65% of cell dry weight, respectively, as compared to the untransformed *A. latus*.

PHA-producing bacteria are classified into two groups based on culture conditions required for efficient PHA synthesis[47]. One group requires the limitation of an essential element such as N, P, Mg, O, or S for the efficient synthesis of PHA and the other group requires no nutrient limitation. Both the groups can accumulate polymer accumulation during growth. Therefore, these characteristics should be considered in developing culture methods for the efficient production of PHAs. Either fed-batch or continuous culture techniques can be used for the production of PHA with high productivity. An initial growth phase in nutrient enriched medium yields sufficient biomass, followed by a product formation phase in nitrogen-depleted medium. Single fed-batch fermentation that is nitrogen limited leads to low amounts of polymer, because there is not enough accumulation of biomass[183].

Patnaik[184] reported the use of open mixed cultures, such as activated sludge which can contribute to decrease the cost of PHAs and therefore increase their commercial potential. A stable methane-utilizing mixed bacterial culture was used for the development of viable large-scale production of PHB using cheap substrates like methane from natural or renewable sources in an open system. PHB content

could be increased to 87% by applying nitrogen limitation in fed-batch culture, which was considerably higher than that of typically obtainable 50% under nitrogen-sufficient conditions[185]. Greater research capabilities are needed to investigate whether continuous culture can truly give higher productivity than fed-batch cultures, without any process problems, such as, culture instability and contamination. Kang[165] developed a stress-induced system by which the PHB biosynthesis pathways can be induced under stress conditions in which fermentation results showed that recombinant *E. coli* DH5α (pQKZ103) harboring this system was able to accumulate polyhydroxybutyrate up to 85.8% of cell dry weight in minimal glucose medium without adding any inducer.

Currently PHA production processes based on mixed microbial cultures (MMC) are being investigated as a possible technology to decrease production costs, as no sterilization is required and bacteria can adapt quite well to the complex substrate present in low-cost substrates. In spite of this 'feast and famine' or aerobic dynamic feeding (ADF) is developed which is based on the supply of a short period of excess carbon (feast) followed by a long period of starvation[186]. Serafim[187] showed that the intracellular PHA content reached 65.4% cell dry weight under ADF conditions, with carbon addition (acetate) by sequential pulses.

In the bacterial cell, carbon substrates are metabolized by 3 different pathways. Pathway I, which generates PHB homopolymer from acetyl-CoA processed from sugars and has been found extensively in a wide range of bacteria like *R. eutropha*. Pathways II and III, which generates mainly mcl-(R)-3HA monomers from fatty acid β-oxidation intermediates and fatty acid biosynthesis intermediates,[188, 189] respectively, have been found in various fluorescent *P.* sp. Xi *et al.*[190] reported the *P. stutzeri* strain 1317 was found to produce PHA up to 77% of cell dry weight when grow on various fatty acids, alcohols, diols as well as glucose and gluconate. Impallomeni *et al.*[191] reported that *P. aeruginosa* ATCC 27853 synthesize random co-polyhydroxyalkanoates (co-PHAs) using Tween 20 as the sole carbon source although it is a mixed carbon source. Tween 20 and its three major fatty acids support both cellular growth and PHA production and its emulsifying and solubilizing properties seems to facilitate its use as carbon source by cells, leading to production of the highest polymer yield. Moreover it could provide fatty acids substrates at lower cost than that of purified fatty acids. Halami[192] reported a native

strain *B. cereus* CFR06 which produces amylase and polyhydroxyalkanoate (PHA) (48% CDW) from the starch containing medium.

Plant oils or their derived fatty acids are good carbon sources for the production of PHA as they are inexpensive renewable carbon sources. A large-scale production of P (3-HB-co-3-HHx) from lauric acid was carried out using *Aeromonas hydrophila* with a final PHA content of 50 %[18].

Different kinds of agricultural products like starch[193]and wastes like beet and cane molasses[194, 195] wheat bran[196], malt waste[197], and dairy wastes like cheese whey[196, 197, 198] with or without nitogen supplement have been used as raw materials for PHA production. Liu *et al*[199] reported that recombinant *E. coli* strain was capable of producing 39.5 $gL^{-1}h^{-1}$ PHB using molasses as the carbon source. *B. megaterium* was grown on various carbon sources such as date syrup and beet molasses[200].Currently efforts are being made to grow bacteria on different renewable vegetable oils and various waste products[67, 201]. The use of these inexpensive carbon sources to produce PHAs could lead to significant economical advantages[202]. Huang *et al*[203] reported *Haloferax mediterranei*, an archea which could produce a PHA content of 55.6 wt.% and 38.7 wt.% by a repeated fed-batch fermentation process using low-cost raw materials like extruded rice bran (ERB) and extruded cornstarch (ECS) respectively. *P. putida* can produce medium chain length PHA (28 gL^{-1}) using corn oil hydrolysate (an inexpensive and renewable carbon source) in fed-batch culture[58].

Moreover novel processes have been investigated to produce PHAs from organic wastes in wastewater[204, 205], industrial wastes[206, 207] and municipal wastes[208]. Different wastes containing volatile fatty acids like palm oil mill effluent[209] banana pseudostem[210] damaged food grains, pea shells, apple pomace are used as carbon sources. A large number of bacteria like *A. eutrophus, B. megaterium, P. oleovorans, Azotobacter* sp, *Beijerinckia* sp, *Rhizobium* sp, *Nocardia* sp utilize this waste as substrates for PHA production[210]. Production of PHAs from organic wastes can provide multiple benefits to the environment and promote sustainable development. But Lee and Yu[211] reported that PHA-producing microbes like *R. eutropha* cannot directly utilize organic wastes as they are usually in the complex form. So, the first step to overcome this problem is hydrolysis and acidogenesis of

the wastes producing short-chain volatile fatty acids such as acetic, propionic and butyric acids that can be used by *R. eutropha* for synthesis of P (HB-co-HV)[52].

CO_2 in the atmosphere is the ultimate feedstock for PHA production. Some wild-type cyanobacteria are capable of accumulating small amounts of P (3-HB) (approx 6%) in the cells from CO_2. Ishizaki *et al*[212] reported that *R. eutropha* can assimilate CO_2 and produce P (3-HB) in the absence of light energy, but with oxidization of hydrogen. It has been also reported by Volova *et al*[213] that the carbon monoxide (CO)-resistant strain *R. eutropha* B5786 is able to synthesize PHAs upto 70-75% in the presence of CO under autotrophic conditions. *Cupriavidus necator* H16 can metabolize a mixture of H and CO_2 to form PHAs[214].

The use of methanol as a carbon substrate is significant because it is a cheap carbon source and can significantly reduce the production costs of PHB. It can also be considered as a renewable substrate since it could be derived from woody materials or from natural gas obtained after anaerobic digestion of organic substances. A new bacterial strain *Methylobacterium* sp. strain GW2 isolated from groundwater was found to be capable of producing the homopolymer P-3HB from various carbon sources such as methanol, ethanol, and succinate. Yezza *et al*[215] reported that the bacterium *Methylobacterium* GW2 showed best PHB production (40% w/w dry biomass) in methanol containing medium.

2.5 Recovery of PHA

In addition to the cost of maintaining pure cultures and the high cost of organic substrates, the recovery of PHA contributes significantly to the production cost of the polymer. In the past two decades, a number of economic methods have been suggested for recovery of purified PHA. After fermentation, bacterial cells containing PHAs are separated from the medium by centrifugation, washed, dried and finally disrupted to recover the polymer. Most of the methods to recover intracellular PHA involve chloroform, methylene chloride, propylene carbonate and dichloroethane which can result in purified PHA[216]. Chen and Wu[12] reported that solvent extraction is a good method for medical application as it gives higher percentage of purified PHAs.

Jiang *et al.*[217] reported the use of cheaper and less toxic solvents such as hexane, acetone and dimethylcarbonate for the PHA recovery process. The extracted

polymer solution containing more than 5% (w/v) P (3HB) is very viscous and the removal of cell debris is difficult. Additionally, the process needs large quantities of toxic and volatile solvents, which increases the total production cost despite being hazardous to the environment[218].

Digestion using sodium hypochlorite has been proposed as an alternative to the unfavorable extraction with organic solvents[116]. Even though this method is effective in digestion, it causes severe degradation of PHA. Surfactant pretreatment and hypochlorite digestion under optimized conditions results in pure isolation of P (3HB) with less degradation and improved molecular weight[219, 220]. An enzymatic digestion method developed by Zeneca has been used for the production of Biopol, but the use of expensive chemicals and complex processes does not seem to be economically feasible.

Fidler and Dennis[221] reported a system for PHB recovered from *E. coli* cells by expressing T7 bacteriophage lysozyme gene. In this system, the lysozyme penetrated and disrupted the bacterial cells resulting PHB granules to be released. Choi and Lee[222] reported a simple alkaline digestion method for the recovery of P (3HB) from the recombinant *E. coli* cells. Recombinant *E. coli* cells having a P (3HB) content of 77% when treated with 0.2 M NaOH for 1 h, recovers P (3HB) of 98.5% purity[223]. Hampson and Ashby[224] developed a simple two-step process to extract and purify mcl-PHAs from *P. resinovorans* cells. In this method supercritical fluid extraction (SFE) of the lyophilized cells was done using CO_2 to remove lipid impurities, followed by chloroform extraction of the cells. By this method a maximum of 42.4% mcl-PHA was obtained which designate that this process saves time, uses much less organic solvent, and produces a pure mcl-PHA biopolymer than previous extraction and purification methods.

In the present scenario, the states of art technology for PHA recovery are supercritical fluid disruption[225] dissolved air floatation[226] and selective dissolution of cell mass[227] has been established. These results highlighted the importance of developing an economical and efficient recovery method.

In most of the organisms so far investigated, the PHB is synthesized from acetyl-coenzyme A (acetyl-CoA) by a sequence of three reactions catalyzed by three biosynthetic enzymes. In the first step, 3-ketothiolase (Pha A) combines two molecules of acetyl-CoA to form acetoacetyl-CoA. Acetoacetyl-CoA reductase (Pha

B) allows the reduction of acetoacetyl-CoA by NADH to 3-hydroxybutyryl-CoA. Finally, PHB synthase (Pha C) polymerizes 3-hydroxybutyryl-CoA to PHB and coenzymeA being liberated (Fig.1.5). During the normal bacterial growth, the 3-kitothiolase will be inhibited by free coenzyme-A coming out of the Krebs cycle. But, when entry of actyl-CoA into Krebs cycle is restricted, the surplus acetyl-Co A is channeled in to PHB biosynthase[228]. In *Rhodospirillum rubrum*, two stereospecific enoyl-Co A hydratases are also involved[229]; these enzymes catalyze the conversion of L-(+)-3-hydroxybutyryl-Co A via crotonyl-Co A to D-(-)-3-hydroxybutyryl-Co A, which is polymerized to yield PHB.

2.6 Chemical structure of PHAs

Although the microbial origin, structure and physicochemical properties of PHAs is quite variable (Fig. 1.1), most PHAs could be grouped in to three. The repeat units of scl-PHAs are composed of hydroxyfatty acids. The pendant group (R) varies from methyl (C_1) to tridecyl (C_{13}). Fatty acids with the hydroxyl group at position 4, 5 or 6 and pendant groups containing substituents or unsaturations are also known. Within bacterial metabolism, carbon substrates are converted to hydroxyacyl-CoA thioesters. In all PHAs that have been characterized so far, the hydroxyl-substituted carbon atom is of the stereochemical (R) configuration. Haywood *et al.*[230] and Williams *et al.*[231] reported that a few bacteria are known to synthesize scl-PHAs containing monomers other than 3HB when grown on simple sugar. It is suggested by Sato *et al*[232] that the most common PHB homopolymers, synthesized by bacteria, always contain less than 1 mol of 3-HV monomers. Steinbuchel[24] reported that some *Pseudomonas* spp have been reported to accumulate PHA copolymers containing mcl monomer. The composition of PHA produced is usually related to the substrate used for growth mostly 2_n carbon shorter than the substrate used[233]. Copolymers of PHB are formed when mixed substrates are used, such as, a mixture of glucose and valerate and convert the carbon substrates to PHBV or PHB4B[234]. Pederson *et al.*[235] reported that when substrates were alternated overtime, it was possible to obtain PHA block copolymers synthesized by bacteria. Labuzek and Radecka[236] reported that gram–positive *B. cereus* UW85 strain could produce tercopolymer by using 3-HB, 3-HV and 6-hydroxyhexanoate units' ε-caprolactone, or ε-caprolactone and glucose as carbon

source. *R. eutropha* synthesized a copolymer of 3-hydroxybutyrate and 3-mercaptopropionate, poly (3-HB-co-3MP) containing sulfur in the backbone, when 3-mercaptopropionic acid or 3, 3′- thiodipropionic acid was provided as carbon source in addition to fructose or gluconic acid under nitrogen-limited growth conditions[237].

But in contrast to the normal production of copolymer when using mixed substrates by the bacteria, the strain *P. nitroreducens* isolated from oil-contaminated soil demonstrated some unusual ability to synthesize PHB homopolymer from medium-chain-length (mcl) fatty acids including hexanoate and octanoate[238].

The surface of a PHA granule is coated with a layer of phospholipids and proteins. Phasins, a class of predominant protein of the PHA granule influence the number and size of it[239, 240]. Karen *et al.*[241] has reported that *P. putida* strain CA-3 accumulates polyphosphate (poly P) and it appears that poly P is not the rate-limiting step for mcl-PHA accumulation in *Pseudomonas* strains.

2.7 Physical properties of PHAs

Among all the reported biopolymers, PHB are the most extensively studied polymer and as such, the properties of PHAs have been elucidated by taking it it into consideration[242]. The weight average molecular weight (Mw) of scl-PHAs, like PHB produced from wild-type bacteria is usually in the range of $1x10^4$ to $4x10^6$ Da with a polydispersity of around 2[243, 244]. But according to Valappil *et al.*[245], the Mw in mcl-PHAs, lies between the range of 60,000 and 412,000. The polydispersity index value of scl-PHAs to be around 1.75, while in mcl-PHA copolymers the polydispersities are in the range of 1.6 to 4.4[245].

The family of PHAs exhibits a wide variety of mechanical properties from hard crystalline to elastic, depending on composition of monomer units which extends its application. Scl-PHAs like P (3HB) homopolymer are highly crystalline, stiff, and brittle material[127, 246]. When spun into fibres it behaves as a hard-elastic material[247, 248]. The glass transition temperature (Tg) and melting temperature (Tm) is 180 °C and 4 °C, respectively. These polymers become fluid and can be moulded above their melting temperature. Mechanical properties like Young's modulus (3.5 GPa) and tensile strength (40 MPa) are close to that of polypropylene, although the elongation to break is about 5%, which is significantly lower than that of

polypropylene, 400%[36]. Ashby *et al.*[249] also reported that the film of mcl PHAs synthesized by *P. resinovorans* from coconut oil, tallow and soybean oil can be improved when subjected to 50 kGy of γ-irradiation. This resulted in the formation of crosslink based on the number of olefinic groups present in the polymer side-chains and improved the tensile strength (104% and 63%), percent elongation (49% and 13%), and Young's modulus (30% and 76%) of the polymer film.

The mcl-PHAs have their mechanical properties similar to that of PHB, but they are less stiff and brittle. Khanna and Srivastava[49] reported that the physical and thermal properties can be regulated by varying the copolymer compositions. Mcl-PHAs are semi-crystalline elastomers due to their low melting point (40-60 °C), low glass transition temperatures (-50 to-25 °C). Sanchez *et al.*[250] reported mcl-PHAs also have low crystallinity due to the presence of large and irregular pendant side groups. In case of 3HV copolymer, the copolymer becomes tougher and more flexible with the increase of 3HV unit. However, the melting temperature becomes decreasing and elongation to break becomes increasing with increasing 3HV fraction[49]. Gunaratne and Shanks[251] reported the melting behavior and crystallization of PHAs which showed multiple melting peak behavior and melting-recrystallization-remelting. Carrasco *et al.*[252] reported that the thermal biodegradation of PHB (Biopol) starts at 246.3 °C, while the value for PHBV (Biopol) is 260.4 °C as the side chain increases in the later which in turn increases the thermal stability. This is due to the presence of valerate in the polymer chain which increases the thermal stability of the polymer. Introduction of co-monomers other than 3HV into PHB chain also give copolymers of improved mechanical properties. The physical properties of some of polymers are compared with polypropylene (PP) and polystyrene in Table 2.1

Table 2.1 Physical properties of some polymers

Polymer	Melting point (°c)	Glass-transition temp (°c)	Crystalline (%)	Young's modulus (GPa)	Tensile strength (MPa)	Elongation to break (%)
P (3HB)	179	4	80	3.5	40	6
P (4HB)	53	-	-	149	104	1000
P (3HB-co-3HV)						
3 mol% 3HV	170	-	-	2.9	38	-
9 mol% 3HV	162	-	-	1.9	37	-
14 mol% 3HV	150	-	-	1.5	35	-
20 mol% 3HV	145	-	-	1.2	32	-
25 mol% 3HV	137	-1	40	0.7	20	-

Polymer	Melting point (°c)	Glass-transition temp (°c)	Crystalline (%)	Young's modulus (GPa)	Tensile strength (MPa)	Elongation to break (%)
P (3HB-co-4HB)						
3 mol% 4HB	166	-	-	-	28	45
10 mol% 4HB	159	-	-	-	24	242
16 mol% 4HB	150	-7	45	-	26	444
64 mol% 4HB	50	-	-	30	17	591
90 mol% 4HB	50	-	-	100	65	1080
P(3HB-10% 3HHx)	127	-1	34	-	21	400
Polypropylene (PP)	176	-10	50-70	1.7	34.5	400
Polystyrene	110	21	-	3.1	50	-

Data adapted from Poirier *et al.*[25], Lee[47], Tsuge[57], Khanna and Srivastava[49] and Verlinden *et al.*[248].

2.8 Biodegradation of PHA

The stereochemistry of PHA fits well with its biodegradability. They are fully biodegradable and innocuous to the environment. Jendrossek *et al.*[253] reported that these degradations enable CO_2 and organic compound recycling in the ecosystem which provides a buffer to climate change. The polymers can degrade both under aerobic and anaerobic conditions. They can also be subjected to thermal degradation and enzymatic hydrolysis.

Different factors like stereoregularity, molecular mass, monomeric composition and crystallinity are accountable for the biodegradability of PHAs. Mochizuki *et al.*[254] and Tokiwa *et al.*[255] reported that biodegradation of PHAs is influenced by the chemical structure i.e. presence of functional groups in the polymer chain. Nishida and Tokiwa[256] described that the development of crystallinity evidently depressed the microbial degradability of PHB. Moreover, Boopathy[257] has reported that the rate of polymer also depends on a variety of factors including surface area, microbial activity of the disposal environment, pH, temperature, moisture and presence of other nutrient materials. Wang *et al.*[258] reported that the rate of degradation of PHAs depend upon the crystallinity and surface area of the polymer. Surface morphology affects degradation by facilitating contact between water, enzyme molecules or bacteria and polymer chains. When exposed to hydrolysis, the degradation starts on the surface and at physical lesions on the polymer and proceeds to the inner part of the material.

Any research on the biodegradation of PHA should clearly distinguish between intracellular and extracellular PHA degradation. Extracellular degradation is the utilization of an exogenous polymer by a not-necessarily accumulating microorganism that secretes extracellular PHA depolymerases. The source of extracellular polymer is PHA released by accumulating cells after their death and cell lysis. A number of microorganisms excrete PHA depolymerases to hydrolyze the ester bonds of a polymer into water-soluble monomers and oligomers small enough to be transported into a microbial cell and metabolized to CO_2 and water[259, 260].

Degradation of PHA polymer by different gram positive, gram negative bacteria and some methanogenic co cultures were reported by different researchers[261, 262, 32]. Mabrouk and Sabry[263] reported that a marine *Streptomyces* sp.

SNG9 utilize PHB and its copolymer P (3HB-co-HV) as the sole carbon source and degraded the polymer particles in 4 days. Many microorganisms like *P. lemoignei, P. pseudomallei, Acidovorax facilis, A. delafieldii, Comamonas testosteroni, Variovorax paradoxus, Zoogloea ramigera, and Bacillus* sp., as well as *Streptomycetes* are able to degrade P (3HB) extracellularly[264]. Colak and Guner[265] reported that three *Pseudomonas* sp. namely *P. fluorescens, P. aeruginosa and P. putida* were isolated from fuel oil contaminated soil to investigate the biodegradation of PHAs where morphological changes in the polymer were observed by the help of scanning electron microscope (SEM). Phithakrotchanakoon *et al.*[266] reported that a thermophilic *Streptomyces* sp BCC23167 isolated from a landfill site is capable of degrading various aliphatic polyesters including polyhydroxyalkanoate copolymers, poly(ε-caprolactone) and polybutylene succinate at 50 °C and neutral pH . Another soil bacterium Actinomadura sp. AF-555 has also the potential to degrade P-3HB-co-HV when exposed to soil[267].

Conversely, intracellular degradation is the active degradation of an endogenous storage reservoir by the accumulating bacterium itself. Enzymes catalyzing the intracellular degradation of PHA are intracellular PHA depolymerases. In case of intracellular degradation, PHAs are degraded by some PHA producing bacteria intracellularly. In this case, the polymer is broken down to acetyl-CoA which under the aerobic conditions enters the citric acid cycle and is oxidised to CO_2[36, 268]. Knoll *et al.*[269] reported that the PHA depolymerase enzyme phaZ is involved in the degradation of the PHAs.

Although the anaerobic degradation of PHAs has not been well documented yet, it has been recommended that PHAs can be degraded in an anaerobic environment such as sewage sludge. It was reported that P (3HB) and the copolymer P (3HB-co-3HV) were fermented (upto 83-96%) to methane and CO_2 within 16 days by using anaerobically digested domestic sewage sludge consortium[261]. Lee[47] reported that P (HB-HV) does not degrade under normal conditions of storage as it is insoluble in water and stable in air.

PHAs can be composted over a wide range of temperatures, even at a maximum of around 60 °C. UV radiation also affects the degradation of bacterial biopolyester poly (3-hydroxybutyrate-co-3-hydroxyhexanoate) (PHBHHx) and significant Mw losses were observed with UV radiation time[131].

Since the fungal biomass in soils generally exceeds the bacterial biomass and thus it is demonstrated by Kim and Rhee[270] that fungi may play a considerable role in degrading bacterial biopolyesters. Lee and Chang[271] studied the degradation of PHB by fungi from samples collected from various environments and found clear zone below and around the fungal colony in the tested plates. Different fungi such as *Penicillium, Cephalosporium, Paecilomyces*, and *Trichoderma*[272], *Ascomycetes, Basidiomycetes, Deuteromycetes, Mastigiomycetes, Myxomycetes*[2], *Aspergillus fumigatus*[273] have also been reported to degrade PHA. Fungal species *Candida albicans* and *Fusarium oxysporum* were reported for the biodegradation of mcl-PHA in our published paper[274].

2.9 PHA application

PHAs have been drawing considerable attention as biocompatible plastics for a wide range of applications[126]. A number of different companies are developing PHAs for use in the plastic industry. Currently, Metabolix (USA) and Kaeka (Japan) are among the startup companies actively teamed up for the commercialization of PHA biopolymers to a product called Nodax. Nodax has already been made in to a variety of different prototype objects such as plastic fiber or twine and molded plastic ware. The extensive range of physical properties of PHA provides them a broad range of potential applications to mankind[132, 133].

Bucci and Tavares[275] reported that P (HB-HV) could be used for films, blow molded bottles, containers and as a creating agent on paper. Composites of bioplastics have already been used in electronic products, like mobile phones.

PHA has the ability to chemically modify their functional groups as well as their biodegradability and biocompatibility properties, making them an attractive material in the biomedical field[276]. PHAs are mainly composed of different chiral hydroxyacids that have potential as synthons for anticancer drugs, anti-HIV drugs, antibiotics and vitamins. In biomedical and tissue engineering applications, PHAs have mainly been involved for biodegradable implants. PHA together with hydroxyapatite (HA) finds application as bioactive and biodegradable composite in hard tissue replacement[12]. Kilicay *et al.*[277] reported that a matrix of PHBHHx nanoparticles has been used to deliver antineoplastic agents to cancer cells. Certain target specific breast cancer cells have also been examined with PHB nanoparticles

functionalized with tumor-specific ligand[278]. Francis[279] tested the P (3HB) microsphere for releasing the antibiotics gentamycin and tetracycline *in vitro*. The slow hydrolytic degradation inside the human body makes PHAs more advantageous for use in reconstructive surgery. According to Lee[47] the degradation product of PHB, D (-)-3-hydroxybutyrate has been detected in relatively large amount in human blood plasma. PHAs can also be used as starting material for other chemicals taking advantage of their uniform chirality. Sudesh *et al.*[17] reported that the 4HB units of PHB compounds have been used in the treatment of alcohol withdrawal syndrome. Partial digestion of PHA and recombination with other polymers can be used to achieve specific properties. Degra Pol, a block–copolyesters urethane chemically synthesized from PHB-diol showed good biocompatibility. In experimental animals, P (3HBHHx) scaffolds have been assessed for use in eyelid reconstruction[280]. Moreover PHA has been used in other biomedical applications, such as tablet formulations[281, 282], surgical sutures[283], wound dressings[284, 285], controlled release contraceptive devices[286, 287].

In addition to biomedical applications, PHAs have diverse applications. Recent studies[288] suggest that PHAs can be used as precursors for biofuels production. Hydrolysis of PHAs followed by methyl esterification provides energy containing 3-hydroxyalkanoates methyl esters comparable to that of bioethanol[289, 290, 291]. Foster *et al.*[292] reported that PHAs has potential role as pollution bioindicator in preliminary assessments of environmental health. Hiraishi and Khan[293] reported that many PHAs used in the solid phase denitrification of water and waste water has several advantages over the conventional system supplemented with liquid organic substrate.

Bourbonnais and Marchessault[294] reported the use of PHA latex in paper industry for surface coating of paper and as a sizing agent. In certain aquaculture applications PHAs have been found useful for controlling bacterial pathogens[295, 296, 297]. PHAs have also been used as controlled-release agents for herbicides in agriculture which can potentially reduce the repeated need of herbicides on non target species[298].

In nano-composites

Silver nanoparticles (SNP) have attracted much attention because of their antibacterial properties. The dominant use of SNP is in cosmetics, antibacterial-water filters and also as drug carriers. But slurries of such particles tend to be unstable and therefore always need some biodegradable but stable polymer support. In this regard, use of a hydrophobic, biodegradable, renewable and non-cytotoxic biopolymer for stabilizing SNP particle would provide advantage for the synthesis, and transportation of the SNP colloids and their use in different biomedical applications. In the light of the above information, an experiment designed for stabilizing the colloidal solution of SNP by using bacterial polyhydroxyalkanoates was reported in our previous studies[299]. The hydrophobic nature of PHA would speed up the process of water filtration as water cannot access the surfaces and pores of these particles where SNP would be in touch with water. In cosmetic technology, the SNP–PHA might act as a consistent stabilizer and the stability may lead to increase in the duration of sun screen protection without adding excess of SNP.

Use in biosensors

Polyhydroxyalkanoates have also been used in the biosensors. Ma *et al.*[300] reported that myoglobin immobilized in P (3HB) film provides a model for constructing a third generation H_2O_2 biosensor. The side effects from the artemisinin class of medications are similar to the symptoms of malaria. A case of significant liver inflammation has been reported in association with prolonged use of a relatively high-dose of artemisinin for an unclear reason. In the treatment of severe malaria, parenteral artesunate have shown promising results by reducing mortality rate in South East Asian patients by 35% when compared to quinine. Therefore, it is very important to develop a simple, sensitive, fast, portable and reliable method for detection and quantification of artemisinin.

2.10 PCR based identification of the PHA biosynthetic genes

The genetic organization of PHA biosynthesis genes varies among PHA producing organisms. The type II of PHA biosynthetic genetic system consists of two PHA synthase genes (phaC1 and phaC2) separated by depolymerase phaZ gene. The type II system is commonly found in mcl-PHA producing *Pseudomonads*.

Solaiman *et al.*[301] reported a rapid and sensitive PCR procedure for the specific detection of phaC type genes using primer pair, I-179L and I-179R, based on the highly conserved sequences found in the coding regions of Pseudomonas phaC1 and phaC2 genes. Solaiman *et al.*[302] has reported the presence of PHA biosynthesis gene locus, phaC1 in *P. resinovorans* and this has subsequently been PCR cloned and expressed in *E. coli*. Zhang *et al.*[303] designed PCR-based cloning approach by using the highly conserved regions of PHA biosynthesis gene locus for cloning of PHA biosynthesis genes from *Pseudomonads*. A semi-nested PCR method was opted by Solaiman[304] for the specific and individual amplification of type II subgenomic fragments phaC1 and phaC2. The method was used to show that strains of *Pseudomonas oleovorans* harbor different pha loci. Jamil *et al.*[305] reported PCR base amplification of PHA polymerase genes C1 and C2 from chromosomal DNA. A portion of polymerase C1 and C2 genes of the pha operon was cloned and sequenced.

CHAPTER 3

MATERIALS AND METHODS

3.1 Plasticware/glassware used

All the sterilized polystyrene tubes were purchased from Tarson, India. The Erlenmeyer flasks and beakers were purchased from Borosil, Mumbai, India.

3.2 Chemicals used

All chemicals and reagents used were of analytical grade and procured from Merck India Ltd., SRL, Qualigen, Himedia, Sigma aldrich, and Bangalore Genei. Chromatography grade reagents were used for Gas chromatography mass spectroscopy (GC-MS) analysis and nuclear magnetic resonance (NMR) analysis.

3.3 Microbial strains

The biopolymer producing bacterium *Bacillus circulans* MTCC8167 was previously isolated by our laboratory from crude oil contaminated soil, taxonomically identified and was provided by my supervisor Prof. B. K. Konwar.

3.4 Equipment used

Equipments used in the present study are listed below:

1. Autoclave - Dainan Labtech, Co. Ltd
2. Deep freezer - New Bunswick Scientific, C34085
3. Laminar Hood - Reico
4. Centrifuge - Remi instruments
5. Cooling centrifuge - Remi cooling
6. Lyophilizer - Lyodel
7. Digital weighing balance - Metler Toledo
8. Water bath - Rectangular water bath, JSGW, India
9. Hot air oven -Remi
10. Incubator - EN500, Labtech
11. Incubator shaker - Scigenics, Orbitech, Biotech
12. Heating mentle - Rivotech, India
13. P^H meter - Cyberscan 500
14. Vortexer - Vortex shaker, JSGW, India

15. Sonicator - Ultrasonic homogenizer, OMNI International
16. UV spectrophotometer - Thermoscientific, UV-10, UV-VIS
17. Fourier transform infrared spectrophotometer (FTIR) - Perkin Elmer, Spectrum 100
18. GC-MS- Perkin Elmer, GC Varian 3800 model and Saturn 2,200 MS spectroscopy
19. NMR - JEOL JNN-ECS 400
20. Differential scanning calorimetry (DSC) - Shimadzu DSC-50 system
21. Thermo gravimetric analyser (TGA) - Shimadzu TGA-50
22. X-ray diffraction spectrophotometer (XRD) - Miniflex Table Top XRD model Rigaku Corporation
23. Photoluminescence spectrophotometer (PL) – Perkin Elmer model LS 55
24. Gel permeation chromatography (GPC) - Waters GPC system
25. Scanning electron microscopy (SEM) - JEOL JSM Model 6390 LV Asia PTE Ltd. Singapore model
26. Transmission electron microscopy (TEM)- JEOL JEM 2100 model
27. Fluorescence microscope - Nikon TS 100 model
28. Polymerase chain reaction (PCR) thermal cycler - Applied Biosystem
29. Electrophoresis system for DNA - Genaxy, horizontal electrophoresis chamber, Genaxy Scientific Pvt. Ltd.
30. DNA sequencer - Applied Biosystem, Hitachi, Lab India
31. Cyclic voltamery (CV) - Autolab Potentiostat/galvanostat, Eco Chemie, Netherlands
32. Electrochemical impedance spectroscopy (EIS) - potentiostat/galvanostat/ZRA Gamry Reference 3000, United States of America

3.5 Media composition

Different media were used during the investigation and the same are listed below.

3.5.1 Maintenance media

The maintenance media is a liquid or solid media designed to maintain the growth of microorganisms. This media contains all the essential nutritional elements for almost all bacterial growth. It is non-selective and used for the general cultivation and maintenance of bacteria kept in laboratory culture collections.

Components in gL^{-1} of distilled water:

Nutrient agar: Peptone: 5.0, NaCl: 5.0, Beef extract: 3.0, Agar: 15.0 (pH 7.0)

3.5.2 Inoculum media

The inoculum media is a culture media which provides appropriate biochemical and biophysical environment for cultivation and propagation of bacteria. This media is even employed in the isolation and maintenance of pure cultures of bacteria and is also used for identification of bacteria according to their biochemical and physiological properties.

Components in gL^{-1} of distilled water:

Luria Bertani medium: Tryptone: 10.0, NaCl: 10.0, Yeast extract: 5.0 (pH 7.0)

3.5.3 Production media

The production media is a type of media which is specific for growth of certain types of bacteria and contains specific substances which can allow the growth of the desired species. This type of media is also useful for identifying unknown bacteria.

Components in gL^{-1} of distilled water:

PHA detection medium (Modified medium of Rehman *et al.* [306]):

$(NH_4)_2SO_4$: 1.0, KH_2PO_4: 13.3, $MgSO_4$: 1.3, citric acid: 1.7, Glucose: 10.0

Trace element: 10 ml of (gL^{-1}, $FeSO_4 \cdot 7H_2O$ (10), $ZnSO_4 \cdot 7H_2O$ (2.25), $CuSO_4 \cdot 5H_2O$ (1), $MnSO_4 \cdot 5H_2O$ (0.5), $CaCl_2 \cdot 2H_2O$ (2.0), $Na_2B_4O_7 \cdot 10H_2O$ (0.23), $(NH_4)_6MO_7O_{24}$ (0.1), HCl (0.1 N) (pH 7.0)

3.6 Microbiological methods

3.6.1 Sterilization of the media and glass wares

Media used for various experiments were sterilized in flasks/tubes plugged with non-absorbent cotton at 121 °C and 15-lbs steam pressure for 20 min. Heat sensitive things were sterilized by proper filtration. Glass wares were sealed with autoclavable polypropylene bags before sterilization.

3.6.2 Collection of environmental samples

The collection areas were crude oil contaminated soil of Assam and Assam-Arkan Basin, ONGC, Jorhat, Assam; Numaligarh Refinery Limited (NRL) waste disposal depit, Numaligarh, Assam and Jagiroad Paper Mill, Nagaon, Assam. Soil samples were collected at random in sterile 50.0 mL polystyrene tubes. A minimum of five samples were collected from each location. A clean shovel was used to take the sample from an average depth of 15.0 cm below surface. This was done to avoid surface bacteria that were likely to be totally aerobic. Each sample was labelled properly with all the related information.

3.6.3 Pure culture of biopolymer producing bacterial isolates

Pure culture of the isolated bacterial strains was established by following the standard procedure. At first, a loopful of bacterial culture was inoculated in nutrient broth with pH adjusted to 7.0 with a 0.5 growth OD at 600 nm. After that 100 µl of culture from the above culture was mixed in 0.9 % (w/v) sterile normal saline and serially diluted upto 10^{-7} with a final volume of 2.0 mL. From the above dilution, 100 µl aliquot was taken and spread over sterile nutrient agar plates and kept for 24h at 37 °C in order to obtain single distinct colonies. For isolation of single pure colony, following techniques were used:

(i) Spread-plate method.

(ii) Streak-plate method.

(i) Spread-plate method

In this method the individual colonies are separated from the culture of mixed populations of micro-organisms. The microorganisms were spread over the

solidified agar medium with a sterile L-shaped glass rod while the Petri dish was spun on a turntable. The cells were separated from each other allowing for formation of colonies without overlapping.

(ii) Streak-plate method

This method offers a scope to obtain discrete colonies and pure cultures. A sterilized loop or transfer needle was dipped into a suitable diluted suspension of bacterial culture which was then streaked on the surface of a solidified agar plate to make a series of parallel, non-overlapping streaks. The plates were incubated at 37 °C for a period in inverted position to get the pure bacterial colonies.

3.6.4 Routine maintenance and preservation of microorganisms

Pure cultures of bacteria were preserved at 4 °C in nutrient agar slants for short time storage and sub cultured by transferring them to fresh slants at an interval of one month. The isolates were also stored in 15 % (v/v) glycerol in nutrient broth and kept at -80 °C for long term storage.

3.6.5 Taxonomic identification of biopolymer producing bacteria

The selected biopolymer producing bacteria were taxonomically identified by (a) standard biochemical tests, (b) studying their morphological characteristics and (c) ribotyping.

3.6.6 Inoculum preparation

Inoculum of the isolated bacterial strains was prepared by transferring single colony from a 24 h old culture plate into 5.0 mL of nutrient broth or LB broth and allowed to incubate at 180 rpm and 37 °C overnight. This seed culture was used for inoculating the production medium at 10^5 v/v. The number of viable cells was presented as CFU/mL by using hemocytometer.

3.7 Polyhydroxyalkanoate (PHA) production

3.7.1 Shake flask culture

An aliquot of 10.0 mL of the above pre-culture inoculum was transferred to 250 mL Erlenmeyer flask containing 100.0 mL sterile PHA medium with the corresponding carbon source (glucose) and then kept at 37 °C and 180 rpm for 48 h. Bacterial growth in the medium was observed by the increase in the turbidity of the culture medium. The flask cultures were harvested and assayed for PHA production. All experiments were carried out in triplicates.

3.7.2 Gram's staining

Crystal violet: 2 gm of crystal violet was dissolved in 20.0 mL of 95 % ethanol and the volume was made up to 100.0 mL with distilled water.

Gram's iodine: 1 gm of iodine was dissolved in 300.0 mL of potassium iodide solution (1 gm/300 mL)

Decolourizer: Absolute alcohol (95% ethyl alcohol)

Safranin stain: 2.0 gm of safranin was dissolved in 20.0 mL of 95% ethyl alcohol and the volume made up to 100.0 mL with distilled water.

Procedure

A thin smear of the 24h old bacterial culture was prepared on a clean glass slide and kept for 5-10 min for air drying followed by heat fixation. Few drops of crystal violet was flooded over the bacterial culture and allowed to stand for 1 min. The excess stain was washed off with distilled water. Gram's iodine was poured over it after primary staining and kept at room temperature for 1 min. The smear was rinsed by washing under tap water followed by addition of a few drops of decolourizer to remove the excess stain. It was washed again with tap water to remove the decolourizer followed by addition of counter stain safranin for 45 seconds. The counterstain was removed with tap water and the slide was kept at room temperature for air-drying. The bacteria were observed under the light microscope (100X).

3.7.3 Staining for intracellular PHA detection

3.7.3.1 Staining of cells with Sudan black B[108]

Bacterial colonies grown on nutrient agar plates were transferred by replica plating to nitrogen-deficient carbon containing medium and incubated at 37 °C for 3 days. Sudan Black B solution (0.02% w/v in 96% ethanol) was prepared and stained for 20 min. The dye was removed after 20 min and the plates were treated for 1 min with 10.0 mL of 96% ethanol. Colonies containing PHA rich cells retained the dye and appeared dark blue.

3.7.3.2 Staining of cells with Nile Blue A[109]

The presence of PHA granules inside the growing bacterial cells was confirmed by fluorescence microscopy after staining with Nile blue A following the method of Ostle and Holt[109]. For the experiment, a loopful of bacterial cells was heat-fixed and stained with 1% aqueous solution of Nile blue A. The stain was mildly heated and filtered before use[109]. After the staining, slides were washed with tap water followed by 8% acetic acid solution for 1 min, washed again, and finally the stained smear was blotted dry with the bibulous paper (remoistened with tap water) and covered with a glass cover slip. The stained smear was observed under the fluorescence microscope at an excitation wavelength of 460 nm to detect the presence of intracellular PHA granules.

3.8 Morphological characterization of bacteria

The bacterial isolates were characterized by observing their different morphological traits, such as:

1. Size and shapes of bacterial colonies
2. Forms of bacterial colonies
3. Margins of bacterial colonies
4. Elevation of bacterial colonies
5. Different pigments of bacterial colonies

3.9 Biochemical characterization study

Biochemical tests conducted for the biochemical characterization of the bacterial isolates were described as follows:

3.9.1 Catalase test

The test was performed to determine the presence of catalase enzyme in the bacterial isolates. 10.0 mL of trypticase soy agar (TSA) slant was streaked with a loopful of 24h bacterial culture and kept at 37 °C for 48 h. 3% (v/v) hydrogen peroxide (H_2O_2) was added to detect catalase production by the bacterial isolates. If bubble formation was observed, it indicated the catalase positive test (production of catalase by bacteria).

Composition of TSA medium:

Pancreatic digest of casein	17.0 gL^{-1}
Enzymatic digest of soybean meal	3.0 gL^{-1}
Dextrose	2.50 gL^{-1}
NaCl	5.0 gL^{-1}
K_2HPO_4	2.50 gL^{-1}
Agar	20.0 gL^{-1}
pH	7.3

3.9.2 Urease test

To detect the production of urease enzyme by the bacterial isolates, urease test was performed. 0.1 mL of 24 h bacterial culture was inoculated in 10.0 mL of sterile urea broth and kept at 37 °C for 48 h. Positive isolates degraded urea present in the urea broth medium by means of urease enzyme. If the phenol red in the medium turned to deep pink, it indicated the presence of urease activity.

Composition of Urea broth:

Urea	20.0 gL^{-1}
Na_2HPO_4	9.50 gL^{-1}
KH_2PO_4	9.10 gL^{-1}
Yeast extract	0.10 gL^{-1}
Phenol red	0.01 gL^{-1}
pH	6.8

3.9.3 Citrate test

The citrate test was performed to detect the production of citrase enzyme by the bacterial isolates. 10.0 mL of sterile Simmons citrate agar slants were prepared and inoculated with 24 h of bacterial culture and kept at 37 °C for 48 h. It was followed by the addition of bromo-thymol blue indicator over the surface. Positive isolates used citrate as the sole source of carbon, producing citrase enzyme in the medium. If citrate is utilized, the bacteria produce alkaline products by changing the colour of bromothymol blue from green (at neutral pH 6.9) to blue (at higher pH 7.6) in the medium.

Composition of Simmons citrate agar slant medium:

Magnesium sulphate	0.2 gL^{-1}
Ammonium dihydrogen phosphate	1.0 gL^{-1}
Potassium phosphate	1.0 gL^{-1}
Sodium citrate	2.0 gL^{-1}
Sodium chloride	5.0 gL^{-1}
Bromothymol blue	0.08 gL^{-1}
Agar	15.0 gL^{-1}
pH	6.8

3.9.4 Triple sugar iron test

The test in tryptic nitrate broth with three sugars and iron was carried out in order to differentiate bacteria for their ability to ferment glucose, lactose and sucrose or to reduce sulphur to hydrogen sulphide. A loopful of 24 h bacterial culture was streaked over TSI agar slants and kept at 37 °C for 48 h. Changes in medium colour were observed over TSI agar slants.

Composition of Triple sugar iron medium:

Casein enzymatic hydrolysate	10.0 gL^{-1}
Peptic digest of animal tissue	10.0gL^{-1}
Yeast extract	3.0 gL^{-1}
Beef extract	3.0 gL^{-1}
Lactose	10.0 gL^{-1}
Sucrose	10.0gL^{-1}
Dextrose	10.0gL^{-1}
Ferric ammonium citrate	0.3 gL^{-1}
Sodium chloride	5.0 gL^{-1}
Sodium thiosulphate	0.3 gL^{-1}
Phenol red	0.024 gL^{-1}
Agar	12.0gL^{-1}
pH	7.4

3.9.5 Nitrate reduction test

The test conducted in the tryptic nitrate medium detects the ability of an organism to reduce nitrate (NO_3) to nitrite (NO_2) or some other nitrogenous compounds such as molecular nitrogen (N_2) using the enzyme nitrate reductase. The nitrate medium contains potassium nitrate as the substrate. 1.0 mL of 24 h of bacterial culture was inoculated in 100.0 mL of sterile trypticase nitrate broth and kept at 37 °C for 48 h. To confirm the nitrate reduction capability of bacterial culture post 48 h of incubation, solution A (sulfanilic acid), solution B (alpha-naphthylamine) and trace amounts of zinc powder were mixed with bacterial culture. If the organism reduces NO_3 to NO_2, the nitrite would react with sulfanilic acid and α- naphthylamine to produce a cherry red colour. If no colour is developed, it indicates either of the following two reactions: (i) nitrate is not reduced or (ii) nitrate is reduced even further to compounds other than nitrite (NH_2 or N_2).

Composition of Tryptic nitrate medium:

Casein enzymatic hydrolysate	20.0 gL^{-1}
Disodium phosphate	2.0gL^{-1}
Dextrose	1.0gL^{-1}
KNO3	1.0 gL^{-1}
Agar	1.0 gL^{-1}
pH	7.6

3.9.6 Indole production test

The indole test was used to identify bacteria capable of producing indole by using the enzyme tryptophanase. Sterile sulphide indole motility (SIM) agar deep tubes were streaked with 24 h bacterial culture over agar surface and kept at 37 °C for 48 h. The by-product indole was identified by this test on addition of Kovac's reagent containing hydrochloric acid and dimethylaminobenzaldehyde and amyl alcohol, a red layer formation referred to the presence of indole.

3.9.7 H_2S production test

This test was used to identify those bacteria capable of reducing sulphur. In this test a loopful of 24 h bacterial culture was inoculated inside the 10.0 mL of sulphide indole motility medium (SIM) agar slants and kept at 37 °C for 48 h. The medium contained cysteine, an amino acid containing sulphur, and sodium thiosulfate with peptonized iron or ferrous sulfate. Formation of black precipitate indicated that the test would be positive for hydrogen sulphide (H_2S) production by anaerobic respiration of bacterial culture. No precipitate formation would refer to a negative test.

Composition of the Sulphide indole motility agar medium (SIM):

Pancreatic digest of casein	20.0 gL^{-1}
Peptic digest of animal tissue	6.1 gL^{-1}
Fe $(NH_4)_2(SO_4)_2.6H_2O$	0.2 gL^{-1}
$Na_2S_2O_3.5H_2O$	0.2 gL^{-1}
Agar	3.5 gL^{-1}
pH	7.3

3.9.8 Litmus milk reaction test

This test was used to identify bacteria capable of transforming the different milk substrates enzymatically into varied metabolic end products. 10.0 mL of sterile litmus milk broth was inoculated with 0.1 mL of 24 h bacterial culture and kept at 37 °C for 48 h. After 48 h of incubation any changes in medium colour, lactose fermentation, gas formation, curd formation, litmus reduction, peptonization and alkaline reaction were observed.

Composition of Litmus milk medium:

Skim milk powder	100.0 gL^{-1}
Litmus	0.5 gL^{-1}
Sodium sulphate	0.5 gL^{-1}
pH	6.8

3.9.9 Methyl red-Voges-Proskauer (MR-VP) test

(a) Methyl red (MR) test[307] was carried out to test the ability of an organism to produce and maintain stable acid end products from the glucose fermentation. In this test, 100.0 mL of sterile methyl red-Voges-Proskauer (MR-VP) broth was inoculated with 1.0 mL of 24 h bacterial culture and kept at 37 °C for 48 h. MR-VP medium was separated into parts A and B. In part A, the pH indicator methyl red was added for confirmation of MR test which detects the presence of large concentrations of acid end products. If the tube turns red in colour, it indicates a positive test and if yellow, it indicates a negative result.

(b) In part B, mixtures of Barritt A and B solutions were added in VP broth. .The Voges-Proskauer (VP) test was used to determine the capability of organisms to produce non-acidic or neutral end products, such as acetylmethylcarbinol (acetoin), a neutral product formed from pyruvic acid in the course of glucose fermentation. The reagent used in the VP test is Barritt's reagent [307] which consists of a mixture of alcoholic α-naphthol and 40 % potassium hydroxide. After 15 minutes of addition of Barritt's reagent a deep rose colour in the culture is developed indicating the presence of acetoin and this represented a positive result. The absence of rose colouration was a negative result.

Composition of MR-VP broth:

Buffered peptone	7.0 gL^{-1}
Dextrose	5.0 gL^{-1}
Dipotassium phosphate	5.0 gL^{-1}
pH	6.9

3.9.10 Extracellular enzyme activity (hydrolysis) test medium

(a) To determine the ability of microorganisms to secrete extracellular hydrolytic enzymes capable of degrading polysaccharides, lipids and proteins (casein and gelatin). The hydrolysis test was carried out in the concerned medium. The test was used to differentiate microbes based on their ability to hydrolyse starch with exoenzyme amylase.

(b) Tributyrin agar was used to determine the hydrolytic activity of lipase as produced by the tested microorganisms. The medium was composed of nutrient agar supplemented with triglyceride tributyrin as the lipid source. In the experiment, milk agar was used to determine the hydrolytic activity of the enzyme. The positive bacterial isolates could produce a clear zone surrounding their growth loosing opacity. But in the absence of protease activity, the medium surrounding the growth of the bacteria remains opaque, which confirms a negative reaction.

(c) Gelatin liquefaction test was used to determine the ability of bacteria to produce hydrolytic exoenzymes called gelatinases that digest and liquefy gelatin. The presence of these enzymes, as determined by the liquefaction, was used for identifying certain bacteria.

Starch agar composition:

Peptone	5.0 gL^{-1}
Beef extract	3.0 gL^{-1}
Starch	2.0 gL^{-1}
Agar	15.0 gL^{-1}
pH	7.0

Tributyrin agar composition:

Peptone	5.0 gL^{-1}
Yeast extract	3.0 gL^{-1}
Agar	15.0 gL^{-1}
pH	6.9

Milk agar composition:

Peptone	5.0 gL^{-1}
Skim milk powder	100.0 gL^{-1}
Agar	15.0 gL^{-1}
pH	6.9

Nutrient gelatin composition:

Peptone	5.0 gL^{-1}
Beef extract	3.0 gL^{-1}
Gelatin	120.0 gL^{-1}
pH	6.8

3.9.11 Carbohydrate fermentation medium

This biochemical test was performed to determine the ability of microorganisms to degrade and ferment carbohydrates with the production of acid and/or gas. For this purpose, different types of carbohydrate enriched media were used:

Composition of phenol red lactose, dextrose and sucrose broths: (in gL^{-1})

Chemicals	Phenol red lactose	Phenol red dextrose	Phenol red sucrose	Phenol red xylose	Phenol red mannitol
Protease peptone	10.0	10.0	10.0	10.0	10.0
Beef extract	1.0	1.0	1.0	1.0	1.0
Sodium chloride	5.0	5.0	5.0	5.0	5.0
Phenol red	0 018	0.018	0.018	0.018	0.018
Lactose	10.0	-	-	-	-
Dextrose	-	1.0	-	-	-
Sucrose	-	-	5.0	-	-
Xylose	-	-	-	5.0	-
Mannitol	-	-	-	-	5.0
pH	7.4	6.9	6.9	6.8	6.8

Fermented carbohydrates with the production of acidic wastes might cause yellowing of phenol from red colour, thereby indicating a positive reaction. In some cases, acid production is accompanied by the evolution of CO_2 gas which becomes visible as bubbles in the inverted tube. Cultures that are not capable of fermenting carbohydrates are negative ones.

3.10 Analytical techniques

3.10.1 Biomass estimation

Biomass was estimated by the gravimetric method. The culture samples of bacteria were taken in a polypropylene tube and centrifuged at 8,000 rpm for 15 min. The precipitated cells were washed with distilled water and dried at 60 °C in a hot air oven until a constant weight was achieved.

3.10.2 Polymer extraction and purification

For the extraction of PHA, biomass of the bacterial cells was harvested by centrifugation of the culture broth at 8,000 rpm. The cell pellet was washed twice with sterilized distilled water and lyophilized. PHA was extracted from the dry biomass by using soxhlet extraction for 24 h using chloroform. The PHA was then

concentrated by rotary vacuum evaporator and precipitated with 10 volumes of ice-cold methanol. The process was repeated thrice for getting the purified polymer [308] and the precipitated polymer was collected by air drying.

3.10.3 *Quantification of* PHA

3.10.3.1 Gravimetric method

PHA content of the bacterial cells was determined gravimetrically[112]. The PHA dissolved in chloroform obtained from soxhlet extraction was washed with ice cold methanol to get purified product. The product was then collected by air drying, weighed and PHA concentration was expressed as % of cellular dry weight (CDW).

% PHA=Weight of PHA x 100/ Weight of biomass

3.10.4 Characterization of PHA

3.10.4.1 UV-Visible spectrophotometer analysis

UV-Visible (UV-Vis) spectrophotometer provides the information about the structure and stability of the materials in both solid and liquid form. Different kinds of electronic excitation may occur in the molecules by absorbing the energies available in the UV-Vis region. The spectrophotometer records the wavelength at which absorption occurs, together with the degree of absorption at each wavelength. The resulting spectrum is presented graphically pertaining absorbance versus wavelength. UV-Visible spectra were recorded on a UV-10, UV-VIS spectrophotometer using chloroform.

3.10.4.2 FTIR analysis

FTIR characterization of the PHA containing cells and that of the purified PHA were done using Perkin Elmer, Spectrum 100 FTIR spectrometer to evaluate the functional groups of the compounds. Purified PHA sample was mixed with potassium bromide (KBr) using a clean and smooth mortar and pestle. After mixing for three minutes, the mass was transferred to a pellet preparation instrument, and a solid pellet was prepared using hydraulic pressure. The pellet was transferred to the holder of the FTIR spectrometer. The spectra were recorded in the range 400 - 4000 cm^{-1}.

3.10.4.3 GC-MS analysis

PHA composition was analysed by gas chromatography using either lyophilized cells or purified polymer samples. To determine the polymer content of the bacterial cells, freeze dried cell samples were subjected to methanolysis in the presence of sulphuric acid according to Brandl *et al.*[38]. In this method approximately 4.0 mg of the bacterial cells was reacted in a screw cap test tube with a solution containing 1.0 mL chloroform, 0.85 mL methanol and 0.15 mL sulphuric acid for 140 min at 100 °C in a thermostat-equipped oil bath. Under this condition, the intracellular PHA was degraded to its constituent 3-hydroxyalkanoic acid methyl esters. After the reaction, 0.5 mL distilled water was added and the tube was vigorously shaken for 1 min. After the phase separation, the bottom organic phase was collected, dried over anhydrous sodium sulphate, filtered and analysed[309]. The methyl esters were analysed by gas chromatography with a Perkin Elmer, GC Varian 3800 model and Saturn 2,200 MS spectroscopy equipped with a CP-Sil 8 CB and CP-Sil 5 CB capillary column and a flame ionization GC detector and quadruple ion trap MS detector. A 2.0 µl portion of the organic phase was analysed after split injection (spilt ratio 1:40) and helium (35cm/min) was used as a carrier gas. The temperature of the injector and the detector were maintained at 230 °C and 275 °C, respectively. For efficient separation of the methyl esters the following temperature program was used: 120 °C for 5 min, temperature rise of 8 °C min^{-1}, 180 °C for 12 min. P (HB) and P (HB-CO-HV) were used as standards. Benzoic acid was used as an internal standard.

3.10.4.4 NMR analysis

To confirm the chemical structure of PHA, ^{1}H and ^{13}C NMR analyses were carried out. The spectra were measured with JEOL JNN-ECS 400 spectrophotometer. A sample of 20.0 mg purified polymer was dissolved in 1 mL deuterated chloroform ($CDCl_3$) and analysed with ^{1}H NMR (400 MHz) and ^{13}C NMR (400 MHz) at 25 °C. Chemical shifts were reported in ppm relative to the signal of tetramethylsilane.

3.10.4.5 Crystallinity study by XRD

X-ray diffraction measurements were done with a Miniflex Table Top XRD model Rigaku Corporation and a Ni filter. The X-ray diffractogram obtained from the polyester pellet samples was aged at room temperature to reach crystallinity equilibrium prior to analysis and recorded at 27 °C in the range 2θ=5°-70° at a scan rate of 0.01/10s. The crystallinity degree (Xc) was calculated from normalized diffractogram data recorded from the relation:

Xc = [(total area)-(amorphous area)] / (total area).

3.10.4.6 Surface study by SEM

A microstructural study for the surface topography of the isolated polymer was done by using a (JEOL JSM Model 6390 LV Asia PTE Ltd. Singapore). Samples were placed in aluminium stubs of 8 mm diameter and then coated with platinum using the spluttering device. The SEM images were taken with an acceleration voltage of 15 kV (maximum) to avoid incineration of the polymer due to the beam heat.

3.10.4.7 Determination of molecular weight by GPC

The molecular weight of the isolated polymer was determined by gel permeation chromatography (GPC) using Waters GPC system. The PHA was dissolved in tetrahydofurane (THF) and analyzed by running at room temperature. A polystyrene standard with a low polydispersity was used to generate a calibration curve equipped with serially connected RI detector. The molecular weight of the product was determined with no further corrections and THF was used as an eluent at the flow rate of 0.5 $mL.min^{-1}$ and 40 °C temperature.

3.10.4.8 Thermal property

3.10.4.8.1 DSC analysis

DSC data of the polymer sample (3 mg) encapsulated with aluminium pans, heating at -30 °C–300 °C was recorded at a heating rate of 20 $°C.min^{-1}$ on a Shimadzu DSC-50 system equipped with a cooling accessory under a nitrogen flow of 30 $mL.min^{-1}$. The testing temperature was maintained at 150 °C for 1 min and quenched

to -30 °C at a rate of -20 °C.min^{-1}. Subsequently, the polymer sample was reheated from -30 °C–300 °C at a heating rate of 20 °C.min^{-1}. The midpoint of increasing step was taken as the glass transition temperature (Tg). An endothermic peak was observed upon heating, and the temperature at the peak was taken as the melting temperature (Tm).

3.10.4.8.2 TGA analysis

The thermal stability and decomposition profile of the polymer sample was determined by using Shimadzu TGA-50 thermogravimetric analyzer which operated at a nitrogen flow rate of 10 mL.min^{-1}. The sample was weighed to ca. 10.0 mg and placed in a platinum pan and heated from 30 °C–600 °C at the heating rate of 10 °C.min^{-1} under a nitrogen atmosphere. The decomposition temperature was recorded from the thermograms to the maximum degradation temperature and determined by analysis of the derivative weight loss curve over temperature.

3.10.4.9 PL study

Photoluminescence spectroscopy is used to analyse fluorescent compounds at very low concentration in both solid and liquid states. Ions or molecules show fluorescence spectra when they absorb electromagnetic radiation at short wavelengths (higher energy) and are capable of radiating at longer wavelengths (lower energy). Photoluminescence spectra were recorded using a Perkin Elmer model LS 55 spectrophotometer, using excitation of the polymer at maximum absorption wavelength. The photoluminescence spectrum of the polymer solution was recorded in the chloroform solvent. Photoluminescence of solid state polymers were measured by preparing the polymer film on the glass substrate. The emission was recorded at two different wave lengths for all the polymers.

3.11 *In vitro* biodegradation study of PHA using different soil microorganisms

3.11.1 Preparation of polymer film

The extracted polymer from isolated bacteria was dissolved in chloroform in a specific amount and cast over a cover slip (2.0 cm^2) homogenously. The film was

kept for 24–36 h at room temperature undisturbed to get a thin film of the PHA polymer.

3.11.2 Microorganisms used

In the present investigation, bacteria and fungi species isolated from crude oil contaminated soils of Assam were used to degrade the extracted polymer. Bacteria used were *Pseudomonas aeruginosa* strains BP4, BP5, BP7, *Bacillus subtilis* (R38-I), *B. circulans* (MTCC8167), *Alacaligens faecalis* (MTCC8164), *P. aeruginosa* (MTCC7815), *Mycobacterium* spp (G-35I). The two fungal strains used were *Candida albicans* (MTCC 3017) and *Fusarium oxysporum* (NCIM 1281). Bacterial and fungal strains used were maintained on the Nutrient agar and Sabouraud dextrose (SD) agar slants, respectively. Mineral salt medium used in the investigation was composed of KNO_3, 2; K_2HPO_4, 1; KH_2PO_4, 0.7; $MgSO_4 \cdot 7H_2O$, 0.7 gL^{-1} in distilled water and the pH adjusted to 7.0. Accordingly, fungal species were grown on SD medium for the polymer degradation test. Aliquots (10.0 mL) of the mineral salt medium and SD medium were dispensed in 100.0 mL conical flasks, each inoculated with 5 pieces of PHA films (2.0 cm^2). Flasks were incubated at 37 °C and 30 °C for bacteria and fungi, respectively for 36 days. The experiment was performed in triplicates. Two flasks containing mineral salt medium and SD medium separately with no PHA film were used as the control for the bacterial and the fungal species, respectively. After completion of incubation, the PHA films were taken out and washed with sterile distilled water. The effect of microbial treatment was monitored by SEM and FTIR.

3.11.3 SEM observation

The surface topology of the PHA films, incubated in sterile fluid for 36 days and those inoculated with bacteria and fungi were analysed through optical microscope (JEOL JSM Model 6390 LV Asia PTE Ltd. Singapore) to verify any structural changes. Images obtained by the SEM analysis on the treated and untreated samples were analysed on comparative basis.

3.11.4 FTIR spectroscopy analysis

FTIR analysis was done to detect the degradation of PHA by using a Perkin Elmer, Spectrum 100 instrument. Part of the polymer film was mixed with KBr and made into a pellet, which was fixed to the FTIR sample plate. Spectra were recorded in triplicates (400–4000 cm^{-1}) for each sample.

3.12 Application of PHA in enhancing the stability of colloidal silver nanoparticles (SNP)

3.12.1 Synthesis of SNP in PHA dispersed colloid

The PHA suspension (0.5%) in distilled water was prepared by sonication for 3 h using ultrasonic water bath homogenizer. The PHA inclusion bodies in the bacterial species *B. circulans* (MTCC 8167) were stained with Nile blue A and observed under the fluorescent light (100 X magnifications). From the PHA stock, an aliquot of 5.0 mL was taken in a 250 mL Erlenmeyer flask and the volume was adjusted to 30.0 mL to get 0.002M sodium borohydride ($NaBH_4$). The Erlenmeyer flask was placed into an ice bath and was allowed to cool for 20 min. The assembly was stirred gently using a magnetic stirrer. Then, 10.0 mL of 0.001M $AgNO_3$ solutions was added drop wise, about 1 drop per second, until the whole amount was used up. After the addition of silver nitrate, the solution turned light yellow in colour and the SNP was synthesized in the PHA dispersed colloidal solution.

3.12.2 Fourier-transform-infrared (FTIR) spectroscopic analysis

The IR (Nicolett Impact 410 spectrometer) spectra of the virgin biopolymer and SNP–PHA samples were recorded using KBr pellet. Spectra showing the functional group were used to study the composition of the biopolymer. The absorption spectra were plotted using a built-in plotter. The spectra were obtained from 400–4000 wave numbers (cm^{-1}). Samples were prepared by dispersing the solid uniformly in a matrix of dry nujol (KBr) mull, compressed to form an almost transparent disc.

3.12.3 Stability analysis of SNP solution using UV-Vis spectrophotometer

Three different solutions of SNP were prepared in triplicates, each containing 0.08% PHA in 30.0 mL distilled water. The bright yellow colour of the solution is a proof of the presence of SNP with a maximum absorption at about 400 nm and the solution was labelled as SNP–PHA *in situ*. Another solution of SNP synthesized by mixing pure SNP colloids and PHA-dispersed solution of 0.25 % (w/v) at 1:1ratio was labelled as SNP–PHA mixture. The analysis was carried out following the principle of absorption maxima shifted towards the longer wavelength and simultaneously the colour of the colloid changed to violet and sometimes greyish as the particles settled down. Based on the spectroscopic data, all three types of SNP colloidal solutions (SNP, SNP–PHA mixture and SNP–PHA *in situ*) were recorded for 30 days with an interval of 5 days in between.

3.12.4 TEM analysis

The colloid prepared in the PHA-dispersed solution was spread on the TEM (JEOL JEM 2100.model). The stub and sample preparations were done using the standard protocol. Consequently each sample was examined.

3.13 Photoluminescence study of the nanoparticles-biopolymer hybrid

3.13.1 Experiment

The fluorescence behavior of PHA polymer extracted from *P. aeruginosa* JQ866912 was studied for the development of a method to estimate different nanoparticles in solution. PHA polymer was prepared by dissolving in chloroform (1.4%). The metal oxide nanoparticles ZnO, NiO and CuO were gifted by Prof. S. K. Dolui, Chemical Sciences, Tezpur University, India. Different concentrations of ZnO, NiO and CuO were mixed with the polymer solution by constant sonication for about 30 min. All PHA-nanoparticle hybrid mixtures were cast on a glass slide and dried in vacuum for the further characterization.

3.13.2 Characterization

For the determination of the size of the nanomaterials, XRD was used. By this technique the crystal size of the nanomaterials and average size of the particles in

the matrix can be detected. XRD study for the biopolymer-nanoparticles was done using Miniflex, Rigaku (Japan) with CuKα radiation (λ = 0.15418 nm) at 30 kV and 15 mA with scanning rate of 0.005 S^{-1} in a 2θ range of 30–70 °.

The optical properties of the PHA-nanoparticles hybrid materials were determined by UV-vis spectroscopy and PL spectroscopy. The distribution of the nanoparticles within the PHA biopolymer matrix and the surface study of the hybrid materials were analysed by using SEM.

3.14 Application of PHA for composite based biosensor preparation with gold nanoparticles (AuNPs) for the detection of antimalarial drug 'artemisinin'

3.14.1 Reagents and materials

Artemisinin (99% purity) was gifted by Dr. N.C. Baruah, Natural Product Chemistry Division, CSIR-NEIST, India. Horse Radish Peroxidase (HRP), aniline monomer (99.5%) of analytical grade, ITO coated glass plates were purchased from Sigma Aldrich (Germany). Serum sample was provided by CSIR-NEIST, Clinical Centre from healthy volunteers and kept frozen at -20 °C for further use. After gentle thawing, the serum sample was spiked with appropriate concentrations of the drug for testing. For experimental investigations, stock solution of artemisinin was prepared by direct dissolution of 1.0 $mg.mL^{-1}$ of artemisinin in freshly prepared 0.05M phosphate buffer saline (PBS) of pH 7.0±0.1. Simultaneously, standard working solutions were prepared by appropriate dilutions of the stock solution. Potassium ferrocyanide $[Fe(CN)_6]^{3-/4-}$ containing PBS of 200 ml capacity with ionic strength 0.05 M in the pH range 5.5-9.0 were prepared in deionized water (TKA Millipore water system) by adding appropriately measured amounts of mono sodium dihydrogen phosphate (NaH_2PO_4), disodium mono hydrogen phosphate (Na_2HPO_4) and the pH was adjusted with 1.0 M HCl and 0.1 M NaOH solution. All the reagents used in the present study were of analytical and molecular biology grade and obtained from Sigma Aldrich.

3.14.2 Characterization

Electrochemical measurements were performed using Autolab Potentiostat/galvanostat (Eco Chemie, Netherlands) with NOVA software and

potentiostat/galvanostat/ZRA (Gamry Reference 3000, USA) with Gamry Echem Analyst Software in which working electrode was replaced with PHA/ITO, PHA/AuNPs/ITO and PHA/AuNPs/HRP/ITO. Platinum wire and Ag/AgCl (3 M KCl) were used as counter and reference electrodes, respectively. CV and EIS were carried out in a 20.0 mL Dr Bob's electrochemical cell stand. The surface topology of respective films was studied by using SEM (JEOL-JSM-6390LV).

3.14.3 Preparation of PHA-Au nanocomposite film

The isolated polymer from *P. aeruginosa* JQ866912 isolate was used to prepare the composites; PHA-Au nanocomposite was prepared by mixing 20.0 µl of PHA solution (3.0 $mg.mL^{-1}$) and 80.0 µl of AuNPs in water (3.0 $mg.mL^{-1}$) and sonicated for 30 min. The mixture was cast over ITO glass plate (0.25 cm^2), 1 with normal casting and 1 with deep coating in specialized chamber.

3.14.4 Immobilization of HRP on PHA-Au nanocomposite film

The bio-electrode for the detection of artemisinin was prepared by immobilizing HRP enzyme (1.0 $mg.mL^{-1}$ solution in phosphate buffer, pH 7.0±0.1) onto the PHA-Au nanocomposite by adsorption technique (in a specially assembled cell) and incubated overnight at 4 °C. In one experiment glutaraldehyde was used as a cross linker, but in the other, none. The condition for the immobilization of the enzyme was used based on prior studies [310, 311]. To remove loosely-bound materials, the biosensors were rinsed with phosphate buffer saline and preserved at 4 °C with pH 7.0±0.1 in the buffer solution for further use.

3.14.5 Preparation of artemisinin samples

Artemisinin solution was prepared in water (0.0011mg.100 mL^{-1}) by sonicating for 3 h as it is sparingly soluble in water. The stock solution of artemisinin was supplemented with the freshly prepared 0.05M PBS (pH 7.0±0.1) to make the desired concentrations. Prior to measurements, human serum samples used were centrifuged and diluted 10 times with the buffer solution. The standard addition method was used for analyzing the pharmaceutical samples and

artemisinin-spiked human serum samples for the validation of the modified electrode.

3.15 Isolation of chromosomal DNA

DNA extraction by alkaline lysis

Genomic DNA from bacteria was prepared as described by Sambrook *et al.*[312]. The cells were pelleted by spinning 4 mL of fresh bacterial culture at 9,450 x g for 10 min in a refrigerated Beckman Centrifuge, UK and supernatant was decanted. The supernatant was then discarded and pellet was dissolved in 0.8 mL of solution I (50.0 mM glucose, 25.0 mM Tris cl pH 8.0, 10.0 mM EDTA pH 8.0) and vortexed. To this resultant mixture, 160.0 µl of lysozyme (10.0 $mg.mL^{-1}$) was added and incubated at room temperature (24 °C) for 20 min. Subsequently, 44.5 µl of 10 % (w/v) SDS solution was added and re-incubated for 10 min at 50 °C. After that, 53.3 µl of RNase (10.0 $mg.mL^{-1}$) was added to the above sample and incubated at 37 °C for 90 min. This was followed by addition of 45.3 µl of Na-EDTA (0.1 M, pH-8.0) and re-incubated at 50 °C for 10 min. To remove the protein, 26.6 µl of proteinase K (5.0 $mg.mL^{-1}$ stock) was added and incubated at 50 °C for 10 min. Equal volume of phenol (saturated with 0.1 M Tris HCl, pH-8.0) was added to the above solution and mixed thoroughly. The mixture was centrifuged at 9,450 x g for 10 min, the upper (aqueous) phase was aspirated into sterile microfuge tube and lower phase was discarded. Then 700.0 µl of (1:1) phenol and chloroform-isoamyl alcohol (24:1) were added and mixed thoroughly. Following centrifugation at 9,450 x g for 10 min, the upper phase was transferred to a sterile microfuge tube and then equal volume of chloroform-isoamyl alcohol (24:1) was added and spun at 9,450 x g for 10 min. The upper phase was transferred to a sterile microfuge tube and $1/10^{th}$ volume of sodium acetate (3M, pH-7.0) was added to it. The DNA was precipitated by adding 2 volumes of ice-cold absolute ethanol in the above solution and the DNA-pellet and was recovered by centrifugation. After removal of alcohol, DNA was resuspended in 10mM Tris HCl-1mM EDTA buffer (pH-8.0) and was stored at 4 °C for further used.

3.15.1 Agarose gel electrophoresis

Reagents: 0.8% agarose gel, 50X and 1X TAE buffer, loading dye and ethidium bromide solution.

Procedure:

- 0.8% agarose gel was prepared with 2% 50X TAE buffer and poured into the gel caster sealed with adhesive tape and fitted with comb.
- The comb and adhesive tape were removed when agarose gel was solidified completely.
- After that the gel was placed in the electrophoresis chamber filled with 1X TAE buffer.
- DNA sample preparation: The DNA samples were mixed with 2.0µl of loading dye for 5.0-10.0 µl of sample.
- The sample was run at 100 volts till the loading dye reached 75% of the gel.
- The gel was removed from the electrophoresis chamber and examined on UV transilluminator.

3.15.2 PCR amplification of 16S- rRNA gene

DNA amplification was performed with Genamp PCR system (Applied Biosystem, USA). Reaction mixture for the PCR contained 10X PCR buffer [200.0 mM Tris–HCl (pH 8.4), 500.0 mM KCl], each deoxynucleotide triphosphate (dNTP) at a final concentration of 2.5mM, 1.5mM $MgCl_2$, 400.0 ng of each oligonucleotide primer and 3.0 units of Taq DNA polymerase (Invitrogen, USA) in a final volume of 100.0 µl. The PCR product was sequenced bi-directionally using the forward, reverse and internal primer of the 16S rDNA. The sequences of the universal primers are presented below:

Table 3.1 Sequences of the primer

Sl. No.	Primers
1	16s Forward Primer (27F):(5'- GAGTRTGATCMTYGCTWAC-3'):19 Mer
2	16s Reverse Primer (1544 R):(5'-CGYTAMCTTWTTACGRCT-3'):18 Mer
3	Internal Primer (13BG):(5'- CAGCAGCCGCGGTAATAC-3'):18 Mer

Standardized PCR condition with respect to each strain is shown in Table 3.2. Amplified DNA was verified by electrophoresis of aliquots of PCR product (5.0 µl) on a 1.0% agarose gel in 1X TAE (Tris-acetate-EDTA) buffer. The PCR products (16S rRNA gene) were purified using gel extraction kit (Bangalore Genei) and sequenced with Big Dye Terminator version 3.1 Cycle sequencing kit and ABI 3500 XL Genetic Analyzer. The sequence data were aligned and compared with published sequences obtained from the Gen Bank database using Seq Scape v 5.2.

Table 3.2 Optimal PCR reaction conditions for amplification of conserved region of 16S rRNA gene of selected polymer producing bacterial strains

PCR conditions	Bacterial strains	
	P. aeruginosa JQ796859	*P. aeruginosa* JQ866912
Initial denaturation	94 °C for 5 min	94 °C for 5 min
Denaturation	94 °C for 30 s	94 °C for 30 s
Annealing	55 °C for 30 s	55 °C for 30 s
Elongation	72 °C for 2 min	72 °C for 2 min
Final elongation	72 °C for 5 min	72 °C for 5 min
Cycles	35	35

Composition of the Sequencing mix (10.0 µl):

- Big Dye Terminator Ready Reaction Mix: 4.0 µl
- Template (100.0 ng.μl^{-1}):1.0 µl
- Primer (10 pmol.λ^{-1}):2.0 µl
- Milli Q Water: 3.0 µl

PCR Conditions for 25 cycles

Initial Denaturation: 96 °C for 1min

Denaturation: 96 °C for 10 sec

Hybridization: 50 °C for 5 sec

Elongation: 60 °C for 4 min

3.15.3 Phylogenetic analysis

The 16S rDNA sequence of bacteria under study was aligned with reference sequences showing homology from the NCBI database (http://blast.ncbi.nlm.nih.gov) using the multiple sequence alignment programme of MEGA 4.0. Phylogenetic trees were constructed using ClustalW by distance matrix analysis and the neighbour-joining method[313]. Phylogenetic trees were displayed using TREEVIEW[314]. The 16S rRNA gene sequence determined in this study was deposited in GenBank of NCBI data library (http://www.ncbi.nlm.nih.gov/GenBank) under different accession numbers with respect to each strain.

3.16 PCR based identification of the PHA biosynthetic genes in bacterial strains

Genomic DNA was isolated from bacterial strains *P. aeruginosa* strains JQ796859 and JQ866912 by using Genei Pure TM Bacterial DNA purification kit (Cat no: 117290).

The primers used in the experiment were I-179L and I-179R[231]; custom-ordered from Bangalore Genei were based on two highly conserved sequences deduced from a multiple sequence alignment analysis of the pseudomonad phaC genes. The sequences of the primers are presented below:

Table 3.3 Sequences of the primers

Sl. No.	Primers
1	Forward Primer: I-179L –5′-ACAGATCAACAAGTTCTACATCTTCGAC-3′):28 Mer
2	Reverse Primer: I-179R–5′-GGTGTTGTCGTTGTTCCAGTAGAGGATGTC-3′):30 Mer

The PCR mixture consisted of 2.0 µl of the genomic DNA template; 0.45 µl (0.3 µM) of each primer, 1.5 µl of 1x PCR buffer, 0.6 µl of 200 µM dNTPs, 0.3 µl of (1.0 U) Taq DNA polymerase in a final volume mixture of 15.0 µl. PCR amplification was performed with a GeneAmp PCR System 9700 (Applied

Biosystems). The thermal cycling was initiated by denaturing the DNA at 95 °C for 2 min followed by 30 cycles of 94 °C for 30 sec, 60 °C for 45 sec and 72 °C for 45 sec, with a final 7 min extension step at 72 °C.

A portion of the amplified PCR reaction mixtures with ethidium bromide were loaded on a 1.0% agarose gel and separated by electrophoresis in TAE buffer (Tris 1.6 M, acetic acid 0.8 M, EDTA 40 mM). 100 bp DNA ladder (Bangalore Genei, India) was used as a molecular marker and loaded in gel. After electrophoretic separation, PCR products were analyzed by UV transilluminator.

3.17 Statistical Analysis

All experiments were repeated thrice. The mean of three experiments was considered. The statistical analysis was done using the origin 6.1-Scientific Graphing and Data Analysis Software (Origin lab Corporation) as well as Microsoft excels 2007. The standard error was calculated using the formulae:

$$SE=s/\sqrt{n}$$

Where, SE is the standard error; s is standard deviation and n is the number of observation.

CHAPTER 4

RESULTS

The investigation was carried out to isolate and screen biopolymer producing bacterial species from the soil samples collected from the various crude oil contaminated sites of Assam and Assam Arakan Basin, ONGC and Numaligarh refinery Limited, Assam. Also some more bacterial strains were isolated from the waste samples of Jagiroad Paper Mill, Nagaon, Assam. The screened bacteria were cultured in suitable media for the production of biopolymers. The production technology of bacterial biopolymers has been standardized. The isolated and purified biopolymers were subjected to physico-chemical characterization. Subsequently biodegradation of biopolymers was assessed. Molecular genetic assessment of the biopolymer producing bacteria was carried out with the amplification of 16s rDNA by polymerase chain reaction and subsequent phylogenetic analysis. Moreover, PCR detection was done for polymer specific genes coding for PHA synthases in the bacterial strains.

The details of the research findings are presented in this chapter.

4.1 Screening of Biopolymer producing microbes

4.1.1 Isolation and pure culture of microbes capable of producing biopolymer

A good number of culturable bacteria were isolated from the soil samples of crude oil contaminated sites of Assam and Assam Arakan Basin, ONGC and Numaligarh refinery Limited, Assam. Also some more bacterial strains were isolated from the waste samples of Jagiroad Paper Mill, Nagaon, Assam. A total of 13 bacterial isolates were screened on the basis of their ability to produce biopolymer. The bacterial isolates were recovered, pure cultured and maintained either in stab agar cultures at 4 °C or preserved in 15% glycerol at -80 °C.

The bacterial isolates were cultured in nutrient broth medium at 37 °C in an incubator shaker at 180 rpm for 24 h and subsequently the pure cultures were used as the seed culture for further screening. The pure cultures were sub-cultured by re-suspending the microbes in fresh polymer detection media with the necessary environmental conditions.

4.1.2 Morphological characterization of bacterial isolates

The morphology of the isolated and pure cultured bacterial strains was studied in the nutrient agar medium. Data thus obtained are presented in Table 4.1.

Table 4.1 Morphological characters of bacterial isolates obtained from different soil and waste samples

Sl No	Bacterial isolate	Size	Form	Margin	Elevation	Pigment	Gram staining
1	BS1	Small	Circular	Entire	Flat	Greenish	Gram negative
2	BS2	Medium	Circular	Entire	Convex	Yellowish	Gram negative
3	BP C1	Large	Circular	Entire	Flat	Bluish green	Gram negative
4	BP C2	Large	Circular	Entire	Flat	Greenish	Gram negative
5	BS4	Medium	Circular	Entire	Flat	Yellowish green	Gram negative
6	BS5	Large	Circular	Entire	Raised	Greenish	Gram negative
7	BS7	Small	Circular	Entire	Flat	Yellowish green	Gram negative
8	BP1	Medium	Circular	Entire	Convex	White	Gram negative
9	BP2	Small	Circular	Serrate	Flat	White	Gram positive
10	BP3	Pinhead	Circular	Entire	Flat	White	Gram negative
11	BP4	Large	Circular	Entire	Raised	White	Gram positive
12	BPr2	Large	Circular	Entire	Flat	White	Gram negative
13	BPr3	Medium	Circular	Entire	Flat	White	Gram positive

Morphological studies of bacteria in terms of colony size, pigmentation, form, margin and elevation displayed variable results.

4.1.3 Screening of biopolymer (PHA) producing bacterial isolates

In screening experiments, all the bacterial isolates were cultured in the nutrient broth (NB) (Sigma, Aldrich) at 37 °C as a pre-culture for 24 h. The PHA detection medium[306] was used with minor modifications for the production of PHA. The pH of the medium was adjusted to 7.0 before autoclaving. The composition of the medium (gL^{-1}) is: $(NH_4)_2SO_4$ (1.0), KH_2PO_4 (13.3), $MgSO_4$ (1.3), citric acid (1.7), trace element solution 10 $mL.L^{-1}$ (gL^{-1}, $FeSO_4 \cdot 7H_2O$ 10, $ZnSO_4 \cdot 7H_2O_2$ 0.25, $CuSO_4 \cdot 5H_2O$ 1, $MnSO_4 \cdot 5H_2O$ 0.5, $CaCl_2 \cdot 2H_2O$ 2.0, $Na_2B_4O_7 \cdot 10H_2O$ 0.23, $(NH_4)_6Mo_7O_{24}$ 0.1 and HCl 10 0 mL) and glucose (10.0 gL^{-1}). Glucose was added to the medium after

autoclaving to avoid reduction of glucose by high temperature and pressure. An aliquot of 10.0 mL of the above pre-cultured inoculum was transferred to 250 mL Erlenmeyer flask containing 100 mL sterile PHA medium with glucose as the carbon source and then cultured in a shaker at 180 rpm for 48 h at 37 °C. Bacterial multiplication was indicated by the increase in the turbidity of the culture medium. The bacterial biomass was harvested by centrifugation and then assessed for PHA production. The screening data are presented in Table 4.2

Table 4.2 Screening of biopolymer producing bacteria

Isolate no	Response in PHA medium	Isolate no	Response in PHA medium
BS1	-	BP1	-
BS2	-	BP2	+
BP C1	+	BP3	-
BP C2	+	BP4	-
BS4	-	BPr2	-
BS5	-	BPr3	-
BS7	-		

As shown in Table 4.2, out of 13 pure bacterial cultures, only 3 viz. BPC1, BPC2 and BP2 showed positive growth in the PHA detection medium. These isolates were found to be promising for the production of biopolymer polyhydroxyalkanoates (PHA). Subsequent studies were carried out with these 3 bacterial isolates.

BPC1 and BPC2 bacterial isolates were identified by 16s rRNA gene sequence analysis and the same were deposited in GenBank NCBI and the accession no. given are *Pseudomonas aeruginosa* BPC1 (JQ796859) [BPC1] and *P. aeruginosa* BP C2 (JQ866912) [BPC2]. The details of the genotypic characterization of the two strains are presented in the subsequent section. The strain BP2 was identified as *Bacillus circulans* MTCC8167 in a previous work by our laboratory. Earlier, the strain BP2 was examined for biosurfactant production but not for biopolymer production.

4.1.4 Screening of PHA producing bacterial isolate by staining procedure

The presence of biopolymer in the growing bacterial cells was confirmed by the Fluorescence Staining as described by Ostle and Holt[109]. Following the staining, the bacterial cultures were observed under a fluorescence microscope with fluorescence excitation using immersion oil attachment. The PHA producing bacteria were also stained by Sudan black B as per the method of Schlegel *et al.*[108] for visualizing the PHA granules in the bacterial cells under a. light microscope. The observation is presented in Table 4.3.

Table 4.3. PHA producing bacterial isolates showing staining response

Strains	Nile Blue A treatment	Sudan Black B treatment
BS1	-ve	-ve
BS2	-ve	-ve
P. aeruginosa JQ796859	+ve	+ve
P. aeruginosa JQ866912	+ve	+ve
BS4	-ve	-ve
BS5	-ve	-ve
BS7	-ve	-ve
BP1	-ve	-ve
B. circulans MTCC8167	+ve	+ve
BP3	-ve	-ve
BP4	-ve	-ve
BPr2	-ve	-ve
BPr3	-ve	-ve

As shown in Table 4.3, out of 13 bacterial isolates, only 3 viz. *P. aeruginosa* JQ796859, *B. circulans* MTCC8167 and *P. aeruginosa* JQ866912 showed orange fluorescence after the Nile blue A treatment (Fig. 4.3). Similarly when Sudan black B (Fig. 4.3) was applied, the PHA rich bacterial cells retained the dye and appeared dark blue under the microscope. Colonies of PHA deficient cells appeared light grey as they lost the dye during the differentiation process. The positive isolates were considered to be promising for the production of biopolymer, PHA.

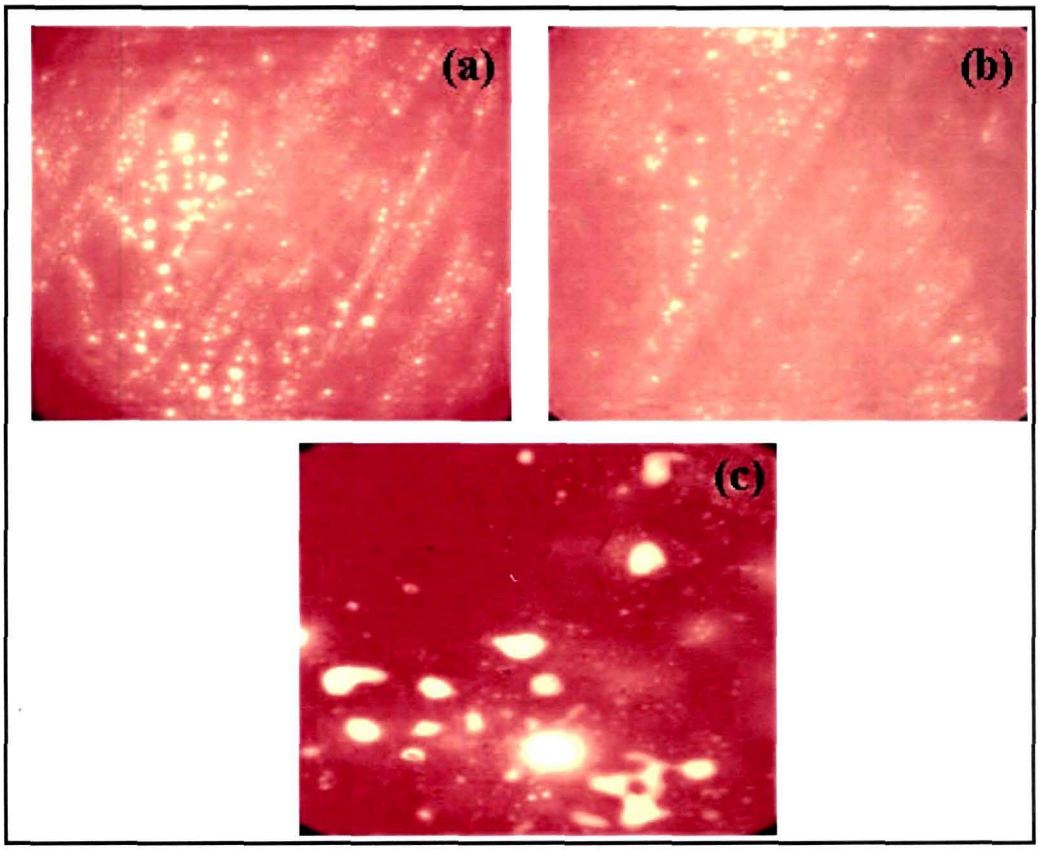

Fig. 4.1 PHA inclusion bodies in bacterial isolates (a) *P. aeruginosa* JQ796859 (b) *B. circulans* MTCC8167 and (c) *P. aeruginosa* JQ866912 stained with Nile blue A and observed under fluorescent light (100 X magnification)

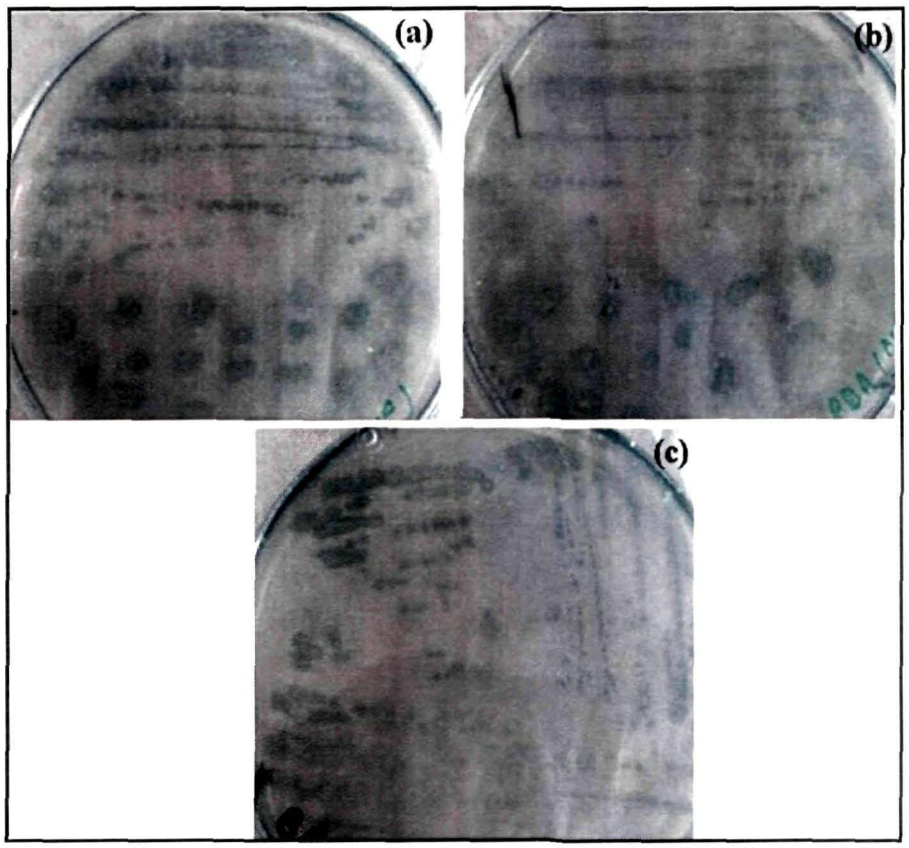

Fig. 4.2 Sudan black B treatment on bacterial isolates (a) *P. aeruginosa* JQ796859 (b) *B. circulans* MTCC8167 and (c) *P. aeruginosa* JQ866912. Positive isolates show bluish black color in the colonies

4.1.5 Cell size determination by SEM analysis

To determine the shape and size of PHA producing bacterial strains, SEM micrography was done on each strain and the photographs thus obtained are presented in Fig. 4.3.

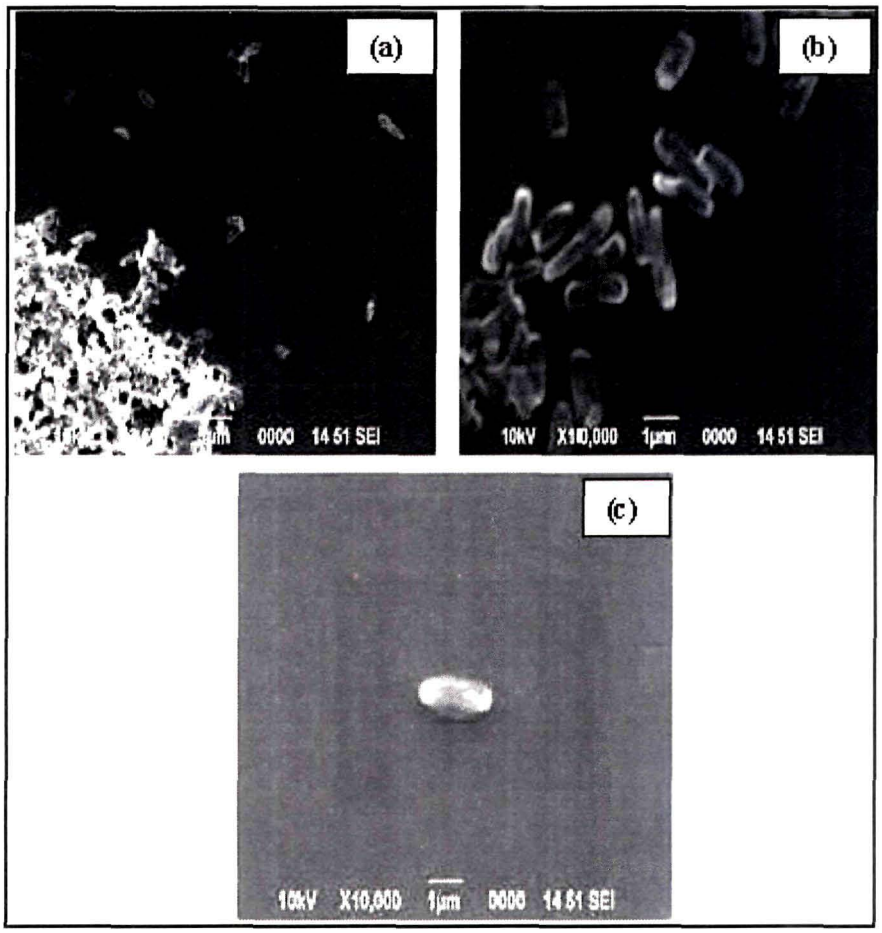

Fig. 4.3 SEM micrograph of bacterial strains (a) *P. aeruginosa* JQ796859 (b) *B. circulans* MTCC8167 and (c) *P. aeruginosa* JQ866912.

The SEM micrograph has revealed all bacterial strains to be rod shaped and each bacterial cell appeared 1.0-2.0 µm in size.

4.1.6 Biochemical characterization of the PHA producing bacterial strains

Different biochemical tests were performed for all 3 bacterial strains by following the standard protocols. Data thus obtained are presented in Table 4.4. Characters recorded for the tests were catalase, urease, citrate, triple sugar iron, nitrate reduction, indole and H_2S production, litmus milk reaction, MR-VP, starch, gelatin and casein hydrolysis, glucose and combination of $(NH_4)_2SO_4$ and glucose utilization and acid production from sugars like lactose, manitol, dextrose, sucrose and xylose.

Table 4.4 Biochemical characterization of the PHA producing bacterial strains

Enzymes	Biochemical characters		
	P. aeruginosa JQ796859	*B. circulans* MTCC8167	*P. aeruginosa* JQ866912
Catalase	+	+	+
Urease	-	+	-
Citrate	+	-	+
Triple sugar iron	+	+	+
Nitrate reduction	+	-	+
Indole production	-	-	-
H_2S production	-	-	-
Litmus milk reaction	Peptonization	Peptonization	Peptonization
Methyl red	-	-	+
Vogues proskauer	-	-	-
Starch hydrolysis	-	+	-
Gelatin hydrolysis	+	+	+
Casein hydrolysis	+	+	+
1% Glucose	+	+	+
$(NH_4)_2SO_4$+ Glucose	+	+	+
Acid production from sugars			
Lactose	+	+	-
Manitol	-	+	+
Dextrose	+	+	+
Sucrose	+	+	+
Xylose	+	+	+

4.2 Growth determination of PHA producing bacterial strains

4.2.1 Growth of bacterial strains at different pH levels

The PHA producing bacterial strains were assessed for their growth at different pH levels ranging from acidic to alkaline (2-10) using glucose containing media. Data thus obtained are presented in Fig. 4.4 (a-e).

All the bacterial strains showed poor growth at high acidic (pH 2.0) and high alkaline (pH 10.0) conditions. At pH 2.0, the bacterial strains *P. aeruginosa* JQ796859, *B. circulans* MTCC8167 and *P. aeruginosa* JQ866912 produced comparatively lower biomass of 0.25-0.34 gL^{-1} having the peak at 96 h. The strains *B. circulans* MTCC8167 and *P. aeruginosa* JQ866912 retarded their growth after 96 h, but *P. aeruginosa* JQ796859 showed stationary growth up to 120 h. At pH 4.0, *P. aeruginosa* JQ796859 showed better growth in comparison to the other strains that exhibited a similar growth pattern. At pH 6.0, *B. circulans* MTCC8167 exhibited better growth with biomass yield of 1.0-1.48 gL^{-1} during the initial culture period of 24-72 h in comparison to the other two strains. However, a further increase in pH (upto pH 10.0) resulted in a decline in growth for all the strains.

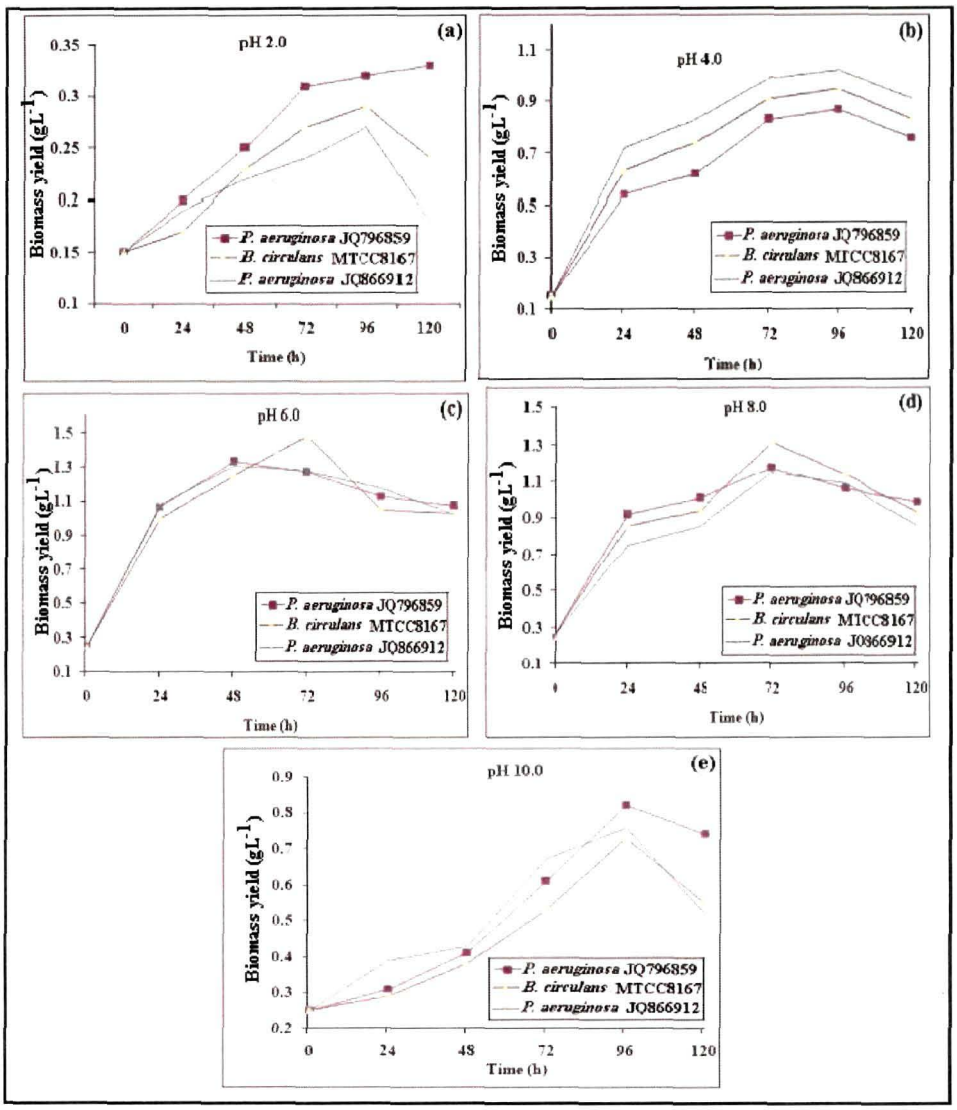

Fig. 4.4 Growth of bacterial strains in glucose supplemented media having pH 2.0-10.0 (a-e)

4.2.2 Growth of bacterial strains at different temperatures

The PHA producing bacterial strains were assessed for their growth at the temperature range of 30-45 °C in the medium containing glucose. Data thus obtained are presented in Fig. 4.5 (a-c). The effect of temperature on growth of the bacterial strains showed that the yield of biomass was significantly increased at temperatures 30-37 °C. At 37 °C, the strains showed good biomass production; *P. aeruginosa* JQ866912 exhibited the highest biomass production of 4.3 gL^{-1} as compared to others. However, all the bacterial strains failed to survive beyond this temperature and the yield of biomass also declined. Therefore, 37 °C was considered as the optimum temperature for the growth of these bacterial strains.

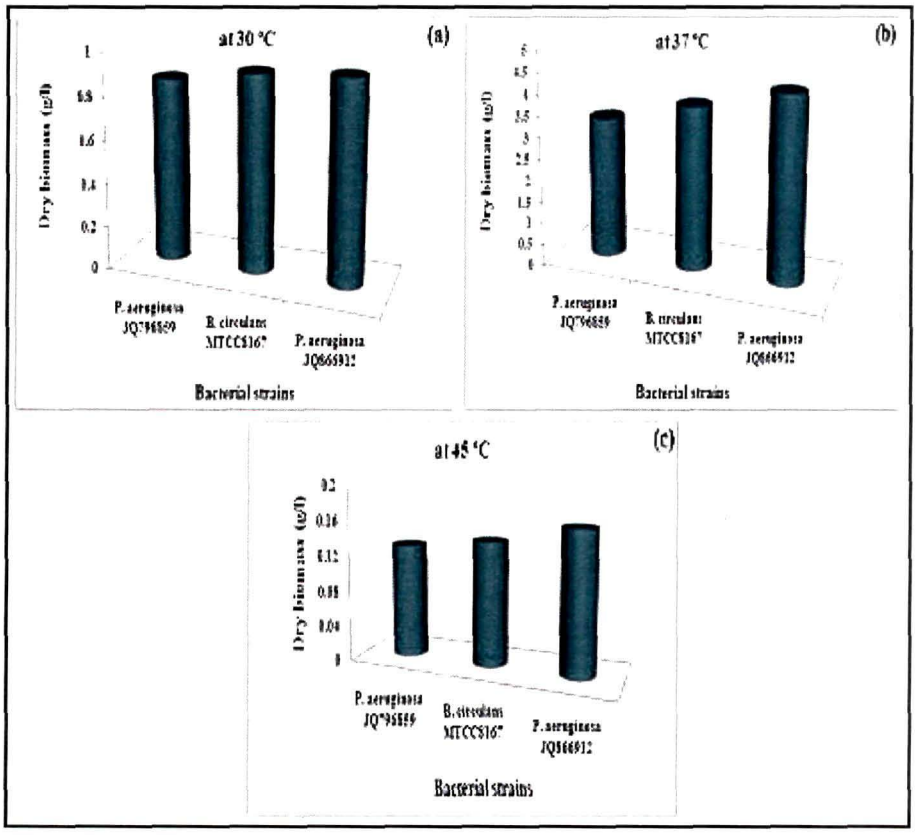

Fig. 4.5 Growth of bacterial strains at the different temperatures: (a) 30 °C (b) 37 °C (c) 45 °C in glucose supplemented medium

4.2.3 PHA production by the bacterial strains at different growth phases

The selected PHA producing bacterial strains were grown in PHA detection medium containing 1% glucose for different time periods for the production and accumulation of PHA. The accumulated PHA was assayed at the time interval of 12h till 96 h. Data thus obtained are presented in Table 4.5.

Table 4.5 PHA production by the bacterial strains at different growth periods

Isolate	PHA (% CDW) in glucose supplemented medium				
	12 h	24 h	48 h	72 h	96 h
P aeruginosa JQ796859	ND	1.4	4 5	6.47	5.1
B circulans MTCC8167	ND	1.9	5.6	9.22	6.9
P. aeruginosa JQ866912	ND	2.5	10.4	18.0	16 2

ND: not detectable, the values presented here are mean of three independent experiments

From the Table 4.5, it was observed that during the first 12 h period there was no accumulation of PHA in all three bacterial strains. At 24 h culture, the strains showed initiation of PHA accumulation. Then the accumulation of PHA gradually increased up to 72 h of culture. The highest PHA accumulation was observed in *P. aeruginosa* JQ866912 that amounted to 18.0% after 48 to 72 h of culture. Other two strains also showed increased accumulation of PHA (*P. aeruginosa* JQ796859: 6.5% and *B. circulans* MTCC8167: 9.2%) after 48 to 72 h of culture. But all the three bacterial cultures exhibited reduction in the accumulated PHA after 96 h of culture (*P. aeruginosa* JQ796859: 5.1%, *B. circulans* MTCC8167: 6.9% and *P aeruginosa* JQ866912: 16.2%).

4.2.4 PHA production by the bacterial strains in different carbon substrates

Different carbon sources were screened for biopolymer production by the isolated bacterial strains. Biopolymers producing bacterial strains were separately inoculated in media supplemented with the different carbon sources: glucose, glycerol, colocasia starch, propionic acid, soy oil, waste mobile (spent engine oil), sugarcane

molasses and glycerol byproduct of kitchen chimney dump lard (KCDL). The growth of the bacterial isolates and PHA yield are presented in Table 4.6.

Table 4.6 PHA production by the bacterial isolates using different carbon sources

Isolate	Carbon source	Biomass (gL^{-1})	PHA (% CDW)
P aeruginosa JQ796859	Glucose (1%)	5 4	6 47
B circulans MTCC8167		6 32	9 22
P aeruginosa JQ866912		6 8	18 0
P aeruginosa JQ796859	Glycerol (1%)	4 5	5 6
B circulans MTCC8167		5 9	8 0
P aeruginosa JQ866912		7 4	14 5
P aeruginosa JQ796859	Colocassia starch (1%)	0 6	-
B circulans MTCC8167		4 8	6 5
P aeruginosa JQ866912		0 3	-
P aeruginosa JQ796859	Glucose (1%) + Propionic acid (0 1%)	3 6	4 6
B circulans MTCC8167		6 8	19 8
P aeruginosa JQ866912		5 5	12 5
P aeruginosa JQ796859	Sugarcane molasses (1%)	4 1	4 7
B circulans MTCC8167		5 3	7 9
P aeruginosa JQ866912		6 3	13 2
P aeruginosa JQ796859	Waste mobile (1%)	2 3	1 2
B circulans MTCC8167		-	-
P aeruginosa JQ866912		2 8	1 4
P aeruginosa JQ796859	Soy oil (1%)	5 9	7 77
B circulans MTCC8167		6 2	8 12
P aeruginosa JQ866912		7 6	17 07
P aeruginosa JQ796859	Glycerol waste of KCDL (1%)	5 7	7 9
B circulans MTCC8167		4 9	6 3
P aeruginosa JQ866912		7 8	22 5

NB The values presented here are mean of three independent experiments

All the bacterial strains were tested for their PHA accumulation against the different carbon sources (1%) in the medium after 72 h of culture. In the glucose containing medium, the isolate *P aeruginosa* JQ866912 exhibited the highest PHA accumulation of 18.0% CDW followed by *B circulans* MTCC8167 and *P aeruginosa* JQ796859. Similar results were obtained in the glycerol containing medium; a highest value of 14.5% PHA accumulation was shown by *P aeruginosa* JQ866912 isolate. But in the case of colocasia starch containing medium, no growth was exhibited by *P aeruginosa* JQ796859 and *P aeruginosa* JQ866912 strains, while *B circulans* MTCC8167 showed 6.5% accumulation. The strain *B circulans* MTCC8167 exhibited the highest PHA accumulation of 19.8% in the medium supplemented with

the combination of 0.1% propionic acid and 1.0% glucose followed by *P. aeruginosa* JQ866912 (12.5%) and *P. aeruginosa* JQ796859 (4.6%). Almost, the similar result was exhibited by *P. aeruginosa* JQ796859 in sugarcane molasses as the carbon source, as well as glucose and propionic acid combination. The strain *P. aeruginosa* JQ866912 accumulated 13.2% PHA in the same source. While using waste mobile as the carbon source in the medium, all the strains showed the least accumulation of PHA. All the strains showed better growth and PHA accumulation in soy oil-supplemented medium. The strain *P. aeruginosa* JQ866912 exhibited 17.07% PHA accumulation followed by *B. circulans* MTCC8167 and *P. aeruginosa* JQ796859. Comparatively, the best PHA accumulation was observed when the glycerol byproduct (waste of KCDL) was used; the strain *P. aeruginosa* JQ866912 showed 22.5% CDW of PHA accumulation followed by *P. aeruginosa* JQ796859 and *B. circulans* MTCC8167 having 7.9 and 6.3% PHA respectively.

The bacterial biomass yield in bacterial shake flask cultures with the use of the above carbon sources as the sole source of carbon (1.0% w/v) are shown in Table 4.6. After 72 h of culture, each 5.0 mL sample was assayed for dry biomass yield. The results revealed that higher cell densities were obtained from glycerol byproduct. Cell growth up to a dry biomass of 7.8 gL^{-1} from the bacterial strain *P. aeruginosa* JQ866912 was obtained while using the glycerol byproduct supplemented medium. In the case of medium with colocassia starch and waste mobile, there was a decrease in the cell biomass yield in both *P. aeruginosa* JQ796859 and *P. aeruginosa* JQ866912 but *B. circulans* MTCC8167 showed an increase in biomass up to 4.8 gL^{-1}.

4.3 Physical and chemical characterization of PHA

4.3.1 UV analysis of PHA

The isolated PHA was dissolved in chloroform and subjected to the wavelength scan to determine the light absorption at 190-600 nm to find the maximum absorption (λ_{max}). Data thus obtained are presented graphically in Fig. 4.6 (a, b and c). PHA isolated from *P. aeruginosa* JQ796859 was found to have its maximum absorption at the wavelength of 261 nm; PHA from *B. circulans* MTCC8167 shows absorption maxima at 289 nm and PHA from *P. aeruginosa* JQ866912 shows maximum absorption at 285-290 nm.

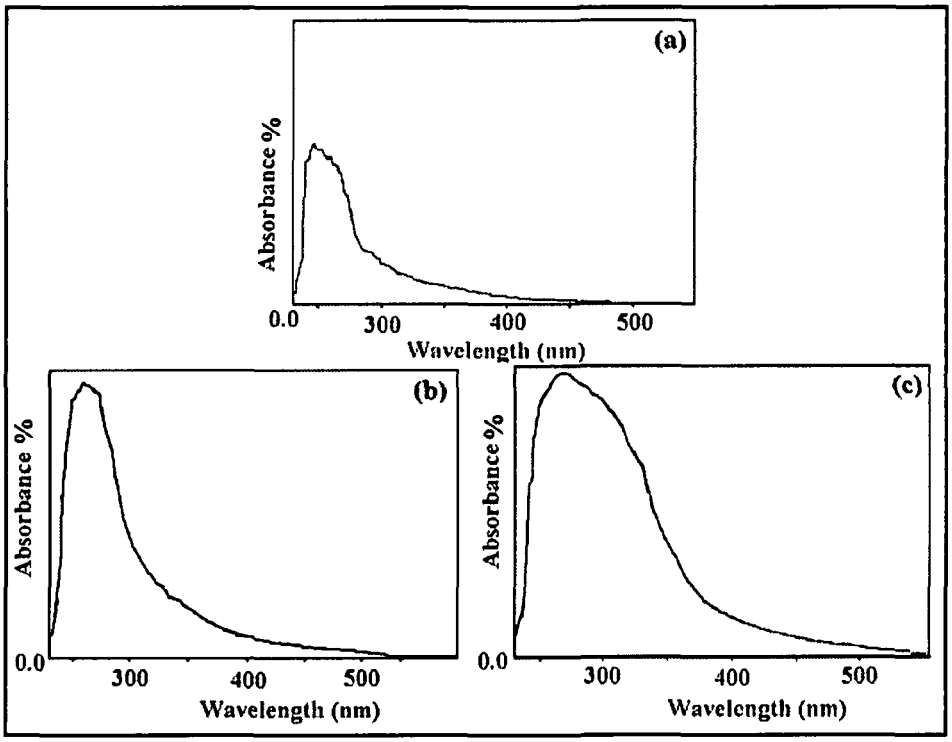

Fig. 4.6 UV-visible absorption spectrum of PHA from the bacterial strains (a) *P. aeruginosa* JQ796859 (b) *B. circulans* MTCC8167 and (c) *P. aeruginosa* JQ866912

4.3.2 FTIR analysis of PHA

Characterization of the extracted and purified PHA was done with the help of Fourier transform infrared spectroscopy (FTIR) technique. FTIR analysis of the isolated polymer of *P. aeruginosa* JQ796859, *B. circulans* MTCC8167 and *P. aeruginosa* JQ866912 revealed absorption bands at 1730–1735 cm^{-1}, corresponding to the ester carbonyl group. Other characteristic bands were observable in the spectrum, albeit at a different position and with weaker bands. The FTIR spectral pattern of the polymer compounds of these bacterial strains were depicted in Fig. 4.7-4.9 and Table 4.7. The data were also compared with the control PHB (Fig. 4.10).

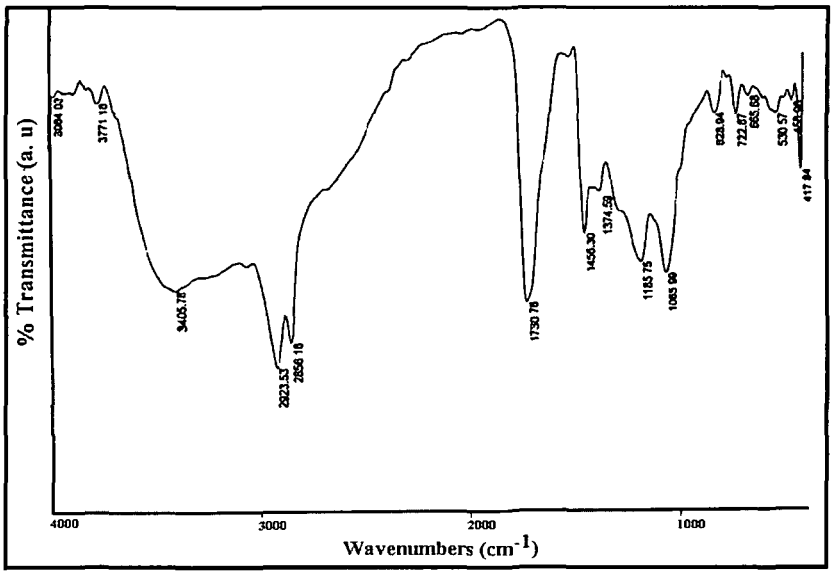

Fig. 4.7 FTIR spectra of purified polymer from the bacterial strain *P. aeruginosa* JQ796859 when cultured in glucose containing media

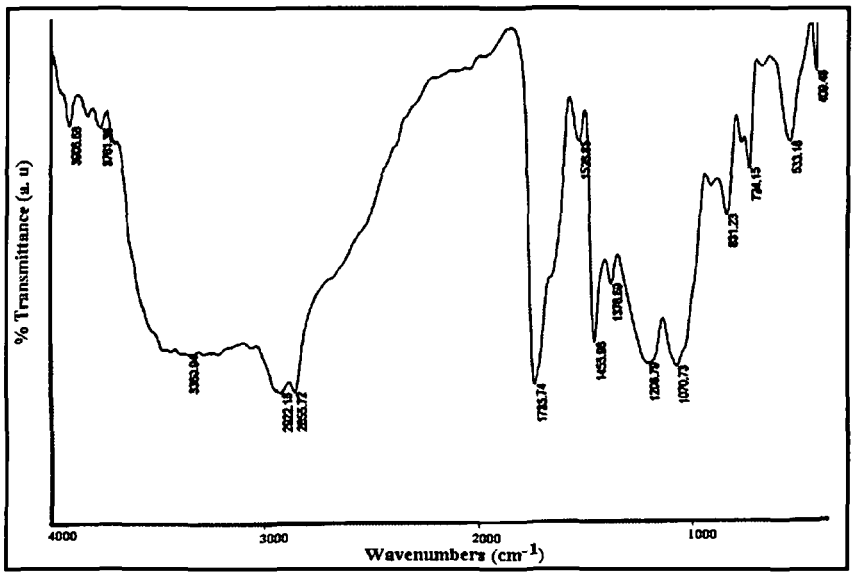

Fig.4.8 FTIR spectra of purified polymer from the bacterial strain *B. circulans* MTCC8167 when cultured in glucose containing media

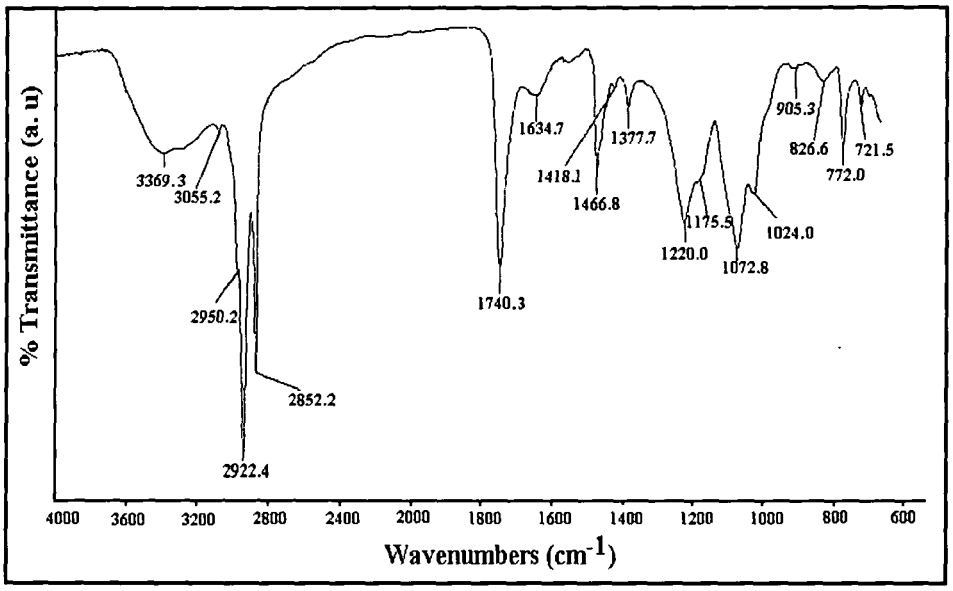

Fig. 4.9 FTIR spectra of purified polymer from the bacterial strain *P. aeruginosa* JQ866912 when cultured in glucose containing media

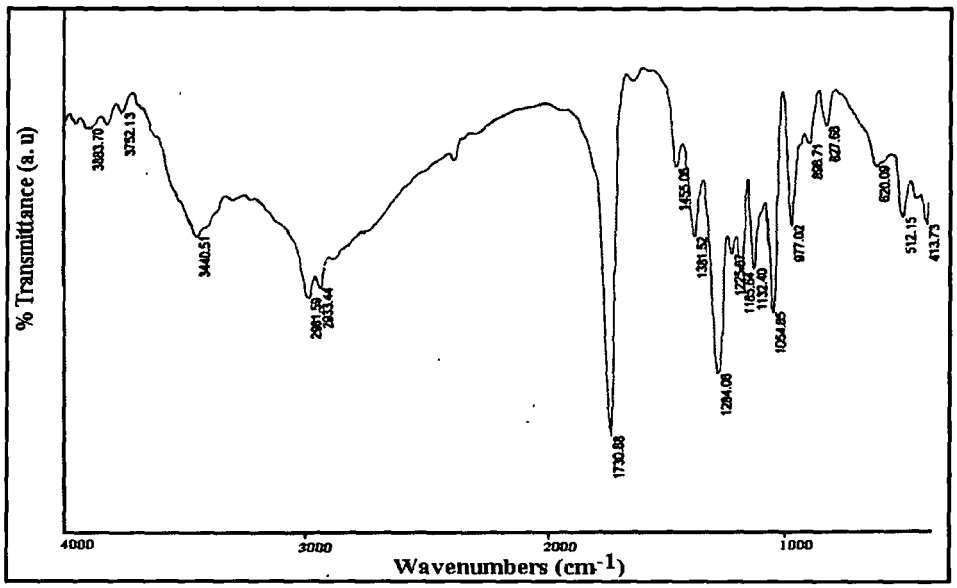

Fig. 4.10 FTIR profiling of PHB (control)

Table 4.7 Structural information generated from FTIR data

Bacterial strain	FTIR peaks (wave number cm^{-1})	Structural information revealed
P.aeruginosa JQ796859	3,405	O-H bonding
	2,923	bands of C-H stretching
	1,730	band of ester carbonyl C=O
	1,670	–C=C stretching
	3,085	Alkene C–H stretching
	1,065	–C–O–C stretching vibrations
B. circulans MTCC8167	3,360	O–H bonding
	2,922	bands of C–H stretching
	1,735	strong absorption band of ester carbonyl C=O,
	1,206	C–O–C group
	1,070	–C–O–C stretching vibrations
P. aeruginosa JQ866912	3,369	O-H bonding
	2,922	bands of C-H stretching
	1,740	strong absorption band of ester carbonyl C=O
	1,634	–C=C
	3,055	alkene C–H stretching
	1,071	–C–O–C stretching vibrations
The FTIR peaks were identical with the data provided by different researchers[19-21]. The comparisons suggested that the polymer compounds might be polyhydroxyalkanoates (PHA).		

4.3.3 GC-MS analysis of PHA

The actual monomeric characterization of the biopolymer obtained from the isolated bacterial strains was done using GC-MS. For GC-MS analysis, both the dry cell sample and the isolated polymer were methanolized to convert the polymer into methyl-3-hydroxyalkanoate with the functional group.

(i) PHA from bacterial strain *P. aeruginosa* JQ796859

In the case of the polymer from *P. aeruginosa* JQ796859 biopolymer, the GC pattern of the total ion chromatogram (Fig. 4.11) possessed two methyl ester peaks. To identify these two major peaks, mass spectroscopy measurement was performed and compared with the mass spectrum of methyl esters in the MS library as shown in Fig. 4.12 (a) and (b).

Fig. 4.11 Total ion chromatogram of the polymer isolated from *P. aeruginosa* JQ796859

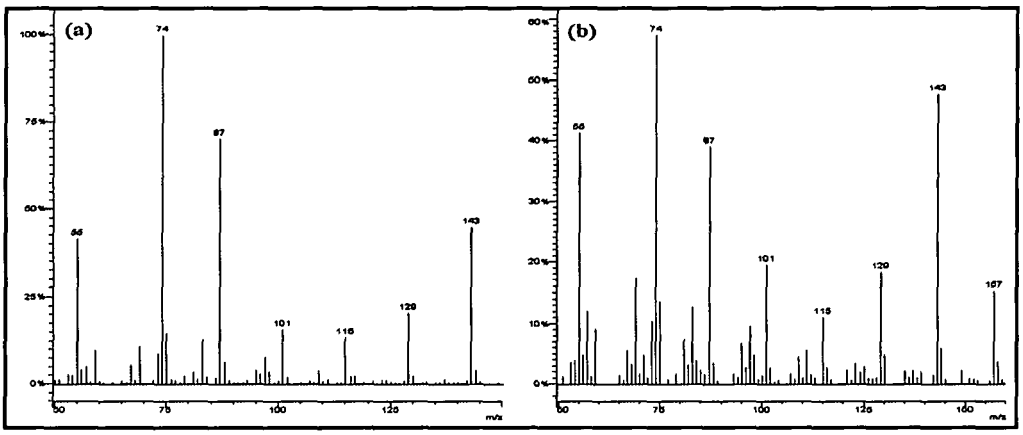

Fig. 4.12 Mass spectra of methyl ester peaks with the retention time RT=11.45 (a) and RT=19.65 (b) min of the polymer isolated from *P. aeruginosa* JQ796859

(ii) PHA from bacterial strain *B. circulans* MTCC8167

The total ion chromatogram (TIC) for the methanolysis product of the isolated PHA from the bacterial isolate *B. circulans* MTCC8167 possessed two methyl ester peaks (Fig. 4.13). To identify these two major peaks, mass spectroscopy measurement

was performed and a similarity was found with the mass spectrum of methyl esters in the MS library as shown in Fig. 4.14 (a) and (b).

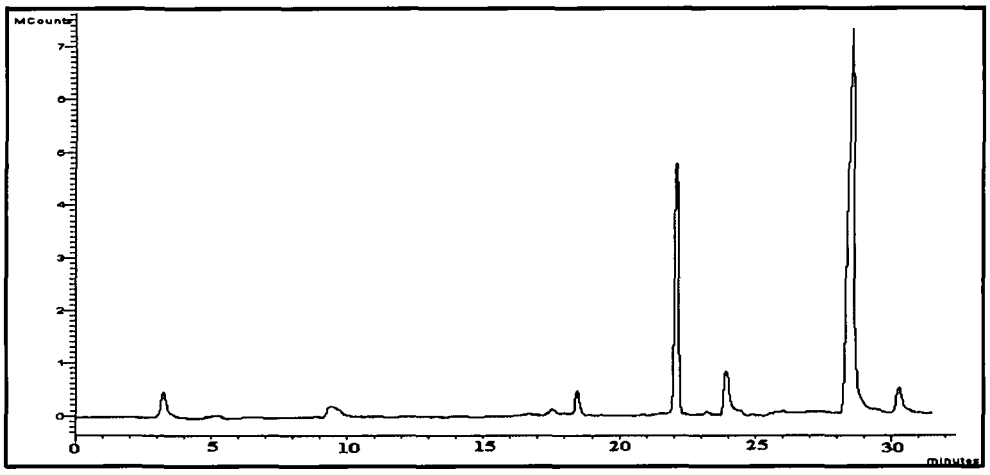

Fig. 4.13 Total ion chromatogram of the polymer isolated from *B. circulans* MTCC8167

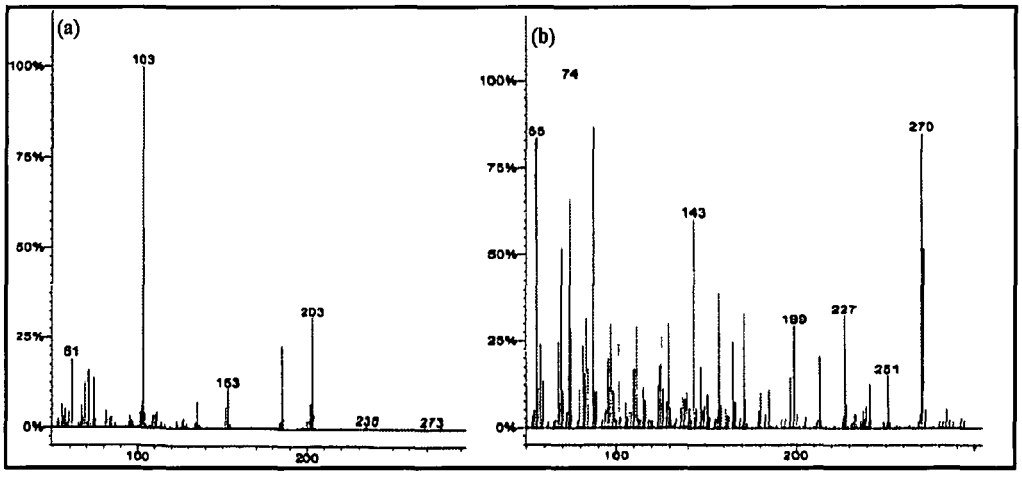

Fig. 4.14 Mass spectra of methyl ester peaks with the retention time RT=22.67 (a) and RT=28.10 (b) min of the polymer isolated from *B. circulans* MTCC8167

(iii) PHA from bacterial strain *P. aeruginosa* JQ866912

In case of the polymer from *P. aeruginosa* JQ866912, the GC pattern of the total ion chromatogram (Fig. 4.15) possessed three methyl ester peaks. To identify these three major peaks, mass spectroscopy measurement was performed and compared with the mass spectrum of methyl ester in the MS library as shown in Fig. 4.16 (a) (b) and (c).

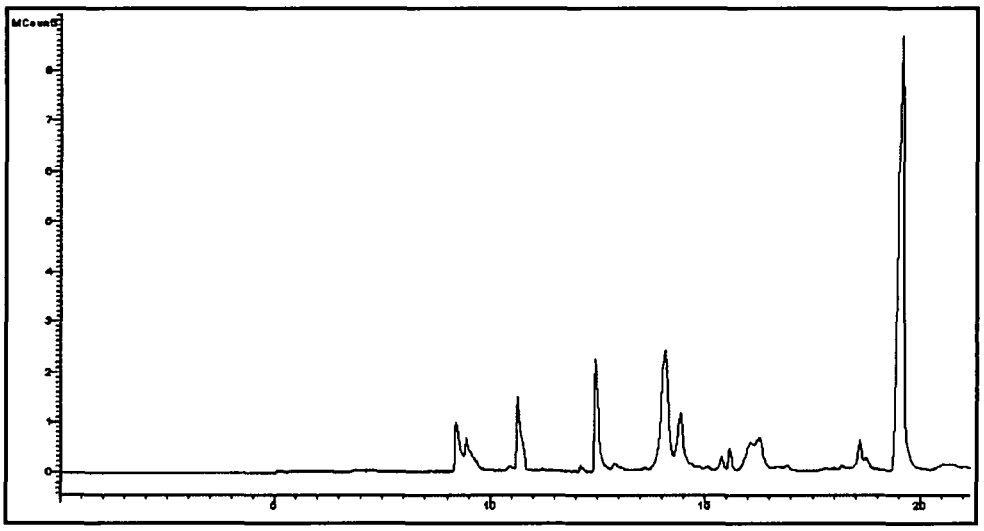

Fig. 4.15 Total ion chromatogram of the biopolymer isolated from *P. aeruginosa* JQ866912 strain

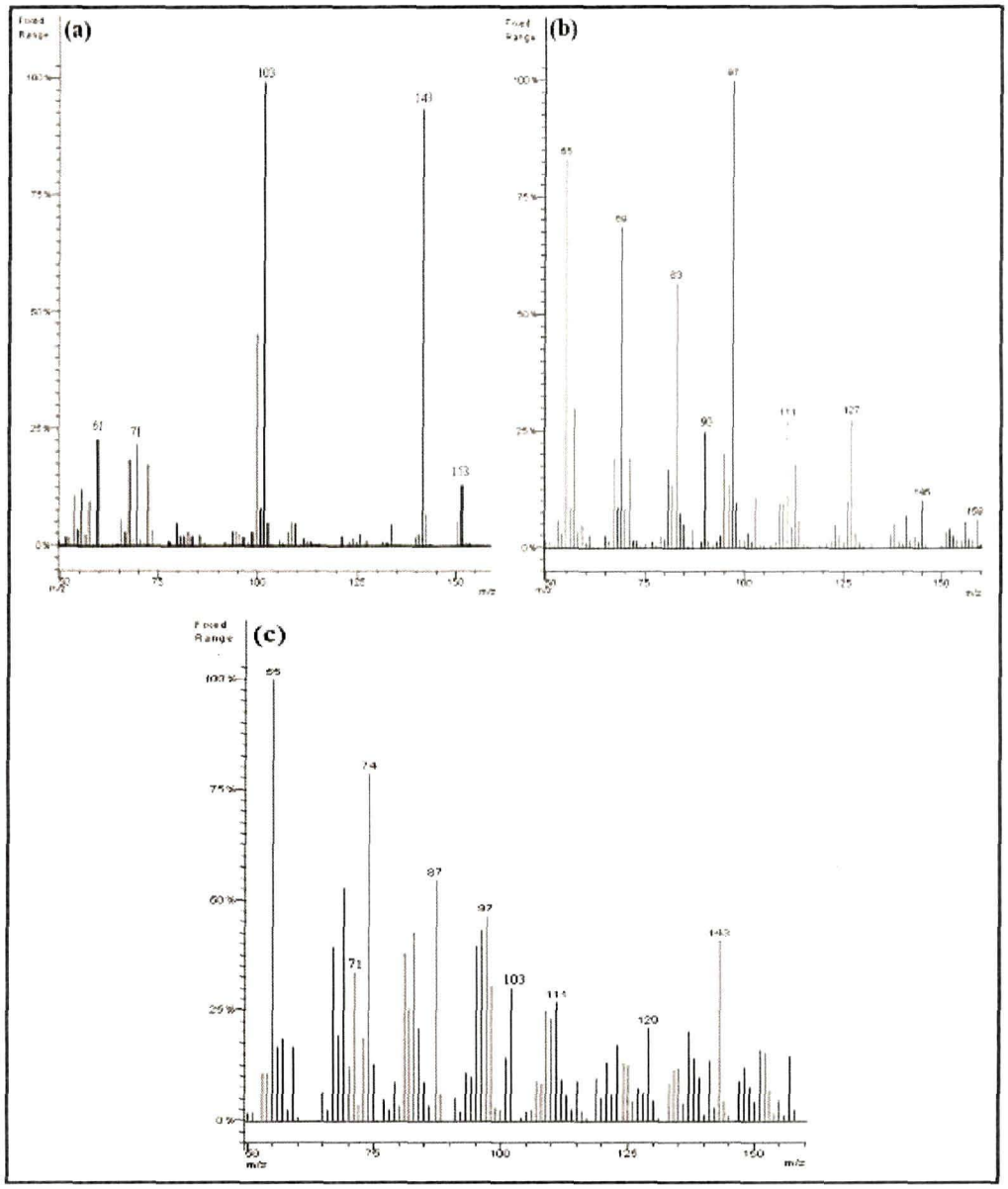

Fig. 4.16 Mass spectra of methyl ester peaks with the retention time RT=11.56 (a), RT=18.46 (b) and RT=19.66 (c) min of the polymer isolated from *P. aeruginosa* JQ866912 strain

4.3.4 NMR analysis of PHA

To confirm the chemical structure of the PHA, ^{1}H and ^{13}C NMR analyses were used. The spectra were measured with JEOL JNN-ECS 400 spectrophotometer. ^{1}H NMR (400 MHz) and ^{13}C NMR (400 MHz) spectra were recorded at 25 °C in a deuterated chloroform ($CDCl_3$) solution. Chemical shifts were reported in ppm relative to the signal of tetramethylsilane.

The ^{1}H NMR and ^{13}C NMR spectra of the polymer sample from *P. aeruginosa* JQ796859, *B. circulans* MTCC8167 and *P. aeruginosa* JQ866912 are presented in Fig. 4.17 (a, b), Fig. 4.18 (a, b) and Fig. 4.19 (a, b) respectively. The characteristics peaks from the figure revealed that all the strains produced copolymer.

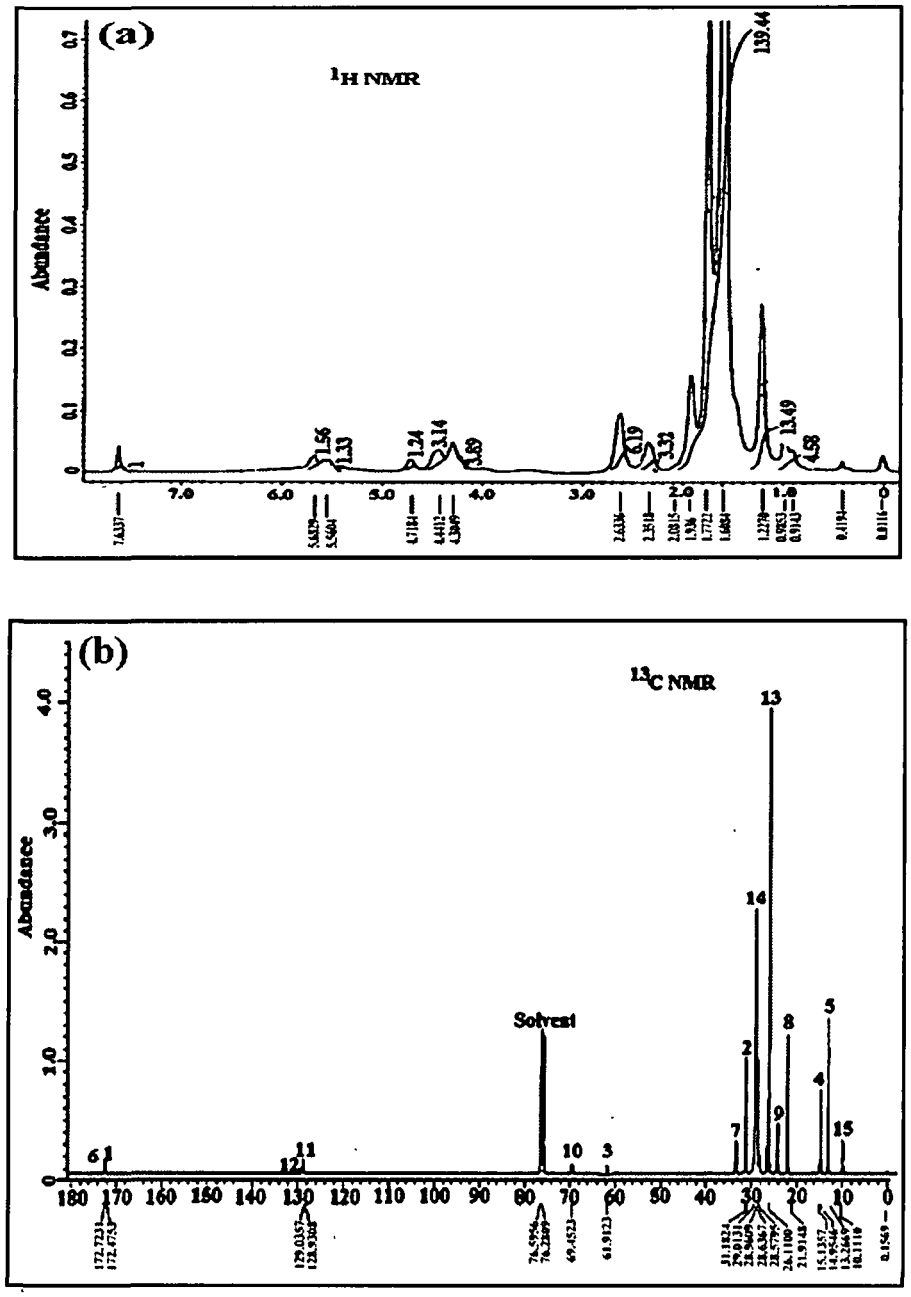

Fig. 4.17 ^{1}H NMR spectrum (a) and ^{13}C NMR spectrum (b) of P-3HV-5-HDE polymer produced by *P. aeruginosa* JQ796859 when grown on glucose as a carbon substrate

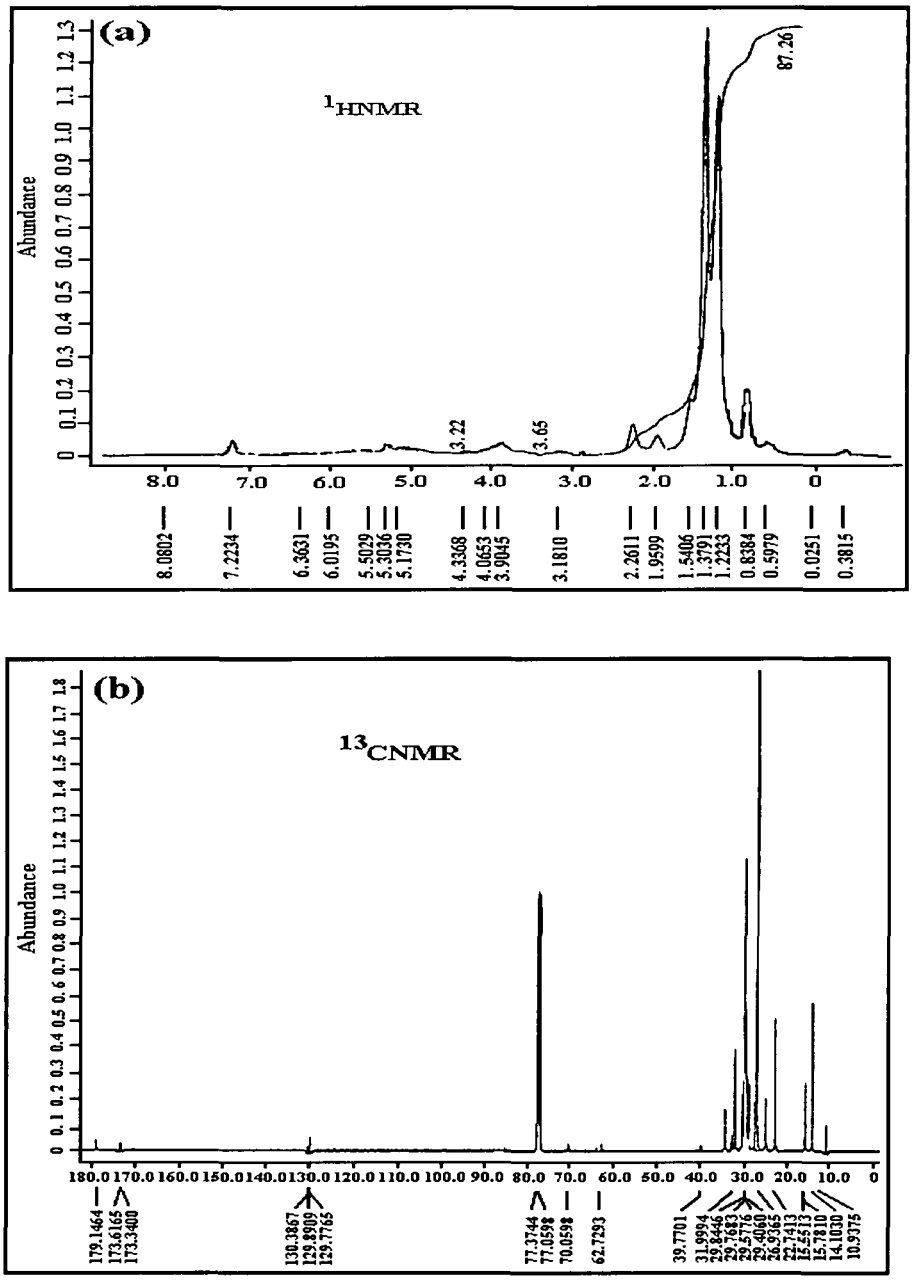

Fig. 4.18 ^{1}H NMR spectrum (a) and ^{13}C NMR spectrum (b) of P-3HB-3-HV polymer produced by *B. circulans* MTCC8167 when grown on glucose as a carbon substrate

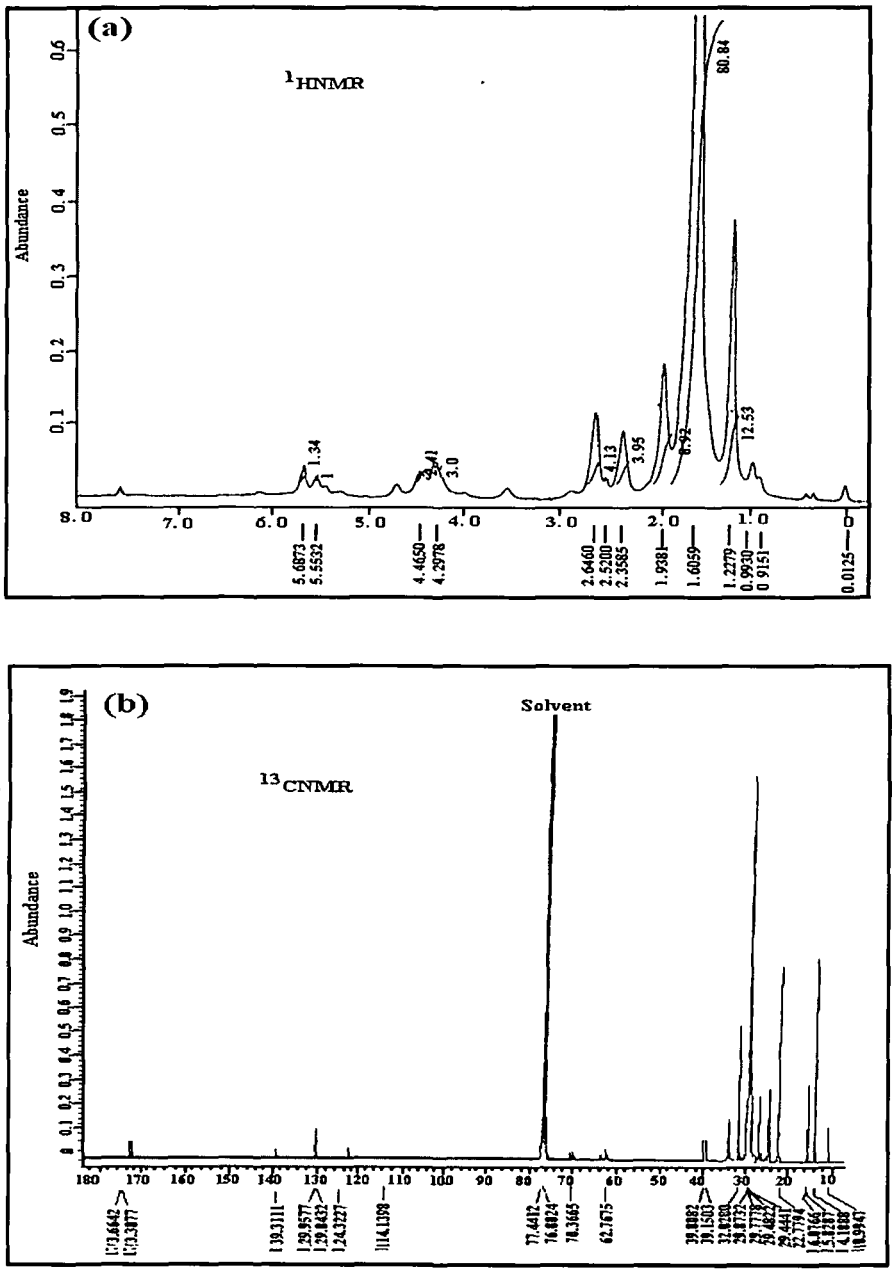

Fig. 4.19 ^{1}H NMR spectrum (a) and ^{13}C NMR spectrum (b) of P-3HV-5HDE-3HODE polymer produced by *P. aeruginosa* JQ866912 when grown on glucose as a carbon substrate

4.3.5 Physical analysis of PHA

4.3.5.1 Molecular weight determination of the PHA by Gel Permeation Chromatography (GPC)

The molecular weight of the biopolymer extracted from the bacterial strains *P. aeruginosa* JQ796859, *B. circulans* MTCC8167, and *P. aeruginosa* JQ866912 was measured by using GPC in THF solution using polystyrene standard. Average molecular weights of the polymers in THF are shown in Table 4.8. GPC curve of the polymers are presented in the Fig. 4.20-4.22.

Table 4.8 Average molecular weight of all three biopolymers

Polymer Sample	$\bar{M}_n$	$\bar{M}_w$	Polydispersity index
P. aeruginosa JQ796859	5.6×10^3	5.9×10^3	1.05
B. circulans MTCC8167	4.2×10^4	5.1×10^4	1.21
P. aeruginosa JQ866912	3.8×10^4	4.1×10^4	1.08

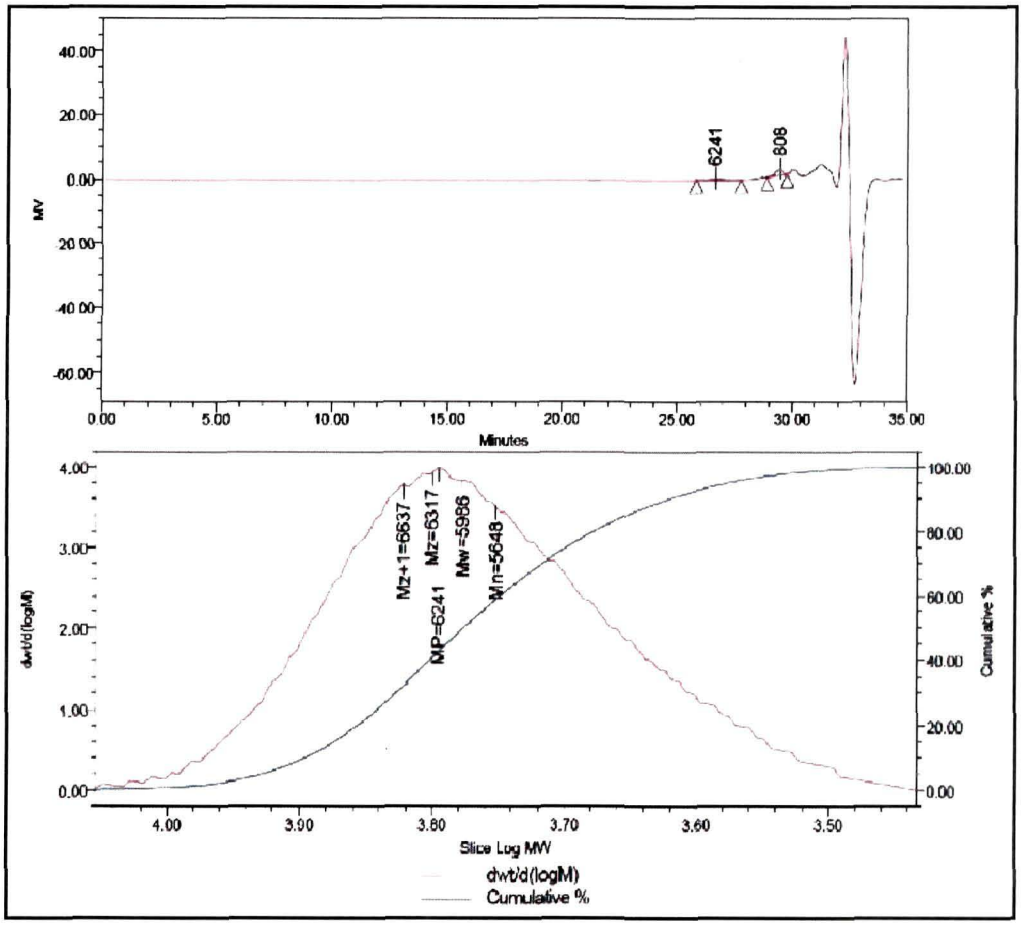

Fig. 4.20 GPC of *P. aeruginosa* JQ796859 biopolymer

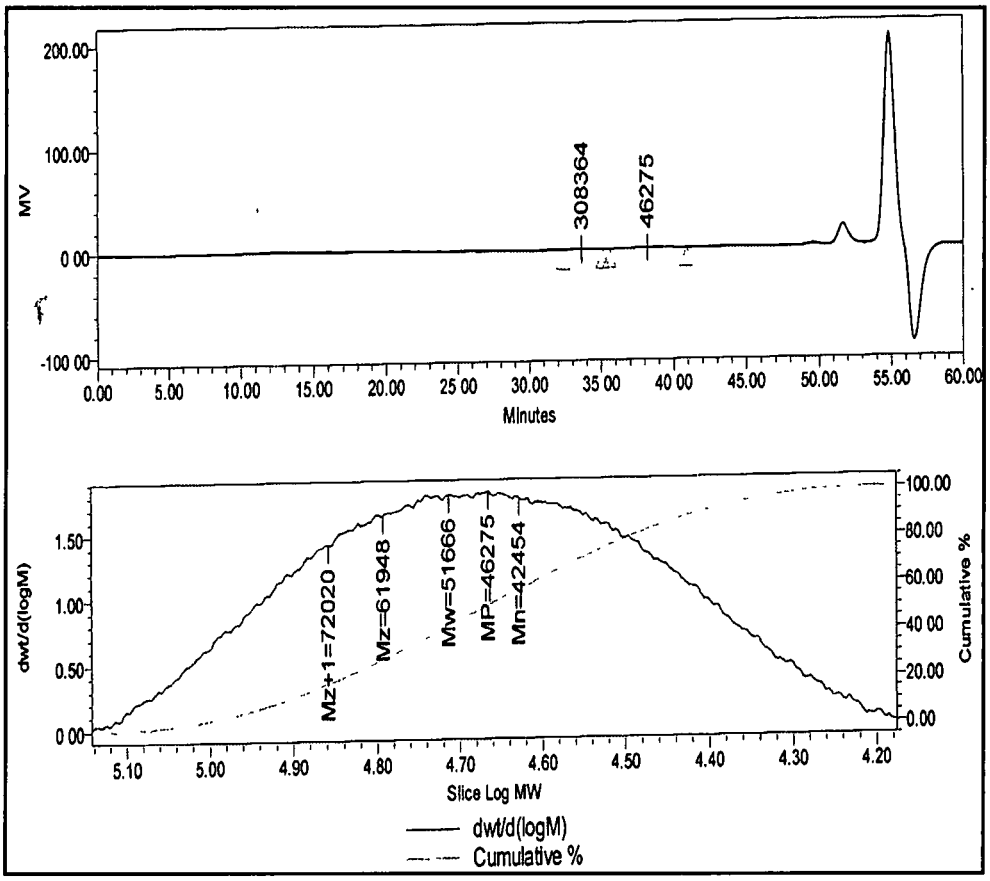

Fig. 4.21 GPC of *B. circulans* MTCC8167 biopolymer

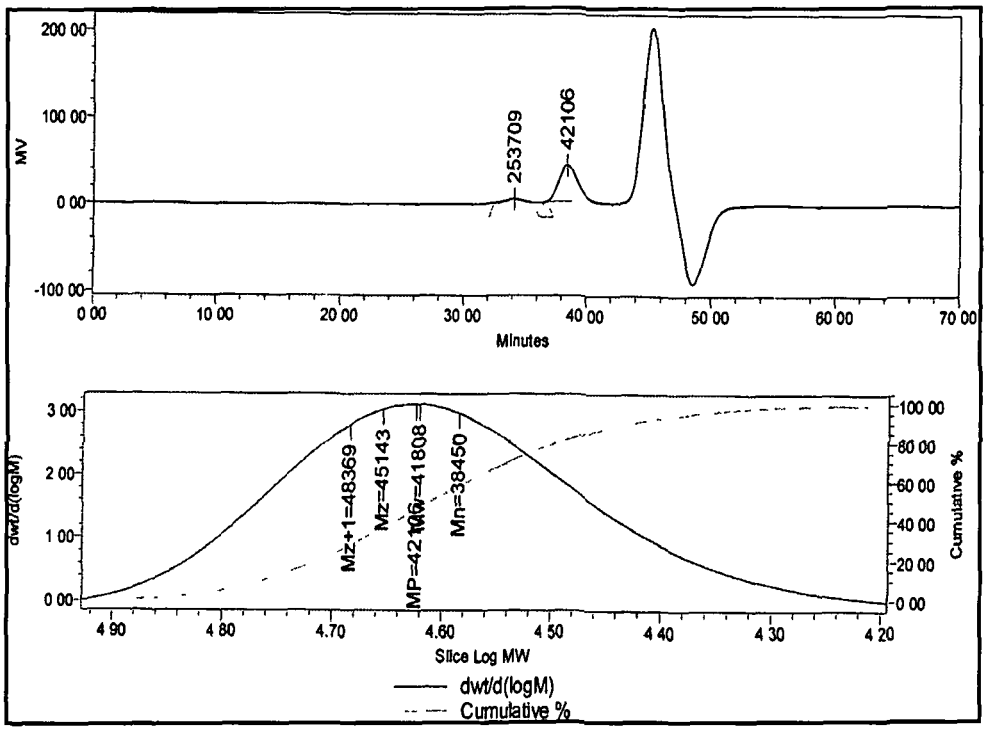

Fig. 4.22 GPC of *P. aeruginosa* JQ866912 biopolymer

4.3.5.2 Crystallinity study of the PHA by X-Ray diffraction (XRD)

X-ray diffraction analysis was performed on the PHA polymers isolated from *P. aeruginosa* JQ796859, *B. circulans* MTCC8167 and *P. aeruginosa* JQ866912 and data thus obtained are shown in Fig. 4.23. The calculation on crystallinity of the polymer samples is also presented in the Fig. 4.23. The XRD data revealed that the polymers are crystalline in nature with large crystal size.

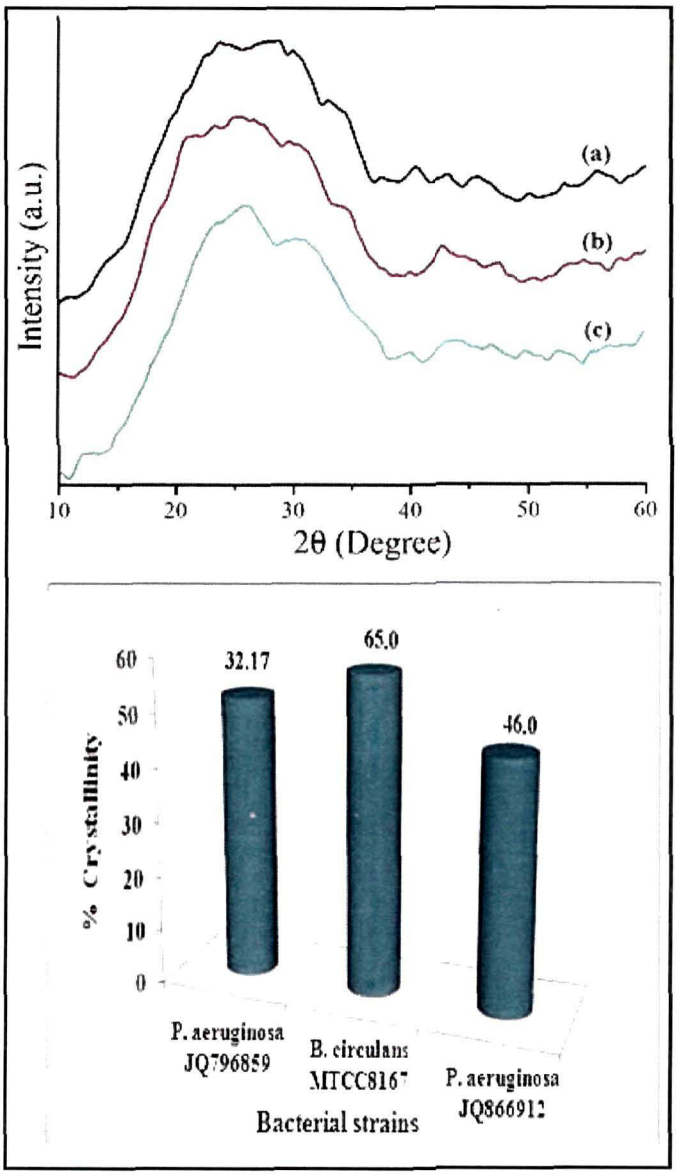

Fig.4.23 XRD result of polymer from *P. aeruginosa* JQ796859 (a), *B. circulans* MTCC8167 (b) and *P. aeruginosa* JQ866912 (c) bacterial strains

4.3.5.3 Thermogravimetric (TGA) analysis of PHA

The TGA of the polymers from the bacterial strains *P. aeruginosa* JQ796859, *B. circulans* MTCC8167 and *P. aeruginosa* JQ866912 is presented in the Fig. 4.24. The figure reveals the thermal degradation profile of all the polymers as compared to the commercially available standard polymer. From the Fig. 4.24, the percentage of weight loss of the polymer samples was calculated. The biopolymers isolated from the strains showed high degree of thermal stability in comparison to the standard polymer.

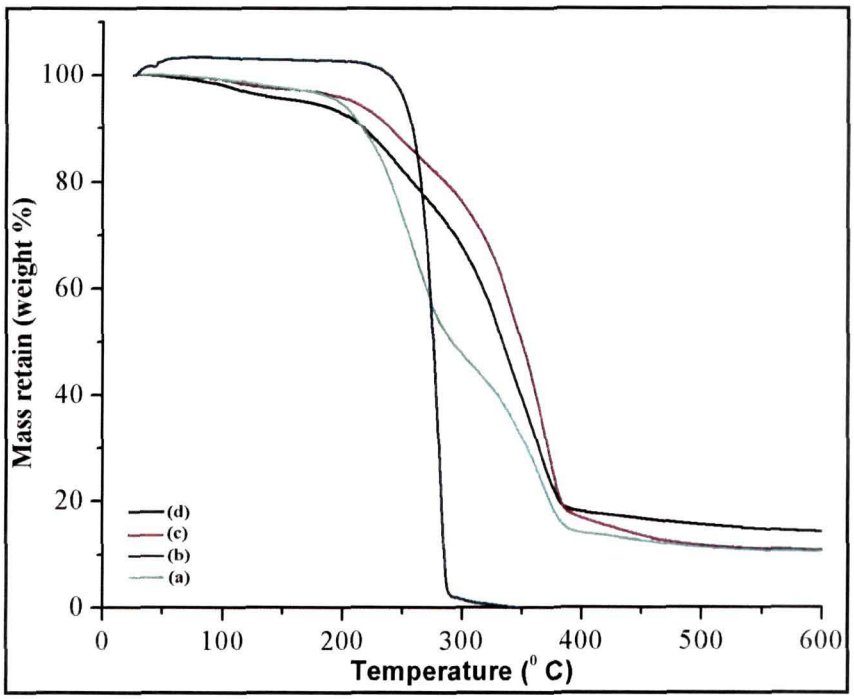

Fig. 4.24 Thermogravimetric analysis of the polymers from the strains *P. aeruginosa* JQ796859 (a), *B.circulans* MTCC8167 (b), *P. aeruginosa* JQ866912 (c) and standard polymer (d)

4.3.5.4 Differential scanning calorimetry (DSC) analysis of PHA

The DSC of the polymer from the bacterial strains *P. aeruginosa* JQ796859, *B. circulans* MTCC8167 and *P. aeruginosa* JQ866912 is presented in Fig. 4.25 (a-c). The figure depicts changes in the degradation pattern of the polymer samples. All the polymers show high thermal stability.

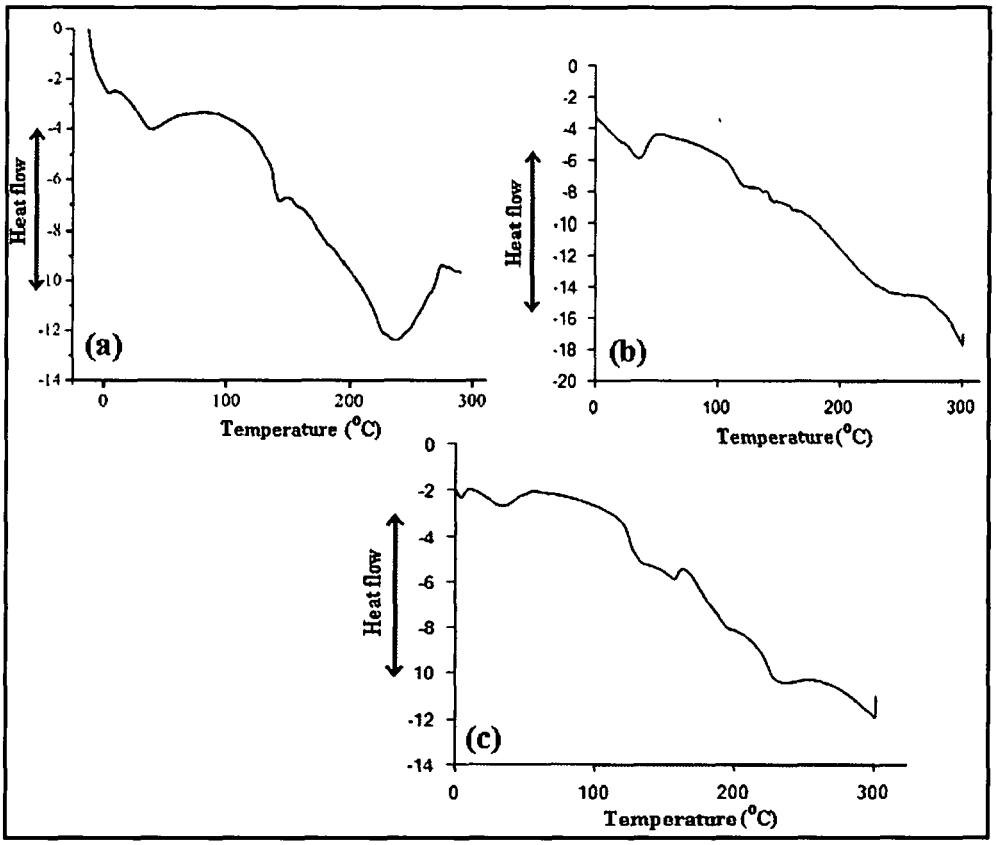

Fig. 4.25 DSC thermogram analysis of the polymer from *P. aeruginosa* JQ796859 (a), *B. circulans* MTCC8167 (b) and *P. aeruginosa* JQ866912(c)

4.3.5.5 Photoluminescence (PL) study of PHA

The PL emission spectra were recorded at two different wavelengths for all three polymers (Fig. 4.26). The PL of the polymers excited at their maximum absorption wavelength is measured. All of the polymers showed luminescence property. The polymer shows luminescence in the range of 300-420 nm with high intensity.

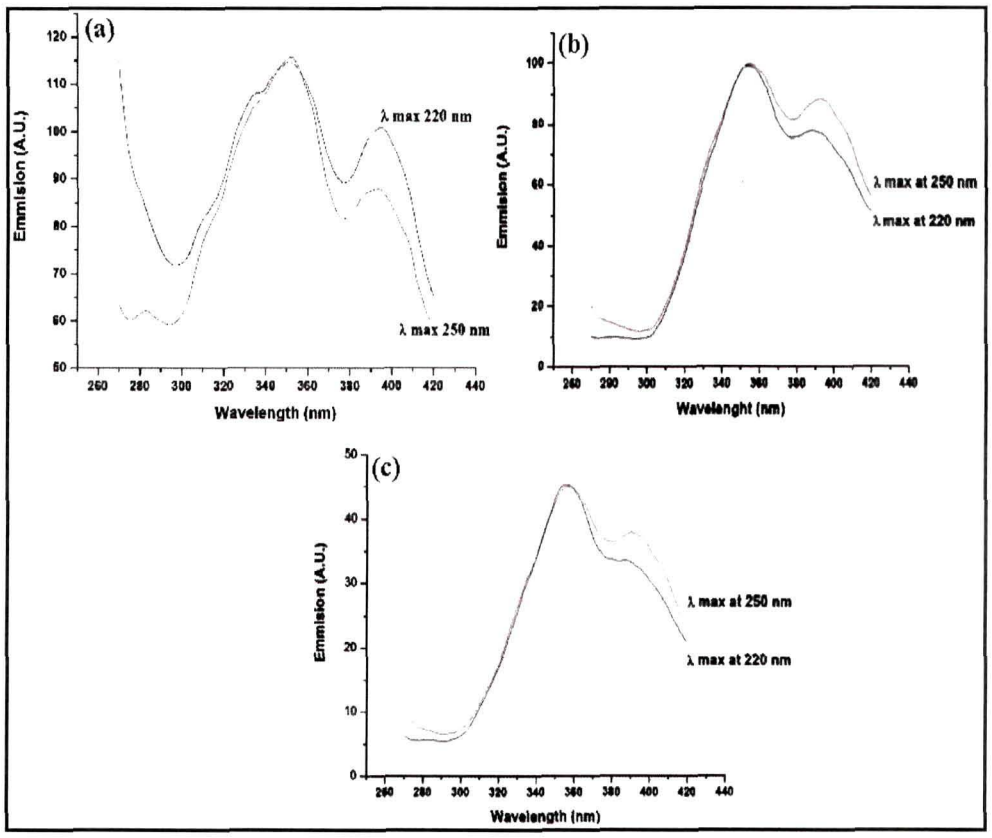

Fig. 4.26 PL intensity of the polymers isolated from *P. aeruginosa* JQ796859 (a), *B. circulans* MTCC8167 (b) and *P. aeruginosa* JQ866912 (c)

4.3.5.6 Surface morphology study of PHA using SEM

The surface morphology of the extracted polymer samples of all three bacterial strains was studied by using SEM. For the analysis, a thin film was prepared on to a thin glass slide by carefully spreading PHA solution in chloroform. After that the slide was left undisturbed for over 24 hours for complete drying. The SEM micrograph of the polymer from *P. aeruginosa* JQ796859, *B. circulans* MTCC8167 and *P. aeruginosa* JQ866912 strains are presented in Fig. 4.27 (a-c). SEM micrograph of the polymer samples showed that the polymers possessed uneven surface with non porous texture.

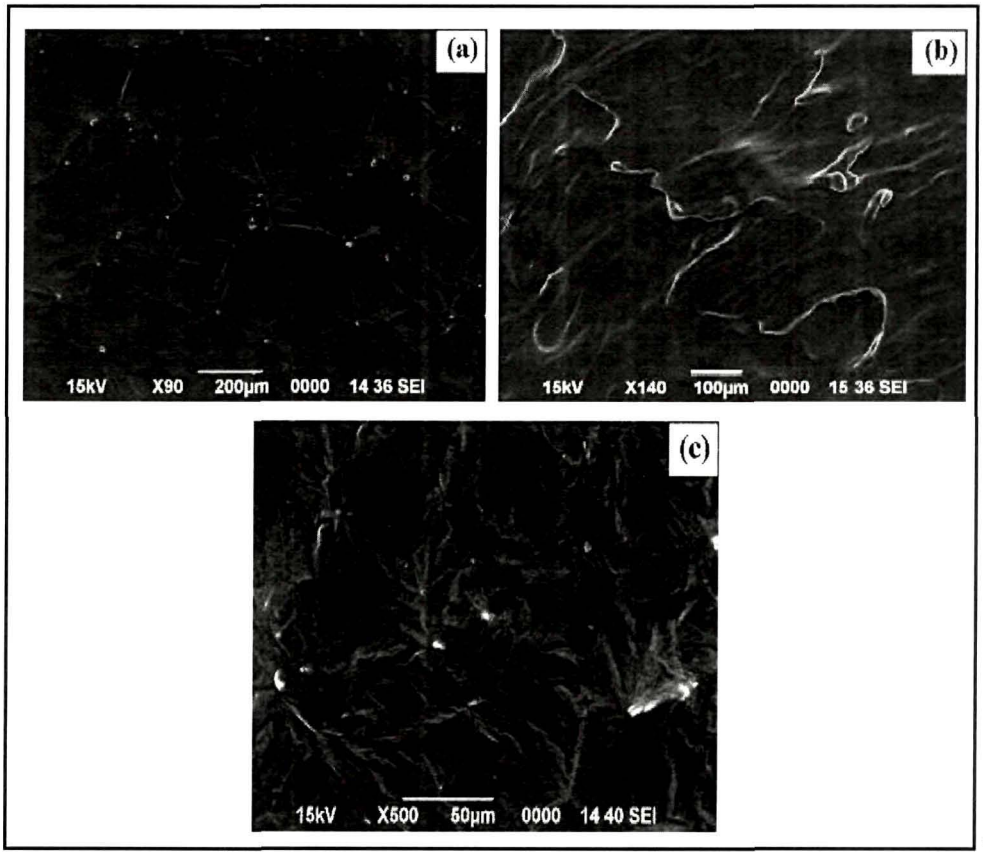

Fig. 4.27 SEM of PHA films obtained from *P. aeruginosa* JQ796859 (a), *B. circulans* MTCC8167 (b) and *P. aeruginosa* JQ866912 (c)

4.4. Biodegradation of PHA from *B. circulans* MTCC8167, *P. aeruginosa* JQ796859 and *P. aeruginosa* JQ866912

Biodegradation of the prepared biopolymer films of *B. circulans* MTCC8167 strain was done by treating it with the different soil bacteria like *Pseudomonas aeruginosa* strains BP4, BP5, BP7, *Bacillus subtilis* (R38-I) and fungal strains *Candida albicans* and *Fusarium oxysporum.* Biodegradation study of *P. aeruginosa* JQ796859 and *P. aeruginosa* JQ866912 biopolymer (PHA) was carried out by treating them with different soil bacteria like *Alacaligens faecalis* (MTCC8164), *B. circulans* (MTCC8167), *P. aeruginosa* (MTCC7815) and *Mycobacterium* spp (G-35I). At first, the biopolymer film was incubated in carbon free mineral salt medium and then the bacterial and fungal strains were inoculated separately in each of the incubated Erlenmeyer flasks. The biopolymer films exhibited slow degradation after 15-36 days of inoculation. The increase in the microbial (bacterial/fungal) biomass on the surface of the PHA film and in the medium indicated that they utilized PHA as the source of carbon and energy.

The FT-IR spectrum (Fig. 4.28) of the PHA film of the B. *circulans* MTCC8167 strain inoculated with the bacterial and fungal strains showed shifting and decrease in the intensity of the peak in comparison to the control (polymer without microbial treatment). Optical microscopic observation (Fig. 4.29) revealed many changes in the surface morphology of the PHA film of *B. circulans* MTCC8167 at the end of the incubation. From the data it could be concluded that the biopolymer from bacterial strain *B. circulans* MTCC8167 is biodegradable.

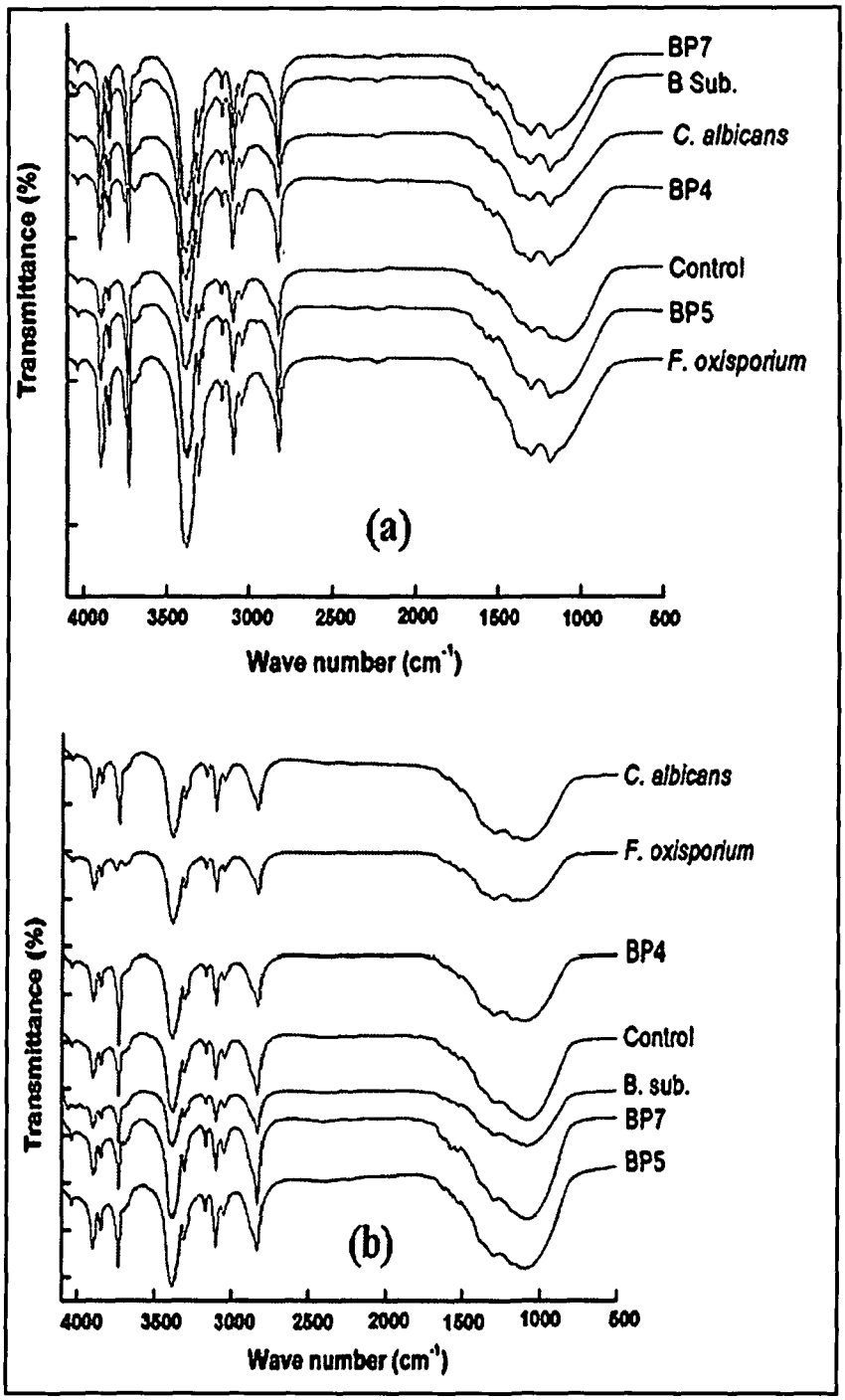

Fig. 4.28 FTIR spectra of the biodegradation of PHA from B. *circulans* MTCC8167 strain (a) after 15 days and (b) after 36 days of treatment with microbes

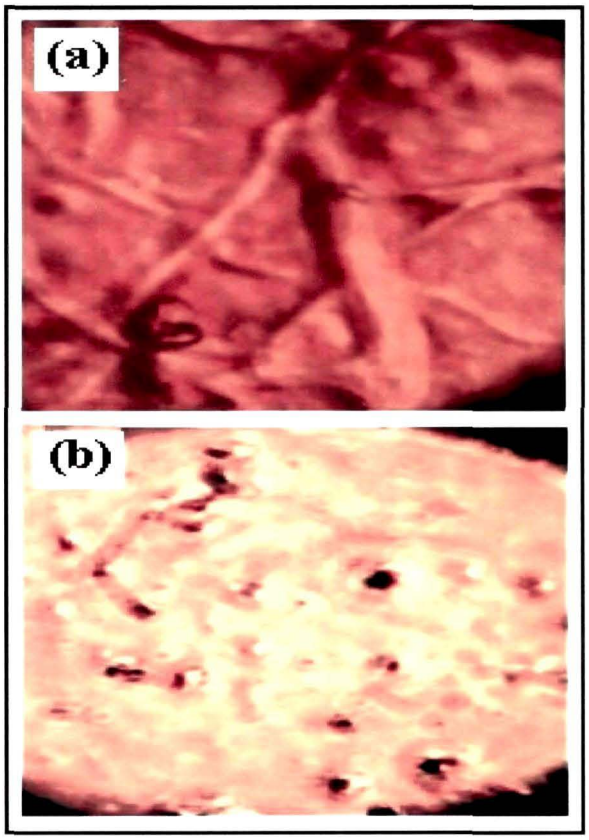

Fig. 4.29 Optical micrograph profiling of the degraded PHA film of B. *circulans* MTCC8167 strain after 15 days (a) and after 30 days (b) of treatment with microbes

The FT-IR spectra (Fig. 4.30 and Fig. 4.31) of the PHA films of the bacterial strains *P. aeruginosa* JQ796859 and *P. aeruginosa* JQ866912 inoculated with each of the bacterial strains also showed shifting and decrease in intensity of the peak in comparison to the control (polymer without microbial treatment). This revealed the degradation pattern of the polymers.

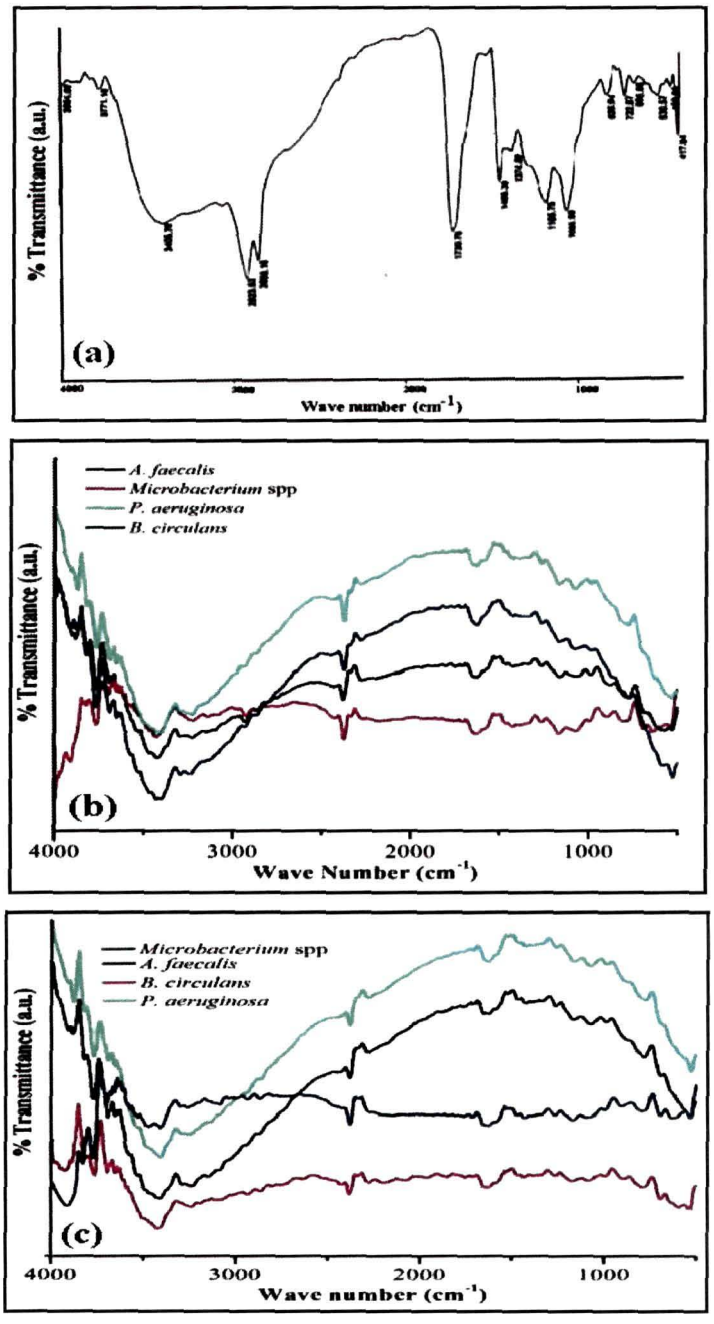

Fig. 4.30 FTIR spectra of biodegradation of PHA from *P. aeruginosa* JQ796859 (a) crude polymer as control without microbial treatment, (b) after 15 days and (c) after 36 days of treatment with each microbial strains

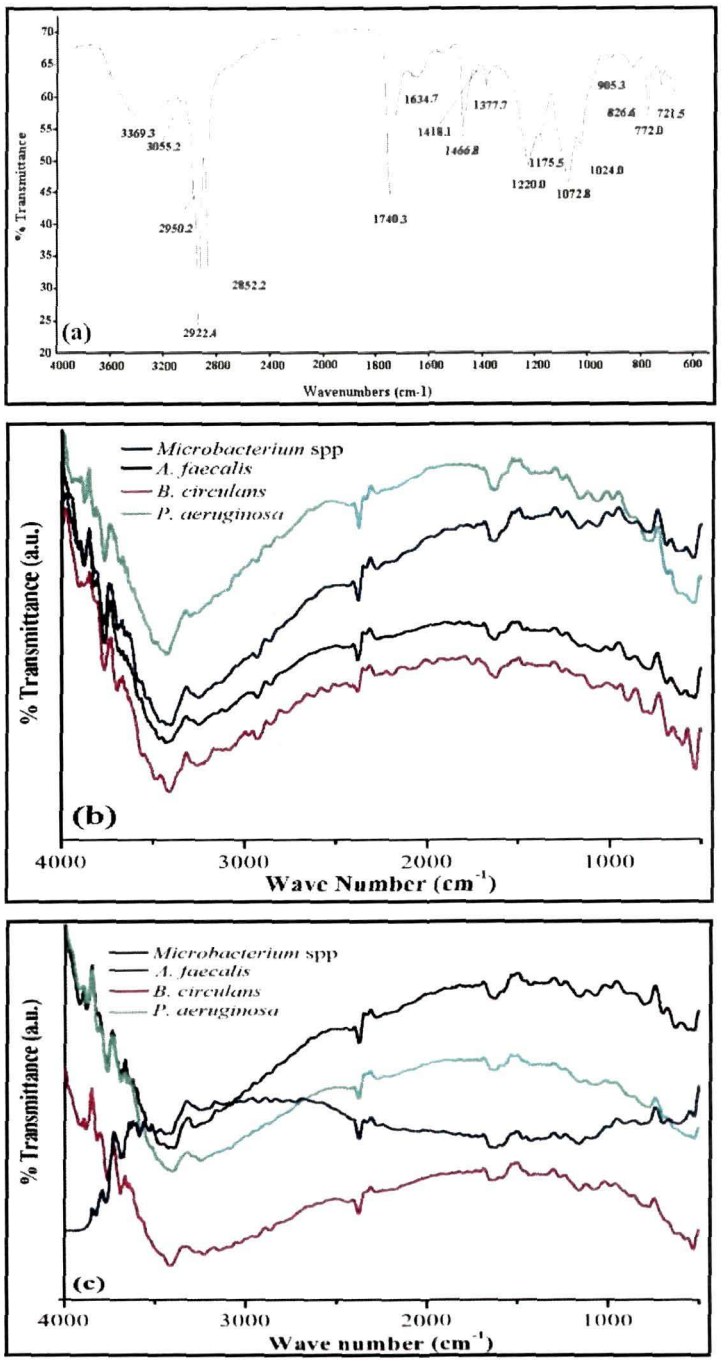

Fig. 4.31 FTIR spectra of biodegradation of PHA from *P. aeruginosa* JQ866912 (a) crude polymer as control without microbial treatment, (b) after 15 days and (c) after 36 days of treatment with each microbial strain

Scanning electron micrographs of the polymer films of bacterial strain *B. circulans* MTCC8167 before and after 36 days of biodegradation are presented in Fig. 4.32. The changes in the morphology of the polymer surface confirm the degradation of the polymer when exposed to microbial action.

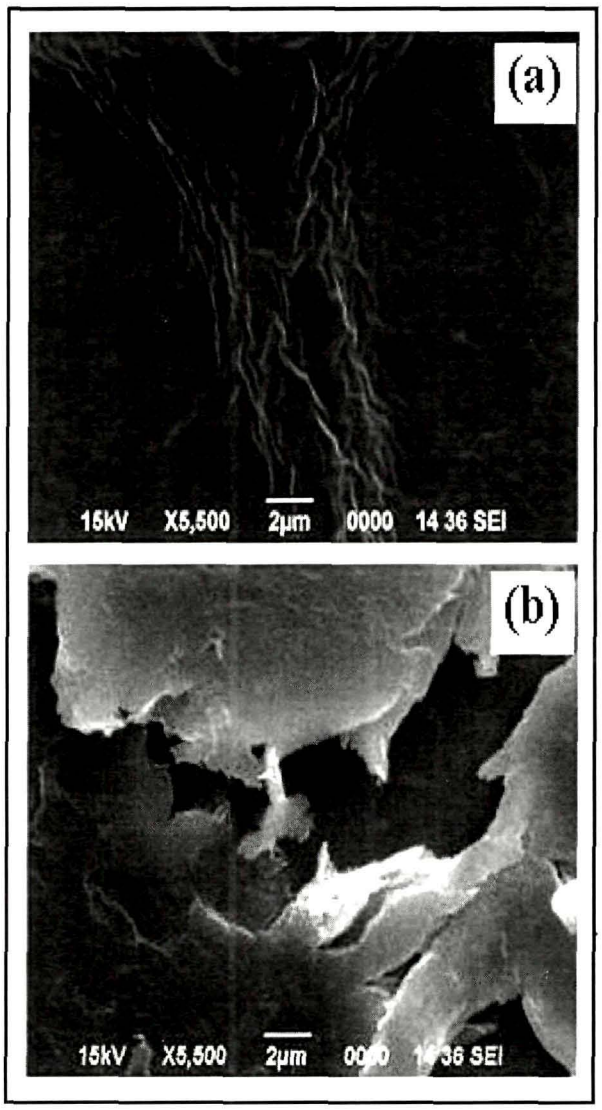

Fig. 4.32 SEM profiling of the degraded PHA film of *B. circulans* MTCC8167 strain, (a) before and (b) after 36 days

Similarly SEM micrograph of the PHA films of the bacterial strains *P. aeruginosa* JQ796859 and *P. aeruginosa* JQ866912 at the end of the incubation period of 36 days are presented in Fig. 4.33 and Fig. 4.34. The micrographs also showed many changes in the surface morphology which depicts the biodegradation of the polymer samples.

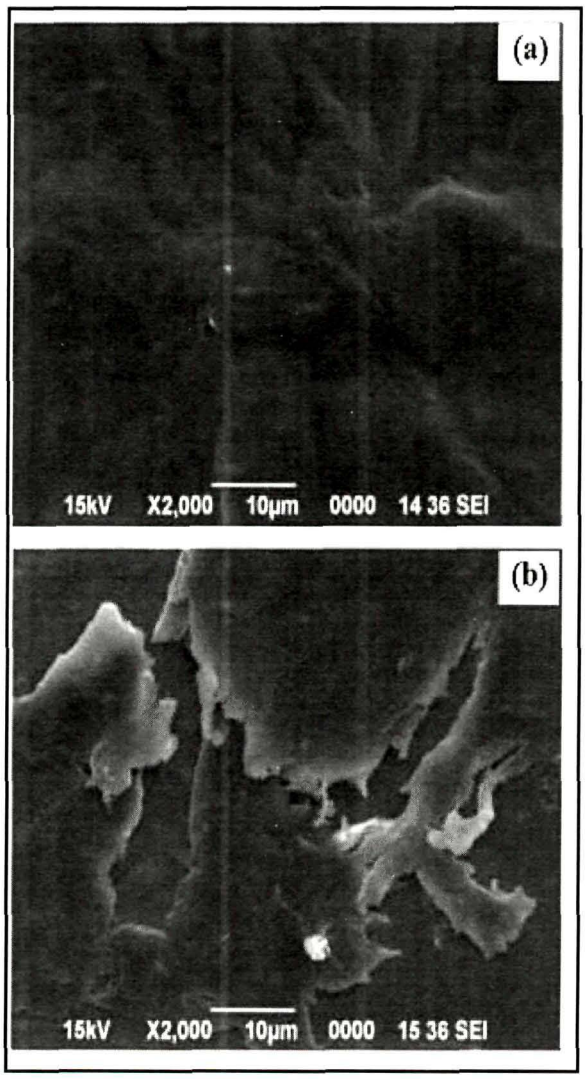

Fig. 4.33 SEM profiling of the degraded PHA film of bacterial strain *P. aeruginosa* JQ796859 (a) before and (b) after 36 days

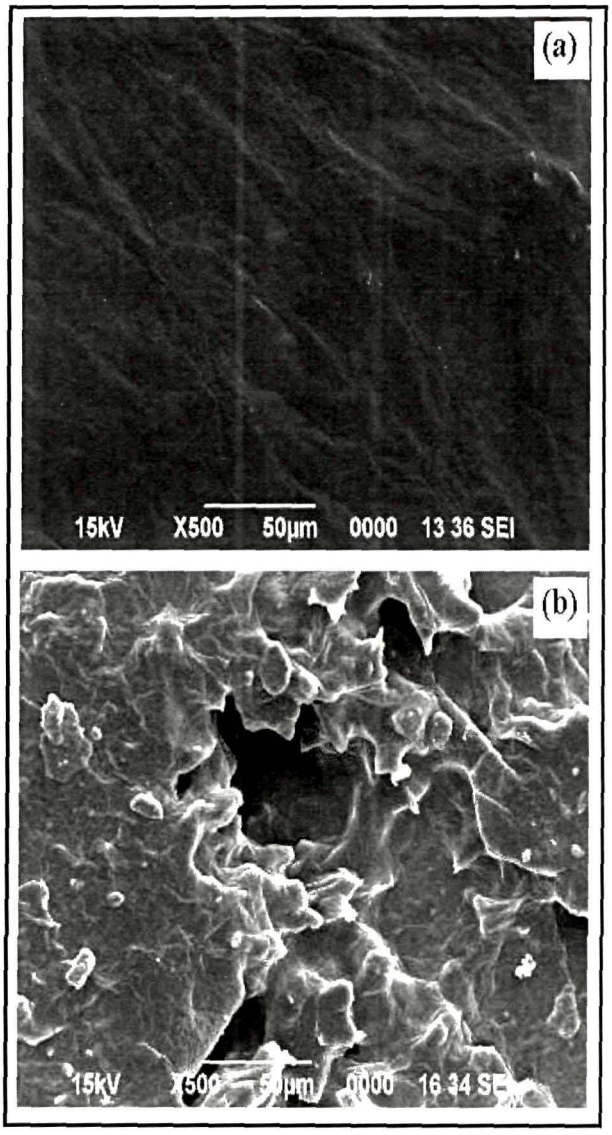

Fig. 4.34 SEM profiling of the degraded PHA film of bacterial strain *P. aeruginosa* JQ866912 (a) before and (b) after 36 days

4.5 Application of PHA of *B. circulans* MTCC8167 strain in enhancing the stability of colloidal silver nanoparticles (SNP)

4.5.1 Characterization by using FTIR spectroscopy

The FT-IR spectrum of the SNP confirmed the presence of silver in the material. The absorption peaks confirmed the presence of silver in the SNP, SNP-PHA *in situ* and SNP-PHA mix (Fig. 4.35). The shifting and decrease in the intensity of the absorption peaks revealed the successful conjugation or the presence of SNP in the SNP-PHA colloids. The photographic evidence (Fig. 4.36) depicted the stabilization of the SNP colloids for 29 days by the different methods.

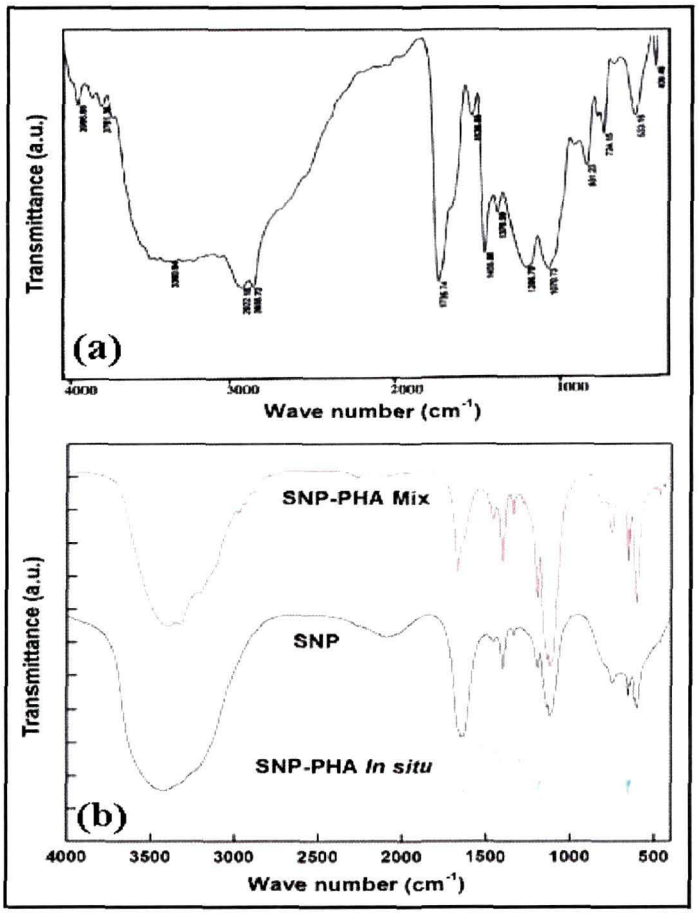

Fig. 4.35 FT-IR spectrum of PHA polymer isolated from *B. circulans* MTCC8167 (a) and the SNP, SNP-PHA *in situ* and SNP-PHA mixture (b)

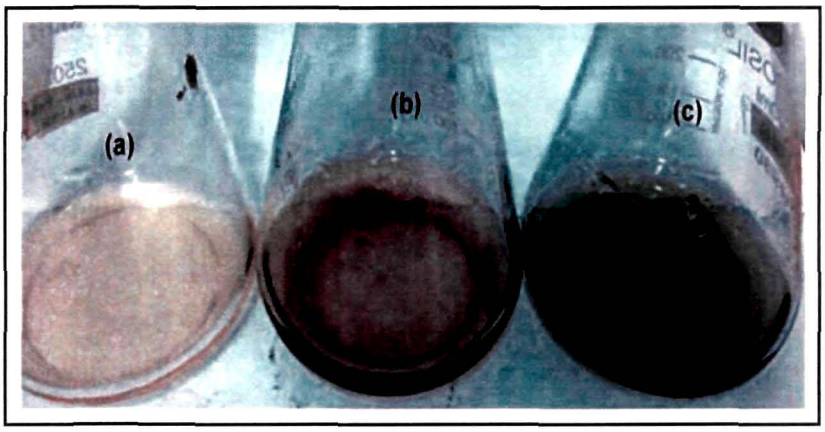

Fig. 4.36 SNP in different colloids: (a) SNP-PHA *in situ*, (b) SNP-PHA mixed and (c) SNP after 30 days aging at room temperature

4.5.2 Characterization of SNP-PHA by TEM

The size and morphology of the SNP are analyzed by TEM and data thus obtained are presented in Fig. 4.37.The TEM image confirms the presence of SNP in SNP-PHA *in situ* colloid.

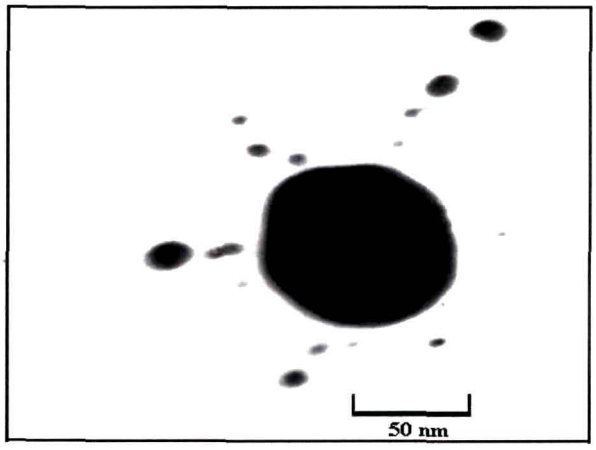

Fig. 4.37 Transmission electron micrograph (TEM) of the silver nano particle in SNP-PHA *in situ*

4.5.3 Characterization of SNP-PHA by UV-Vis spectroscopy

The UV-Vis spectra of the SNP colloids are presented in Fig. 4.38 (A). After 29 days the UV-Vis spectrum of the SNP shifted towards 420 nm. It was probably due to the aggregation of the SNP in the colloid. In the case of SNP-PHA *in situ*, the UV-Vis spectra showed the maximum absorption near 400 nm from day 1 to day 30 [Fig. 4.38 (B)].

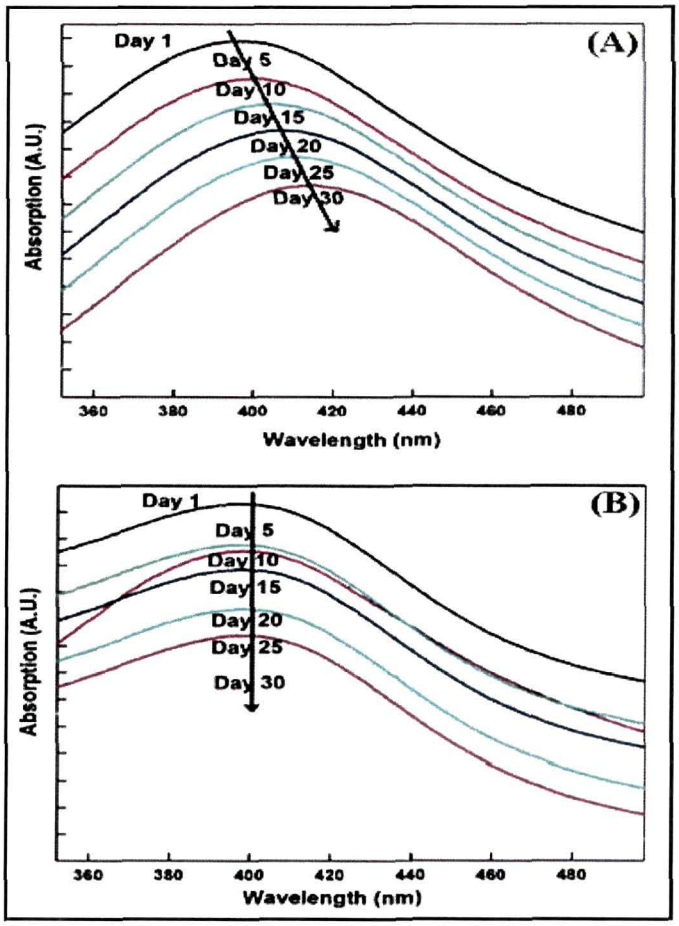

Fig. 4.38 UV-Vis wavelength scanning of the SNP in colloid (A) and SNP-PHA *in situ* (B)

The stability of the SNP-PHA *in situ* colloid can be seen from the consistency of the absorption maxima near 400 nm after 29 days of synthesis.

4.6 Photoluminescence study of PHA from *P. aeruginosa* JQ866912, its behavior study using different nanoparticles

4.6.1 XRD analysis of PHA- metal oxide nanoparticles hybrids

In order to determine the crystalline nature of the PHA/nanoparticles (NPs) hybrids, the thin film on the glass substrate was used for the XRD analysis. The XRD pattern of the prepared virgin PHA biopolymer, virgin nanoparticles and PHA/NiO NPs, PHA/ZnO NPs and PHA/CuO NPs hybrids with different concentrations is shown in the Fig. 4.39. The comparative study with the virgin nanoparticles, virgin polymer sample and the hybrid materials show the successful incorporation of the nanoparticles in the polymer matrix indicating that the crystal planes arise from the process.

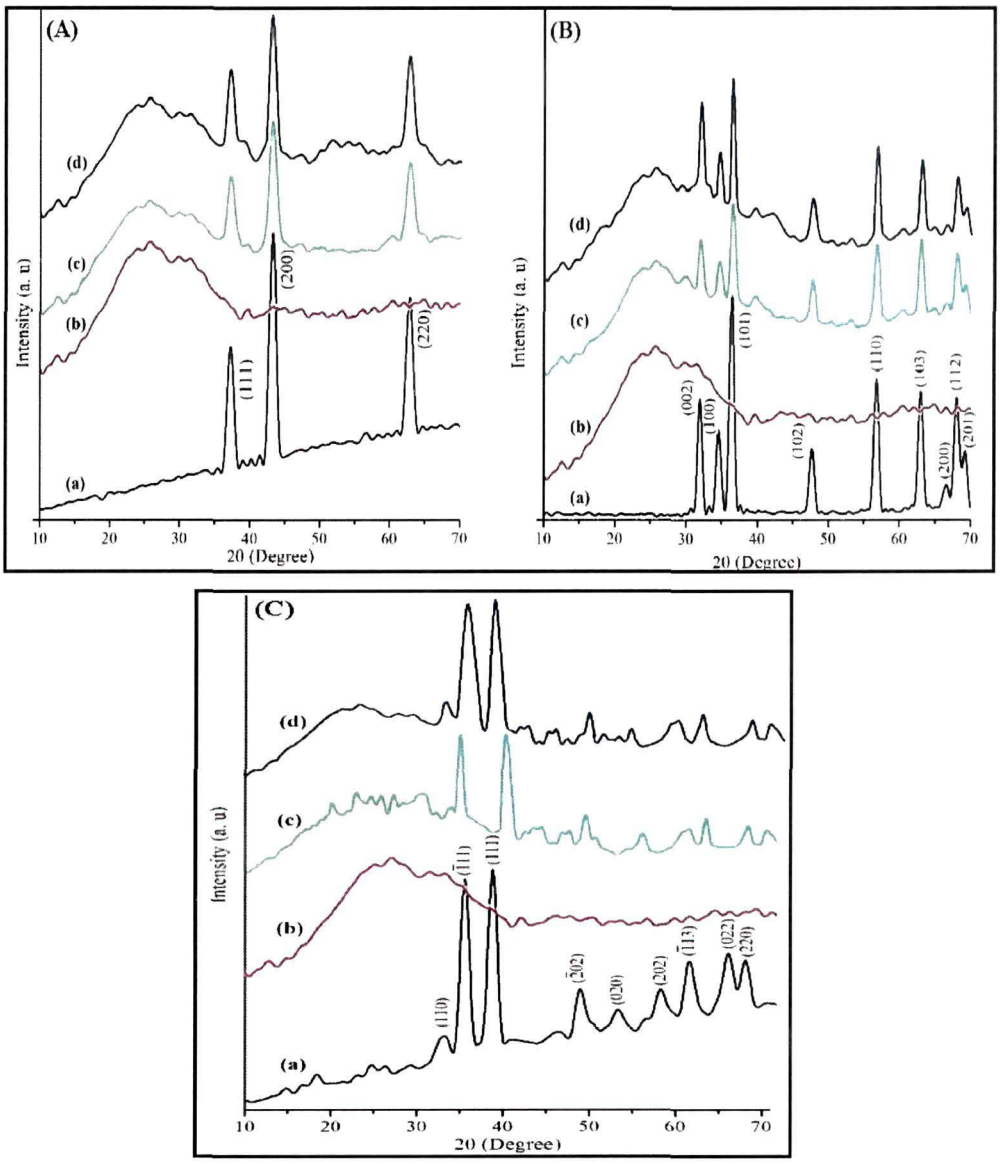

Fig 4.39 (A) XRD for NiO NPs (a), PHA (b), PHA/NiO NPs (1:1) hybrid (c), PHA/NiO NPs (1:3) hybrid (d), (B) XRD for ZnO NPs (a), PHA (b), PHA/ZnO NPs (1:1) hybrid (c), PHA/ZnO NPs (1:3) hybrid (d) and (C) XRD for CuO NPs (a), PHA (b), PHA/CuO NPs hybrid (1:1) (c), PHA/CuO NPs hybrid (1:3) (d) materials

4.6.2 Optical properties of PHA- metal oxide nanoparticle hybrids

The absorption and emission spectra of the polymer metal nano-particle hybrids were recorded with UV-Vis spectrophotometer and Fluorescence spectrophotometer. The UV absorbance spectra (Fig. 4.40) showed shifting of the absorption maxima of the PHA polymer when incorporated with the metal nanoparticles. The photoluminescence (PL) spectra (Fig. 4.41) of the polymer-nanoparticle hybrids were recorded by preparing thin films over glass plates. The PL spectra of the material showed a dramatic change in the emission nature to that of the virgin polymer. The intensity of the PL spectra also increased with the increase in concentration of metal oxide nanoparticles.

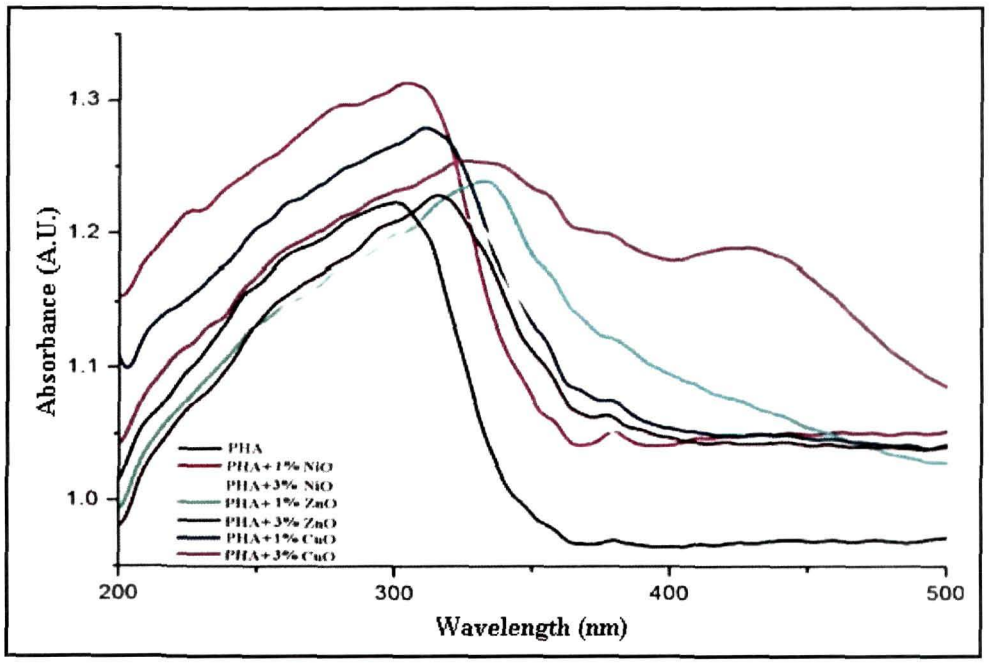

Fig. 4.40 UV-Vis spectra of crude polymer and polymer with different concentration of different nanoparticles in chloroform

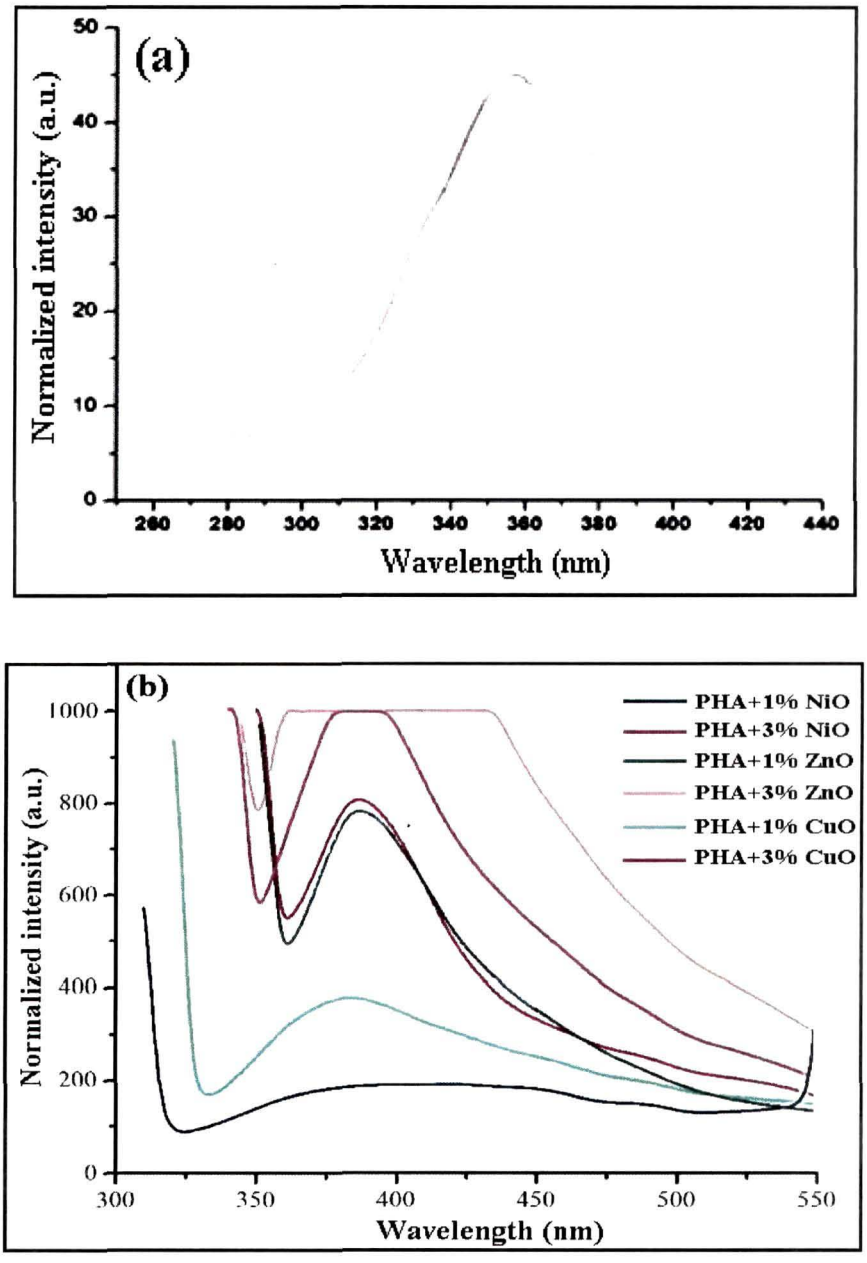

Fig. 4.41 Fluorescence spectra of (a) polymer (b) polymer in the presence of various nanoparticles in chloroform at their excitation wavelength

4.6.3 SEM analysis

The SEM micrograph of the virgin polymer and polymer-nanoparticle hybrids is presented in Fig. 4.42. The particle sizes observed in the image demonstrated the presence of nanoparticles within the polymer matrix.

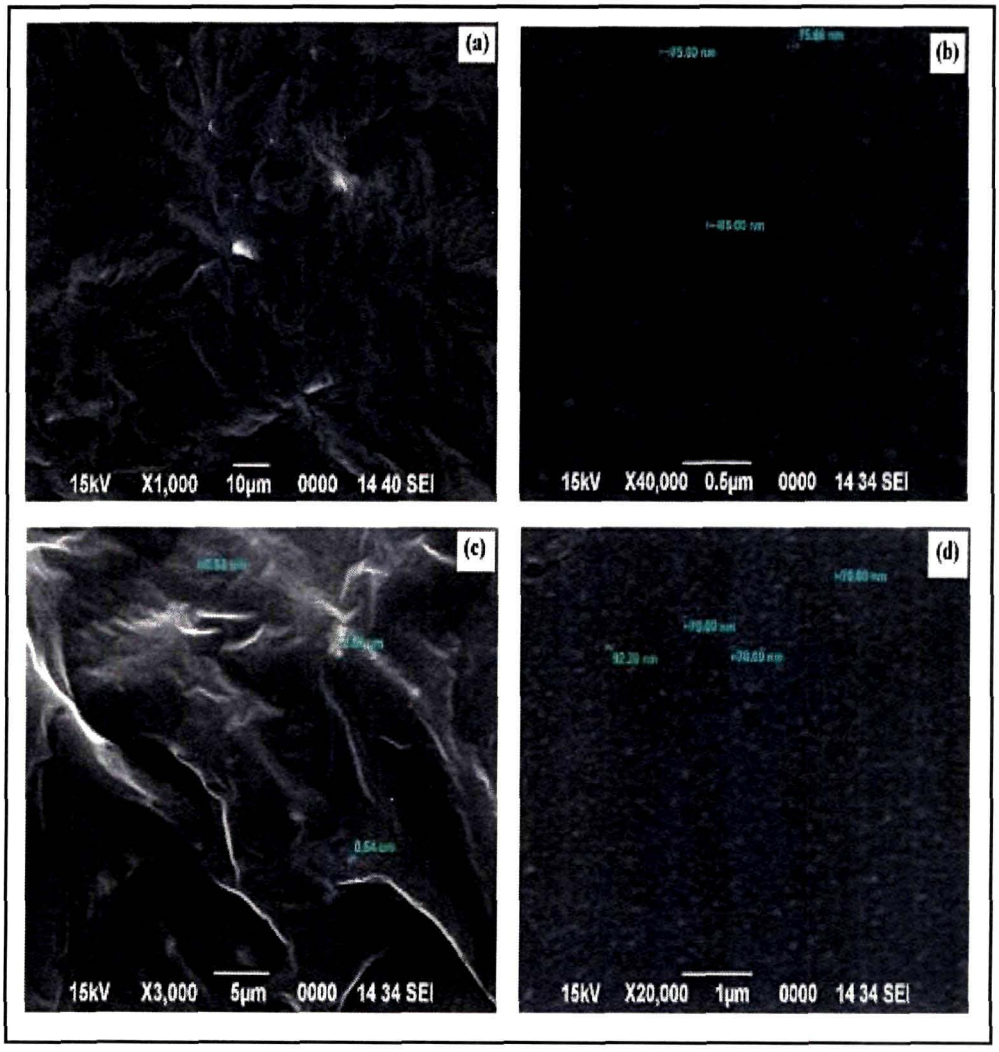

Fig. 4.42 SEM photograph of crude PHA (a), PHA/NiO NPs hybrid (b), PHA/ZnO NPs hybrid (c) and PHA/CuO NPs hybrid (d)

4.7 Application of PHA for composite based biosensor preparation with gold nanoparticles (AuNPs) for detection of antimalarial drug-Artemisinin

4.7.1 Cyclic voltametry (CV)

The electrochemical behavior of the PHA/AuNPs/HRP/ITO based biosensor was investigated by using CV. The cyclic voltametric behavior of the PHA/ITO (A), PHA/AuNPs/ITO (B) and PHA/AuNPs/HRP/ITO (C) films was studied at different scan rates (5 to 40 mV s^{-1}) in phosphate buffered saline (PBS) [50mM, pH 7.0 ±0.1, 0.9% NaCl] containing 5mM $[Fe(CN)_6]^{3-/4}$ (Fig. 4.43). It can be seen that the anodic peak potential (Fig. 4.43 B and C) shifts towards the positive side and the cathodic peak potential shifts in the reverse direction. Moreover, the redox peak currents are proportional to the square root of scan rate, $\upsilon^{1/2}$ (Fig. 4.44) indicating a diffusion electron transfer process. The effect of pH on the peak current was investigated in the pH range from 5.5 to 9.0 in the presence of 0.01 $\mu g.mL^{-1}$ artemisinin (Fig. 4.43 D). The plot of current versus pH showed the presence of the maximum peak current and a peak shape at pH 7.0±0.1 of PBS.

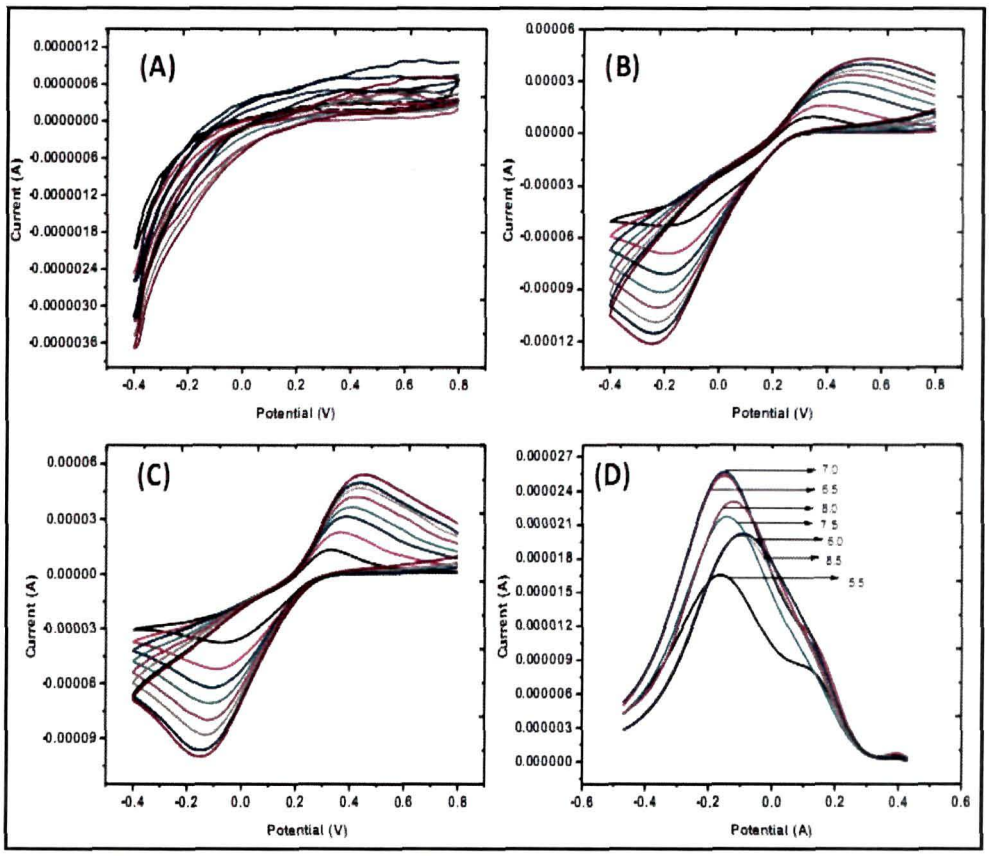

Fig. 4.43 Cyclic voltammograms of (A) PHA/ITO, (B) PHA/AuNPs/ITO, (C) PHA/AuNPs/HRP/ITO electrodes in PBS containing (5mM) $[Fe(CN)_6]^{3-/4-}$ at scan rate from 5.0 mV s^{-1} to 40.0 mV s^{-1} and (D) study of pH

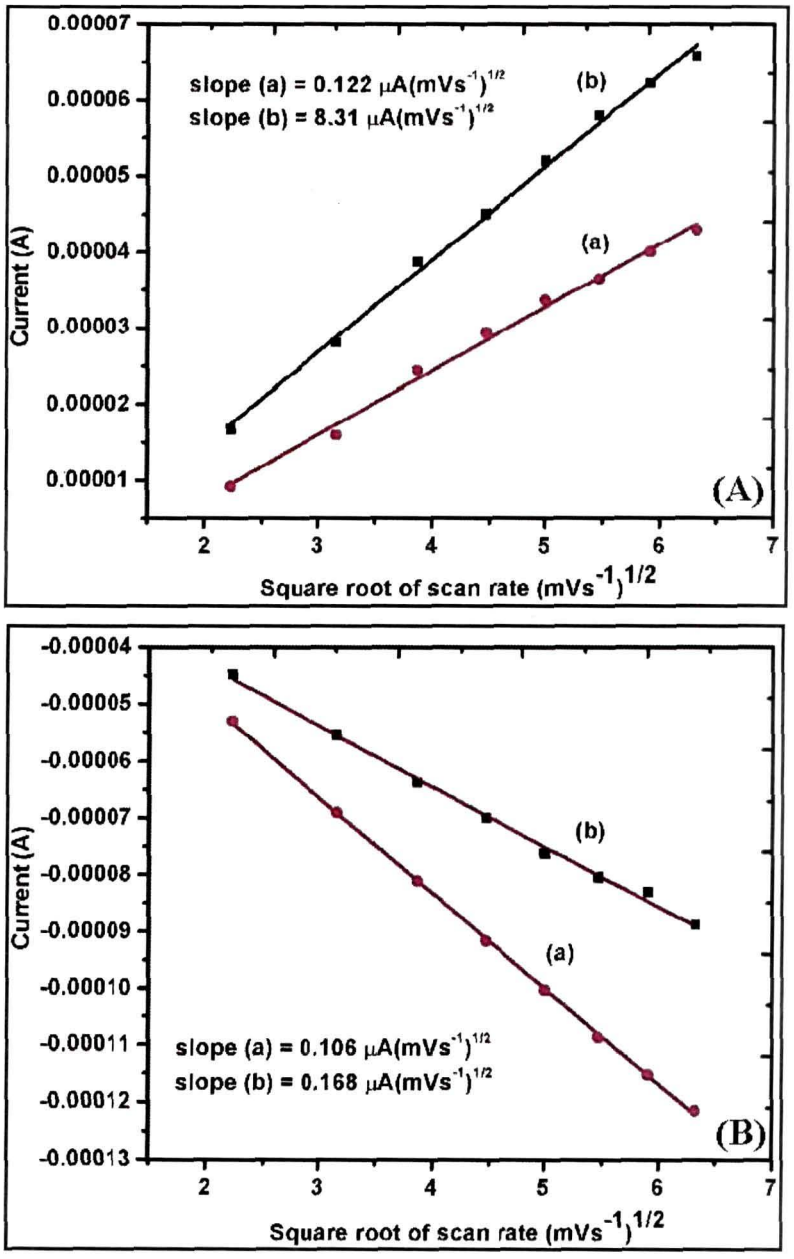

Fig. 4.44 Oxidations (A) and Reduction (B) peaks current with square root of scan rate for PHA/AuNPs/ ITO (a) and PHA/AuNPs/HRP/ITO (b)

4.7.2 EIS study

To investigate the effect of surface charge modulation for the determination of relative change in the surface resistance at zero potential, EIS was carried out on (a) PHA/ITO, (b) PHA/AuNPs/ITO and (c) PHA/AuNPs/HRP/ITO films (Fig. 4.45 B). From the figure, the surface charge transfer resistance, R_{CT} in the impedance spectrum of PHA/AuNPs /ITO electrode is observed to be lower in comparison to the others which depicted the successful incorporation of AuNPs into the PHA films. This could also be supported by the study of relative variation in CV at constant scan rate (5 mVs^{-1}) in PBS buffer containing 5mM $[Fe(CN)6]^{3-/4-}$ for three electrodes (a) PHA/ITO, (b) PHA-AuNPs /ITO and (c) PHA-AuNPs-HRP/ITO (Fig. 4.45 A) which also showed enhancement of current in PHA-AuNPs /ITO electrode in comparison to the others.

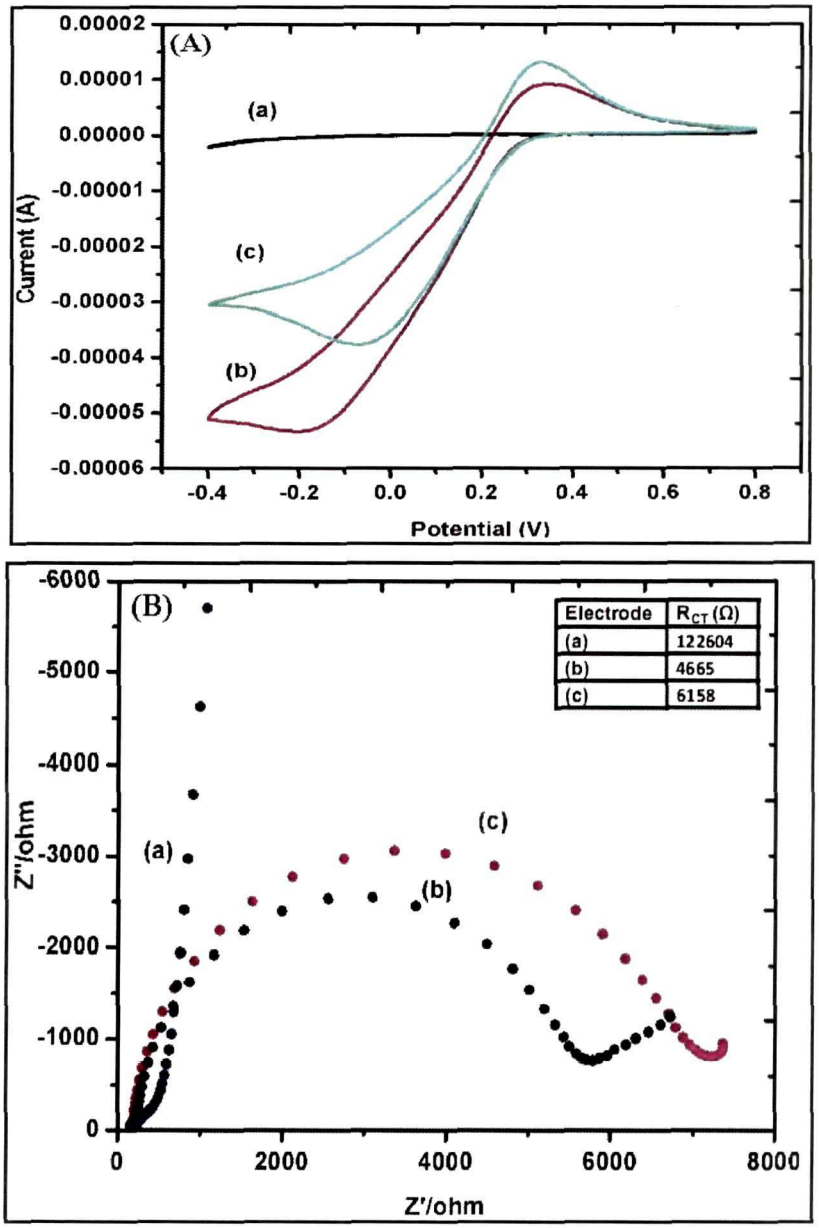

Fig. 4.45 Cyclic voltammograms of (A): (a) PHA/ITO (b) AuNPs/PHA/ITO (c) AuNPs/PHA/HRP/ITO scan rate at 5.0 mV s^{-1}, and (B): electro-chemical Nyquist plots of (a) PHA/ITO (b) AuNPs/PHA/ITO (c) AuNPs/PHA/HRP/ITO electrodes in PBS buffer (50mM) containing 5mM $[Fe(CN)6]^{3-/4-}$

4.7.3 SEM study

In order to get insight into the surface morphology of the working electrodes, the SEM micrograph was investigated. Fig. 4.46 (a) shows non-porous and smooth surface of the PHA, Fig. 4.46 (b) shows the surface of the electrodes consisting of uneven porous matrix of PHA, embedded with Au nanoparticles and Fig. 4.46 (c) shows immobilization of HRP to the PHA/AuNPs film.

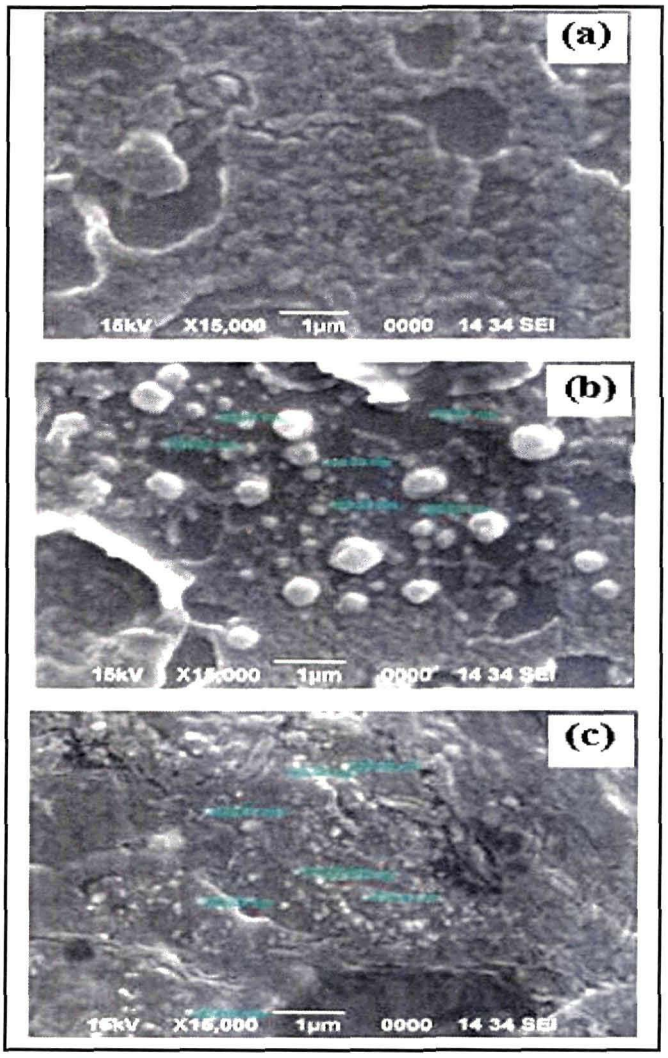

Fig. 4.46 SEM micrograph of the surface of (a) PHA/ITO (b) PHA/AuNPs/ITO (c) PHA/AuNPs/HRP/ITO biofilms

4.7.4 Application to real sample

The applicability of the proposed PHA/AuNPs/HRP/ITO bio-electrode based electro-chemical biosensor was assessed for antimalarial drug artimisinin in bulk and spiked human serum. The representative voltammograms and calibration curve are presented in Fig. 4.47. The figure shows that the current is proportional to the concentration of artimisinin over a convenient range. The precision was estimated for 0.01-0.08 $\mu g.mL^{-1}$ of the drug using the calibration curve and the standard addition method. The calibration equation parameters and the related validation data are presented in Table 4.9.

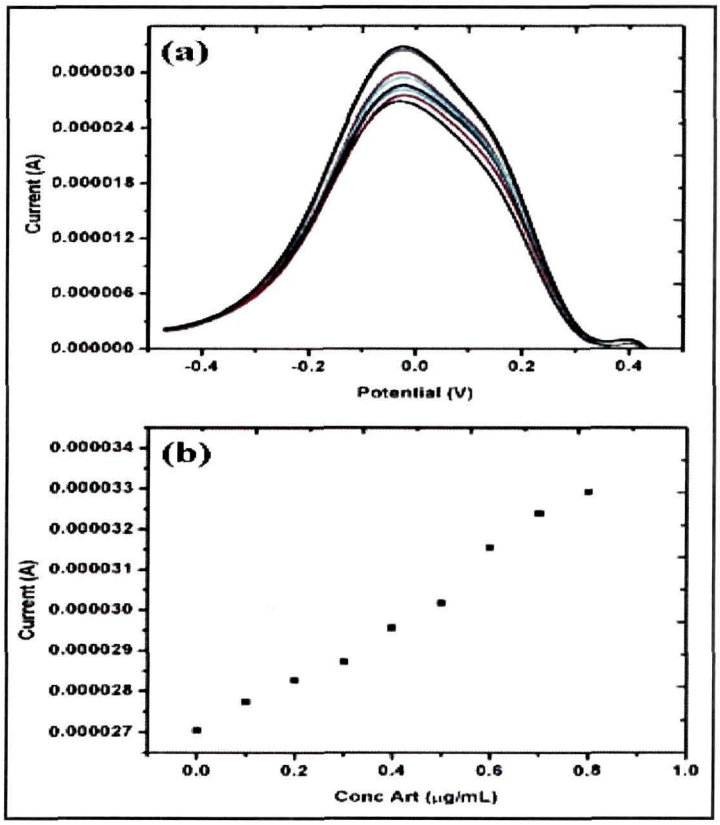

Fig. 4.47 (a) Shows biosensors response with increase in concentration of artemisinin and (b) calibration curve shows linearity for artemisinin as 0.01-0.08 $\mu g.mL^{-1}$

Table.4.9 Regression data of the calibration lines for the quantitative determination of *Artemisinin* by *organic-inorganic hybrid nanocomposite* AuNPs//PHA/HRP based biosensor in bulk form and spiked human serum using DPV waveform

Parameters	Bulk form	Human Serum
Linearity range ($\mu g\ mL^{-1}$)	0.01 – 0.08	0.01 – 0.06
Slope($A/\mu gmL^{-1}$)	8.8641×10^{-6}	9.1050×10^{-6}
Intercept (A)	2.6222×10^{-5}	2.6172×10^{-5}
Correlation coefficient (r^2)	0.985	0.984
RSD of the intercep	1.0438×10^{-8}	1.0762×10^{-8}
RSD of the slope	3.8728×10^{-7}	4.6491×10^{-7}
Reproducibility (%RSD)	1.01	1.13
Repeatability (%RSD)	0.66	1.01
LOD ($\mu g\ mL^{-1}$)	0.0035	0.0036
LOQ($\mu g\ mL^{-1}$)	0.0110	0.0121

4.8 Molecular genetic assessment of PHA producing bacterial isolates

4.8.1 Phylogenetic analysis of PHA producing bacterial isolates based on sequencing the conserved region of 16S rRNA gene

The genomic DNA isolated from the bacterial isolates BPC1 and BPC2 was used for the amplification of 16S rRNA gene by PCR. The 16S rRNA gene was amplified and sequenced and the sequences are shown in Fig. 4.48 and Fig. 4.49.

```
CGGGGGGCAGGCCTACACATGCAGTCGAGCGGATGAAGGGAGCTTGCTCCTGGATTCAGCGGCGGACGGGTGA
GTAATGCCTAGGAATCTGCCTGGTAGTGGGGGATAACGTCCGGAAACGGGCGCTAATACCGCATACGTCCTGA
GGGAGAAAGTGGGGGATCTTCGGACCTCACGCTATCAGATGAGCCTAGGTCGGATTAGCTAGTTGGTGGGGTA
AAGGCCTACCAAGGCGACGATCCGTAACTGGTCTGAGAGGATGATCAGTCACACTGGAACTGAGACACGGTCC
AGACTCCTACGGGAGGCAGCAGTGGGGAATATTGGACAATGGGCGAAAGCCTGATCCAGCCATGCCGCGTGTG
TGAAGAAGGTCTTCGGATTGTAAAGCACTTTAAGTTGGGAGGAAGGGCAGTAAGTTAATACCTTGCTGTTTTG
ACGTTACCAACAGAATAAGCACCGGCTAACTTCGTGCCAGCAGCCGCGGTAATACGAAGGGTGCAAGCGTTAA
TCGGAATTACTGGGCGTAAAGCGCGCGTAGGTGGTTCAGCAAGTTGGATGTGAAATCCCCGGGCTCAACCTGG
GAACTGCATCCAAAACTACTGAGCTAGAGTACGGTAGAGGGTGGTGGAATTTCCTGTGTAGCGGTGAAATGCG
TAGATATAGGAAGGAACACCAGTGGCGAAGGCGACCACCTGGACTGATACTGACACTGAGGTGCGAAAGCGTG
GGGAGCAAACAGGATTAGATACCCTGGTAGTCCACGCCGTAAACGATGTCGACTAGCCGTTGGGATCCTTGAG
ATCTTAGTGGCGCAGCTAACGCGATAAGTCGACCGCCTGGGGAGTACGGCCGCAAGGTTAAAACTCAAATGAA
TTGACGGGGGCCCGCACAAGCGGTGGAGCATGTGGTTTAATTCGAAGCAACGCGAAGAACCTTACCTGGCCTT
GACATGCTGAGAACTTTCCAGAGATGGATTGGTGCCTTCGGGAACTCAGACACAGGTGCTGCATGGCTGTCGT
CAGCTCGTGTCGTGAGATGTTGGGTTAAGTCCCGTAACGAGCGCAACCCTTGTCCTTAGTTACCAGCACCTCG
GGTGGGCACTCTAAGGAGACTGCCGGTGACAAACCGGAGGAAGGTGGGGATGACGTCAAGTCATCATGGCCCT
TACGGCCAGGGCTACACACGTGCTACAATGGTCGGTACAAAGGGTTGCCAAGCCGCGAGGTGGAGCTAATCCC
ATAAAACCGATCGTAGTCCGGATCGCAGTTTGCATCTAGCTTGCGGGAAGTCGGAATCGCTAGTAATCGCCAA
TCAGAATGTCACGGTGAATACGTTCCCGGACCTTGTACACACCGCCCGTCACACCATGGGAGTGGGTTTCTCC
AGAAGTAGCTAGTACAACCGCAAGGGGGACGGTACCACGGAGTGATTCATGACTGGGGTGAAGTCGAACAACG
AGCCAAGCTGT
```

Fig. 4.48 Partial DNA sequences of conserved region of 16S rRNA gene of the PHA producing bacterial isolate BPC1

CGGTGGCGGCGGCCTAACACATGCAAGTCGAGCGGATGAAGGGAGCTTGCTCCTGGATTCAGCG
GCGGACGGGTGAGTAATGCCTAGGAATCTGCCTGGTAGTGGGGGATAACGTCCGGAAACGGGCG
CTAATACCGCATACGTCCTGAGGGAGAAAGTGGGGGATCTTCGGACCTCACGCTATCAGATGAGC
CTAGGTCGGATTAGCTAGTTGGTGGGGTAAAGGCCTACCAAGGCGACGATCCGTAACTGGTCTGA
GAGGATGATCAGTCACACTGGAACTGAGACACGGTCCAGACTCCTACGGGAGGCAGCAGTGGGG
AATATTGGACAATGGGCGAAAGCCTGATCCAGCCATGCCGCGTGTGTGAAGAAGGTCTTCGGATT
GTAAAGCACTTTAAGTTGGGAGGAAGGGCAGTAAGTTAATACCTTGCTGTTTTGACGTTACCAACA
GAATAAGCACCGGCTAACTTCGTGCCAGCAGCCGCGGTAATACGAAGGGTGCAAGCGTTAATCGG
AATTACTGGGCGTAAAGCGCGCGTAGGTGGTTCAGCAAGTTGGATGTGAAATCCCCGGGCTCAAC
CTGGGAACTGCATCCAAAACTACTGAGCTAGAGTACGGTAGAGGGTGGTGGAATTTCCTGTGTAG
CGGTGAAATGCGTAGATATAGGAAGGAACACCAGTGGCGAAGGCGACCACCTGGACTGATACTGA
CACTGAGGTGCGAAAGCGTGGGGAGCAAACAGGATTAGATACCCTGGTAGTCCACGCCGTAACGA
TGTCGACTAGCCGTTGGGATCCTTGAGATCTTAGTGGCGCAGCTAACGCGATAAGTCGACCGCCT
GGGGAGTACGGCCGCAAGGTTAAAACTCAAATGAATTGACGGGGGCCCGCACAAGCGGTGGAGC
ATGTGGTTTAATTCGAAGCAACGCGAAGAACCTTACCTGGCCTTGACATGCTGAGAACTTTCCAGA
GATGGATTGGTGCCTTCGGGAACTCAGACACAGGTGCTGCATGGCTGTCGTCAGCTCGTGTCGTG
AGATGTTGGGTTAAGTCCCGTAACGAGCGCAACCCTTGTCCTTAGTTACCAGCACCTCGGGTGGG
CACTCTAAGGAGACTGCCGGTGACAAACCGGAGGAAGGTGGGGATGACGTCAAGTCATCATGGCC
CTTACGGCCAGGGCTACACACGTGCTACAATGGTCGGTACAAAGGGTTGCCAAGCCGCGAGGTGG
AGCTAATCCCATAAAACCGATCGTAGTCCGGATCGCAGTCTGCAACTCGACTGCGTGAAGTCGGA
ATCGCTAGTAATCGTGAATCAGAATGTCACGGTGAATACGTTCCCGGGCCTTGTACACACCGCCC
GTCACACCATGGGAGTGGGTTGCTCCAGAAGTAGCTAGTCTAACCGCAAGGGGGACGGTACCTCT
GGAGGTTTCCCT

Fig. 4.49 Partial DNA sequences of conserved region of 16S rRNA gene of the PHA producing bacterial isolate BPC2

4.8.1.1 Phylogeny of BPC1 strain

A homologous search result of the bacterial strain BPC1 demonstrated 98-99% similarity of 16S rDNA sequence with other species of the genus *Pseudomonas* as shown in Table 4.10. The phylogenetic tree constructed from the sequence data by the neighbour-joining method showed that *Pseudomonas aeruginosa* P21 (HQ697283) has 99% homology with BPC1 and represented its closest phylogenetic neighbor (Fig. 4.50).

Table 4.10 Homologous search results of partial sequence of 16S-rRNA gene of strain BPC1 using Basic Local Alignment Search Tool (BLAST) from National Centre for Biotechnology Information (NCBI). The 16S-rDNA sequences from microbes showing up to 99% identity are shown

Accession	Organism name	S_ab score
EU147007	*Pseudomonas putida;* CGL-3	0.994
EU826025	*Pseudomonas. aeruginosa* CDB35	0.997
GQ472194	*Pseudomonas* sp. XQ-ph1	0.995
EU449119	*Pseudomonas* sp. 9 GUW	0.995
HM355700	*Pseudomonas aeruginosa;* BAC3111	0.994
HM355726	*Pseudomonas aeruginosa;* BAC1137	0.994
HQ697283	*Pseudomonas aeruginosa;* P21	1.000
HQ697284	*Pseudomonas aeruginosa;* P22	1.000
HQ697285	*Pseudomonas aeruginosa;* P28	0.998
HQ697286	*Pseudomonas aeruginosa;* P43	0.998

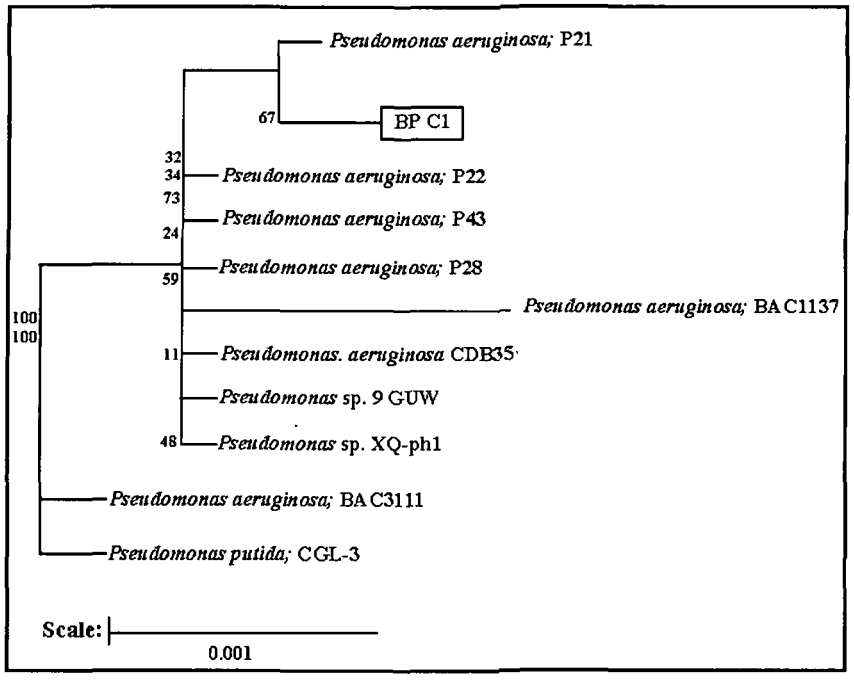

Fig. 4.50 Phylogenetic relationships of strain BPC1 and other closely related *Pseudomonas* species based on 16S rDNA sequencing. The tree was generated using the neighbour-joining method

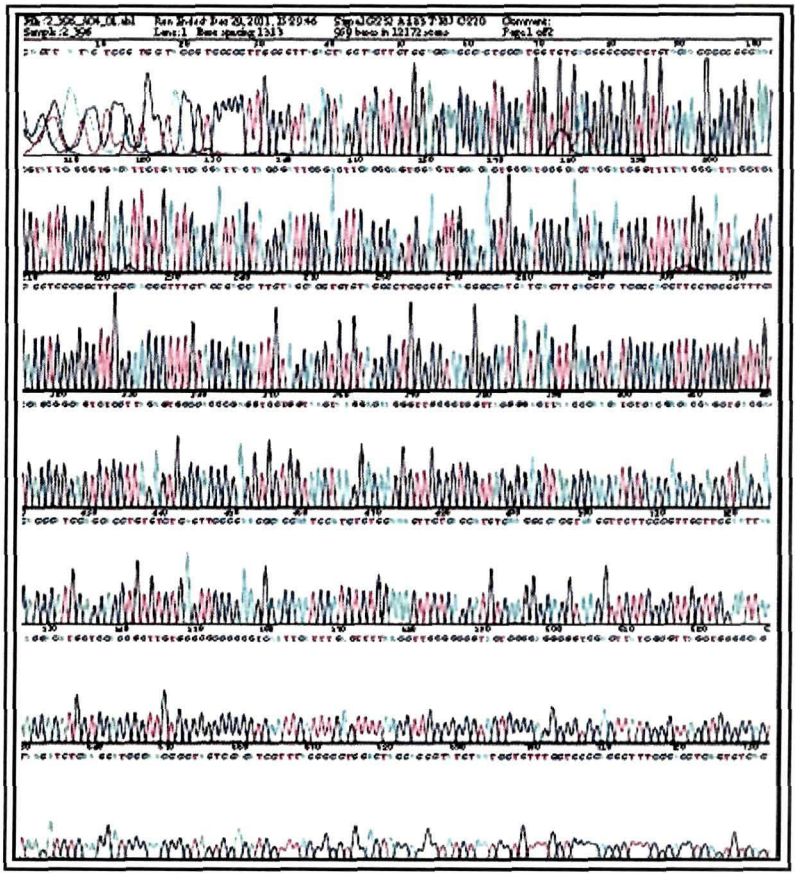

Fig. 4.51 Electropherogram of 16S rRNA gene of strain BPC1

4. 8.1.2 Phylogeny of strain BPC2

A homologous search result of 16S-rDNA sequence of strain BPC2 demonstrated 98-99% similarity with other species of the genus *Pseudomonas* as shown in Table 4.11. The phylogenetic tree was constructed from the 16S rDNA partial sequence data by the neighbour-joining method. It was observed that *Pseudomonas aeruginosa* MTH8 (HQ202541) showed 99% homology with BPC2 and represented its closest phylogenetic neighbor (Fig. 4.52).

Table 4.11 Homologous search results of 16S-rRNA gene partial sequence of strain BPC2 using Basic Local Alignment Search Tool (BLAST) from National Centre for Biotechnology Information (NCBI). The 16S-rDNA sequences from microbes showing upto 99% identity are shown

Accession	Organism name	S_ab score
DQ237950	*Pseudomonas* sp. Bxl-1	0.999
FJ462714	*Pseudomonas. aeruginosa;* Y-4	1.000
GQ926937	*Pseudomonas aeruginosa;* DM2	0.998
GU272400	*Pseudomonas* sp. YKM_M4	0.997
GU726840	*Pseudomonas aeruginosa;* 1242	1.000
HQ202541	*Pseudomonas aeruginosa;* MTH8	0.997
HM448980	*Pseudomonas* sp. NEHU. BSSRJ.2	0.999
HM448981	*Pseudomonas* sp. NEHU. BSSRJ.3	0.999
HM448983	*Pseudomonas* sp. NEHU. BSSRJ.5	0.999
JF331665	*Pseudomonas aeruginosa;* NL01	0.991

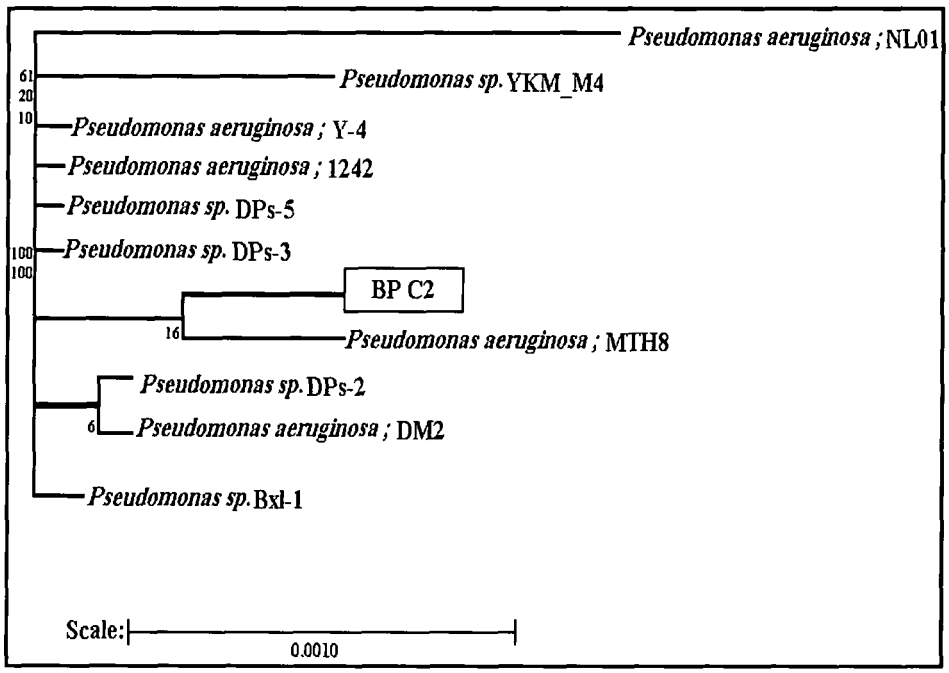

Fig. 4.52 Phylogenetic relationship (neighbour-joining method) of the strain BPC2 and other closely related *Pseudomonas* species based on 16S rDNA sequencing

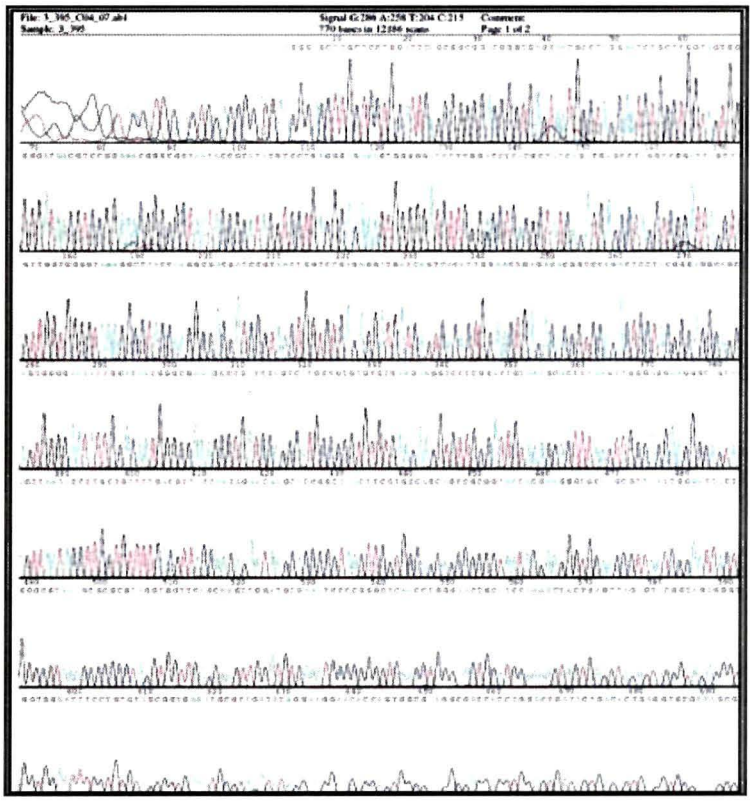

Fig. 4.53 Electropherogram of 16S rRNA gene of strain BPC2

4.8.1.3 Bacterial identification and re-designation

The 16S-rDNA sequences of *P. aeruginosa* strain BPC1 and *P. aeruginosa* strain BPC2 were deposited to GenBank NCBI and GenBank ID of partial 16S-rDNA sequence was given as *P. aeruginosa* BPC1 (JQ796859) and *P. aeruginosa* BPC2 (JQ866912) for BPC1 and BPC2 respectively.

4.8.1.4 Taxonomic identification of BP2 strain

The strain BP2 was previously isolated and taxonomically identified in IMTECH, Chandigarh as *B. circulans* MTCC8167. Further this was screened for biosurfactant production. The biopolymer production from this strain was investigated for the first time.

4.8.2. PCR based identification of the PHA biosynthetic genes in *P. aeruginosa* strains JQ796859 and JQ866912

PCR was performed using forward (I-179L; 5′-ACAGATCAACAAGTTCTACATCTTCGAC-3′) and reverse (I-179R; 5′-GGTGTTGTCGTTGTTCCAGTAGAGGATGTC-3′) primers based on two highly conserved sequences deduced from a multiple sequence alignment analysis of *Pseudomonas* phaC1 and phaC2 genes. The PCR product obtained from the bacterial strains *P. aeruginosa* JQ796859 and JQ866912 was about 540 bp (Fig. 4.54). The size of the PCR products agrees with the length of the phaC1 and phaC2 genes flanked by the I-179L/ I-179R primer-pair and also provides evidence for the presence of phaC genes in the above two *P. aeruginosa* strains.

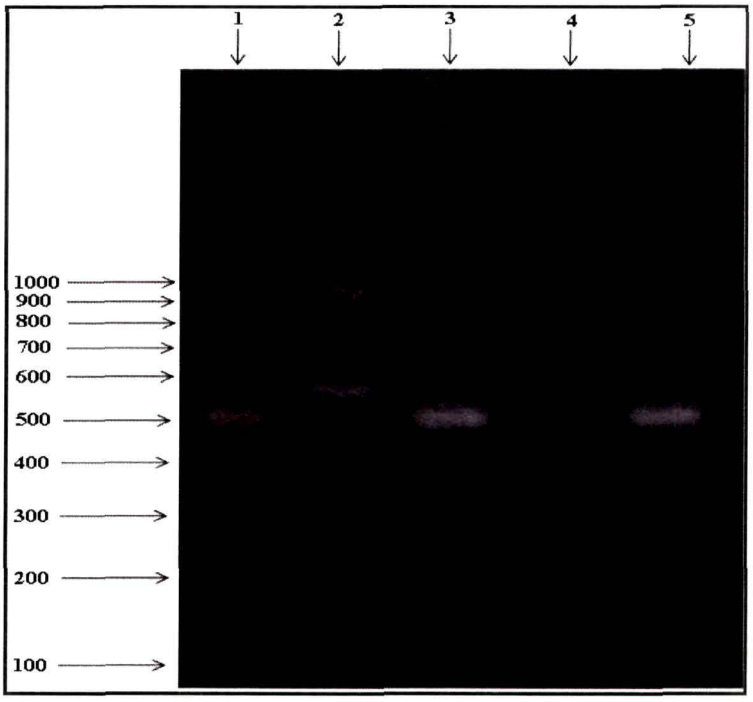

Fig. 4.54. PCR detection of phaC1/phaC2 genes. Purified genomic DNA and regular *Taq* DNA polymerase were used in the reactions. Lane 1, 5: *P. aeruginosa* JQ866912, Lane 2: DNA size marker, Lane 3, 4: *P. aeruginosa* JQ796859

CHAPTER 5

DISCUSSION

5.1 Screening of biopolymer producing bacteria

5.1.1 Isolation and pure culture of bacteria

A total of 13 pure bacterial strains were isolated from the soil samples of crude oil contaminated sites of Assam and Assam Arakan Basin, ONGC, Numaligarh refinery Limited, Numaligarh, Assam and wastes samples of Jagiroad Paper Mill, Nagaon, Assam on the basis of their morphological variations. Dalal *et al.*[315] reported the isolation of different bacterial strains from soil samples contaminated with oily sludge procured from different oil refineries for biopolymer polyhydroxyalkanoates production. They assumed that petroleum hydrocarbon sites constitute an environment of excess carbon coupled with nitrogen stress, can be potential source for most bacteria for PHA production. Different workers[316, 317, 318] have reported that *Pseudomonas* species is the most commonly studied bacterial strain producing PHAs from oil-contaminated soils. Reddy and Thirumala[319] has also reported potent PHA-producing bacterial strain from crude oil contaminated ecosystem.

5.1.2 Morphological characteristics of bacteria

Morphological studies of bacteria in terms of colony size, pigmentation, form, margin and elevation displayed wide variations. The size of colonies was observed (Table 4.1) to fall in the categories of large, moderate, small and pinhead. While in most of the cases, white colonies were seen, although some were yellowish and green. Difference in morphology existed among bacterial community at the oil contaminated surface and sub-surface soil and also due to complexity in environmental conditions could potentially influence bacterial diversity.

5.1.3 Screening of biopolymer producing bacterial strains

In the present investigation, out of 13 pure bacterial strains, only 3 strains viz. BPC1 (*P. aeruginosa* JQ796859), BPC2 (*P. aeruginosa* JQ866912) and BP2 (*B. circulans* MTCC8167) (as shown in Table 4.2) showed positive growth in the PHA detection medium. Rehman *et al.*[306] reported the screening of different soil bacteria by using PHA detection medium. These strains were considered to be promising for the production of biopolymer PHA. Subsequent studies were carried out with these 3 bacterial strains.

Orange color observed under the fluorescence microscope reinforced the hypothesis that out of 13 bacterial strains, only 3 such as *P. aeruginosa* JQ796859, *P. aeruginosa* JQ866912 and *B. circulans* MTCC8167 could produce biopolymer in the respective culture medium (Table 4.3). The observation is presented in Fig. 4.1. The three bacterial strains also showed bluish black colour in the colonies (Fig. 4.2) on staining with the Sudan Black B. Ostle andHolt[109] reported emission of orange fluorescence by poly-β-hydroxybutyrate granules on staining with 1% Nile blue A; but it failed to stain glycogen and polyphosphate. This established the specificity of Nile blue A stain towards poly-β-hydroxybutyrate in contrast to the other stain Sudan black B. William and Chistopher[320] also reported the presence of inclusion bodies of poly-β-hydroxybutyrate inside the bacteria *Azotobacter vinelendi* UWD cells produced fluorescence emission when stained with Nile blue A. Naheed *et al.*[321] also reported the screening of *Enterobacter* sp. SEL2 and *Enterobacteriaceae* bacterium PFW1 by staining with Sudan black B and Nile blue A. The stain could be used in the quantitative assay of PHB in a variety of cells. It might, therefore, be inferred that *P. aeruginosa* JQ796859, *P. aeruginosa* JQ866912 and *B. circulans* MTCC8167 strains produced the metabolite PHA.

5.2 Biochemical characterization of the PHA producing bacterial strains

Biochemical tests were performed (Table 4.4) as bacteria may possess different biological catalysts called enzymes to regulate different kinds of cellular metabolites to run different cellular pathways.

In this investigation, biochemical characterization of the gram negative bacterial strain *P. aeruginosa* JQ796859 exhibited catalase positive, urease negative, citrate positive, triple sugar iron negative, nitrate reduction positive, MR and VP negative reaction. The microbe did not show activity for the utilization of starch, H_2S and indole production. The strain possessed the ability to hydrolyze gelatin and casein; also the ability to peptonize the milk protein. Biochemical tests showed that the strain could produce acid from lactose, dextrose, sucrose and xylose, but cannot from manitol.

The gram positive strain *B. circulans* MTCC8167 was found to be spore forming, catalase positive, urease positive, triple sugar iron positive, and MR-VP negative. Biochemical test confirmed its ability to produce acid from lactose, manitol, dextrose, sucrose and xylose. It failed to reduce nitrate to nitrite and could

not uptake glucose. The bacterium hydrolyzed gelatin and casein; and possessed the ability to utilize triple sugar iron and also to peptonize milk. The microbe did not show any activity for the citrate, H_2S and indole production, but could hydrolyze starch.

The gram negative bacterial strain *P. aeruginosa* JQ866912 was found to be catalase positive, citrate positive, triple sugar iron positive, MR and VP negative. The strain possessed the ability to reduce nitrate to nitrite and could utilize glucose. The strain did not show any ability in the utilization of starch and urease. It showed negative results in the production of H_2S and indole. The microbe could peptonize milk protein and hydrolyze gelatin and casein. Except lactose, it showed positive results for acid production from manitol, dextrose, sucrose and xylose.

5.3 Growth of bacterial strains at different pH levels

Each microbial species has a definite pH growth range and pH growth optimum. Some microorganisms can survive within a wide range of pH, while others can only resist small variations. Excessive variations in hydrogen ion concentration can affect microorganisms by disrupting the plasma membrane or inhibiting the activity of enzymes and membrane transport proteins. In the present study, all the bacterial strains were examined in the medium having acidic to alkaline (2.0-10.0). At high acidic (pH 2.0) condition, the growth of the bacterial strains exhibited poor (0.25-0.34 gL^{-1}) biomass yield [Fig. 4.4 (a-e)]. In pH range 6.0-8.0, the bacterial strain *B. circulans* MTCC8167 possessed better growth with comparatively higher biomass yield to the other two strains *P. aeruginosa* JQ796859 and *P. aeruginosa* JQ866912. Thus, the strain was identified to be the most efficient when compared to rest of the two strains in terms of growth/biomass yield over a wider pH range. But at pH 10.0, *P. aeruginosa* JQ796859 possessed comparatively better growth in comparison to the other strains which exhibited a slow growth rate. Garland[322] reported that generally in bacteria, intracellular pH is maintained in near neutral range, but when the cell is subjected to an acidic environment the intracellular pH can decrease considerably[323]. Russell and Dombrowski[324] also reported that since many enzymes are markedly sensitive to pH, the growth inhibition occurring at low pH could be caused by direct effect of the H^+ ion on cellular components.

5.4 Growth of bacterial strains at different temperatures

The PHA producing bacterial strains were cultured in glucose containing medium for their growth at temperatures ranging from 30-45 °C [Fig. 4.5 (a-c)]. At 30 °C, all the bacterial strains *P. aeruginosa* JQ796859, *B. circulans* MTCC8167 and *P. aeruginosa* JQ866912 exhibited better growth rate with dry biomass yield within the range 0.86-0.94 gL^{-1}. At 37 °C, *P. aeruginosa* JQ866912 exhibited highest biomass production of 4.3gL^{-1} in comparison to the others. However, at the high temperature of 45 °C, all bacterial strains failed to survive in the medium. Temperature affects the growth rate of bacteria since their enzyme-catalyzed reactions are sensitive to temperature. High temperatures can damage microorganisms by denaturing their enzymes, transport carriers, proteins and thereby disrupting the microbial cell membranes. Parr *et al.*[325] reported that most of the soil microorganisms are mesophiles and exhibits maximum growth in the range of 20-35 °C.

5.5 PHA production by the bacterial strains at different growth phases

The rate of production and accumulation of PHA by the bacterial strains were grown in PHA detection medium containing glucose (1.0%) was maximum at 72 h when the cells reached their stationary phase. From the Table 4.5, it was observed that there was no accumulation of PHA by all three bacterial strains during the first 12 h period. The strain *P. aeruginosa* JQ866912 followed by *B. circulans* MTCC8167 exhibited highest PHA accumulation after 48 to 72 h of culture. However, all three bacterial cultures exhibited reduction in the accumulated PHA after 96 h of culture. According to Zinn *et al.*[326], PHA accumulating microbes cultured in a medium with carbon excess and nitrogen limitation have to grow maximum upto the available nutrient in the medium. Following the onset of the stationary phase microbial growth is terminated, after which PHA accumulation begins within their cell as an energy rich material.

5.6 PHA production by the bacterial strains in different carbon substrates

In the present investigation the three bacterial strains were tested for PHA production with different carbon substrates such as glucose, glycerol, colocassia starch, propionic acid, soy oil, waste mobile, sugarcane molasses and glycerol byproduct of kitchen chimney dump lard (KCDL). The accumulation of PHA by the

bacterial strains in glucose containing medium was in the order of *P. aeruginosa* JQ866912> *B. circulans* MTCC8167> *P. aeruginosa* JQ796859 (Table 4.6). Similar results were obtained in the glycerol containing medium. But, in the case of colocasia starch containing medium, the strains *P. aeruginosa* JQ796859 and *P. aeruginosa* JQ866912 possessed no growth. When combination of 0.1% propionic acid and 1% glucose was used as the carbon source, PHA accumulation by the strains was in the order of *B. circulans* MTCC8167> P. aeruginosa JQ866912> P. aeruginosa JQ796859. In the case of sugarcane molasses and soy oil, *P. aeruginosa* JQ866912 accumulated the highest PHA accumulation followed by *B. circulans* MTCC8167 and *P. aeruginosa* JQ796859. In the case of waste mobile, *B. circulans* MTCC8167 showed no PHA accumulation and the rest of the two showed the least. Comparatively, when the glycerol byproduct (waste of KCDL) was used, *P. aeruginosa* JQ866912 showed the highest PHA accumulation in comparison to all of the above carbon sources followed by *P. aeruginosa* JQ796859 and *B. circulans* MTCC8167.

The same results were observed in case of biomass yield by the bacterial strains with variable carbon sources like glucose, glycerol, colocassia starch, propionic acid, soy oil, waste mobile, sugarcane molasses and glycerol byproduct of KCDL (1.0% w/v) (Table 4.6). The results revealed that higher cell densities were obtained by *P. aeruginosa JQ866912* strain when glycerol byproduct was used as carbon source. In case of medium with colocassia starch, *P. aeruginosa* JQ796859 and *P. aeruginosa* JQ866912 showed no growth in the medium while *B. circulans* MTCC8167 showed least. But in case of waste mobile, *B. circulans* MTCC8167 showed no growth while the others showed least.

It has been reported that genetically engineered *P. putida* GPp104 synthesized poly (3-hydroxybutyrate-co-3-hydroxyhexanoate) (PHBHHx) using gluconate and glucose, rather than fatty acids[327]. Solaiman *et al.*[328] reported that the cellular yields were higher than those obtained with *P. corrugata* grown on E medium supplemented with glucose (1.52 g CDW.L^{-1}) or oleic acid (1.62 g CDW.L^{-1}). But the PHA yields from the strains were low than PHA yields of 31 and 61% CDW from *P. corrugata* grown on glucose or oleic acid. This value can also be compared with the mcl-PHA accumulation from the bacterial species *P. oleovorans* NRRL B-778 grown on glucose, octanoic acid and oleic acid[329] and are found higher. The composition of polyester synthesized was determined mainly by the specificity of

the enzymes involved in the synthesis of PHAs; genetically encoded availability of metabolic links of fatty acid metabolism to PHA synthesizing system and also on the composition of the substrate. Ashby *et al.*[330] reported that *P. oleovorans* NRRL B-14682 and *P.corrugata* 388 synthesized mcl-PHA upto 13-27% and 42% and cellular growth upto 1.3±0.1 gL^{-1} and 1.7–2.1 gL^{-1} respectively, when cultured in soy-based biodiesel production containing glycerol, fatty acid soaps and residual fatty acid methyl esters (FAME). Wong *et al.*[331] reported that the PHA accumulation by *Staphylococcus epidermidis* was 2.5 gL^{-1} and cell density of 2.68% was achieved when grown on sesame oil. While Obruca *et al.*[332] proved that efficient production of co-polymers was found from waste oil in comparison to pure oil and also to glucose. Verlinden *et al.*[333] also reported that *Cupriavidus necator* produced 1.2 gL^{-1} of PHB homopolymer from waste and heated frying oil which is alike when glucose is used as the carbon source. They stated that the unsaturated fatty acids, residual carbohydrates, proteins and fats from foods, available nitrogen compounds, peroxides and heat-degradation products in the waste or frying oil could also be metabolized and may have contributed to increased PHB production by bacteria. This indicated that glycerol byproduct from KCDL may contribute towards PHA accumulation by the bacterial strain *P. aeruginosa* JQ866912 when compared to other carbon sources.

5.7 Physicochemical characterization of PHA

5.7.1 Light absorption by PHA

As observed in the Fig. 4.6 (a-c), the PHA of the three bacterial strains *P. aeruginosa* JQ796859, *B. circulans* MTCC8167 and *P. aeruginosa* JQ866912 showed maximum absorption (λ_{max}) in the UV region (260-290 nm).

5.7.2 FTIR analysis of PHA

The results obtained from FT-IR analysis are presented in Table 4.7. The PHA isolated from all the three strains *P. aeruginosa* JQ796859, *B. circulans* MTCC8167 and *P. aeruginosa* JQ866912 contained the main characteristic ester carbonyl (C=O) group confirmed by the spectral pattern (Fig. 4.7-4.9). The peak between 3,405–3,369 cm^{-1} might be attributed due to O-H bonding in the polymer material. The peaks between 2,923–2,922 cm^{-1} might be ascribed to the bands of C-H stretching in

all the three polymers isolated. The absorption from 1,065–1,071 cm^{-1} might be due to –C–O–C stretching vibrations in the polymer material in all the three strains. In case of *P. aeruginosa* JQ796859 and *P. aeruginosa* JQ866912 polymer, the band from 1,670–1,634 cm^{-1} might be ascribed to the –C=C– stretching. In case of the polymers from these two strains *P. aeruginosa* JQ796859 and *P. aeruginosa* JQ866912, the band from 3,085–3,055 cm^{-1}.corresponds to C–H stretch.

From these observations it could be concluded that the presence of a marked peak for the ester carbonyl bond strongly indicates the accumulation of PHA in the bacterial strains. Moreover, these bands at the above ranges were identical to those reported earlier for PHA[334, 335].

5.7.3 GC-MS analysis of PHA

GC-MS is an innovative method for qualitative and quantitative analysis of PHA polymer.

In case of *P. aeruginosa* JQ796859 bacterial strain, the structural confirmation of the PHA monomers was done using GC-MS. GC-MS revealed the production of a copolymer containing hydroxyvalerate and hydroxydecenoate in the polymer of *P. aeruginosa* JQ796859. Fig. 4.11 shows the total ion current chromatogram (TIC) for the methanolysis products of the PHA from *P. aeruginosa* JQ796859. Two methyl ester peaks with the retention time RT=11.45 min, an additionally large peak with a retention time RT=19.65 and some minor peaks at RT=12.59 and 14.81 were observed. These two major peaks showed similarity to the corresponding standard mass spectra of hydroxyvalerate and hydroxydecenoate in the MS (NIST) library. In Fig. 4.12 (a), the mass spectra of the methyl ester of the saturated 3-hydroxy valeric acid were being dominated by m/z=74, caused by Mc Laff Herty rearrangement[336] of the methyl ester. m/z=143 probably caused by expulsion of methanol from m/z=270. Similarly, in Fig. 4.12 (b), the mass spectra of the methyl ester of the unsaturated decenoic acid methyl esters were being dominated by m/z=74 and 143. Therefore it was concluded that *P. aeruginosa* JQ796859 produced a copolymer of poly-hydroxyvalerate-co-hydroxydecenoate.

Fig. 4.13 shows the total ion current chromatogram (TIC) for the methanolysis product of the isolated PHA from the bacterial strain *B. circulans* MTCC8167. The GC pattern of the isolated polymer possessed two methyl ester peaks with the retention time RT=22.67 min, an additionally large peak with a retention time

RT=28.10 and some minor peaks at RT=3.49, 24.95 and 30.91. In Fig. 4.14 (a), the mass spectra of the methyl ester of the saturated 3-hydroxy butyric acid were being dominated by m/z=103, caused by an α–cleavage between C3 and C4. Further, important ions at m/z=61 was probably of the methyl ester, but m/z=203, would not be indicative of a special functionality in the molecule. Similarly, in Fig. 4.14 (b), the mass spectra of the methyl ester of the saturated 3-hydroxyl velerate were being dominated by m/z=270. Further, important ions at m/z=74, caused by Mc Laff Herty rearrangement of the methyl ester. m/z=143 was probably caused by expulsion of methanol from m/z=270. The other ions were not indicative. Therefore, it was concluded that a copolymer of poly-3-hydroxybutyrate-co-3-hydroxyvalerate (PHB-HV) was produced by *B. circulans* MTCC8167.

In case of the polymer from *P. aeruginosa* JQ866912, the GC pattern of the total ion chromatogram Fig 4.15 possessed three methyl ester peaks with the retention time RT=11.56 min, 18.46 and an additionally large peak with a retention time RT=19.66 and some minor peaks at RT=12.59 and 14.61. In Fig. 4.16 (a), the mass spectra of the methyl ester of the saturated 3-hydroxy valeric acid were being dominated by m/z=103 caused by an α–cleavage between C3 and C4 and M/Z=143 probably caused by expulsion of methanol. Similarly, in Fig. 4.16 (b), the mass spectra of the decanoic acid methyl esters pattern showed the m/z peak at 90.1 which originated from the carbonyl end of the molecule. This was due to the cleavage between C2 and C3 carbon atoms following McLafferty rearrangement. The fragmentation pattern of the methyl esters of octadecanoic acid methyl esters [Fig. 4.16 (c)] showed the m/z peak at 74.1. This peak originated from the carbonyl end of the molecule due to cleavage between C3 and C4 carbon atoms following McLafferty rearrangement[333]. The peak at m/z=103.1 represented the hydroxyl end of the molecule which occurred due to the cleavage at bonds between C3 and C4; the alkyl end of this cleavage resulted in the peak at m/z=71.1. Therefore it was concluded that a copolymer of poly-hydroxyvalerate-co-hydroxydecenoate-co-octadecanoate was produced by *P. aeruginosa* JQ866912.

5.7.4 NMR analysis of PHA

To confirm the chemical structure of the PHA, ^{1}H and ^{13}C NMR analyses were used. ^{1}H NMR and ^{13}C NMR of the polymer sample in $CDCl_3$ solution was done to illustrate the structure of the extracted polymer from *P. aeruginosa* JQ796859 bacterial strain. Fig. 4.17 (a) shows that in ^{1}H NMR chemical shift (δ) values ranging from 0.91–0.98 ppm attributed the protons of methyl terminal groups, while δ values at 1.22–2.08 ppm corresponded to all internal $-CH_2-$ groups in the polymer. The peak at 4.30–4.71 ppm was due to the presence of ester (–O–CH) proton and at 5.56–5.68 ppm clearly indicated –CH=CH– moiety in the polymer chain. Likewise, ^{13}C NMR peaks [Fig. 4.17(b)] appearing at 10-30 ppm represented methyl and methylene carbons. The ^{13}C signal at 128 and 129 ppm indicates –CH=CH– carbons and that at 172–173 ppm were the representative peaks for two types of C=O (carbonyl) carbons of the copolymer composition. From the NMR information, it could be proposed that the polymer isolated from *P. aeruginosa* JQ796859 is poly (3-hydroxyvalerate) co- (5-hydroxydecenoate) (P-3HV-5-HDE). Moreover, the copolymer composition in P-3HV-5-HDE was determined from the integration height in ^{1}H NMR spectrum and it was found that % molar compositions of 3HV and 5-HDE were 45% and 55%, respectively.

In case of *B. circulans* MTCC8167 strain, ^{1}H NMR and ^{13}C NMR clearly supported the proposed structure [Fig. 4.18 (a, b)] of the extracted polymer[337]. In the ^{1}H NMR chemical shift values (δ) ranging from 0.83 ppm represented the protons of methyl terminal groups, while δ values at 1.22–1.95 ppm represented all internal $-CH_2-$ groups in the polymer. The peak at 3.99–4.33 ppm was due to the presence of ester (–O–CH) proton and δ values at 5.30–5.50 ppm clearly indicated the –CH=CH– moiety in the polymer chain. Likewise, ^{13}C NMR peak appearing at 10–30 ppm has represented methyl and methylene carbons. The ^{13}C signal at 129 and 130 ppm indicated the –CH=CH– carbons and that at 173.34–173.61 ppm was the representative peaks for two types of –C=O (carbonyl) carbons of the copolymer composition. With reference to the above, a chemical structure was prescribed as poly-3-hydroxybutyrate-co-3-hydroxyvalerate (P-3HB-3HV), a medium chain length copolymer.

In the ^{1}H NMR [Fig. 4.19 (a)], chemical shift (δ) values ranging from 0.91–0.99 ppm attributed the protons of methyl terminal groups, while δ values at 1.22–

1.93 ppm corresponded to all internal $-CH_2-$ groups in the polymer. The peak at 4.29–4.72 ppm was due to the presence of ester (–O–CH) proton and at 5.25–5.68 ppm clearly indicates –CH=CH– moiety in the polymer chain. Likewise, ^{13}C NMR peaks [Fig. 4.19 (b)] appearing at 10-30 ppm represented methyl and methylene carbons. The ^{13}C signal at 124.32–139.31 ppm indicated –CH=CH– carbons and that at 173.38–173.66 ppm were the representative peaks for two types of C=O (carbonyl) carbons of the copolymer composition. Presence of –CH=CH– moiety in the polymer chain indicates unsaturation in one monomer of the polymer. The spectrum closely resembles the spectra of the PHA isolated from *P. putida* cultivated on glucose[338] and PHA isolated from *P. aeruginosa* MTCC 7925 with different carbon sources[339]. From the NMR information, it can be inferred that the polymer isolated from *P. aeruginosa* JQ866912 contain 3-hydroxyvalerate (3HV), 5-hydroxydecenoate (5HDE) and 3- hydroxyoctadecenoate (3HODE).

5.8 Physical analysis of PHA

5.8.1 Molecular weight determination of PHA

Table 4.8 and Fig. 4.20–4.22 depict the molecular weight of the biopolymer extracted from the bacterial strains *P. aeruginosa* JQ796859, *B. circulans* MTCC8167, and *P. aeruginosa* JQ866912. The weight-average molecular weight (Mw) and the number-average molecular weight (Mn) were $5.9x10^3$ and $5.6x10^3$ Da, respectively for P-3HV-5-HDE isolated from *P. aeruginosa* JQ796859 bacterial strain (Fig. 4.20). The polydispersity index (I=Mw/Mn) bears a narrow value of 1.059, which suggests possession of uniform chain length and this is essential for the food and pharmaceutical industries as it does not require further processing for polymer chain uniformity. The average Mw of P-3HV-5-DE was considerably smaller than other reported mcl-PHA polymers. The molar mass was almost one order smaller than mcl-PHA polymers from *P. putida* (Mn of $3.3x10^4$ Da and Mw of $5.6x10^4$ Da) where as the polydispersity index was slightly higher (1.7)[340].

In case of *B. circulans* MTCC8167 bacterial strain, GPC analysis indicated the molecular mass of PHBV polymer to be $5.1x10^4$ Da (Fig. 4.21). Oliveira *et al.*[341] reported the molecular weight of the extracted PHB to be about $5.2x10^5$ Da. In the present study PHBV obtained has a very low polydispersity index (1.21). The present polydispersity index of PHBV polymer is comparable to the PHB-4 polymer reported from recombinant *R. eutropha*[342]. Ma *et al.*[343] reported the production of

copolymer 3-hydroxyoctanoate and 3-hydroxydecanoate from *P. putida* strain KT2047A having polydispersity index almost similar (1.24) to that of the extracted PHBV polymer sample. Lower polydispersity index of the extracted PHBV samples suggest that it can be used for commercial purpose without any major processing to confer uniformity to the polymer chain.

The number average molecular weights (Mn) of the P-3HV-5HDE-3HODE polymer of *P. aeruginosa* JQ866912 strain was found to be $3.8x10^4$ Da (Fig. 4.22). The weight average molecular weight (Mw) of the polymer was $4.1x10^4$ Da with polydispersity index (PDI) of 1.08 (Table 4.8). Ouyang *et al.*[344] reported that *P. putida* KT2442 has produced mcl-PHA containing hydroxydodecanoate fractions with the number average molecular weights (Mn) of $8.0x10^4$ Da. But the polydispersity index of this polymer is slightly higher (1.25) than the polymer isolated from *P. aeruginosa* JQ866912 strain. Allen *et al.*[345] also reported that *P. oleovorans* (ATCC 29347) grown in medium supplemented with saponified jatropha seed oil produced PHA copolymer having molecular weight (MP) of $1.79x10^5$ with polydispersity (Mw/Mn) of 1.3 which is almost similar in range with the polymer from *P. aeruginosa* JQ866912. They also suggested that the lower polydispersity index of the polymer has uniform chain length, i.e., only one length of polymer is present in the PHA.

5.8.2 Crystallinity study of the PHA

The experiment revealed that polymers isolated from *P. aeruginosa* JQ796859, *B. circulans* MTCC8167, and *P. aeruginosa* JQ866912 strains were crystalline in nature (Fig. 4.23). The X-ray diffraction pattern supported the finding that the polymer obtained from the solvent casting of *P. aeruginosa* JQ796859 strain was crystalline possessing 32.17% crystallinity. The X-ray diffractogram of the synthesized P-3HB-co-3HV polymer of *B. circulans* MTCC8167 strain showed crystalline size of 2.260 Å. The extracted polymer showed crystalline nature with 65% of crystallinity. Abe *et al.*[346] reported that the crystallinity of P3HB produced by *R. eutrophus* from 4-hydroxybutyric acid was 59%. Further analysis of XRD data was done to determine the strain among the polymer chains with the use of Voigt-function model described by de-Keijser *et al.*[347] and the strain between crystals was found to be 36.69%. The polymer from *P. aeruginosa* JQ866912 strain also showed crystalline nature with 46% crystallinity.

5.8.3 Thermogravimetric (TGA) analysis

The TGA graph (Fig. 4.24) revealed that the standard polymer from the market possessed the lowest thermal degradation temperature in comparison to all the polymers. From the TGA thermogram the polymer from *P. aeruginosa* JQ796859 showed that the first step thermal degradation was found to be at 225 °C and about 90% of the degradation of the neat PHA occurred at 385 °C indicating high degree of temperature resistivity of the polymer. The polymer from *P. aeruginosa* JQ866912 and *B. circulans* MTCC8167 bacterial strains was found to be thermally stable upto the range of 220–229 °C. The initial weight loss step in the TG analysis curves was at around 80–120 °C which corresponds to the loss of moisture. The second step where major weight loss occurred (about 80%) in the TGA curves between 350–360 °C was due to degradation of polymers. About 10% of residue of the all the polymers was finally left when heated to 600 °C. Liu and Chen[348] reported that mcl-PHA was being more thermostable and PHB and P (3HB–12mol %3HHx) degraded at 226 and 239 °C, respectively. The high thermal degradability temperature and melting temperature of the isolated PHA from these strains suggests the potential applicability of mcl-PHAs in different industries. Li *et al.*[349] reported that mcl–PHAs consisting of 30 mol% 3HV, the degradation temperature lies between 296 °C and 307 °C. Bengtsson *et al.*[350] also reported that decomposition temperatures of the PHAs produced from fermented molasses and synthetic feeds containing single volatile fatty acids (VFAs) by an open mixed culture were 277.2 °C and 294.9 °C, respectively.

5.8.4 Differential scanning calorimetry (DSC) analysis

DSC analysis of polymer from the bacterial strain *P. aeruginosa* JQ796859 revealed that the Tm value was 139 °C [Fig. 4.25 (a)]. A second melting peak at 227 °C further indicated the presence of a second monomer. Loo *et al.*[351] reported that two melting peaks were found in DSC of a copolymer when incorporation of second monomer occurs. The polymer was found to be melt-stable when heated above their Tm to 190 °C, quenched to -30 °C, and reheated to 300 °C; the peak at their Tm was obtained again on second heating, suggesting their stability. This Tm value can be compared with the Tm value of the polymer isolated from other *Pseudomonas* sp reported[352, 353] using glucose as carbon source. Savenkova *et al.*[354] reported that Tm of the P3HB homopolymer produced by *Azotobacter chroococcum* 23 was 180 °C

and Tg 3.9 °C which was similar with the glass transition temperature, Tg of the isolated PHA from *P. aeruginosa* JQ796859 (4 °C). The polymer was also shows some segmental melting of polymer chain at around 34–55 °C. In case of *B. circulans* MTCC8167 polymer, the DSC graph [Fig. 4.25 (b)] revealed that Tg was found to be 14.79 °C. The melting temperature of the polymer was about 116 °C and the second melting peak was at 234 °C. This Tm data was similar to the Tm data (116.4 °C) of the P (3HB) with 20 mol % 3HV produced by *A. chroococcum* 23[354]. They also stated that Tg of the polymers and melting range decreases with increase in side chain length. At around 28.7 °C, the polymer was also shows some segmental melting of polymer chain. The Tg of the polymer from *P. aeruginosa* JQ866912 strain was 1.03 °C [Fig. 4.25 (c)]. Here the first melting point (Tm) starts at around 150 °C and second melting peak at around 226 °C. This thermal behavior of the polymer from *P. aeruginosa* JQ866912 was similar with the Tm (155 °C) and Tg (1.2 °C) of the polymer produced from fermented molasses with 44 mol% non-3HB by an open mixed culture[355]. No ashes have been found, in the thermal degradation of all these polymers and all are copolymer in nature.

5.8.5 Photoluminescence (PL) study

The emission was recorded at two different wave lengths for all three polymers (Fig. 4.26). All of the polymers showed luminescence property. The emission maxima (λPL max) of the polymers have been found in the range of 340–390 nm which is due to $\pi \rightarrow \pi^*$ transition of different monomers present in the copolymers. This value was similar with the fluorescence spectra of glycogen biopolymer from bovine liver reported by Bozani *et al.*[356].

5.8.6 Surface morphology study of PHA

SEM micrograph of the polymer sample isolated from *P. aeruginosa* JQ796859 and *P. aeruginosa* JQ866912 strain (Fig. 4.27) showed that the polymer possessed a coralloid surface which was decorated with many star shaped protrusions. In case of *B. circulans* MTCC8167 polymer, the polymer film showed no star shaped protrusions and the polymer film showed two non-uniform layers. But, in both cases there was absence of pore in the polymer film surface. Thire *et al.*[357] has reported that the SEM micrograph of pure PHB film has fractured surface

with relatively smooth topography, indicating a brittle fracture holding several cracks and voids.

5.9 Biodegradation of PHA from *B. circulans* MTCC8167, *P. aeruginosa* JQ796859 and *P. aeruginosa* JQ866912

Biodegradation of the prepared biopolymer films was done by treating with the different soil bacteria and fungal strains. FTIR spectra of the PHA film of *B. circulans* MTCC8167, *P. aeruginosa* JQ796859 and *P. aeruginosa* JQ866912 strains was analyzed following the microbial exposure that indicated the formation of new peaks, breakdown of some bonds and increase in the band intensity which might be due to the production of monomers via break down of the polymer. In case of *B. circulans* MTCC8167 polymer (Fig. 4.28), the decrease in the intensity of the bands around 1,127–1,140 cm^{-1} assigned to the stretching vibration of C–O–C group, indicating oxidative breakage of the polymer chain. Similarly, in case of *P. aeruginosa* JQ796859 and *P. aeruginosa* JQ866912 polymer samples (Fig. 4.30-31), the decrease in the intensity of the bands around 1185–1211 cm^{-1} assigned to the stretching vibration of C–O–C group, indicated degradation of the polymer chain. Changes also occurred in the region of 1,675–1,735 cm^{-1} of the *B. circulans* MTCC8167 polymer associated with C=O stretching ester carbonyl bond, showing shifting and decrease in the peak intensity which might correspond to the breakdown of ester bond in polymer films after treatment with different microbes[358]. Similarly, the PHA films of *P. aeruginosa* JQ796859 and *P. aeruginosa* JQ866912 strains inoculated with each bacterial strain possessed a shifting in the peak from 1730–1735 cm^{-1} associated with C=O stretching ester carbonyl bond referring to a decrease in the peak intensity which might correspond to the breakdown of ester bond in the polymer films following the inoculation. This was probably due to the externally secreted enzymes by microbes in the culture medium. FTIR spectra of PHA film of all the bacterial strains showed disappearance of a peak present in the control at 2922 cm^{-1} and 2919–2923 cm^{-1} respectively, indicating the breakdown of –C–H bonds in the treated one by exo-cleavage activity of PHA depolymerase. The breakdown of the polymer evidenced by decrease in amorphous nature was observed as a decrease in the intensity of the peak between 764–775 cm^{-1} (Fig. 4.28) and the peak between 722 and 724 cm^{-1} (Fig. 4.30-4.31). Similarly, the shapes and intensities of some IR bands in the copolymer are sensitive to the degree of crystallinity and,

thus, some bands decrease in intensity, while others increase as a response to greater crystallinity[359]. Various workers reported the same changes in the case of synthetic polymers (polyethylene and polyurethane) before and after the microbial treatment, through FTIR spectroscopy[360, 361]. Bordoloi *et al.*[362] also reported that *P. aeruginosa* (MTCC7815), *P. aeruginosa* (MTCC7812), *P. aeruginosa* (L43-I), *B. subtilis* (R38-I) produced biosurfactant and was able to degrade petroleum derived different complex hydrocarbon components by reducing surface tension. Here, in this experiment we have used the four above *Pseudomonas* and *Bacillus* sp, and surfactant produced by these bacteria might be one of the reasons for the degradation of the polymer films. It could be assumed that bacterial and fungal species can potentially be used for the biodegradation of PHA. Minor bond degradation of some polymers enhances the degradation process via change in crystallinity; such as, poly-propylene is resistant to decomposition by microorganisms, although these can be appearance of cracks as caused by the contraction of surface layers as one of the consequences of ''semi-crystallization''.

Scanning electron micrographs of the original films and the films after 36 days of biodegradation are presented in Fig. 4.32-4.34 (a-b) for the polymer of *B. circulans* MTCC8167 and *P. aeruginosa* JQ796859 and *P. aeruginosa* JQ866912, respectively. The change in the morphology of the polymer surface appeared to indicate the instability of the materials when exposed to microbial action. The films subjected to microbial degradation showed surface erosion in different areas, grooves, cavities and pit formation when compared to the original film. Sang *et al.*[363] reported the formation of different cavities and grooves on the surface of PHBV films which demonstrated degradation due to the synergistic effect of a microbial consortium (fungi, bacteria, and actinobacteria) colonizing the surface of the film. The PHA films clearly possessed morphological and structural changes as visible after 36 days of treatment with different microbes, indicating the biodegradation process. Dutta *et al.*[358] also reported the degradation of polyurethane/epoxy blends by different *P. aeruginosa* bacterial strains with SEM micrograph. The degradation of polymer film occurs through microbial attack, which might be due to the action of exo and/ or endo-enzymes produced by the microbes themselves. The attack might begin at more accessible enzymatic sites such as the amorphous phase and in the chain ends at the crystal edges, as in the case of PCL films. Accordingly, it was concluded that the biopolymer from the *B.*

circulans MTCC8167 and *P. aeruginosa* JQ796859 and *P. aeruginosa* JQ866912 bacterial strains is biodegradable though it needs modified procedures and other parameters.

Optical microscopic observation (Fig. 4.29) showed that the PHA film of bacterial strain *B. circulans* MTCC8167 at the end of incubation showed many changes in surface morphology, such as erosion and extensive roughening with pit formation as compared to the untreated one.

5.10 Application of PHA of *B. circulans* MTCC8167 in enhancing the stability of colloidal silver nanoparticles (SNP)

5.10.1 Characterization by using FTIR spectroscopy

The FT-IR spectrum of the SNP confirmed the presence of silver in the material. The absorption peaks near 600 cm^{-1} indicating N–H stretching, 1100 cm^{-1} assigned as the absorption peaks of–C–O–, 1400 and 1600 cm^{-1} indicating the stretching vibration of C=C. Therefore, this absorption peaks revealed the presence of silver in the SNP and SNP-PHA colloids (Fig. 4.35). The peak near 1,666 cm^{-1} of the SNP-PHA mix might be due to the ester carbonyl C=O of the PHA which shifted due to conjugation or presence of SNP. The same peak towards the smaller wave number showed a small valley which might be due to the SNP. This low intensity of the SNP peak might be due to double dilution of the SNP colloids with PHA dispersed solution. The same peak in the case of SNP-PHA *in situ* broadened up due to the presence of PHA and SNP. In the case of SNP, the peak near 1,666 cm^{-1} was broad but different from that of SNP-PHA *in situ*. The pattern clearly revealed the presence of the silver nanoparticles in the medium.

The photographic evidence for the SNP colloids stabilized for 29 days by different methods has been depicted in Fig. 4.36. As seen in the figure after 29 days of incubation, the SNP-PHA *in situ* remained stable, whereas the other two samples showed color pattern aggregation of the SNP[364]. The bright yellow color of the SNP-PHA *in situ* suggests the stability of the SNP in the colloid[365].

5.10.2 Characterization of SNP-PHA by TEM

The TEM image shown in the Fig. 4.37 revealed the existence of the SNP in SNP-PHA *in situ* colloid. The morphology of the nanoparticles was found to be spherical and the size as observed in the figure was 5.0-60.0 nm. However, the number of small particles (5.0-15.0 nm) was more as compared to larger (60.0 nm) particles. Saha *et al.*[366] has reported the TEM image of silver nanoparticles produced by a phytopathogenic fungus *Bipolaris nodulosa* possessed spherical, semi-pentagonal structure having 10.0-60.0 nm in diameter. This can also be supported by silver nanoparticles synthesized by using sodium borohydride as reducing agent[367]. They reported that the nanoparticles formed are spherical in shape and uniform having a size range from 7.0-25.0 nm.

5.10.3 Characterization of SNP-PHA by UV-Vis spectroscopy

The UV–Vis spectra of the SNP colloids (Fig. 4.38) showed absorption spectra near 400 nm in day1 due to its surface Plasmon resonance phenomenon to indicate the particle size[367] After 29 days, the UV–Vis spectrum of the SNP shifted towards 420 nm along with a decrease in the intensity of the surface Plasmon absorption. It was probably due to the aggregation of the SNP in the colloid with time and larger particles require lesser energy and hence longer wavelength[368]. The aggregation of SNP was stimulated by two different phenomenons. One was due to the reaction of excess sodium borohydride with SNP which increased overall ionic strength[369] and the other reason might be due to the addition of the electrolytes such as NaCl. Salt tends to shield the charges allowing the particles to clump together to form aggregates[370]. The colloidal silver solution turned dark yellow, violet and then grayish (Fig. 4.36)[363] whereas in the case of SNP–PHA *in-situ*, the UV–Vis spectra showed maximum wave length near 400 nm in day1 consistent upto day 30. From the consistency of color and the range of maximum wave length of the SNP–PHA *in situ* formation indicated their stability throughout the period. Udapudi *et al.*[371] reported that no change was observed in peak position for 30 days of silver nanoparticles synthesized from aqueous solution of silver nitrate using trisodium citrate as a reductant which depicts its stability. The high stability of the SNP–PHA *in situ* might be due to the presence of hydrophobic PHA in the colloid. The PHA in the colloids might be acting as a stabilizer by providing a surface for immobilization of the SNP[372]. It was evident from FTIR spectroscopy, that there was no evidence in

the formation of new bond, but physical immobilization of SNP in the PHA (in SNP–PHA *in situ* and SNP–PHA mixed) was evident while doing filtration through 0.45µm nitrocellulose membrane filter. The SNP–PHA mixed sample showed an intermediate absorption maxima shift near 415 nm after 29 days of aging. The low stability of the mixed sample in comparison to the *in situ* one might be due to the low immobilization of the SNP on it. The observations warrant further investigation.

5.11 Photoluminescence study of PHA from *P. aeruginosa* JQ866912, its behavior study using different nanoparticles

5.11.1 XRD analysis of PHA- metal oxide nanoparticles hybrids

In order to determine the crystalline nature of the PHA/nanoparticles hybrids, a thin film on the glass substrate was used for the XRD analysis (Fig. 4.39). From this study, the diffraction peak at 2θ=38° for the plane (111), 2θ=43.15° for the plane (200) and 2θ at 64.8° for the plane (220) of NiO nanoparticles are observed in case of virgin nanoparticles[373]. But in case of PHA/NiO hybrid these peaks show slight shifting and slight decreasing of the peak intensity. 2θ=31.94° (100), 34.55° (002), 36.45° (101), 47.65° (102), 56.75° (110), 62.95° (103), 66.45° (200), 68.10° (112) and 69.20° (201) of the ZnO confirms the formation of the nanoparticles[374] which were also present in the PHA/ZnO hybrids but slightly at different positions and decrease in their peak intensity. Different peaks were observed at (2θ)=33.33° (110), 35.69° ($\bar{1}$11), 38.90° (111), 48.91° ($\bar{2}$02), 53.36° (020), 58.24° (202), 61.72° ($\bar{1}$13), 65.8° (022) and 66.2° (220) corresponds to different planes of CuO nanoparticles which confirms the formation of CuO nanoparticles[375]. In case of the PHA/nanoparticles hybrids, the broadening and shifting of the peaks and the position of the crystal planes as per literature proves the formation of the nanoparticles within the polymer.

5.11.2 Optical properties of PHA- metal oxide nanoparticles hybrids

From the UV absorbance spectra (Fig. 4.40) it was revealed that the absorption maximum of the PHA polymer has been shifted when incorporated with the metal nanoparticles. The polymer absorbed in the region of 285–295 nm. The absorption intensity of the polymer became the highest with incorporation of 1.0% NiO nanoparticles with the polymer than the other two nanoparticles. But there was a

decrease in the intensity of the polymer hybrid with the incorporation of 3.0% NiO nanoparticles. The increased concentration of NiO nanoparticles affect the UV absorption as NiO nanoparticles do not absorb in the UV region. Therefore, it decreases the absorption intensity of the polymer/metal oxide nanoparticles hybrid. The other two polymer hybrid nanoparticles (CuO and ZnO) possessed the same effect like that of the NiO hybrid material but their absorption spectra showed shifting of the absorption maxima as compared to the crude polymer material.

The photoluminescence (PL) spectra (Fig. 4.41) of the material showed a dramatic change in the emission nature to that of the virgin polymer which accounts for the interaction of the metal nanoparticle with the polymer. The change in the surface states of the metal nanoparticles enhanced the luminescence of the polymer metal oxide nanoparticles hybrids. The density of the surface would have increased with the decrease in the particle size due to the large surface to volume ratio[376]. The PL spectra clearly exhibited with the increase in nanoparticles concentration, the intensity of PL also increased. This was due to energy transfer mechanism. The polymer materials generally form clusters and transfer their energy to each other and thereby causing decrease in PL intensity. Bur when nanoparticles are incorporated with the polymer, nanoparticles break the cluster thereby allowing polymer chains to absorb and emit light independently. As such, the enhancement of PL intensity takes place.

5.11.3 SEM analysis

The surface morphology of the polymer-metal oxide nanoparticles hybrids thin film was investigated using SEM [Fig. 4.42(a-d)]. The SEM micrograph shows the presence of nanoparticles within the polymer matrix. The SEM images also show the well distribution of the nanoparticles within the polymer matrix. The size of the particles was found to be 70.0-92.0 nm. Kausik *et al.*[377] has reported the surface morphology of polyaniline-ZnO nanocomposite and suggested that embedding of nanoparticles in the polymer matrix could impart novel properties with regard to sensing application.

5.12 Application of PHA for composite based biosensor preparation with gold nanoparticles (AuNPs) for detection of antimalarial drug-Artemisinin

5.12.1 Cyclic voltametric (CV) study

The electrochemical behavior using the cyclic voltammetric behavior of the (A) PHA/ITO (B) PHA/AuNPs/ITO (C) PHA/AuNPs/ HRP/ITO electrode studied at different scan rate (5 to 40 mV s^{-1}) in PBS (50 mM, pH 7.0 ±0.1) containing 5 mM $[Fe(CN)6]^{3-/4-}$ was shown in Figure 4.43. In the CV curve of biopolymer PHA [Fig 4.43 (A)], no significant redox peak was observed which indicated PHA is not electroactive in nature. In the CV curves of PHA/AuNPs/ITO and PHA/AuNPs/HRP/ITO [Fig 4.43 (B), (C)], the peaks shifted towards more positive potential. The improved electrochemical behavior of the AuNPs modified electrode can be attributed to the improved charge propagation within the electrode on incorporation of conducting Au nanoparticles. The effect of pH on the peak current was investigated in the pH range from 5.5 to 8.5 in presence of 0.01 $\mu g.mL^{-1}$ artemisinin [Fig. 4.43 (D)]. It was observed that the electrodes showed a maximum peak current as well as good redox behavior at pH 7.0±0.1 of PBS. Therefore, in order to maximize the biosensors current signal, a PBS solution (pH 7.0±0.1) was optimized as the optimum solution for all further experiments. The change in redox current with scan rate represented that with increasing scan rate, both peak current and peak potential increased steadily. Also good uniformity of current function, $ip/AC\upsilon^{1/2}$ was observed from plot. The plot of ip against $\upsilon^{1/2}$ evidenced significant straight line relationship of Randles-Sevcik nature with positive correlation coefficient of 0.99 supporting mass transport as a means of diffusion.

$$ip\ (\mu A) = 8.3 \times \upsilon^{1/2}\ (mVs^{-1}) + 9.1;\ r2 = 0.992;\ n = 8\ (PHA\ /AuNPs/\ ITO)$$

$$ip\ (\mu A) = 0.12 \times \upsilon^{1/2}\ (mVs^{-1}) + 9.8;\ r2 = 0.996;\ n = 8\ (PHA\ /AuNPs/HRP/ITO)$$

As no significant peak was observed in case of PHA, therefore no slope was assigned to it. But after addition of AuNPs into PHA a sharp anodic and cathodic peaks were observed with slope 0.122 $\mu A\ (mV^{-1})^{1/2}$ and 8.31$\mu A\ (mV^{-1})^{1/2}$, respectively in Fig. 4.44 [(A) (a) & (b)], respectively. This is because highly conducting AuNPs facilitates the oxidation-reduction process inside the electrodes. After immobilization of HRP, slopes were decreased to 0.106 $\mu A\ (mV^{-1})^{1/2}$ and 0.168 $\mu A\ (mV^{-1})^{1/2}$, respectively [Fig. 4.44 [(B) {(a) & (b)}] which was due to the

successful immobilization of (HRP) retaining their bioactivity onto the PHA/AuNPs/ITO. Further, Fig. 4.45 (A) shows relative variation in CV at constant scan rate (5 mVs^{-1}) in PBS (50 mM, pH 7.01,) containing 5 mM $[Fe(CN)6]^{3-/4-}$ for three electrodes (a) PHA/ITO (b) PHA/AuNPs/ITO (c) PHA/AuNPs/HRP/ITO electrodes. In the PHA/ITO electrode, no significant redox peak was observed which was due to the fact that PHA acts as a barrier in electron transport. CV curve of PHA/AuNPs/ITO showed significant redox peaks with nearly rectangular shape. This improved electrochemical behavior of the electrode was due to the addition of AuNPs which facilitates the charge transfer within the system. However, in PHA/AuNPs/HRP/ITO, the peak current decreased in comparison to PHA/AuNPs/ITO [Fig. 4.45 A (c)] which may be due to slow redox process after immobilization of HRP.

5.12.2 EIS study

To investigate the effect of surface charge modulation for determination of relative change in surface resistance at zero potential, EIS was carried out on (a) PHA/ITO, (b) PHA/AuNPs/ITO and (c) PHA/AuNPs/HRP/ITO electrode in Fig. 4.45 (B). R_{CT} is the surface charge transfer resistance as R_p, the polarization resistance obtained at zero potential and C_d is the double layer capacitance at the electrode/solution interface. The frequency associated with maximum Z'' (imaginery impedance) and R_{CT} were used to calculate C_d using the following equation[378].

$$R_{CT}C_d = 1 / 2\pi f_{max}$$

Where f_{max} is the frequency at which maximum Z'' obtained.

From the Nyquist plot it was seen that the Nyquist diameter of the electrode deposited with PHA [Fig. 4.45 B (a)] is much larger than that of the PHA/AuNPs electrode [Fig. 4.45 B (b)], which manifested that the formation of PHA layer on the electrode surface, and it in some degree blocked the redox probe of $[Fe\ (CN)_6]^{3-/4-}$ contacting with the electrode surface. This clearly indicated that the AuNPs were not only self-assembled on the outer surface of the PHA, but also partly distributed within the film as tiny conduction centers which facilitated electron-transfer[379] and evidenced more conductive. However, AuNPs act as electron- conducting tunnel which can greatly promote the direct electron transfer[380]. This change in the

capacitance suggested that AuNPs were successfully incorporated into the PHA films and this is further supported by CV study which shows drastic enhancement of current in PHA/AuNPs as compared to PHA in Fig. 4.45(A). It has also been noticed in the impedance spectrum of the resulting electrode immobilized with HRP [Fig. 4.45 B (c)] that the increase in R_{CT} was due to the dielectric and insulating features at the electrodes electrolyte interface and was associated with successive immobilization of HRP. The change in R_{CT} after HRP immobilization may be due to the hindrance of the macromolecular structure of HRP to the electron-transfer, and it also confirms the successful immobilization of HRP[379].

5.12.3 SEM study

In order to get insight into the surface morphology of the working electrodes SEM micrograph was investigated. Fig. 4.46 (a) shows non-porous and smooth surface of the PHA which is in agreement with CV (Fig. 4.44) studies confirming non-conductivity of the PHA that is non electro-active in nature. Fig. 4.46 (b) shows that the surface of the electrodes surface consists of uneven porous matrix of PHA, embedded with Au nanoparticles of 66.67 nm which increased the conductivity of the film. From Fig. 4.46 (c) it can be assumed that PHA/AuNPs could provide a matrix for the successful immobilization of the HRP enzyme[381]. Lin *et al.*[381] has developed a disposable biosensor for rapid determination of H_2O_2 by incorporating HRP enzyme in Au–chitosan membrane to modify ITO electrode. They reported that the presence of the Au–chitosan membrane played an important role in immobilization of HRP enzyme and also facilitated immobilization to expose enzyme activity sites. This could make the substrate more easily accessible to the enzyme, resulting in a good amperometric response of the biosensor. The presence of the Au nanoparticles attributed increase in roughness of the surface area and demonstrated effective sensitivity of the biosensor.

5.12.4 Application to real sample

The applicability of the proposed PHA/AuNPs/HRP/ITO bio-electrode based electrochemical biosensor has been studied in bulk and spiked human serum. Representative voltammograms and calibration curve are shown in Fig. 4.47. The figure shows that the current is proportional to the concentration of artemisinin over a convenient range in Fig. 4.47 (a). The precision was estimated for 0.01-0.08

$\mu g.mL^{-1}$ of the drug using the calibration curve and the standard addition method in Fig. 4.47 (b). The calibration equation parameters and related validation data are presented in Table 4.9. Recovery experiments were performed using the standard addition method. The recovery values of artemisinin (0.01 $\mu g.mL^{-1}$) in spiked human serum was 95.41% with % RSD of 1.05, n=5. Moreover it demonstrated considerable repeatability and reproducibility, along with accuracy and precision in experimental study and offers candidature as a promising alternative method for the direct determination of artemisinin in pharmaceutical formulations and spiked biological fluids. The strategy described here has many attractive advantages: simplicity, rapidity, and low cost could be a useful method for pharmaceutical analysis. The electrochemical behavior of artemisinin under the conditions described in this work is an irreversible process controlled by diffusion. A first hand report on the electrochemical determination of artemisinin using a PHA/AuNP/HRP hybrid nanocomposite based biosensor in bulk and spiked human serum has been presented. The proposed method has distinct advantages over other existing methods regarding sensitivity, selectivity, time saving and minimum detectability. Furthermore, in an earlier HPLC and GC methods[382, 383] for the determination of artemisinin, sensitivity and lower limit of detection were found to be 5.0 $ng.mL^{-1}$, 50 $ng.mL^{-1}$ and 30 $ng.mL^{-1}$ but in the present developed method it could be estimated upto a level of 0.0035 $\mu g.mL^{-1}$. The method when applied to spiked human serum could be detected upto 0.0036 $\mu g.mL^{-1}$ which is more sensitive to HPLC methods[384, 385]. Consequently, the proposed method has potential of a good analytical alternative in comparison to chromatographic methods for determining artemisinin.

5. 13 Molecular genetic assessment of PHA producing bacterial strains

5.13.1 Genotypic characterization of strain *P. aeruginosa* JQ796859 and *P. aeruginosa*

16S rRNA gene sequences are highly conserved and specific in all organisms and provide the degree of similarity among the groups of the organisms indicating evolutionary relatedness, which helps to place an organism in the proper group. In this investigation, the phylogenetic analysis (Fig. 4.50), indicated that the sequence similarity of 16S rDNA of *P. aeruginosa* JQ796859 strain within the species was 99%, other closely related species of the strain was found to be *Pseudomonas aeruginosa* P21 (GenBank entry: HQ697283) having a homology of 99.98%.

Further, a BLAST (NCBI) search showed 99% homology to other known *P. aeruginosa* 16S rDNA gene sequences and accordingly it was named as *P. aeruginosa* JQ796859 (GeneBank entry: JQ796859). As shown in Fig 4.52, phylogenetic analysis indicated a comparative search for the sequence of the strain *P. aeruginosa* JQ866912 revealed 99.98% homology to the *Pseudomonas aeruginosa*; MTH8 ;(GenBank entry: HQ202541) 16S rDNA gene sequence. Further, BLAST (NCBI) search showed 99% homology to other known *P. aeruginosa* 16S rDNA gene sequences and accordingly it was named as *Pseudomonas aeruginosa P. aeruginosa* JQ866912 (GeneBank entry: JQ866912).

5. 13.2 PCR based identification of the PHA biosynthetic genes in *P. aeruginosa* strains JQ796859 and JQ866912

In this experiment, the conserved sequences were identified by using the specific primer-pair I-179L / I-179R for the identification PHA biosynthetic genes pha C1and C2 genes. Solaiman *et al.*[301] reported this primer pair, I-179L and I-179R which are highly specific for the coding regions of *Pseudomonas* phaC1 and phaC2 genes. The 540 bp PCR product obtained in the experiment (Fig. 4.54) reveals the presence of the coding regions of phaC1 and C2 genes flanked by the primer-pair[301, 305]. Solaiman[304] also reported that the semi-nested PCR reaction should specifically yield the 540 bp subgenomic fragments of phaC1 and phaC2 on *P. resinovorans* NRRLB-2649 and *P. corrugata* strains. The results suggested the successful amplification of the specific coding regions and also confirmed the production of mcl-PHA by the *P. aeruginosa* strains JQ796859 and JQ866912. However, the identification of these PHA synthetic genes will need further confirmation by sequence determination, followed by restriction digestion, cloning into an expression vector and the subsequent transformation into an expression host.

CHAPTER 6

CONCLUSION AND FUTURE PROJECTIONS

6.1 Conclusion

The findings of the thesis are described below:

- Three different PHA producing bacterial isolates BPC1, BPC2 and BP2 were isolated from the crude oil contaminated soil site of Assam and Assam Arakan Basin, ONGC, Assam.
- BP2 was previously identified by our laboratory and confirmed by IMTECH, Chandigarh to be *Bacillus circulans* MTCC8167.
- 16s rDNA analysis was performed for molecular characterization of the selected biopolymer producing bacterial isolates BPC1 and BPC2. Subsequently the 16S rDNA gene sequence was deposited in GenBank of NCBI data library and they were named as *Pseudomonas aeruginosa* JQ796859 and *Pseudomonas aeruginosa* JQ866912 respectively.
- The optimum conditions of the bacterial strains for the growth and production of PHA was found to be at pH 7.0, 37 °C temperature and 72 h culture period.
- The glycerol byproduct of kitchen chimney dump lard (KCDL) was found to be good carbon source for the highest PHA accumulation by the bacterial strain *P. aeruginosa* JQ866912 in comparison to other carbon sources used.
- Based on FTIR, GCMS and ^{1}H and ^{13}C NMR, their characterization lead to identification of the biopolymers isolated from *P. aeruginosa* JQ796859, *B. circulans* MTCC8167 and *P. aeruginosa* JQ866912 to be poly (3-hydroxyvalerate) co- (5-hydroxydecenoate) (P-3HV-5-HDE), poly-3-hydroxybutyrate-co-3-hydroxyvalerate (P-3HB-3HV) and poly-3-hydroxyvalerate-co-5-hydroxydecenoate-co-3-hydroxyoctadecenoate(P-3HV-5HDE-3HODE), respectively.
- The average (number) molecular weight of the biopolymers is in the range of $5.6x10^3$ to $4.2x10^4$ Da and the polydispersity index bears a narrow value in the range of 1.05 to 1.21.
- All the biopolymers possessed high degree of thermal as well as melting stability.
- XRD data revealed that the polymers are crystalline in nature having large crystal size. The polymers possess luminescence property.
- The biopolymers are biodegradable when exposed to microbial action.

- ❖ The PHA of *B. circulans* MTCC8167 is useful enhancing the stabilization of colloidal solution of SNP.
- ❖ By incorporating the metal oxide nanoparticles with biopolymer, the intensity of the emission peak could be increased. The increase in concentration of metal oxide nanoparticles, the PL intensity of the polymer metal oxide hybrid material becomes increase. The resulting nanocomposites could be used for further application as sensors.
- ❖ A selective and sensitive PHA/AuNPs/HRP/ITO biosensor based nanocomposite probe is developed for direct determination of artemisinin in bulk and spiked human serum. The proposed method has distinct advantage over other existing methods regarding sensitivity, selectivity, time saving and minimum detectability.
- ❖ The resultant specific 540-bp PCR product has represented the presence of mcl biosynthesis genes phaC1/C2 in the bacterial strains *P. aeruginosa* JQ796859 and *P. aeruginosa* JQ866912.

6.2 Future projections

- Sequencing of PCR amplified product of pha synthase gene has to be taken up.
- Gene expression studies for pha synthase gene to be carried out using *E. coli* model system.
- Techno-economic evaluation/comparison of the biopolymer has to be taken up for future application.

BIBLIOGRAPHY

1. Atlas, R.M. *Microbial Ecology: Fundamentals and Applications*, 3rd ed., Benjamin-Cummings Publishing Company Inc. Redwood City, CA, 1993.
2. Jendrossek, D., & Handrick, T. Microbial degradation of polyhydroxyalkanoates, *Annual Rev Microbiol.* **56**, 403--432, 2002.
3. Kim, D.Y., & Rhee, Y.H. Biodegradation of microbial synthetic polyesters by fungi, *Appl Microbiol Biotechnol.* **61**, 300--308, 2003.
4. Tokiwa, Y., & Calabia, B.P. Degradation of microbial polyesters, *Biotechnol Lett.* **26,** 1181--1189, 2004.
5. Kragelund, C., et al. Ecophysiology of the filamentous *Alphaproteobacterium meganema perideroedes* in activated sludge, *FEMS Microbiol Ecol.* **54,** 111--122, 2005.
6. Akar, A., et al. Accumulation of polyhydroxyalkanoates by *Microlunatus phosphovorus* under various growth conditions, *J Ind Microbiol Biotech.* **33,** 215--220, 2006.
7. Steinbuchel, A., & Fuchtenbusch, B. Bacterial and other biological systems for polyester production, *Trends Biotechnol.* **16,** 419--427, 1998.
8. Angelova, N., & Hunkeler, D. Rationalizing the design of polymeric biomaterials, *Trends Biotechnol.* **17**, 409--421, 1999.
9. Zinn, M., et al. Occurrence, synthesis and medical application of bacterial polyhydroxyalkanoates, *Adv Drug Rev.* **53**, 5--21, 2001.
10. Williams, S.F. & Martin, D.P. Application of PHAs in medicine and pharmacy. in: *Biopolymers. Polyesters III: Applications and Commercial Products,* Y. Doi, & A. Steinbuchel eds., Weinhein, Germany: Wiley-VCH, 2002.
11. Reddy, C.S., et al. Polyhydroxyalkanoates: an overview, *Bioresour Technol.* **87,** 137--146, 2003.
12. Chen, G.Q., & Wu, Q. The application of polyhydroxyalkanoates as tissue engineering materials, *Biomaterials* **26**, 6565--6578, 2005a.
13. Chen, G.Q., & Wu, Q. Microbial production and applications of chiral hydroxyalkanoates, *Appl Microbiol Biotechnol.* **67,** 592--599, 2005b.
14. Steinbuchel, A. Non-biodegradable biopolymers from renewable resources: perspectives and impacts, *Curr Opin Biotechnol.* **16**, 607--613, 2005.

15. Lebo Jr., S.E., Gargulak, J.D. & McNally, T.J. *Lignin. Kirk–Othmer Encyclopedia of Chemical Technology*. John Wiley & Sons Inc. 2001.
16. Barnard, G.N., & Sanders, J.K. The poly-beta-hydroxybutyrate granule *in vivo*. A new insight based on NMR spectroscopy of whole cells, *J. Biol. Chem.* **264**, 3286--3291, 1989.
17. Sudesh, K., et al. Synthesis, structure and properties of polyhydroxyalkanoates: biological polyesters, *Prog. Polym. Sci.* **25**, 1503--1555, 2000.
18. Chen, G., et al. Industrial scale production of poly (3-hydroxybutyrate-co-3-hydroxyhexanoate), *Appl. Microbiol. Biotechnol.* **57**, 50--55, 2001.
19. Kadouri, D., et al. S. Ecological and Agricultural Significance of Bacterial Polyhydroxyalkanoates, *Crit. Rev. Anal. Chem.* **31**, 55--67, 2005.
20. Berlanga, M., et al. Rapid spectrofluorometric screening of poly-hydroxyalkanoate-producing bacteria from microbial mats, *International Microbiology* **9**, 95--102, 2006.
21. Williamson, D.H, & Wilkinson, J.F. The isolation and estimation of poly-β-hydroxybutyrate inclusions of Bacillus species, *J Gen Microbiol.* **19**, 198--209, 1958.
22. Steinbuchel, A., et al. Considerations on the structure and biochemistry of bacterial polyhydroxyalkanoic acid inclusions, Can. *J. Microbiol.* **41**, 94--105, 1995.
23. Anderson, A.J., & Dawes, E.A. Occurrence, metabolism, metabolic role, and industrial use of bacterial polyhydroxyalkanoates, *Microbiol. Rev.* **54**, 450--472, 1990.
24. Steinbuchel, A. Biomaterials: Novel Materials from Biological Sources, D. Byrom ed., Macmillan., New York, NY, 1991, 123–213.
25. Poirier, Y., et al. Production of polyhydroxyalkanoates, a family of Biodegradable plastics and elastomers, in bacterial and plant, *Biotechnol.* **13**, 142--150, 1995.
26. Braunegg, G., et al. Polyhydroxyalkanoates, biopolyesters from renewable resources: Physiological and engineering aspects, *J. Biotechnol.* **65**, 127--161, 1998.

27. Chowdhury, A.A. Poly-β-hydroxybuttersaure abbauende Bakterien und exo-enzyme, *Arch. Microbiol.***47**, 167--200, 1963.
28. Lemoigne, M. Produits de deshydration *et* de polymerisation de l'acide b-oxybutyric, *Bull. Soc. Chem. Biol.* **8**, 770--782, 1926.
29. Steinbuchel, A., Perspectives for biotechnological production and utilization of biopolymers: metabolic engineering of polyhydroxyalkanoate biosynthesis pathways as a successful example, *Macromol. Biosci.* **1,** 1--24, 2001.
30. Williams,S.F., et al. PHA applications: addressing the price performance issue: I. Tissue engineering, *Int. J. Biol. Macromol.* **25**, 111--121, 1999.
31. Shishatskaya, E.I., et al. Tissue response to the implantation of biodegradable polyhydroxyalkanoate sutures, *J. Mater. Sci.: Mater. Med.***15**, 719--728, 2004.
32. Mergaert, J., et al. Microbial degradation of poly (3-hydroxybutyrate) and poly(3-hydroxybutyrate-co-3-hydroxyvalerate) in soils, *Appl Environ Microbiol.* **59**, 3233--3238, 1993.
33. Brown Jr., R.M. The Biosynthesis of Cellulose, *J. Macromol. Sci., Pure Appl. Chem.* **33**, 1345--1373, 1996.
34. Tsuji, H. Polylactides. in *Biopolymers. Polyesters III: Applications and commercial products,* Y. Doi, & A. Steinbuchel, eds., Weinheim, Germany: Wiley-VCH, 2002, 129–177.
35. Flieger, M., et al. Biodegradable Plastics from Renewable Sources, *Folia Microbiol.* **48**, 2--44, 2003.
36. Lee, S.Y. Review Bacterial Polyhydroxyalkanoates, *Biotechnol. Bioeng.* **49,** 1--14, 1995.
37. Madison, L.L., & Huisman, G.W. Metabolic engineering of poly (3-hydroxyalkanoates): from DNA to plastic, *Microbiol. Mol. Biol. Rev.* **63**, 21--53, 1999.
38. Brandl, H., et al. *Pseudomonas oleovorans* as a source of poly (β-hydroxyalkanoates) for potential applications as biodegradable polyesters, *Appl. Environ. Microbiol.* **54,** 1977--1982, 1988.
39. Lageveen, R.G., et al. Formation of polyesters by Pseudomonas oleovorans: effect of substrates on formation and composition of poly-(R)-3-hydroxyalkanoates and poly-(R)-3-hydroxyalkenoates, *Appl. Environ. Microbiol.* **54,** 2924--2932, 1988.

40. Huisman, G.W., et al. Synthesis of poly-3-hydroxyalkanoates is a common feature of fluorescent *Pseudomonads*, *Appl. Environ. Microbiol.* **55**, 1949--1954, 1989.

41. Oeding, V., & Schlegel, H.G. Beta-ketothiolase from *Hydrogenomonas eutropha* HI6 and its significance in the regulation of poly-beta-hydroxybutyrate metabolism, *Biochem. J.* **134**, 239--248, 1973.

42. Wang, J.G., & Bakken, L.R. Screening of soil bacteria for poly-beta-hydroxybutyric acid production and its role in the survival of starvation, *Microb. Ecol.* **35**, 94--101, 1998.

43. Peters, V., & Rehm, B.H.A. *In vivo* monitoring of PHA granule formation using GFP-labeled PHA synthases, *FEMS Microbiol. Lett.* **248**, 93--100, 2005.

44. Byrom, D. Polymer synthesis by microorganisms: Technology and economics, *Trends Biotechnol.* **5**, 246--250, 1987.

45. Choi, J., & Lee, S.Y. Factors affecting the economics of polyhydroxyalkanoate production by bacterial fermentation, *Appl. Microbiol. Biotechnol.* **51**, 13--21, 1999.

46. Lee, S.Y. Bacterial polyhydroxyalkanoates, *Biotechnol. Bioeng.* **49**, 1--14, 1996a.

47. Lee, S.Y. Plastic bacteria? Progress and prospects for polyhydroxyalkanoate production in bacteria, *Trends Biotechnol.* **14**, 431--438, 1996b.

48. Khanna, S., & Srivastava, A.K. Recent advances in microbial polyhydroxyalkanoates, *Process Biochem.* **40**, 607--619, 2005.

49. Zinn, M., & Hany, R. Tailored Material Properties of Polyhydroxyalkanoates through Biosynthesis and Chemical Modification, *Advanced Engineering Materials* **7**, 408--411, 2005.

50. Byrom, D. Polyhydroxyalkanoates, *in Plastic from microbes: microbial synthesis of polymers and polymer precursors*, D.P. Mobley, eds., Hanser Munich, 1994, 5–33.

51. Yu, J. Production of PHA from starch wastewater via organic acids, *J. Biotechnol.* **86**, 105--112, 2001.

52. Du, G., & Yu, J. Green technology for conversion of food scraps to biodegradable thermoplastic polyhydroxyalkanoates, *Environ. Sci. Technol.* **36**, 5511--5516, 2002.

53. De Smet, M.J., et al. Characterization of intracellular inclusions formed by Pseudomonas oleovorans during growth on octane, *J. Bacteriol.* **154**, 870--878, 1983.

54. Otari, S.V., & Ghosh, S.J. Production and characterization of the polymer Polyhydroxybutyrate-co-polyhydroxyvalerate by *Bacillus megaterium* NCIM 2475, *Curr. Res. J. Biol. Sci.*, **1**, 23--26, 2009.

55. Khanna, S., & Srivastava, A.K. Recent advances in microbial polyhydroxyalkanoates, *Process Biochem.* **40**, 607--619, 2005.

56. Tsuge, T. Metabolic improvements and use of inexpensive carbon sources in microbial production of polyhydroxyalkanoates, *J Biosci Bioeng.* **94**, 579--584, 2002.

57. Shang, L., et al. Mass production of medium-chain-length poly(3-hydroxyalkanoates) from hydrolyzed corn oil by fed-batch culture of *Pseudomonas putida*, *World J. Microbiol. Biotechnol.* **24**, 2783--2787, 2008.

58. Hassan, M.A.,·et al. A proposal for zero emission from palm oil industry incorporating the production of polyhydroxyalkanoates from palm oil mill effluent, *J. Chem. Eng. Jpn.* **35**, 9--14, 2002.

59. Bhubalan, K., et al. Controlled biosynthesis and characterization of poly (3-hydroxybutyrate-co-3-hydroxyvalerate-co-3-hydroxyhexanoate)from mixtures of palm kernel oil and 3HV-precursors, *Polym. Degrad. Stab.* **93**, 17--23, 2008.

60. Lee, W.H., et al. Biosynthesis of polyhydroxyalkanoate copolymers from mixtures of plant oils and 3-hydroxyvalerate precursors, *Bioresour. Technol.* **99**, 6844--6851, 2008.

61. Pozo, C., et al. Effects of culture conditions on the production of polyhydroxyalkanoates by *Azotobacter chroococcum* H23 in media containing a high concentration of alpechin (wastewater from olive oil mills) as primary carbon source, *J. Biotechnol.* **97**, 125--131, 2002.

62. Dionisi, D., et al. Olive oil mill effluents as a feedstock for production of biodegradable polymers, *Water Res.* **39**, 2076--2084, 2005.

63. Kahar, P., et al. High yield production of polyhydroxyalkanoates from soybean oil by *Ralstonia eutropha* and its recombinant strain, *Polym. Degrad. Stab.***83**, 79--86, 2004.

64. Albuquerque, M.G.E., et al. Strategies for the development of a side stream process for polyhydroxyalkanoate (PHA) production from sugar cane molasses, *J. Biotechnol.* **130**, 411--421, 2007.
65. Solaiman, D., et al. Biosynthesis of medium-chain-length poly (hydroxyalkanoates) from soy molasses, *Biotechnol. Lett.* **28**, 57--162, 2006.
66. Koller, M., et al. Production of polyhydroxyalkanoates from agricultural waste and surplus materials, *Biomacromolecules* **6**, 561--565, 2005.
67. Chen, C.W., et al. Enzymatic extruded starch as a carbon source for the production of poly (3-hydroxybutyrate-co-3-hydroxyvalerate) by *Haloferax mediterranei*, *Proc. Biochem.* **41**, 2289--2296, 2006.
68. Haas, R., et al. Production of poly (3-hydroxybutyrate) from waste potato starch, *Biosci. Biotechnol. Biochem.* **72**, 253--256, 2008.
69. Koller, M., et al. Polyhydroxyalkanoate production from whey by *Pseudomonas hydrogenovora*, *Bioresour. technol.* **99**, 4854--4863, 2008.
70. Nielsen, L. Polyhydroxyalkanoate production in sugarcane recognizing temporospatial complexity, *J. Biotechnol.* **131**, S28--S29, 2007.
71. Goff, M., et al. Improvement of the conversion of polystyrene to polyhydroxyalkanoate through the manipulation of the microbial aspect of the process: A nitrogen feeding strategy for bacterial cells in a stirred tank reactor, *J. Biotechnol.* **132**, 283--286, 2007.
72. Yu, J., & Heiko, S. Microbial utilization and biopolyester synthesis of bagasse hydrolysates, *Bioresour. Technol.* **99**, 8042--8048, 2008.
73. Bengtsson, S., et al. Production of polyhydroxyalkanoates by activated sludge treating a paper mill wastewater, *Bioresour. Technol.* **99**, 509--516, 2008.
74. Yong, K.H. *Biosynthesis and characterization of polyhydroxyalkanoates by locally isolated Chromobacterium sp. USM2,* Master Thesis, Universiti Sains Malaysia, Malaysia, 2009.
75. Lu, Y.P. Advance on the production of polyhydroxyalkanoates by mixed cultures, *Front. Biol. China.* **2**, 21--25, 2007.
76. Griebel, R., et al. Metabolism of poly (β-hydroxybutyrate). I. Purification, composition, and properties of native poly (β-hydroxybutyrate) granules from *Bacillus megaterium*, *Biochemistry* **7**, 3676--3681, 1968.

77. Mayer, F., et al. Electron microscopic observation on the macromolecular organization of tha boundary layer of bacterial PHA inclusion bodies, *J. Gen. Appl. Microbiol.* **42**, 445--455, 1996.

78. Tian, J., et al. Analysis of transient polyhydroxybutyrate production in Wautersia eutropha H16 by quantitative Western analysis and transmission electron microscopy, *J. Bacteriol.* **187**, 3825--3832, 2005.

79. Griebel, R. J., & Merrick, J.M. Metabolism of poly- -hydroxybutyrate: effect of mild alkaline extraction on native poly- -hydroxybutyrate granules, *J. Bacteriol.* **108**, 782--789, 1971.

80. Lundgren, D.G., et al. Characterization of poly-β-hydroxybutyrate extracted from different bacteria, *J. Bacteriol.* **89**, 245--251, 1964.

81. Jendrossek, D., & Handrick, R. Microbial degradation of polyhydroxyalkanoates, *Annu. Rev. Microbiol.* **56**, 403--432, 2002.

82. Gerngross, T.U., et al. Immunocytochemical analysis of poly-β-hydroxybutyrate (PHB) synthase in *Alcaligenes eutrophus* H16: localization of the synthase enzyme at the surface of the of PHB granules, *J. Bacteriol.* **175**, 5289--5293, 1993.

83. Liebergesell, M., et al. Purification and characterization of the poly(hydroxyalcanoic acid) synthase from *Chromatium vinosum* and localization of the enzyme at the surface of poly (hydroxyalkanoic acid) granules, *Eur. J. Biochem.* **226**, 71--80, 1994.

84. McCool, G.J., & Cannon, M.C. PhaC and PhaR are required for polyhydroxyalkanoic acid synthase activity in *Bacillus megaterium*, *J. Bacteriol.* **183**, 4235--4243, 2001.

85. Mukai, K., et al. Substrate specificities in hydrolysis of polyhydroxyalkanoates by microbial esterases, *Biotechnol. Lett.* **15**, 601--604, 1993.

86. Jaeger, K.E., et al. Substrate specificities of bacterial polyhydroxyalkanoate depolymerases and lipases: Bacterial lipases hydrolyze poly (ω-hydroxyalkanoates), *Appl. Environ. Microbiol.* **61**, 3113--31118, 1995.

87. Kusaka, S., et al. Molecular mass of poly [(R)-3-hydroxybutyric acid] produced in a recombinant *Escherichia coli*, *Appl. Microbiol. Biotechnol.* **47**, 140--143, 1997.

88. Sim, S. J., et al. PHA synthase activity controls the molecular weight and polydispersity of polyhydroxybutyrate *in vivo, Nat. Biotechnol.* **15**, 63--67, 1997.

89. Kraak, M.N., et al. Polymerase C1 levels and poly(R-3-hydroxyalkanoate) synthesis in wild-type and recombinant Pseudomonas strains, *J. Bacteriol.* **179**, 4985--4991, 1997.

90. Jendrossek, D. Extracellular polyhydroxyalkanoate depolymerases: the key enzymes of PHA degradation, *in Biopolymers*; Y. Doi, & A. Steinbuchel, eds., Wiley-VCH: Weinheim, Germany, 2002, 4184.

91. York, G.M., et al. *Ralstonia eutropha* H16 encodes two and possibly three intracellular poly [D-(-)-3-hydroxybutyrate] depolymerase genes, *J. Bacteriol.* **185**, 3788--3794, 2003.

92. Schwartz, E., et al. Complete nucleotide sequence of pHG1: a *Ralstonia eutropha* H16 megaplasmid encoding key enzymes of H (2)-based ithoautotrophy and anaerobiosis, *J. Mol. Biol.* **332**, 369--383, 2003.

93. Potter, M., et al. The complex structure of polyhydroxybutyrate (PHB) granules: four orthologous and paralogous phasins occur in *Ralstonia eutropha*, *Microbiology* **150**, 2301--2311, 2004.

94. Wieczorek, R., et al. Analysis of a 24-kilodalton protein associated with the polyhydroxyalkanoic acid granules in *Alcaligenes eutrophus*, *J. Bacteriol.* **177**, 2425--2435, 1995.

95. Bohmert, K., et al. Constitutive expression of the β-ketothiolase gene in transgenic plants. A major obstacle for obtaining polyhydroxybutyrate-producing plants, *Plant Physiol.* **128**, 1282--1290, 2002.

96. Pieper-Furst, U., et al. Identification of the region of a 14-kilodalton protein of *Rhodococcus ruber* that is responsible for the binding of this phasin to polyhydroxyalkanoic acid granules, *J. Bacteriol.* **177**, 2513--2523, 1995.

97. Rehm, B.H.A. Polyester synthases: natural catalysts for plastics, *Biochem. J.* **376**, 15--33, 2003.

98. Salehizadeh, H., & Loosdrecht, M.C.M.V. Production of polyhydroxyalkanolates by mixed culture: recent trends and biotechnological importance, *Biotechnology Advances* **22**, 261--279, 2004.

99. Asrar, J., et al. Biosynthesis and properties of poly(3-hydroxybutyrate-co-3-hydroxyhexanoate) polymers, *Biomacromolecules* **3**, 1006--1012, 2002.

100. Kim, Y.B., & Lenz, R.W. Polyesters from microorganisms, *Advances in Biochemical Engineering/Biotechnology* **71**, 51--79, 2001.

101. Kessler, B., & Witholt, B. Factors involved in the regulatory network of polyhydroxyalkanoate metabolism, *J. Biotechnol.* **86**, 97--104, 2001.

102. Quillaguaman, J., et al. Synthesis and production of polyhydroxyalkanoates by halophiles: current potential and future prospects, *Appl. Microbiol. Biotechnol.* **85**, 1687--1696, 2010.

103. Qi, Q., & Rehm, B.H.A. Polyhydroxybutyrate biosynthesis in *Caulobacter crescentus*: molecular characterization of the polyhydroxybutyrate synthase, *Microbiology* **147**, 3353--3358, 2001.

104. Liebergesell, M., et al. Isolation and identification of granule-associated proteins relevant for poly (3-hydroxyalkanoic acid) biosynthesis in *Chromatium vinosum* D, *FEMS Microbiol. Lett.* **78**, 227--232, 1992.

105. Mc Cool, G.J., & Cannon, M.C. PhaC and Pha R are required for polyhydroxyalkanoic acid synthase activity in *Bacillus megaterium*, *J. Bacteriol.* **183,** 4235--4243, 2001.

106. Philip, S., et al. Polyhydroxyalkanoates: biodegradable polymers with a range of applications, *J. Chem. Technol. Biotechnol.* **82,** 233--247, 2006.

107. Rehm, B.H.A., et al. A new metabolic link between fatty acid de novo synthesis and polyhydroxyalkanoic acid synthesis, *J. Biol. Chem.* **273**, 24044--24051, 1998.

108. Schlegel, H.G., et al. The isolation of mutants not accumulating poly-b-hydroxybutyric acid, *Arch. Microbiol.* **71**, 283--294, 1970.

109. Ostle, A.G., & Holt, J.G. Nile Blue A as a fluorescent stain for poly-b-hydroxybutyrate, *Appl. Environ. Microbiol.* **44**, 238--241, 1982.

110. Kranz, R.G., et al. Positive selection systems for discovery of novel polyester biosynthesis genes based on fatty acid detoxification, *Appl. Environ. Microbiol.* **63**, 3010--3013, 1997.

111. Degelau, A., et al. Fluorometric measurement of poly-b-hydroxybutyrate in *Alcaligenes eutrophus* by flow cytometry and spectrofluorometry, *Appl. Microbiol. Biotechnol.* **42**, 653--657, 1995.

112. Williamson, D.H., & Wilkinson, J.F. The isolation and estimation of poly-beta- hydroxybutyrate inclusions of *Bacillus* species, *J. Gen. Microbiol.* **19**, 198--200, 1958.

113. Hahn, S.K., et al. The recovery of poly (3-hydroxybutyrate) by using dispersions of sodium hypochlorite solution and chloroform, *Biotechnol. Tech.* **7**, 209--212, 1993.

114. Barham, P.J. Physical properties of poly (hydroxybutyrate) and poly (hydroxybutyrate-co-hydroxyvalerate), *in Novel Biodegradable Microbial Polymers,* E.A. Dawes, eds., Kluwer, Dordrecht, 1990, 8196.

115. Jacquel, N., et al. Isolation and purification of bacterial poly (3-hydroxyalkanoates), *Biochemical Engineering Journal* **39**, 15--27, 2008.

116. Berger, E., et al. PHB recovery by hypochlorite digestion of non-PHB biomass, *Biotechnol. Tech.* **3**, 227--232, 1989.

117. Hahn, S.K., et al. Optimizaton of microbial poly (3-hydroxbytyrate) recovery using dispersions of sodium hypochlorite solution and chloroform, *Biotechnol. Bioeng.* **44,** 256--261, 1994.

118. Law, J., & Slepecky, R.A. Assay of poly-hydroxybutyric acid, *J. Bacteriol.* **82**, 52--55, 1969.

119. Kansiz, M., et al. Quantitative determination of the biodegradable polymer poly (b-hydroxybutyrate) in a recombinant Escherichia coli strain by use of mid-infrared spectroscopy and multivariative statistics, *Appl. Environ. Microbiol.* **66**, 3415--3420, 2000.

120. Randriamahefa, S., et al. Fourier transform infrared spectroscopy for screening and quantifying production of PHAs by *Pseudomonas* grown on sodium octanoate, *Biomacromolecules* **4,** 1092--1097, 2003.

121. Braunegg, G., et al. A rapid gas chromatographic method for the determination of poly-β-hydroxybutyric acid in microbial biomass, *European J. Appl. Microbiol. Biotechnol.* **6,** 29--37, 1978.

122. Cornibert, J., & Marchessault, R.H. Physical properties of poly-hydroxybutyrate. IV. Conformational analysis and crystalline structure, *J. Mol. Biol.* **71**, 735--756, 1972.

123. Sato, H., et al. Infrared and Raman spectroscopy and quantum chemistry calculation studies of C-H center dot center dot center dot O hydrogen

bondings and thermal behavior of biodegradable polyhydroxyalkanoates, *J. Mol. Struct.* **744,** 35--46, 2005.

124. Tsz-Chun, M., et al. Microbial synthesis and characterization of physiochemical properties of polyhydroxyalkanoates (PHAs) produced by bacteria isolated from activated sludge obtained from the municipal wastewater works in Hong Kong, *Appl. Biochem. Biotechnol.* **122**, 731--740. 2005.
125. Agus, J., et al. Molecular weight characterization of poly [(R)-3-hydroxybutyrate] synthesized by genetically engineered strains of *Escherichia coli*, *Polym. Degrad. Stab.* **91**, 1138--1146, 2006.
126. Holmes, P.A. Applications of PHB- a microbially produced biodegradable thermoplastic, *Phys. Technol.* **16,** 32--36, 1985.
127. Padermshoke, A., et al. Melting behavior of poly (3- hydroxybutyrate) investigated by two-dimensional infrared correlation spectroscopy, *Spectrochim. Acta, Part A–Mol Biomol Spectrosc.* **61**, 541--550, 2005.
128. Jendrossek, D., & Handrick, R. Microbial degradation of polyhydroxyalkanoates, *Annu. Rev. Microbiol.* **56**, 403--432, 2002.
129. Choi, G.G., et al. Enzymatic and non-enzymatic degradation of poly (3-Hydroxybutyrate-co-3-Hydroxyvalerate) copolyesters produced by *Alcaligenes* sp. MT-16, *J. Microbiol.* **42**, 346--352, 2004.
130. Philip, S., et al. Polyhydroxyalkanoates: biodegradable polymers with a range of applications, *J. Chem. Technol. Biotechnol.* **82**, 233--247, 2007.
131. Shangguan, Y.Y., et al. The mechanical properties *and in vitro* biodegradation and biocompatibility of UV-treated poly (3-hydroxybutyrate-co-3-hydroxyhexanoate), *Biomaterials* **27**, 2349--2357, 2006.
132. Gao, Y., et al. Improvement of mechanical properties of poly (DL-lactide) films by blending of poly (3-hydroxybutyrate-co-3-hydroxyhexanoate), *Eur. Polym. J.* **42**, 764--775, 2006.
133. Kunze, C., et al. *In vitro* and in vivo studies on blends of isotactic and atactic poly (3-hydroxybutyrate) for development of a dura substitute material, *Biomaterials* **27**, 192--201, 2006.

134. Foster, L.J.R., et al. Environmental concentrations of polyhydroxyalkanoates and their potential as bioindicators of pollution, *Biotechnol. Lett.* **23**, 893--898, 2001.

135. Dubnau, D., et al. Gene conservation in Bacillus species, I. conserved genetic and nucleic acid base sequence homologies, *Proc. Natl. Acad. Sci. U.S.A.* **54**, 491--497, 1965.

136. Shang, L., et al. Poly (3-hydroxybutyrate) synthesis in fed-batch culture of *Ralstonia eutropha* with phosphate limitation under different glucose concentrations, *Biotechnol. Lett.* **25**, 1415--1419, 2003.

137. Smibert, R.M., & Krieg, N.R. General characterization, *in Manual of methods for general bacteriology,* P. Gerhardt et. al, eds., American Society for Microbiology, Washington, D.C.,1981, 409443.

138. Spiekermann, P., et al. A sensitive, viable-colony staining method using Nile red for direct screening of bacteria that accumulate polyhydroxyalkanoic acids and other lipid storage compounds, *Arch. Microbiol.* **171**, 73--80, 1999.

139. Jendrossek, D., et al. Poly (3-hydroxybutyrate) granules at the early stages of formation are localized close to the cytoplasmic membrane in *Cryophanon latum*, *Appl. Environ. Microbiol.* **73**, 586--593, 2007.

140. Lemos, P.C., et al. Microbial characterisation of polyhydroxyalkanoates storing populations selected under different operating conditions using a cell-sorting RT-PCR approach, *Appl. Microbiol. Biotechnol.* **78**, 351--360, 2008.

141. Vaneechoutte, M., et al. Wautersia gen. nov., a novel genus accommodating the phylogenetic lineage including *Ralstonia eutropha* and related species, and proposal of Ralstonia [Pseudomonas] syzygii (Roberts et al. 1990) comb. nov, *Int. J. Syst. Evol. Microbiol.* **54**, 317--327, 2004.

142. Kim, B.S., et al. Production of poly (3-hydroxybutyric acid) by fed-batch culture of *Alcaligenes eutrophus* with glucose concentration control, *Biotechnol. Bioeng.* **43**, 892--898, 1994.

143. Madden, L.A., et al. Production and characterization of poly (3-hydroxybutyrate-co-3-hydroxyvalerate-co-4-hydroxybutyrate) synthesized by *Ralstonia eutropha* in fed-batch cultures, *Polymer* **41**, 3499--3505, 2000.

144. Volova, T.G., et al. Physiological and biochemical characteristics and capacity for polyhydroxyalkanoates synthesis in a Glucose-Utilizing Strain of

Hydrogen-Oxidizing Bacteria, *Ralstonia eutropha* B8562, *Microbiology* **74**, 684--689, 2005.

145. Foollner, C.G., et al. Biosynthesis of poly-3-hydroxybutyric acid by the facultatively methanol-assimilating bacterium *Mycoplana rubra* B346 and *recombinant strains*, *J. Basic Microbiol.* **35**, 179--188, 1995.
146. Ueda, S., et al. Synthesis of poly (3-hydroxybutyrate-co-3-hydroxyvalerate) from methanol and n-amyl alcohol by the methylotrophic bacteria *Paracoccus denitrtificans* and *Methylobacterium extorquens*, *Appl. Environ. Microbiol.* **58** 3574--3579, 1992.
147. Suzuki, T., et al. Kinetics and effects of nitrogen source feeding on production of poly-β-hydroxybutyric acid by fed-batch culture, *Appl. Microbial. Technol.* **24**, 366--369, 1986a.
148. Suzuki, T., et al. Mass production of poly-β-hydroxybutyric acid by fed batch culture with control carbon/nitrogen feeding, *Appl. Microbial. Biotechnol.* **24**, 370--374, 1986b.
149. Bourque, D., et al. Production of poly-β-hydroxybutyrate from methanol: characterization of a new isolate of *Methylobacterium extorquens*, *Appl. Microbial. Technol.* **37**, 7--12, 1992.
150. Haywood, G.W., et al. The importance of PHB-synthase substrate specificity in polyhydroxyalkanoates synthesis by *Alcaligenes eutrophus*, *FEMS Microbiol. Lett.* **57**, 1--6, 1989.
151. Huisman, G.W., et al. Synthesis of poly-3-hydroxyalkanoates is a common feature of fluorescent *Pseudomonads*, *Appl. Environ. Microbiol.* **55**, 1949--1954, 1989.
152. Hoffmann, N., et al. The Pseudomonas aeruginosa phaG gene product is involved in the synthesis of polyhydroxyalkanoic acid consisting of medium-chain-length constituents from non-related carbon sources, *FEMS Microbiol. Lett.* **184**, 253--259, 2000.
153. Ayub, N.D., et al. Polyhydroxybutyrate-producing *Pseudomonas* sp. isolated from antarctic environments with high stress resistance, *Curr. Microbiol.* **49**, 170--174, 2004.

154. Borah, B., et al. The influence of nutritional and environmental conditions on the accumulation of poly-β-hydroxybutyrate in *Bacillus mycoides* RLJ B-017, *Journal of Applied Microbiology* **92**, 776--783, 2002.

155. Rawte, T., et al. Incidence of marine and mangrove bacteria accumulating polyhydroxyalkanoates on the mid-west coast of India, *World J. Microbiol. Biotechnol.* **18**, 655--659, 2002.

156. Tajima, K., et al. Isolation and characterization of *Bacillus* sp. INT005 accumulating polyhydroxyalkanoate (PHA) from gas field soil, *J. Biosci. Bioeng.* **95**, 77--81, 2003.

157. Wang, Y., et al. Construction of Recombinant *Bacillus subtilis* for production of polyhydroxyalkanoates, *Appl. Biochem. biotechnol.* **129-132,** 1015--1022, 2006.

158. Lakshman, K., & Shamala, T. R. Enhanced biosynthesis of polyhydroxyalkanoates in a mutant strain of *Rhizobium meliloti*, *Biotechnol. Lett.* **25**, 115--119, 2003.

159. Van-Thuoc, D., et al. Utilization of agricultural residues for poly (3-hydroxybutyrate) production by *Halomonas boliviensis* LC1, *Journal of Applied Microbiology* **104,** 420--428, 2008.

160. Schubert, P., et al. Cloning of the *Alcaligenes eutrophus* genes for synthesis of poly-beta-hydroxybutyric acid (PHB) and synthesis of PHB in *Escherichia coli*, *J. Bacteriol.* **170**, 5837--5847, 1988.

161. Slater, S. C., et al. Cloning and expression in *Escherichia coli* of the *Alcaligenes eutrophus* H16 poly-beta-hydroxybutyrate biosynthetic pathway, *J. Bacteriol.* **170,** 4431--4436, 1988.

162. Peoples, O.P., & Sinskey, A.J. Poly-beta-hydroxybutyrate (PHB) biosynthesis in *Alcaligenes eutrophus* H16. Identification and characterization of the PHB polymerase gene (phbC), *J. Biol. Chem.* **264**, 15298--15303, 1989.

163. Langenbach, S., et al. Functional expression of the PHA synthase gene phaC1 from *Pseudomonas aeruginosa* in *Escherichia coli* results in poly (3-hydroxyalkanoate) synthesis, *FEMS Microbiol. Lett.* **150**, 303--309, 1997.

164. Qi, Q., et al. Synthesis of poly (3-hydroxyalkanoates) in *Escherichia coli* expressing the PHA synthase gene phaC2 from *Pseudomonas aeruginosa*: comparison of PhaC1 and PhaC2, *FEMS Microbiol. Lett.* **157**, 155--162, 1997.

165. Kang, Z., et al. Construction of a stress-induced system in *Escherichia coli* for efficient polyhydroxyalkanoates production, *Appl. Microbiol. Biotechnol.* **79**, 203--208, 2008.

166. Sujatha, K., & Shenbagarathai, R. A study on medium chain length-polyhydroxyalkanoate accumulation in *Escherichia coli* harbouring phaC1 gene of indigenous *Pseudomonas* sp. LDC-5, *Letters in Applied Microbiology* **43**, 607--614, 2006.

167. Abu-Elreesh, G., et al. Exo biopolymer from polyhydroxyalkanoate-producing transgenic yeast, *Afr. J. Biotechnol.* **10,** 6558--6563, 2011.

168. Abd-El-Haleem, D.A.M., et al. Biosynthesis of polyhydroxyalkanotes in wild type yeasts, *J. Appl. Sci. Environ. Manage.***11**, 5--10, 2007.

169. Poirier, Y., et al. Synthesis of polyhydroxyalkanoate in the peroxisome of *Pichia pastoris*, *FEMS Microbiol. Lett.* **207**, 97--102, 2002.

170. Buelhamd, A.T., et al. Genetic engineering of *Schizosaccharomyces pombe* to produce bacterial polyhydroxyalkanoates, *J. Appl. Sci. Environ. Manage.* **11**, 83--90, 2007.

171. Williams, M.D., et al. Production of a polyhydroxyalkanoate biopolymer in insect cells with a modified eukaryotic fatty acid synthase, *Appl. Environ. Microbiol.* **62**, 2540--2546, 1996.

172. Reddy, C.S.K., et al. Polyhydroxyalkanoates: an overview, *Bioresour. Technol.* **87,** 137--146, 2003.

173. Snell, K.D., & Peoples, O.P. Polyhydroxyalkanoate polymers and their production in transgenic plants, *Metab. Eng.* **4**, 29--40, 2002.

174. Poirier, Y., et al. Polyhydroxybutyrate, a biodegradable thermoplastic, produced in transgenic plants, *Science* **256**, 520--523, 1992.

175. Bohmert, K., et al. Transgenic Arabidopsis plants can accumulate polyhydroxybutyrate to up to 4% of their fresh weight, *Planta* **211**, 841--845, 2000.

176. John, M.E., & Keller, G. Metabolic pathway engineering in cotton: Biosynthesis of polyhydroxybutyrate in fiber cells, *Proc. Natl. Acad. Sci. USA.* **93**, 12768--12773, 1996.

177. Hahn, J.J., et al. Peroxisomes as sites for synthesis of polyhydroxyalkanoates in transgenic plants, *Biotechnol. Prog.* **15,** 1053--1057, 1999.

178. Houmiel, K.L., et al. Poly (b-hydroxybutyrate) production in oilseed leucoplasts of *Brassica napus*, *Planta* **209**, 547--550, 1999.

179. Nakashita, H., et al. Production of biodegradable polyester by a transgenic tobacco, *Biosci. Biotechnol. Biochem.* **63**, 870--874, 1999.

180. Slater, S., et al. Metabolic engineering of Arabidopsis and Brassica for poly (3-hydroxybutyrate-co-3-hydroxyvalerate) copolymer production, *Nat. Biotechnol.* **17**, 1011--1016, 1999.

181. Bohmert-Tatarev, K., et al. High levels of bioplastic are produced in fertile transplastomic tobacco plants engineered with a synthetic operon for the production of polyhydroxybutyrate, *Plant Physiol.* **155**, 1690--1708, 2011.

182. Ahn, W.S., et al. Production of Poly (3-Hydroxybutyrate) by Fed-Batch Culture of Recombinant *Escherichia coli* with a Highly Concentrated Whey Solution, *Appl. Environ. Microbiol.* **66,** 3624--3627, 2000.

183. Katircioglu, H., et al. Production of poly-β-hydroxybutyrate (PHB) and differentiation of putative *Bacillus mutants* strains by SDS-PAGE of total cell protein, *Afr. J. Biotechnol.* **2**, 147--149, 2003.

184. Patnaik, P.R. Perspectives in the Modeling and optimization of phb production by pure and mixed cultures, *Crit. Rev. Biotechnol.* **25,** 153--171, 2005.

185. Wang, F., & Lee, S.Y. Production of poly (3-hydroxybutyrate) by fed-batch culture of filamentation-suppressed recombinant *Escherichia coli*, *Appl. Environ. Microbiol.* **63**, 4765--4769, 1997.

186. Majone, M., et al. Influence of storage on kinetic selection to control aerobic filamentous bulking, *Water Sci. Technol.* **34,** 223--232, 1996.

187. Serafim, L.S., et al. Optimization of polyhydroxybutyrate production by mixed cultures submitted to aerobic dynamic feeding conditions, *Biotechnol. Bioeng.* **87**, 145--160, 2004.

188. Aldor, I.S., & Keasling, J.D. Process design for microbial plastic factories: metabolic engineering of polyhydroxyalkanoates, *Curr. Opin. Biotechnol.* **14,** 475--483, 2003.

189. Steinbuchel, A., & Lutke-Eversloh, T. Metabolic engineering and pathway construction for biotechnological production of relevant polyhydroxyalkanoates in microorganisms, *Biochemical Engineering Journal* **16**, 81--96, 2003.

190. Xi, J., et al. Hyperproduction of polyesters consisting of medium-chain-length hydroxyalkanoate monomers by strain *Pseudomonas stutzeri* 1317, *Antonie van Leeuwenhoek* **78,** 43--49, 2000.

191. Impallomeni, G., et al. Tween 20 and its major free fatty acids as carbon substrates for the production of polyhydroxyalkanoates in *Pseudomonas aeruginosa* ATCC 27853, *J. Polym. Environ.* **8**, 97--102, 2000.

192. Halami, P.M. Production of polyhydroxyalkanoate from starch by the native isolate *Bacillus cereus* CFR06, *World J. Microbiol. Biotechnol.* **24**, 805--812, 2008.

193. Lillo, J.G., & Rodriguez-Valera, F. Effects of culture conditions on poly (β-hydroxybutyric acid) production by *Haloferax mediterranei*, *Appl. Environ. Microbiol.* **56**, 2517--2521, 1990.

194. Page, W.J. Production of polyhydroxyalkanoates by *Azotobacter vinelandii* UWD in beet molasses culture, *FEMS Microbiol. Lett.* **103**, 149--157, 1992.

195. Zhang, H., et al. Production of polyhydroxyalkanoates in sucrose-utilizing recombinant *Escherichia coli* and *Klebsiella* strains, *Appl. Environ. Microbiol.* **60**, 1198--1205, 1994.

196. Yellore, V., & Desai, A. Production of poly-3-hydroxybutyrate from lactose and whey by *Methylobacterium* sp. ZP24, *Lett. Appl. Microbiol.* **26**, 391--394, 1998.

197. Povolo, S., & Casella, S. Bacterial production of PHA from lactose and cheese whey permeate, *Macromol. Symp.* **197**, 1--9, 2003.

198. Bosco, F., & Chiampo, F. Production of polyhydroxyalcanoates (PHAs) using milk whey and dairy wastewater activated sludge: Production of bioplastics using dairy residues, *J. Biosci. Bioeng.* **109**, 418--421, 2010.

199. Liu, F., et al. Production of poly-b-hydroxybutyrate on molasses by recombinant *Escherichia coli*, *Biotechnol. Lett.* **20**, 345--348, 1998.

200. Omar, S., et al. Optimization of cell growth and poly (3-hydroxybutyrate) accumulation on date syrup by a Bacillus megaterium strain, *Biotechnol. Lett.* **23**, 1119--1123, 2001.

201. Lee, K.M., & Gilmore, D.F. Modeling and optimization of biopolymer (polyhydroxyalkanoates) production from ice cream residue by novel

statistical experimental design, *Appl. Biochem. Biotechnol.* **133**, 113--148, 2006.

202. Quillaguaman, J., et al. Poly (b-hydroxybutyrate) production by a moderate halophile, Halomonas boliviensis LC1 using starch hydrolysate as substrate, *J. Appl. Microbiol.* **99**, 151--157, 2005.
203. Huang, T.Y., et al. Production of polyhydroxyalkanoates from inexpensive extruded rice bran and starch by Haloferax mediterranei, *J. Ind. Microbiol. Biotechnol.* **33**, 701--706, 2006.
204. Chua, H., et al. Coupling of waste water treatment with storage polymer production, *Appl. Biochem. Biotechnol.* **63-65**, 627--635, 1997.
205. Kumar, M.S., et al. Production of biodegradable plastics from activated sludge generated from a food processing industrial wastewater treatment plant, *Bioresour. Technol.* **95**, 327--330, 2004.
206. Rusendi, D., & Sheppard, J.D. Hydrolysis of potato processing waste for the production of poly-β-hydroxybutyrate, *Bioresour. Technol.* **54**, 191--196, 1995.
207. Khardenavis, A., et al. Activated sludge is a potential source for production of biodegradable plastics from wastewater, *Environ. Technol.* **26**, 545--552, 2005.
208. Takabatake, H., et al. Recovery of biodegradable plastics from activated sludge process, *Water Sci. Technol.* **42**, 351--356, 2000.
209. Kalia, V.C., et al. Biomethanation of plant materials, *Biores. Technol.* **41**, 209--212, 1992.
210. Kalia, V.C., et al. Anaerobic digestion of banana stem waste, *Bioresour. Technol.* **73**, 191--193, 2000.
211. Lee, S., & Yu, J. Production of biodegradable thermoplastics from municipal sludge by a two-stage bioprocess, *Resources, Conservation and Recycling* **19**, 151--164, 1997.
212. Ishizaki, A., et al. Microbial production of poly-D-3-hydroxybutyrate from CO_2, *Appl. Microbiol. Biotechnol.* **57**, 6--12, 2001.
213. Volova, T.G., et al. Autotrophic synthesis of polyhydroxyalkanoates by the bacteria *Ralstonia eutropha* in the presence of carbon monoxide, *Appl. Microbiol. Biotechnol.* **58**, 675--678, 2002.

214. Pohlmann, A., et al. Genome sequence of the bioplastic-producing "Knallgas" bacterium *Ralstonia eutropha* H16, *Nat. Biotechnol.* **24**, 1257--1262, 2006.

215. Yezza, A., et al. Production of polyhydroxyalkanoates from methanol by a new methylotrophic bacterium *Methylobacterium* sp. GW2, *Appl. Microbiol. Biotechnol.* **73**, 211--218, 2006.

216. Ramsay, J.A., et al. Extraction of poly-3-hydroxybutyrate using chlorinated solvents, *Biotechnol. Tech.* **8**, 589--594, 1994.

217. Jiang, X., et al. Acetone extraction of mcl-PHA from *Pseudomonas putida* KT 2440, *J. Microbiol. Methods.* **67**, 212--219, 2006.

218. Choi, J., & Lee, S.Y. Process analysis and economic evaluation for poly (3-hydroxybutyrate) production by fermentation, *Bioprocess Eng.* **17**, 335--342, 1997.

219. Ramsay, J.A., et al. Recovery of poly-b-hydroxybutyric acid granules by a surfactant-hypochlorite treatment, *Biotechnol. Tech.* **4**, 221--226, 1990.

220. Ryu, H.W., et al. Recovery of Poly (3-hydroxybutyrate) from coagulated *Ralstonia eutropha* using a chemical digestion method, *Biotechnol. Prog.* **16**, 676--679, 2000.

221. Fidler, S., & Dennis, D. Polyhydroxyalkanoate production in recombinant *Escherichia coli*, *FEMS Microbiol. Lett.* **103**, 231--235, 1992.

222. Choi, J., & Lee, S.Y. Efficient and economical recovery of poly (3-hydroxybutyrate) from recombinant *Escherichia coli* by simple digestion with chemicals, *Biotechnol. Bioeng.* **62**, 546--553, 1999.

223. Jung, I.L., et al. Spontaneous liberation of intracellular polyhydroxybutyrate granules in *Escherichia coli*, *Res. Microbiol.* **156**, 865--873, 2005.

224. Hampson, J.W., & Ashby, R.D. Extraction of lipid-grown bacterial cells by supercritical fluid and organic solvent to obtain pure medium chain-length polyhydroxyalkanoates, *JAOCS* **76**, 1371--1374, 1999.

225. Khosravi-Darani, K., et al. Effect of process variables on supercritical fluid disruption of *Ralstonia eutropha* cells for poly(r-hydroxybutyrate) recovery, *Biotechnol. Prog.* **20**, 1757--1765, 2004.

226. Hee, P.V., et al. Selective recovery of polyhydroxyalkanoate inclusion bodies from fermentation broth by dissolved-air flotation, *J. Colloid Interface Sci.* **297**, 595--606, 2006.

227. Yu, J., & Chen, L.X.L. Cost-effective recovery and purification of polyhydroxyalkanoates by selective dissolution of cell mass, *Biotechnol. Prog.* **22**, 547--553, 2006.

228. Ratledge, C. & Kristiansen, B. *Basic Biotechnology*, 2nd ed., Cambridge University Press, Cambridge, 2001.

229. Moskowitz, G.J., & Merrick, J.M. Metabolism of poly-β-hydroxybutyrate. II. Enzymic synthesis of D-(-)-β-hydroxybutyryl coenzyme A by an enoyl hydrase from R*hodospirillum rubrum, Biochemistry* **8**, 2748--2755, 1969.

230. Haywood, G.W., et al. Accumulation of a poly (hydroxyalkanoate) copolymer containing primarily 3-hydroxyvalerate from simple carbohydrate substrates by *Rhodococcus* sp. NCIMB 40126, *Int. J. Biol. Macromol.* **13**, 83--88, 1991.

231. Williams, R.D., et al. Production of a co-polyester of 3-hydroxybutyric acid and 3-hydroxyvaleric acid from succinic acid by *Rhodococcus ruber*: biosynthetic considerations, *Appl. Microbiol. Biotechnol.* **40**, 717--723, 1994.

232. Sato, H., et al. Compositional analysis of poly (3-hydroxybutyrate-co-3-hydroxyvalerate) by pyrolysis-gas chromatography in the presence of organic alkali, *J. Anal. Appl. Pyrolysis.* **74**, 193--199, 2005.

233. Poirier, Y., et al. Production of polyhydroxyalkanoates, a family of biodegradable plastics and elastomers, in bacteria and plant, *Biotechnol.* **13**, 142--150, 1995.

234. Yan, Q., et al. Biosynthesis of short-chain-length polyhydroxyalkanoates during the dual-nutrient-limited zone by *Ralstonia eutropha*, *World J. Microbiol. Biotechnol.* **21**, 17--21, 2005.

235. Pederson, E.N., et al. Bacterial synthesis of PHA block copolymer, *Biomacromolecules* **6**, 1904--1911, 2006.

236. Labuzek, S., & Radecka, I. Biosynthesis of copolymers of PHB tercopolymers by *Bacillus cereus* UW85 strain, *J. Appl Microbiol* **90**, 353--357, 2001.

237. Eversloh Lutke, T., et al. Identification of a class of biopolymer: bacterial synthesis of a sulfur containing polymer with thioester linkages, *Microbiology* **147**, 11--19, 2001.

238. Yao, J., et al. Production of polyhydroxyalkanoates by *Pseudomonas nitroreducens*, *Antonie van Leeuwenhoek* **75**, 345--349, 1999.

239. Potter, M., et al. Regulation of phasin expression and PHA granule formation in *Ralstonia eutropha* H16, *Microbiology* **148**, 2413--2426, 2002.

240. Potter, M., & Steinbuchel, A. Poly (3-hydroxybutyrate) granule-associated proteins: impacts on poly (3-hydroxybutyrate) synthesis and degradation, *Biomacromolecules* **6**, 552--560, 2005.

241. Tobin, K.M., et al. Polyphosphate accumulation by *Pseudomonas putida* CA-3 and other medium-chain-length polyhydroxyalkanoate accumulating bacteria under aerobic growth condition, *Appl. Environ. Microbiol.* **73**, 1383--1387, 2007.

242. Khanna, S., & Srivastava, A.K. Recent advances in microbial polyhydroxyalkanoates, *Process Biochem.* **40**, 607--619, 2005.

243. Macrae, R.M., & Wilkinson, J.R. Poly-β-hydroxybutyrate metabolism in washed suspensions of *Bacillus cereus* and *Bacillus megaterium*, *J. Gen. Microbiol.* **19**, 210--22, 1958.

244. Agus, J., et al. Molecular weight characterization of poly [(R)-3-hydroxybutyrate] synthesized by genetically engineered strains of *Escherichia coli*, *Polym. Degrad. Stab.* **91**, 1138--1146, 2006.

245. Valappil, S.P., et al. Large-scale production and efficient recovery of PHB with desirable material properties, from the newly characterized *Bacillus cereus* SPV, *J. Biotechnol.* **132**, 251--258, 2007.

246. Martin, D.P., & Williams, S.F. Medical applications of poly-4-hydroxybutyrate; a strong flexible absorbable biomaterial, *Biochemical Engineering Journal* **16**, 97--105, 2003.

247. Antipov, E.M., et al. Strain-induced mesophase and hard-elastic behaviour of biodegradable polyhydroxyalkanoates fibers, *Polymer* **47**, 5678--5690, 2006.

248. Verlinden, R.A.J., et al. Bacterial synthesis of biodegradable polyhydroxyalkanoates, *J. Appl. Microbiol.* **102**, 1437--1449, 2007.

249. Ashby, R.D., et al. Improved film properties of radiation treated medium-chain-length poly (hydroxyalkanoates), *Biotechnol. Lett.* **20**, 1047--1052, 1998.

250. Sanchez, R., et al. Medium-chain-length polyhydroxyalkanoic acids (PHA mcl) produced by *Pseudomonas putida* IPT 046 from renewable sources, *Eur. Polym. J.* **39**, 1385--1394, 2003.

251. Gunaratne, L.M.W.K., & Shanks, R.A. Melting and thermal history of poly (hydroxybutyrate-co-hydroxyvalerate) using step-scan DSC, *Thermochim. Acta* **430**, 183--190, 2005.

252. Carrasco, F., et al. Thermal stability of polyhydroxyalkanoates, *J. Appl. Polym. Sci.* **100**, 2111--2121, 2006.

253. Jendrossek, D., et al. Degradation of poly (3-hydroxybutyrate), PHB, by bacteria and purification of a novel PHB depolymerase from Comamonas sp. J. *Environ. Polym. Degrad.* **1**, 53--64, 1993.

254. Mochizuki, M., et al. Structural Effects upon Enzymatic Hydrolysis of Poly (butylene succinate-co-ethylene succinate) s, *Macromolecules* **30**, 7403--7407, 1997.

255. Tokiwa, Y., & Calabia, B.P. Degradation of microbial polyesters, *Biotechnol. Lett.* **26**, 1181--1189, 2004.

256. Nishida, H., & Tokiwa, Y. Effects of higher-order structure of poly (3-hydroxybutyrate) on its biodegradation. II. Effects of crystal structure on microbial degradation, *J. Environ. Polym. Degrad,* **1**, 65--80, 1993.

257. Boopathy, R. Factors limiting bioremediation technologies, *Bioresour. Technol.* **75**, 63--67, 2000.

258. Wang, Y.W., et al. Biodegradation studies of poly (3-hydroxybutyrate-co-3-hydroxyhexanoate), *Polym. Degrad. Stab.* **85**, 815--821, 2004.

259. Lim, S.P., et al. degradation of medium-chain-length polyhydroxyalkanoates in tropical forest and mangrove soils, *Appl. Biochem. Biotechnol.* **126**, 23--33, 2005.

260. Sridewi, N., et al. Degradation of commercially important polyhydroxyalkanoates in tropical mangrove ecosystem, *Polym. Degrad. Stab.* **91**, 2931--2940, 2006.

261. Budwill, K., et al. Methanogenic degradation of poly (3-hydroxyalkanoates), *Appl. Environ. Microbiol.* **58**, 1398--1401, 1992.

262. Janssen, P.H., & Schink, B. Pathway of anaerobic poly-β-hydroxybutyrate degradation by Ilyobacter delafieldii, *Biodegradation* **4**, 179--185, 1993.

263. Mabrouka, M.M., & Sabry, S.A. Degradation of poly (3-hydroxybutyrate) and its copolymer poly (3-hydroxybutyrate-co-3-hydroxyvalerate) by a marine *Streptomyces* sp. SNG9, *Microbiol. Res.* **156**, 323--335, 2001.

264. Jendrossek, D., & Handrick, R. Microbial Degradation of Polyhydroxyalkanoates, *Annu. Rev. Microbiol.* **56**, 403--432, 2002.

265. Colak, A., & Guner, S. Polyhydroxyalkanoate degrading hydrolase-like activities by *Pseudomonas* sp. isolated from soil, *International Biodeterioration & Biodegradation* **53**, 103--109, 2004.

266. Phithakrotchanakoon, C., et al. Microbial degradation and physico-chemical alteration of polyhydroxyalkanoates by a thermophilic *Streptomyces* sp. *Biologia* **64**, 246--251, 2009.

267. Shah, A.A., et al. Degradation of poly (3-hydroxybutyrate-co-3-hydroxyvalerate) by a newly isolated *Actinomadura* sp. AF-555, from soil, *International Biodeterioration & Biodegradation* **64**, 281--285, 2010.

268. Philip, S., et al. Polyhydroxyalkanoates: biodegradable polymers with a range of applications, *J. Chem. Technol. Biotechnol.* **82**, 233--247, 2007.

269. Knoll, M., et al. The PHA Depolymerase Engineering Database: A systematic analysis tool for the diverse family of polyhydroxyalkanoate (PHA) depolymerases, *BMC Bioinformatics* **10**, 1--8, 2009.

270. Kim, D.Y., & Rhee, Y.H. Biodegradation of microbial and synthetic polyesters by fungi, *Appl. Microbiol. Biotechnol.* **61**, 300--308, 2003.

271. Lee, S.Y., & Chang, H.N. Effect of complex nitrogen source on the synthesis and accumulation of poly (3-hydroxybutyric acid) by recombinant *Escherichia coli* in flask and fed-batch cultures, *J. Environ. Polymer Degrad.* **2**, 169--176, 1994.

272. Savenkova, L., et al. Mechanical properties and biodegradation characteristics of PHB-based films, *Process Biochem.* **35**, 573--579, 2000.

273. Bhatt, R., et al. Synthesis, characterization, and biodegradation of carboxy methyl chitosan-g-medium chain length polyhydroxyalkanoates, *J. Appl. Polym. Sci.* **110**, 975--982, 2008.

274. Phukon, P., et al. Bio-plastic (P-3HB-co-3HV) from *Bacillus circulans* (MTCC 8167) and its biodegradation, *Colloids Surf. B* **92**, 30--34, 2012.

275. Bucci, D.Z., & Tavares, L.B.B. PHB packaging for the storage of food products, *Polym. Test.* **24**, 564--571, 2005.

276. Jain, R., et al. Polyhydroxyalkanoates: A way to sustainable development of bioplastics, *Chron Young Sci.* **1**, 10--15, 2010.

277. Kilicay, E., et al. Preparation and characterization of poly (3-hydroxybutyrate-co-3-hydroxyhexanoate) (Phbhhx) based nanoparticles for targeted cancer therapy, *Eur. J. Pharm. Sci.* **44,** 310--320, 2011.

278. Lee, J., et al. Tumor-specific hybrid polyhydroxybutyrate nanoparticle: surface modification of nanoparticle by enzymatically synthesized functional block copolymer, *Bioorg. Med. Chem. Lett.* **21**, 2941--2944, 2011.

279. Francis, L. *Biosynthesis of polyhydroxyalkanoates and their medical applications,* Ph. D. Thesis, University of Westminster, Westminster, 2011.

280. Zhou, J., et al. The use of poly (3-hydroxybutyrate-co-3-hydroxyhexanoate) scaffolds for tarsal repair in eyelid reconstruction in the rat, *Biomaterials* **31**, 7512--7518, 2010.

281. Patel, A.R., & Velikov, K.P. Colloidal delivery systems in foods: a general comparison with oral drug delivery, *LWT- Food Sci Technol.* **44**, 1958--1964, 2011.

282. Riekes, M.K., et al. Evaluation of oral carvedilol microparticles prepared by simple emulsion technique using poly (3-hydroxybutyrate-co-3-hydroxyvalerate) and polycaprolactone as polymers, *Mater. Sci. Eng. C* **31**, 962--968, 2011.

283. Ra, R., et al. Medium chain length polyhydroxyalkanoates, promising new biomedical materials for the future, *Mater. Sci. Eng. R: Reports* **72**, 29--47, 2011.

284. Ozturk, F., & Ermertcan, A.T. Wound healing: a new approach to the topical wound care, *Cutan Ocul Toxicol* **30**, 92--99, 2011.

285. Uppal, R., et al. Hyaluronic acid nanofiber wound dressing—production, characterization, and in vivo behavior, *J Biomed Mater Res B Appl Biomater.* **97**, 20--29, 2011.

286. Bansal, S.S., et al. Development and in vitro-in vivo evaluation of polymeric implants for continuous systemic delivery of curcumin, *Pharm. Res.* **28**, 1121--1130, 2011.

287. Waknis, V., & Jonnalagadda, S. Novel poly-DL-lactidepolycaprolactone copolymer based flexible drug delivery system for sustained release of ciprofloxacin, *Drug Delivery* **18**, 236--245, 2011.

288. Gumel, A.M., et al. Recent advances in the production, recovery and applications of polyhydroxyalkanoates, *J Polym Environ.* **21**, 580--605, 2012.

289. Zhang, X., et al. Application of (R)-3-hydroxyalkanoate methyl esters derived from microbial polyhydroxyalkanoates as novel biofuels, *Biomacromolecules* **10**, 707--711, 2009.

290. Wang, S.Y., et al. Properties of a new gasoline oxygenate blend component: 3-hydroxybutyrate methyl ester produced from bacterial poly-3-hydroxybutyrate, *Biomass Bioenerg.* **34**, 1216--1222, 2010.

291. Gao, X., et al. Polyhydroxyalkanoates as a source of chemicals, polymers, and biofuels, *Curr. Opin. Biotechnol.* **22**, 768--774, 2011.

292. Foster, L.J.R., et al. Environmental concentrations of polyhydroxyalkanoates and their potential as bioindicators of pollution, *Biotechnol. Lett.* **23**, 893--898, 2001.

293. Hiraishi, A., & Khan, S.T. Application of polyhydroxyalkanoates for denitrification in water and wastewater treatment, *Appl. Microbiol. Biotechnol.* **61**,103--109, 2003.

294. Bourbonnais, R., & Marchessault, R.H. Application of polyhydroxyalkanoates granules for sizing of paper, *Biomacromolecules* **11**, 989--993, 2010.

295. Nhan, D.T., et al. The effect of poly [beta]-hydroxybutyrate on larvi culture of the giant freshwater prawn *Macrobrachium rosenbergii*, *Aquaculture* **302,** 76--81, 2010.

296. De Schryver, P., et al. Convergent dynamics of the juvenile European sea bass gut microbiota induced by polyhydroxybutyrate, *Environ. Microbiol.* **13,** 1042--1051, 2011.

297. Defoirdt, T., et al. Alternatives to antibiotics for the control of bacterial disease in aquaculture, *Curr. Opin. Microbiol.* **14,** 251--258, 2011.

298. Grillo, R., et al. Controlled release system for ametryn using polymer microspheres: preparation, characterization and release kinetics in water, *J. Hazard. Mater.* **186**, 1645--1651, 2011.

299. Phukon, P., et al. Enhancing the stability of colloidal silver nanoparticles using polyhydroxyalkanoates (PHA) from *Bacillus circulans* (MTCC 8167) isolated from crude oil contaminated soil, *Colloids Surf., B* **86**, 314--318, 2011.

300. Ma, X., et al. Hydrogen peroxide biosensor based on the direct electrochemistry of Myoglobin immobilized in poly-3-hydroxybutyrate film, *American J of Biochemistry and Biotechnology* **1,** 43--46, 2005.

301. Solaiman, D.K.Y., et al. Rapid and specific identification of medium-chain-length polyhydroxyalkanoates synthase gene by polymerase chain reaction, *Appl. Microbiol. Biotechnol.* **53**, 690--694, 2000a.

302. Solaiman, D.K.Y. PCR cloning of *Pseudomonas resinovorans* polyhydroxyalkanoates biosynthesis genes and expression in *Escherichia coli*, *Biotechnol. Lett.* **22**, 789--794, 2000b.

303. Zhang, G., et al. PCR cloning of type II polyhydroxyalkanoate biosynthesis genes from two *Pseudomonads*, *FEMS Microbiol. Lett.* **198,** 165--170, 2001.

304. Solaiman, D.K.Y. Polymerase-chain-reaction-based detection of individual polyhydroxyalkanoates synthase phaC1 and phaC2 genes, *Biotechnol. Lett.* **24**, 245--250, 2002.

305. Jamil, N., et al. Characterization of biopolymer produced by Pseudomonas sp. CMG607w of marine origin, *J. Gen. Appl. Microbiol.* **53**, 105--109, 2007.

306. Rehman, S., et al. Screening of different contaminated environments for polyhydroxyalkanoates-producing bacterial strains, *Biol. Bratislava.* **62**, 650--656, 2007.

307. Cappuccino, G.J. & Sherman, N. *Microbiology: A Laboratory Manual* 3rd ed., Benjamin/cummings Pub. Co., New York, 1992.

308. Ashby, R.D., et al. Poly (ethylene glycol)-mediated molar mass control of short-chain- and medium-chain-length poly (hydroxyalkanoates) from *Pseudomonas oleovorans*, *Appl. Microbiol. Biotechnol.* **60**, 154--159, 2002.

309. Huijberts, G.N., et al. 13C Nuclear Magnetic Resonance Studies of *Pseudomonas putida* Fatty Acid Metabolic Routes Involved in Poly(3-Hydroxyalkanoate) *Synthesis, J. Bacteriol.* **176**, 1661--1666, 1994.

310. Wang, Y., et al. Kevlar oligomer functionalized graphene for polymer composites, *Polymer* **52**, 3661--3670, 2011.

311. Monkman, A.P., & Adams, P. Optical and electronic-properties of stretch-oriented solution-cast polyaniline films, *Synth. Met.* **40**, 87--96, 1991.

312. Sambrook, J. & Russell, D.W. *Molecular Cloning: A laboratory Manual*, 3rd ed., Cold Spring Harbor Laboratory Press, New York, 2001.

313. Saitou, N., & Nei, M. The neighbor-joining method: a new method for reconstructing phylogenetic trees, *Mol. Biol. Evol.* **4**, 406--425, 1987.

314. Page, R.D. TREEVIEW: an application to display phylogenetic trees on personal computers, *Comput. Appl. Biosci.* **12**, 357--358, 1996.

315. Dalal, J., et al. Evaluation of bacterial strains isolated from oil-contaminated soil for production of polyhydroxyalkanoic acids (PHA), *Pedobiologia* **54**, 25--30, 2010.

316. He, W., et al. Production of novel polyhy-droxyalkanoates by *Pseudomonas stutzeri* 1317 from glucose and soy bean oil, *FEMS Microbiol.Lett.* **169**, 45--49, 1998.

317. Kaplan, C.W., & Kitts, C.L. Bacterial succession in petroleum land treatment unit, *Appl. Environ. Microbiol.* **70**, 1777--1786, 2004.

318. Haba, E., et al. Poly-3- (hydroxyalkanoate) produced from oily substrates by *Pseudomonas aeruginosa* 47T2 (NCBIM40044): effect of nutrients and incubation temperature on polymer composition, *Biochem. Eng. J.* **35**, 99--106, 2007.

319. Reddy, S.V., & Thirumala, M. Isolation of polyhydroxyalkanoates (PHA) producing bacteria from contaminated soils, *International Journal of Environmental Biology* **2**, 104--107, 2012.

320. William, J. P., & Chistopher, J.T. Quantitation of poly-β-hydroxybutyrate by fluorescence of bacteria and granules stained with Nile blue A, *Biotechnol. Tech.* **10**, 215--220, 1996.

321. Naheed, N., et al. Biosynthesis of polyhydroxybutyrate in *Enterobacter* sp. SEL2 and *Enterobacteriaceae* bacterium sp. PFW1 using sugar cane molasses as media, *African Journal of Biotechnology* **11**, 3321--3332, 2012.

322. Garland, P. B. Energy transduction in microbial systems, *Symp. Soc. Gen. Microbiol.* **27**, 1--21, 1977.

323. Riebeling, V., et al. The internal-alkaline pH gradient, sensitive to uncoupler and ATPase inhibitor, in growing *Clostridum pasteurianum, Eur. J. Biochem.* **55**, 445--453, 1975.

324. Russell, J.B., & Dombrowski, D.B. Effect of pH on the efficiency of growth by pure cultures of rumen bacteria in continuous culture, *Appl. Environ. Microbiol.* **39**, 604--610, 1980.

325. Parr, J.F., Sikora, L.J. & Burge, W.D. Factors affecting the degradation and inactivation of waste constituents in soils, *in land treatment of hazardous wastes,* J.F. Parr et. al, eds., Noyes Data Corp., park Ridge, NJ, 1983, 321337.

326. Zinn, M., et al. Occurrence, synthesis and medical application of bacterial polyhydroxyalkanoates, *Adv. Drug Delivery Rev.* **53**, 5--21, 2001.

327. Qiu, Y.Z., et al. Production of poly (3-hydroxybutyrate-co-3-hydroxyhexanoate) from gluconate and glucose by recombinant *Aeromonas hydrophila* and *Pseudomonas putida*, *Biotechnol. Lett.* **27,** 1381--1386, 2005.

328. Solaiman, D.K.Y., et al. Physiological characterization and genetic engineering of *Pseudomonas corrugata* for medium-chain-length polyhydroxyalkanoates synthesis from triacylglycerols, *Curr. Microbiol.* **44,** 189--195, 2002.

329. Ashby, R.D., et al. The synthesis of short- and medium- chain-length poly (hydroxyalkanoate) mixture from glucose- or alkanoic acid-grown *Pseudomonas oleovorans, J. Ind. Microbiol. Biotechnol.* **28**, 147--153, 2002.

330. Ashby, R.D., et al. Bacterial poly (hydroxyalkanoate) polymer production from the biodiesel co-product stream, *J. Polym. Environ.* **12**, 105--112, 2004.

331. Wong, A.L., et al. Microbial production of polyhydroxyalkanoates by bacteria isolated from oil wastes, *Appl. Biochem. Biotechnol.* **84–86**, 843--857, 2000.

332. Obruca, S., et al. Production of poly (3-hydroxybutyrate-co-3-hydroxyvalerate) by *Cupriavidus necator* from waste rape seed oil using propanol as a precursor of 3-hydroxyvalerate, *Biotechnol. Lett.* **32**, 1925--1932, 2010.

333. Verlinden, R.A.J., et al. Production of polyhydroxyalkanoates from waste frying oil by *Cupriavidus necator*, *AMB Express* **1**, 1--8, 2011.

334. Misra, A.K., et al. Screening of poly-hydroxybutyrate-producing microorganisms using Fourier transform infrared spectroscopy, *Biotechnol. Lett.* **22**, 1217--1219, 2000.

335. Khardenavis, A.A., et al. Utilization of molasses spent wash for production of bioplastics by waste activated sludge, *Waste Manage.* **29**, 2558--2565, 2009.

336. McLafferty, F.W. Mass spectrometric analysis broad applicability to chemical research, *Anal. Chem.* **28**, 306--316, 1956.

337. Doi, Y. *Microbial Polyesters*, VCH publishers, New York, 1990.

338. Huijberts, G.N., et al. *Pseudomonas putida* KT2442 cultivated on glucose accumulates poly (3-hydroxyalkanoates) consisting of saturated and unsaturated monomers, *Appl. Environ. Microbiol.* **58**, 536--544, 1992.

339. Singh, A.K., & Mallick, N. Enhanced production of SCL-LCL-PHA co-polymer by sludge-isolated *Pseudomonas aeruginosa* MTCC 7925, *Letters in Applied Microbiology* **46**, 350--357, 2008.

340. Vander Walle, G.A.M., et al. Development of environmentally friendly coatings and paints using medium-chain-length poly (3-hydrox-yalkanoates) as the polymer binder, *Int. J. Biol.* **25,** 123--128, 1999.

341. Oliveira, F.C., et al. Characterization of poly (3-hydroxybutyrate) produced by *Cupriavidus necator* in solid-state fermentation, *Bioresour. Technol.* **98**, 633--638, 2007.

342. Luo, R., et al. Polyhydroxyalkanoate copolyesters produced by *Ralstonia eutropha* PHB–4 harboring a low-substrate-specificity PHA synthase PhaC2Ps from *Pseudomonas stutzeri* 1317, *Biochemical Engineering Journal* **32**, 218--225, 2006.

343. Ma, L., et al. Production of two monomer structures containing medium-chain-length polyhydroxyalkanoates by β-oxidation-impaired mutant of *Pseudomonas putida* KT2442, *Bioresour. Technol.* **100**, 4891--4894, 2009.

344. Ouyang, S.P., et al. Production of polyhydroxyalkanoates with high 3-hydroxydodecanoate monomer content by fadB and fadA knockout mutant of *Pseudomonas putida* KT2442, *Biomacromolecules* **8,** 2504-- 2511, 2007.

345. Allen, A.D., et al. Biosynthesis and characterization of copolymer poly (3HB-co-3HV) from saponified *Jatropha curcas* oil by *Pseudomonas oleovorans*, *J. Ind. Microbiol. Biotechnol,* **37**, 849--856, 2010.

346. Abe, H., et al. Physical properties and enzymatic degradability of Poly (3-hydroxybutyrate) stereoisomers with different stereoregularities, *Macromolecules* **27**, 6018--6025, 1994.

347. de-Keijser, T.H., et al. Use of the Voigt function in a single-line method for the analysis of X-ray diffraction line broadening, *J. Appl. Cryst.* **15**, 308--314, 1982.

348. Liu, W.K., & Chen, G.Q. Production and characterization of mcl-PHA with high 3-hydroxy tetradecanoate monomer content by fadB and fadA knockout

mutant of *Pseudomona sputida* KT2442, *Appl. Microbiol. Biotechnol.* **76**, 1153--1159, 2007.

349. Li, Z.G., et al. Study of enzymatic degradation of microbial copolyesters consisting of 3-hydroxybutyrate and medium-chain-length 3-hydroxyalkanoates, *Polym. Degrad. Stab.* **92**, 1708--1714, 2007.
350. Bengtsson, S., et al. Molecular weight and thermal properties of polyhydroxyalkanoates produced from fermented sugar molasses by open mixed cultures, *J. Biotechnol.* **147**, 172--179, 2010.
351. Loo, C.Y., et al. Biosynthesis and characterization of poly (3-hydroxybutyrate-co-3-hydroxyhexanoate) from palm oil products in a *Wautersia eutropha* mutant, *Biotechnol Lett.* **27**, 1405--1410, 2005.
352. Haywood, G.W., et al. Accumulation of a polyhydroxyalkanoate containing primarily 3-hydroxydecanoate from simple carbohydrate substrates by *Pseudomonas* sp. strain NCIMB 40135, *Appl. Environ. Microbiol.* **56**, 3354--3359, 1990.
353. Taguchi, S., et al. Biosynthesis of biodegradable polyesters from renewable carbon sources by recombinant bacteria, *Polym Int.* **51**, 899--906, 2002.
354. Savenkova, L., et al. Mechanical properties and biodegradation characteristics of PHB-based films, *Process Biochemistry.* **35**, 573--579, 2000.
355. Bengtsson, S., et al. Molecular weight and thermal properties of polyhydroxyalkanoates produced from fermented sugar molasses by open mixed cultures, *J. Biotechnol.* **147**, 172--179, 2010.
356. Bozani, D.K., et al. Silver nanoparticles encapsulated in glycogen biopolymer: Morphology, optical and antimicrobial properties, *Carbohydrate Polymers* **83**, 883--890, 2011.
357. Thire, R.M.S.M., et al. Effect of starch addition on compression-molded Poly (3-hydroxybutyrate)/starch blends, *J. Appl. Polym. Sci.* **100**, 4338--4347, 2006.
358. Dutta, S., et al. Biodegradation of epoxy and MF modified Polyurethane films derived from a sustainable resource, *J Polym Environ* **18**, 167--176, 2010.
359. Luo, S., & Netravali, A.N. A study of physical and mechanical properties of poly (hydroxybutyrate-co-hydroxyvalerate) during composting, *Polym. Degrad. Stab.* **80**, 59--66, 2003.

360. Shah, A.A., et al. Biological degradation of plastics: A comprehensive review, *Biotechnology Advances* **26**, 246--265, 2008.

361. Yamada-Onodera, K., et al. Degradation of polyethylene by a fungus, *Penicillium simplicissimum* YK, *Polym. Degrad. Stab.* **72**, 323--327, 2001.

362. Bordoloi, N.K., & Konwar, B.K. Microbial surfactant-enhanced mineral oil recovery under laboratory conditions, *Colloids Surf. B.* **63**, 73--82, 2008.

363. Sang, B.I., et al. Fungal contribution to in situ biodegradation of poly (3-hydroxybutyrate-co-3-hydroxyvalerate) film in soil, *Appl. Microbiol. Biotechnol.* **58**, 241--247, 2002.

364. Mulfinger, L., et al. Synthesis and Study of Silver Nanoparticles, *J. Chem. Educ.***84**, 322, 2007.

365. Solomon, S.D., et al. Synthesis and study of silver nanoparticles, *J. Chem. Educ.* **84**, 322--325, 2007.

366. Saha, S., et al. Production of silver nanoparticles by a phytopathogenic fungus bipolaris nodulosa and its antimicrobial activity, *Digest Journal of Nanomaterials and Biostructures* **5**, 887--895, 2010.

367. Wani, I.A., et al. Silver nanoparticles: Ultrasonic wave assisted synthesis, optical characterization and surface area studies, *Mater. Lett.* **65**, 520--522, 2011.

368. Ratyakshi, R., & Chauhan, P. Colloidal synthesis of silver nano particles, *Asian J. Chem.* **21**, 113--116, 2009.

369. Van Hyning, D.L., et al. Characterization of colloidal stability during precipitation reactions, *Langmuir* **17**, 3120--3127, 2001.

370. Solomon, S. D., et al. Synthesis and Study of Silver Nanoparticles, *J. Chem. Educ.* **84**, 322--325, 2007.

371. Udapudi, B.B., et al. Synthesis and characterization of silver nanoparticles, *International Journal of Pharmacy and Biological Sciences* **2**, 10--14, 2012.

372. Jain, P., & Pradeep, T. Potential of Silvernanoparticle-coated polyurethane foam as an antibacterial water filter, *Biotechnol. Bioeng.* **90**, 59--63, 2005.

373. Niasari, M.S., et al. Preparation of NiO nanoparticles from metal-organic frameworks via a solid-state decomposition route, *Inorg. Chim. Acta.* **362**, 3691--3697, 2009.

374. Wu, H.Q., et al. Synthesis of zinc oxide nanorods using carbon nanotubes as templates, *J. Cryst. Growth* **265,** 184--189, 2004.

375. Wu, H.Q., et al. Synthesis of copper oxide nanoparticles using carbon nanotubes as templates, *Chem. Phys. Lett.* **364**, 152--156, 2002.

376. Choulis, S.A., et al. Influence of metallic nanoparticles on the performance of organic electrophosphorescence devices, *Appl. Phys. Lett.* **88**, 213503--213503-3, 2006.

377. Kausik, A., et al. Fabrication and characterization of polyaniline-ZnO hybrid nanocomposite thin films, *J. Nanosci. Nanotechnol.* **8**, 1757--1761, 2008.

378. Khan, R., & Dhayal, M. Chitosan/polyaniline hybrid conducting biopolymer base impedimetric immunosensor to detect Ochratoxin-A, *Biosens. Bioelectron.* **24,** 1700--1705, 2009.

379. Luo, X.L., et al. Electrochemically deposited chitosan hydrogel for horseradish peroxidase immobilization through gold nanoparticles self-assembly, *Biosens. Bioelectron.* **21**, 190--196, 2005.

380. Zhang, L., et al. Attachment of gold nanoparticles to glassy carbon electrode and its application for the direct electrochemistry and electrocatalytic behavior of hemoglobin, *Biosens. Bioelectron.* **21**, 337--345, 2005.

381. Lin, J., et al. Disposable biosensor based on enzyme immobilized on Au–chitosan-modified indium tin oxide electrode with flow injection amperometric analysis; *Anal. Biochem.* **360,** 288--293, 2007.

382. Jastrebova, J., et al. On-line deoxygenation for reductive electrochemical detection of artemisinin and dihydroartemisinin in liquid chromatography, *Analyst* **123**, 313--317, 1998.

383. Peng, C.A., et al. Direct analysis of artemisinin from Artemisia annua L. using high-performance liquid chromatography with evaporative light scattering detector, and gas chromatography with flame ionization detector, *J. Chromatogr., A.* **1133,** 254--258, 2006.

384. Amponsaa-Karikari, A., et al. Determination of artemisinin in human serum by high-performance liquid chromatography with on-line UV irradiation and peroxyoxalate chemiluminescence detection, *Biomed. Chromatogr.* **20**, 1157--1162, 2006.

385. Green, M.D., et al. Chemiluminescent detection of artemisinin novel endoperoxide analysis using luminol without hydrogen peroxide, *J. Chromatogr., A.* **695**, 237--242, 1995.

Papers in Journals

1. Kamrupi, I.R., **Phukon, P.,** Konwer, B.K., & Dolui, S.K. Synthesis of silver-polystyrene nanocomposite particles in water in supercritical carbon dioxide medium and its antimicrobial activity, *J. Supercrit. Fluids* **55,** 1089--1094, 2011.
2. **Phukon, P.,** Saikia, J.P., & Konwar, B.K. Enhancing the stability of colloidal silver nanoparticles using polyhydroxyalkanoates (PHA) from *Bacillus circulans* (MTCC 8167) isolated from crude oil contaminated soil, *Colloids Surf., B* **86** 314--318, 2011.
3. **Phukon, P.,** Saikia, J.P., & Konwar, B.K. Bio-plastic (P-3HB-co-3HV) from *Bacillus circulans* (MTCC 8167) and its biodegradation, *Colloids Surf., B* **92,** 30--34, 2012.
4. **Phukon, P.,** Pokhrel, B., Konwar, B.K., & Dolui, S.K. Biosynthesis and characterization of a new copolymer, poly (3-hydroxyvalerate-co-5-hydroxydecenoate), from *Pseudomonas aeruginosa, Biotechnol Let.* **35**, 607--611, 2013.
5. **Phukon, P.,** Radhapyari, K., Konwar, B.K., & Khan, R. Natural polyhydroxyalkanoate-gold nanocomposite based biosensor for detection of antimalarial drug-artemisinin, *Materials Science and Engineering C* (under review).
6. Phukan, M.M., Singh, S.P., **Phukon, P.,** Borah, T., Konwar, B.K., & Dutta, N. Production and statistical optimization of biodiesel from kitchen chimney dump lard, *Sustainable Chemical Processes* (under review)

Presentation in conference

1. **Phukon, P.,** & Konwar, B. K. Biopolymer Isolated from Bacteria available in Oil well sites of Assam, 96th Indian Science Congress, NEHU, Shillong, January 3-7, 2009.
2. **Phukon, P.,** & Konwar, B. K. Biopolymer from crude oil scavanging bacteria, National seminar on Emerging Trends in Polymer Science and Technology (Poly-2009), Dept. of Chemistry, saurashtra university, Rajkot, Gujrat, October 8-10, 2009 (Adjudged as the best paper).